SCHOOL OF
CIVIL ENGINEERING

INDIANA
DEPARTMENT OF TRANSPORTATION
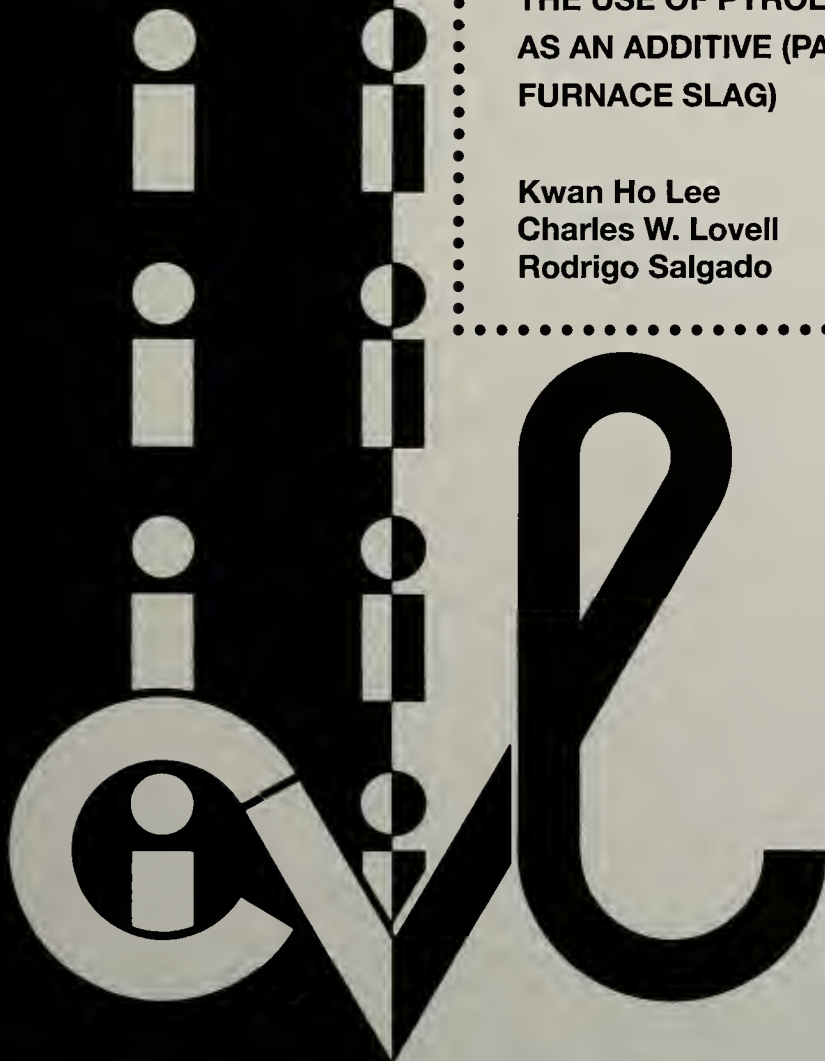
THE USE OF PYROLYZED CARBON BLACK AS AN ADDITIVE (PART III: AIR-COOLED FURNACE SLAG)

Kwan Ho Lee
Charles W. Lovell
Rodrigo Salgado

PURDUE UNIVERSITY

FINAL REPORT

FHWA/IN/JHRP-96/19

THE USE OF PYROLYZED CARBON BLACK AS AN ADDITIVE
(PART III: AIR-COOLED FURNACE SLAG)

by

Kwan-ho Lee
Research Assistant

and
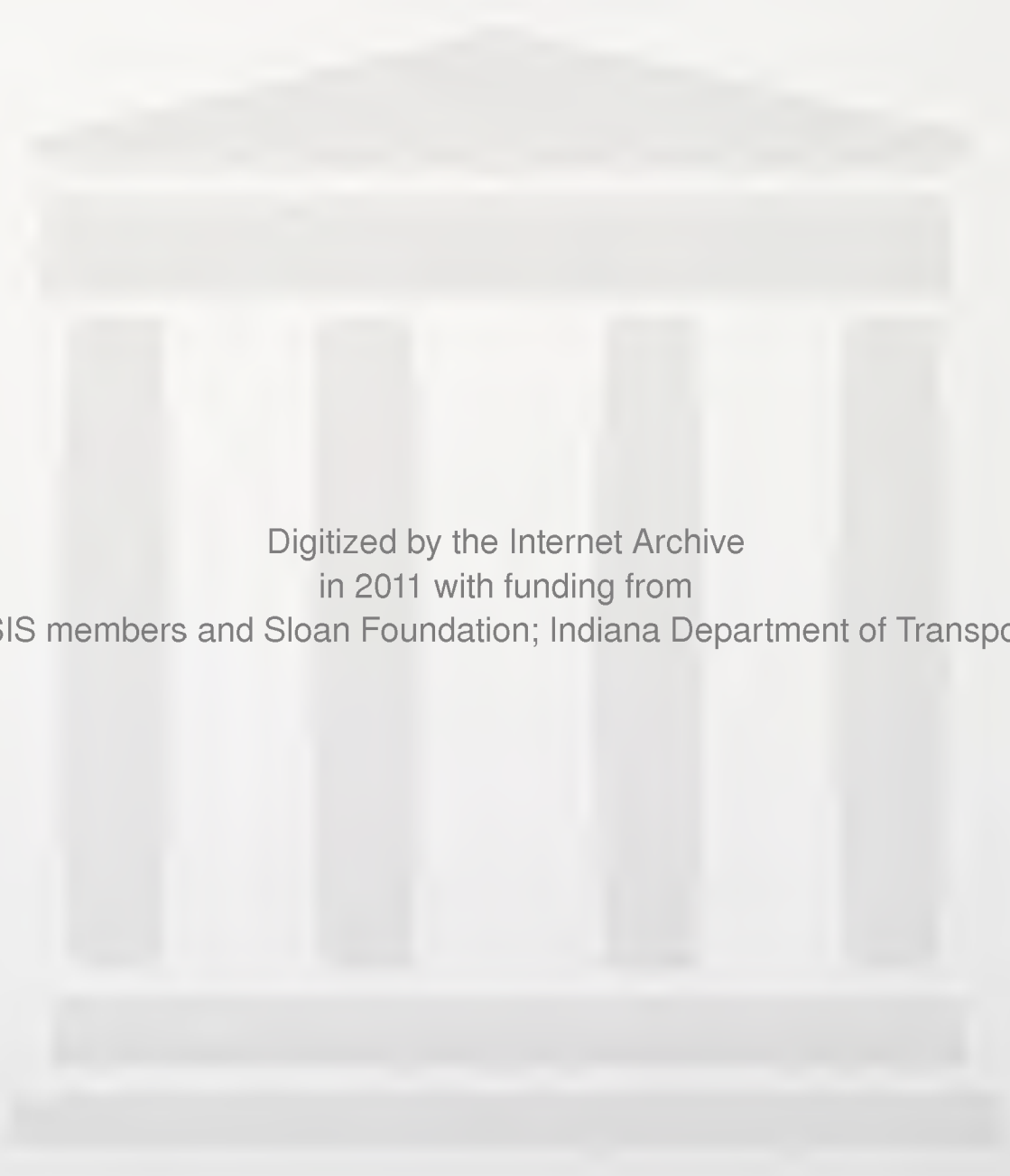
Charles W. Lovell
and
Rodrigo Salgado
Research Engineers

Purdue University
Department of Civil Engineering

Purdue University
West Lafayette, IN 47907
November 20, 1996

1. Report No. FHWA/IN/JHRP-96/19	2. Government Accession No.	3. Recipient's Catalog No.
4. Title and Subtitle The Use of Pyrolyzed Carbon Black as an Additive (Part III: Air-Cooled Furnace Slag)		5. Report Date November 20, 1996
		6. Performing Organization Code
7. Author(s) Kwan-Ho Lee, Charles W. Lovell, and Rodrigo Salgado		8. Performing Organization Report No. FHWA/IN/JHRP-96/19
9. Performing Organization Name and Address Joint Highway Research Project 1284 Civil Engineering Building Purdue University West Lafayette, Indiana 47907-1284		10. Work Unit No.
		11. Contract or Grant No. SPR-2096
12. Sponsoring Agency Name and Address Indiana Department of Transportation State Office Building 100 North Senate Avenue Indianapolis, IN 46204		13. Type of Report and Period Covered Final Report
		14. Sponsoring Agency Code

15. Supplementary Notes

Prepared in cooperation with the Indiana Department of Transportation and Federal Highway Administration.

16. Abstract

The purpose of this research was to characterize the fundamental properties and to evaluate the performance of asphalt mixtures modified by pyrolyzed carbon black (CB_p) as an additive and air-cooled furnace slag as a coarse aggregate. Laboratory tests were conducted at INDOT and Koch Materials. The optimum binder content and the relationship of density and voids were determined from Marshall mix design. The range of the optimum binder content was 6.3% to 7.8%. The Marshall stability as a strength value and flow increased within the accepted ranges due to the inclusion of Cb_p. The gyratory tests were conducted by the US Army Corps of Engineers 8A/6B/4C model. The resilient modulus (M_R) test and indirect tensile test were conducted to determine the stiffness of the mixture at low temperatures which is related to the cracking potential of pavements. The inclusion of commercial CB and Cb_p produced an increase of M_R and tensile strength. Dynamic confined creep tests were carried out to check the rutting potential of pavement at high temperature, which is one of the important problems for pavements. The mixtures modified by Cb_p showed lower creep strain than the unmodified mixtures.

17. Key Words pyrolyzed carbon black, Marshall stability, tensile strength, resilient modulus, stripping inflection point.	18. Distribution Statement No restrictions. This document is available to the public through the National Technical Information Service, Springfield, VA 22161

19. Security Classif. (of this report) Unclassified	20. Security Classif. (of this page) Unclassified	21. No. of Pages 222	22. Price

Form DOT F 1700.7 (8-69)

TABLE OF CONTENTS

LIST OF TABLES

LIST OF FIGURES

LIST OF ABBREVIATIONS

AAMAS : Asphalt-Aggregate Mixture Analysis System

AAPT : Association of Asphalt Paving Technologist

AASHTO : American Association of State Highway and Transportation Offices

AC : Asphalt Cement

AEA : Atomic Energy Authority

AI : Asphalt Institute

ASTM : American Society for Testing and Materials

BBR : Bending Beam Rheometer

CB : Commercial Carbon Black

CB_p : Pyrolyzed Carbon Black

DMA : Dynamic Mechanical Analysis

DTT : Direct Tension Test

EPA : Environmental Protection Agency

FHWA :Federal Highway Administration

G_b : The Specific Gravity of the Asphalt Binder

GCI : Gyratory Compactability Index

G_{mb} : The Specific Gravity of the Sample Mixtures

G_{mm} (TMSG) : The Theoretical Maximum Specific Gravity

G_{sb} : The Blended Aggregate Bulk Specific Gravity

GSF : Gyratory Shear Factor

GSI : Gyratory Stability Index

GTM : Gyratory Testing Machine

HAF : High Abrasion Furnace

HMA : Hot Mix Asphalt

INDOT : Indiana Department of Transportation

ISTEA : The Inermodal Surface Transportation Efficiency Act

LVDT : Linear Variable Differential Transducer

MTS : Material Testing System

M_R : Resilient Modulus

PDU : A Vacuum Pyrolysis Process Development Unit

PI : Penetration Index

RTFOT : Rolling Thin Film Oven Test

S_g : Gyratory Shear

SHRP : Strategic Highway Research Program

S_t : Tensile Strength

TRB : Transportation Research Board

VFA : Voids Filled with Asphalt Cement

VMA : Voids in Mineral Aggregate

VTM : Voids in Total Mix

IMPLEMENTATION REPORT

The main purpose of this research is to evaluate the potential of the use of pyrolyzed carbon black as an additive and air-cooled furnace slag as coarse aggregates in hot mix asphalt.

The following recommendations are made to INDOT to implement the finding of this research.

- The slag mixture showed better performance than the limestone mixture, including higher Marshall stability and ultimate tensile strength, as well as higher resistance for water-susceptibility.

- The inclusion of CB and CB_p reduced the permanent deformation of AC-10 and AC-20 asphalt mixtures at high testing temperature.

- The effect of CB and CB_p as an additive for AC-10 asphalt cement is better than for AC-20 asphalt cement at low testing temperature.

- The inclusion of CB_p in hot mix asphalt can compensate for the initial construction cost due to its good performance, such as the increase of strength and ductility at high temperature, the increase of rutting resistance, the decrease of the potential of low-temperature cracking, and the decrease of water-susceptibility.

- Although asphalt mixtures modified by pyrolyzed carbon black have shown relatively good performance, the long-term performance should be monitored. Therefore, test sections should be constructed and monitored for a long time, using the mixtures which have been shown to be most effective in the laboratory.

CHAPTER 1

INTRODUCTION

1.1 Background

Scrap tires, generated at the rate of over 242 million each year in the United States, are recognized as one of the most significant environmental problems. Most of these scrap tires have been disposed of in landfills, stockpiles, and illegal dumps (EPA 1991). There is a need to find more useful, environmentally friendly applications for these tires. Extensive researches have been conducted in the past years on the utilization of the scrap tires. The use of scrap tires for asphalt pavement, which is complicated by the complex behavior of asphalt, has received major attention.

This research aims to describe the performance of mixtures of asphalt using pyrolyzed carbon black (CB_p) as an additive. Commercial carbon black (CB) is an intensely black, fine powdery substance. Due to the excellent properties of carbon black, it has been used as a fundamental raw material for rubber, plastic products, printing ink, and others. Tire companies are the largest consumers of CB, using two-thirds of the commercial CB supply as a reinforcing agent. However, the major disadvantage to use of CB is its high cost. The use of CB as a reinforcing agent for hot mixed asphalt may produce a similar benefit. It has been reported that CB also be used to reinforce asphalt cement pavements (Rostler et al., 1977). Yao and Monismith (1986) and Vallerga and Gridley (1980) reported that the use of CB increased the rutting resistance at high temperature and the durability of asphalt. They found that the temperature susceptibility and the cracking propagation potential of asphalt at low temperature decreased. In spite of its effectiveness as a modifier, however, the use of CB has been somewhat limited due to its relatively high material cost (Park, 1995).

Pyrolysis of scrap tires is currently receiving renewed attention, since the derived oils may be used directly as fuels or added to petroleum refinery feedstock; they may also be an important source of refined chemicals. The yield products are significantly altered as the pyrolysis temperature and heating rate were increased. CB_p as a byproduct of the pyrolysis of scrap tires, typically yields 55% oil, 25% carbon black, 9% steel, 5% fiber, and 6% gas. Pyrolyzed carbon black includes 75% carbon black, 9% ash, 4% sulfur, and 12% of butadiene copolymer (Roy et al, 1990). CB_p is inferior to commercially available CB due to its high ash content, the presence of solid hydrocarbons and the larger particle size. However, CB_p is suitable for use in low-grade rubber products such as conveyor belts, footwear and automobile mud flaps. In this research, the possibility of using CB_p in hot mix asphalt was evaluated.

1.2 The Distress in Asphalt Pavement

It is generally considered that permanent deformation, fatigue cracking and thermal cracking are the three primary types of distress in asphalt pavements.

Permanent deformation occurs only on flexible pavements and is characterized by a surface cross section that is no longer in its proper position. It cannot be recovered. Wheel path rutting is the most common form of permanent deformation due to weak subgrade, low shear strength of asphalt pavement, moisture damage, and traffic densification. Two design procedures have been used to control permanent deformation: (i) limit the vertical compressive strain on the top of subgrade, and (ii) limit the rutting to a tolerable amount, 0.5 in or 13 mm (Huang, 1993).

Fatigue cracking is a distress type that often occurs in wheel paths where repeated heavy loads are applied (McGennis et al., 1994). The failure criterion relates the allowable number of load repetitions to the tensile strain based on the laboratory fatigue test. An early sign of fatigue cracking is intermittent longitudinal wheel path cracks and is a progressive type of distress. Alligator cracking is an intermediate stage of fatigue cracking because the crack pattern looks like an alligator's skin. A possible way to overcome fatigue cracking is to use paving materials that are resilient enough to withstand normal deflections.

Thermal cracking includes both low-temperature cracking and thermal fatigue cracking. Low-temperature cracking is usually associated with flexible pavements in northern parts of the United States and most of Canada, where winter temperatures can fall below -10°F or -23°C. Thermal fatigue cracking can occur in much milder regions if an excessively hard asphalt is used or the asphalt becomes hardened due to aging. Asphalt binder acts the key role in thermal cracking. In general, hard asphalt binders are more prone to thermal cracking than soft asphalt binders.

1.3 Objective and Test Procedure

A binder study for the rheological behavior of AC-10 and AC-20 asphalt modified by commercial carbon black (CB) and pyrolyzed carbon black (CB_p) was conducted by Zeng and Lovell (1995). In general, AC-10 asphalt binder has lower viscosity and higher penetration than AC-20 asphalt. This research included several laboratory tests, such as penetration test, softening test, ductility test, specific gravity test, and kinematic viscosity test. The major conclusions suggested by them were:

- Pyrolysis is one of the most desirable ways of disposing scrap tires from an economic and environmental standpoint.
- The inclusion of CB_p improved the temperature susceptibility of asphalt cement binder.

Another similar research was conducted by Lesueur et al. (1995). They ran many laboratory tests, such as particle size analysis, dynamic mechanical analysis (DMA), Brookfield viscosity, rolling thin film oven test (RTFOT), pressure aging test, bending beam rheometer (BBR), and direct tension test (DTT). Most of the laboratory tests followed the Strategic Highway Research Program (SHRP) test protocols. Four different fillers passing the No. 200 sieve (75 μm) were used, such as pyrolyzed carbon black, Ralston quarries from Colorado, crushed sieve pits, and Ball clay. This study showed that ;

- The rheology of asphalt binder is mainly governed by the volume content of the fillers at temperature less than 65°C.

- Pyrolyzed carbon black greatly improved the rutting resistance of the binders.
- Fracture mechanics experiments are needed to understand and qualify the temperature toughening effect of the fines.

The main purpose of this study is to evaluate the performance of asphalt mixtures modified by CB and CB_p. Many laboratory tests were conducted in the research laboratory of Indiana Department of Transportation (INDOT). Figure 1.1 shows the laboratory testing program.

Marshall Mix Design
- Proper gradation
- Optimum binder content
- Relationship between density and voids properties

Compaction
- Marshall
- Gyratory

Dynamic Confined Creep Test
- at 50°C
- Permanent deformation
- Stress and strain with time
- Rutting resistance

Gyratory Test
- Stress-strain relationship
- Plastic deformation

Resilient Modulus Test
- at 5°C and 25°C
- Strength

Indirect Tensile Test
- at 5°C
- Ultimate strength

Hamburg Wheel Tracking Test
- at 50°C in water
- Asphalt stripping potential
- Resistance to moisture damage
- Resistance to permanent deformation

Evaluation of Asphalt Mixtures Modified by CB and CB_p

Figure 1.1 Summary for Laboratory Test Procedures

CHAPTER 2
PYROLYSIS OF SCRAP TIRES

2.1 Introduction

Scrap tires, which are generated at the rate of over 242 million each year in the United States and 1.5 million tons per year in the European Community, are recognized as one of the more significant environmental problems (Elliot, 1990, EPA, 1991). Over 70 percent of scrap tires is disposed of in landfill sites, open dumping or stockpiled (EPA, 1991). Incineration currently disposes of a small percent of scrap tires, however, this may not maximize the potential economic recovery of energy and chemical materials from the scrap tires. Moreover, the large centralized facilities that are required for environmentally acceptable incineration require transportation of scrap tires over considerable distance. This transportation carries its own environmental consequences and costs.

Pyrolysis of scrap tires is currently receiving renewed attention, since the derived oil may be used directly as fuels, or added to petroleum refinery feedstocks. It may also be an important source for refined chemicals (Williams et al., 1993). A number of commercial, pilot and bench-scale systems for tire pyrolysis has been reported and the yield of each of the products can be optimized by altering the process conditions. The products yielded are significantly altered as the pyrolysis temperature and heating rate are increased.

2.2 Methods of Pyrolysis

There are many different pyrolysis methods. For example, Williams et al. (1990) used a gas purged static batch reactor for pyrolysis of shredded tires; Kaminsky and Sinn

(1980) used a fluidized bed pyrolyser; Kawakami et al. (1980) used a rotary kiln pyrolyser; and Roy and Unsworth (1989) used a vacuum pyrolysis unit. Only two different pyrolysis units will be discussed in this chapter.

The whole tire batch pyrolysis unit is produced by AEA-Beven, Harwell, a joint venture company between AEA (Atomic Energy Authority), Harwell and Herbert Beven and Company, Colchester, England. This consists of a 4.3 m^3 capacity inner kiln into which the halved and whole tires are loaded. The capacity allows in excess of one ton of tires to be loaded and with a pyrolysis cycle time of 12-14 hours, the throughput is approximately two tons per day. Figure 2.1 shows a schematic diagram of the unit. The inner kiln is loaded into an outer holder which consists of a ceramic-lined vessel fitted with a gas-tight lid to ensure pyrolysis conditions are maintained in the unit. The system is purged with nitrogen to eliminate any oxygen. The inner kiln is heated initially by natural gas burners, but as the pyrolysis of the tires proceeds the natural gas is replaced by the gas derived from the tire pyrolysis.
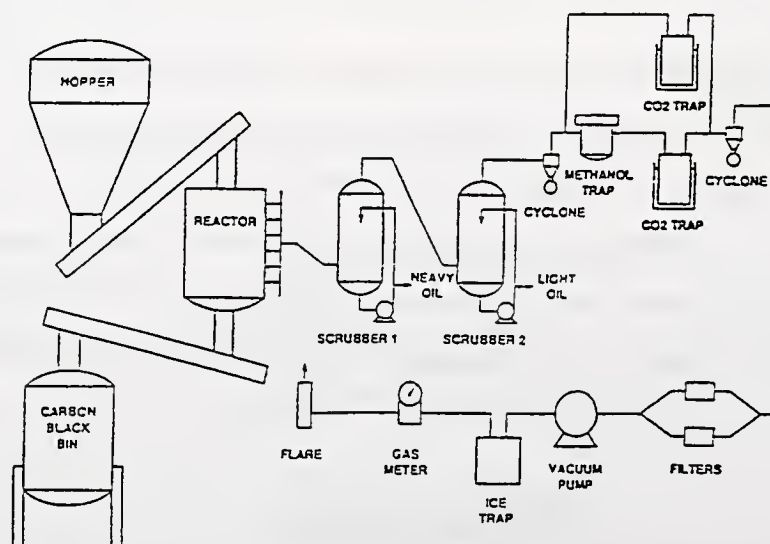
Figure 2.1 Schematic Diagram of the AEA-Beven Tire Pyrolysis Unit (Williams et al., 1993)

The maximum temperature of pyrolysis and the mass of tires loaded into the inner kiln were varied for each experiment from 700 to 950 °C and 305 to 1015 kg respectively. The evolved pyrolysis oil vapors and gases pass through a heat exchanger (to cool the vapors), and into an oil condensing tank. The non-condensed gases then pass to a scrubbing unit to clean the gases, before passing to the burner or to storage. The oil from the condensing tank is pumped to storage, or can also be used to provide auxiliary fuel for the burners. The batch pyrolysis system alleviates many of the problems encountered with continuously fed systems, such as non-maintenance of pyrolysis conditions, feed problems and in-bed fouling by the metal core of the tires.

Vacuum pyrolysis is an old concept. It enables the production of large quantities of pyrolysis oils from organic matter. Vacuum can minimize secondary reactions such as thermal cracking, repolymerization and recondensation reactions, gas phase collision, catalytic cracking and reduction, and oxidation reactions. Figure 2.2 shows a vacuum pyrolysis process development unit (PDU). The system, operated on a semi-continuous feed mode using shredded regular, used tire material sieved to 6.4 - 12.7 mm mesh size.
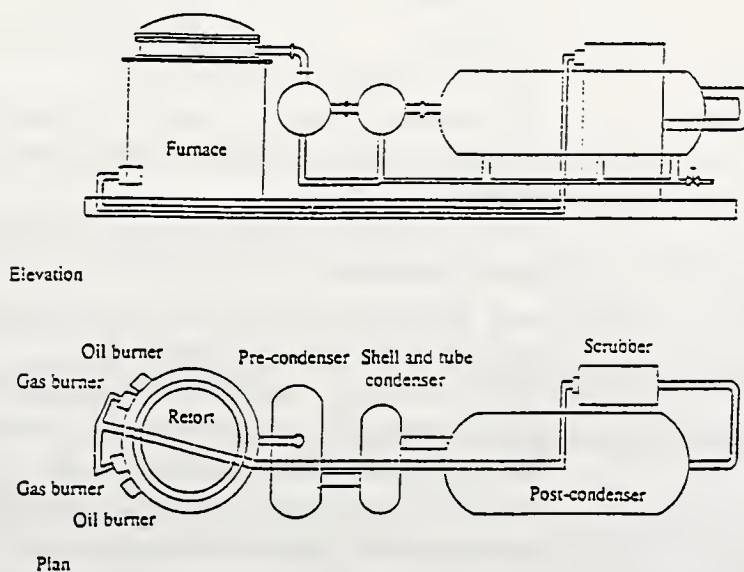
Figure 2.2 Schematic of the Vacuum Pyrolysis Process Development Unit (Roy et al., 1990)

The reactor was a six hearth furnace, 2 m in height and 0.7 m in diameter. It was externally heated by electric elements surrounding the reactor chamber. The maximum throughput reached was 13 kg/h. An important engineering parameter to be considered when designing a full scale pyrolysis plant is the quantity of energy required for the pyrolysis reactions.

Pyrolyzed carbon black (CB_p), which was used in this research, was provided by Wolf Industries, Brazil, Indiana. The information provided by Wolf Industries specified that pyrolysis is a method of decomposing tires by a cooking process in order to break down the tire rubber into salable byproducts. The process by which CB_p is produced is highly protected as confidential and proprietary by the manufacturer, however, a limited and general outline of the pyrolysis of waste tires in the production of CB_p by Wolf Industries is given in Table 2.1 (Park, 1995).

Table 2.1 The Process of the Pyrolysis of Waste Tires by Wolf Industries (Park, 1995)

Process	Subject
Tire Collection and Handling	• Semi-tractor collects used tires for 90 days. • Tires inspection (only light weight tires are accepted).
Production Area	• The tires are sent by the conveyor. • The tires sent are cut 6 in length and cleaned. • The cut tires are sent to the main machinery for next process
The Retort	• The tire bundles evaporating at approximately 800°F (pyrolysis process). • As a result, the solids in the tires, carbon black and steel, fall to the bottom of the tubes.
End Processing of Solid	• The carbon black and steel are moved through a water cooled table to begin the cooling processing. • The upgraded carbon black is sent to a wet pulverizer and milled to reduce the particle size.
Final Processing of Vapors and Liquid	• The separation of volatiles and non-volatiles. • The recovery of oil through a distillation process. • The distillation of the condensable vapor. • Fuel gas from the process.

2.3 Product Yield

The yield from the pyrolysis of scrap tires depends on the source of scrap tires. Table 2.2 shows an example of the composition of scrap tires used by Ogasaware et al. (1987). Yields include oil, carbon black, steel, fiber, and gas. The derived pyrolytic oil has a high calorific value of the order of 42 MJ/kg, with a sulfur content at about 0.8 to 1.65 percent depending on tire sources and process conditions. The oil has been shown to be aromatic and to contain high concentrations of potentially valuable chemical feedstocks, for example benzene, xylene, toluene, styrene and d-limonene (Williams et al., 1990).

Table 2.2 Composition of the Initial Tire Samples (Ogasaware et al., 1987)

Component	Weight	Percent (%)
natural rubber	80	52.2
styrene-butadiene rubber	20	13.0
carbon black (HAF*)	45	29.4
zinc oxide	5	3.3
sulfur	3.2	2.1

* HAF : High Abrasion Furnace

Benzene, xylene and toluene are well-known chemical feedstocks. The concentrations of these components are sufficient to allow the tire oils to be used as a chemical stocks. Limonene has a tremendously increasing wide industrial application (Pakdel et al., 1991). It is used in the formulation of industrial solvents, resins and adhesives and as a dispersing agent for pigments. It is biodegradable, a natural solvent, environmentally safe with excellent solvency, rinseability and high wetting, penetrating, and detergent properties.

Carbon black derived from tire pyrolysis is inferior to commercially available carbon black due to its high ash content, the presence of solid hydrocarbons and larger particle size (Dodds et al., 1983). However, the carbon black is suitable for use in low-

grade rubber products such as conveyor belts, footwear and automobile mud flaps (Roy et al., 1990). One manufacturer concluded that this material could be used as a substitute for up to 20-40 % of N-990 grade in a particular application. An other found that the recycled black has the potential to partially substitute for N-774 commercial grade.

The gas derived from the pyrolysis of scrap tires has been shown to consist of CO_2, CO, H_2, CH_4, C_2H_2, C_2H_6, C_3H_6, C_3H_8, C_4H_6, C_4H_8, and C_4H_{10} with minor concentrations of other hydrocarbon gases. The maximum gas yield was 14.8 percent per mass of tires at the heating rate of 80 kJ/min and final temperature of pyrolysis of 720 °C. The calorific value of gases is around 45 MJ/m^3, depending on type of plant and pyrolysis conditions (Williams et al., 1990). Kaminsky and Sinn (1980) have shown that the calorific value of the gases is sufficient to provide the energy requirements for the pyrolysis process.

CHAPTER 3

THE PROPERTIES OF MATERIALS USED

3.1 Aggregates

3.1.1 Literature Review of Slag

About 200 million metric tons of non-hazardous industrial wastes have been annually generated in the USA (Ciesielski and Collins, 1993). The detailed information on industrial wastes is shown in Table 3.1.

Table 3.1 Detailed Information on Industrial Wastes (Ciesielski and Collins, 1993)

Major	Minor		Amount (mil. ton /yr)	Application
Coal Ash By- products	• fly ash • bottom ash • boiler slag		49.0 12.7 3.6	• structural fill • road base and subbases • asphalt filler
Iron and Steel Slag	blast furnace slag	• air-cooled • granulated • expanded	12.7 0.8 0.6	• all-purpose construction aggregate
	steel slag	• open hearth • basic oxygen • electric arc	7.0 (total)	• aggregate
Reclaimed Pavement	• concrete • asphalt		- 90.7	• unbound base course • cement treated base
Foundry Wastes	• furnace dust • arc dust • sand reclaimed residue		9-14 (total)	• fine aggregate in HMA

Among these, slags are of major interest to this project. Slags are classified according to source as iron blast furnace slag and steel slag.

Iron Blast Furnace Slag

Iron blast furnace slag is defined as " the non-metallic by-product consisting essentially of silicates and aluminosilicates of lime and other bases", and "flows from the blast furnace resembling molten lava" (Miller and Collins, 1976). Four distinct types of blast furnace slags are produced (Ahmed, 1991):

- air cooled (solidification under ambient conditions), which finds extensive use in conventional aggregate applications
- expanded or foamed (solidified with controlled quantities of water), mainly used as light weight aggregate
- granulated (solidified by quick water quenching to a vitrified state), mainly used in slag cement manufacture
- pelletized (solidified by water and air quenching in conjunction with a spinning drum), which is used both as a light-weight aggregate and in slag cement manufacture

Among these, the air-cooled blast furnace slag produced in North America is used in concrete, asphalt, road base, ballast, and as an all-purpose construction aggregate and fill material. More than 15 state highway agencies have used blast furnace slag in various highway applications. The relatively low cost and high performance are the major advantages. According to the report by Emery (1982), the advantages of air-cooled blast furnace slag include:

- low compacted bulk density (typically 1200 to 1450 kg/m^3) that reduces dead load, lateral pressures, and transportation costs on a volumetric basis
- high density (California Bearing Ratio $\geq$ 100), and friction angle (approximately 45°)
- ability to stabilize wet, soft underlying soils at an early construction stage
- placeable in almost any weather, very durable with good resistance to weathering and erosion
- free draining and non-frost susceptible
- almost complete absence of settlement after compaction
- non-corrosive to steel and concrete.

The detailed composition of iron blast furnace slag is shown in Table 3.2. The main components of iron blast furnace slags are calcium oxide and silicon dioxide. The typical characteristics of air-cooled blast furnace slags are shown in Table 3.3.

Table 3.2 Composition of Iron Blast Furnace Slag and Steel Slag (Noureldin and McDaniels, 1991)

Composition (%)	Iron Blast Furnace Slag	Steel Slag
Calcium Oxide	36 - 45	25 - 42
Silicon Dioxide	33 - 42	15 - 17
Aluminum Oxide	8 - 16	2 - 3
Magnesium Oxide	3 - 16	6 - 10
Iron (FeO, Fe_2O_3)	0.3 - 2	20 - 26
Calcium Sulfate	1 - 3	-
Manganese Oxide	0.2 - 1.5	8 - 12
Titanium Dioxide	0 - 1	0 - 1
Free Lime	0 - 1	2 - 4

Steel Slag

Steel slag is a by-product of the steel industry. It is generated as the lime flux reacts with molten iron ore, scrap metal, or other ingredients charged into the steel furnace at melting temperatures (around 2800°F). During this process, part of the liquid metal becomes entrapped in the slag. This molten slag flows from the furnace into the pit area where it solidifies, after which it is transferred to cooling ponds. Metallics are removed by magnetic separation (Miller and Collins, 1976). There are three basic types of steel furnaces, which produce three different types of slag (Lewis, 1982): open hearth furnace, basic oxygen furnace, and electric arc furnace. About half of all currently operating steel furnaces are electric ore furnaces. All steel slags are air-cooled. Steel slags are highly variable, even for the same plant and furnace. The detailed composition of steel slags is shown in Table 3.2. The main components of steel slags are calcium

oxide, iron and silicon dioxide. The typical characteristics of steel slags are shown in Table 3.3. As it can be seen in Table 3.3, steel slags have high bulk specific gravity (3.2-3.6) and a potential expansive nature (volume change of up to 10% attributed to the hydration of calcium and magnesium oxides).

The main applications of steel slag in highway construction have been in pavement bases and shoulders, fills, asphalt mixes, and ice control grit. About nine state highway agencies have used steel slags in several highway applications. From their experience, the use of steel slags in highway applications have proven generally economical, technically feasible and environmentally acceptable. However, the expansive nature of the steel slag should be considered as a potential problem.

Table 3.3 Typical Characteristics of Steel Slag and Air-cooled Blast Furnace Slag
(Noureldin and McDaniels, 1991)

Property	Air-Cooled Blast Furnace	Steel Slag
Bulk Sp. Gravity	2.1 - 2.5	3.2 - 3.6
Porosity	up to 5%	up to 3%
Rodded Unit Weight (ASTM C28), pcf	75 - 90	100 - 120
Los Angeles Abrasion (ASTM C131), %	35 - 45	20 - 25
Sodium Sulfate Loss (ASTM C88), %	≤ 12	≤ 12
Angle of Internal Friction	40° - 45°	40° - 50°
Hardness (measured by Moh's scale)	5 - 6	6 - 7
California Bearing Ratio (top size 3/4 inch)	up to 250%	up to 300%
Unit Weight (pcf)	125 - 145	160 - 190
Polarity	Alkaline, pH 8 - 10	Alkaline, pH 8 - 10
Asphalt Cement Requirements in Dense Grade Mixes	up to 8%	up to 6.5%

* Hardness of dolomite measured on same scale is 3-4.
** Typical CBR value for crushed limestone is 100%.

3.1.2. The Properties of Aggregates Used

Air-cooled blast furnace slag form the Levy Company (at Portage, IN) and natural sands from Vulcan Materials (at W. Lafayette, IN) were used for the mix. A vibrating table sieve shaker (Gilson Model 323333) was used to sieve the aggregate retained on the #4 (4.75mm), and 8 inch diameter sieve used for the #8 (2.36mm) aggregate to # 200 (0.075mm) aggregate. The Indiana Department of Transportation specification for # 9 binder aggregate (INDOT, 1993) was adopted for the target gradation and the gradation of the aggregate was carefully controlled after an initial round of Marshall tests. The upper limit and lower limit gradation for # 9 binder are shown in Figure 3.1. The target gradation that was used is shown in Figure 3.1. Table 3.4 summarizes the gradation of the aggregate used for all the mix design.

The specific gravity test for the coarse aggregate was carried out in accordance with ASTM C127-93 and for the fine aggregate, in accordance with ASTM C128-93. The bulk specific gravity is defined as the overall volume of the aggregate particles as well as the volume of pores that become filled with water after a 24-hour soaking and the apparent specific gravity is defined as only the volume of the aggregate particles. The bulk specific gravity and apparent specific gravity of the coarse aggregate is 2.420 and 2.587. The bulk specific gravity and apparent specific gravity of the fine aggregate is 2.579 and 2.581.

3.2 Asphalt

The ASTM D3381-93 shows the requirements for viscosity graded asphalt cements for each commercial asphalt grade. In this research, AC-10 and AC-20 were used. The main reason is that AC-10 has been used in northern Indiana, and AC-20 has been used in southern Indiana. These two types of asphalt are used very widely in the USA.

The physical properties of AC-10 and AC-20 are summarized in Table 3.5. The physical values from the supplier are in accordance with the INDOT specifications.

According to the physical properties in Table 3.5, the viscosity of AC-10 is less than that of AC-20. On the other hand, penetration of AC-10 is higher than that of AC-20.

Table 3.4 The Gradation of the Aggregate

Sieve Size	% Passing (Used)	Specific % Passing Range
3/4" (19mm)	100	100
1/2" (12.5mm)	81	70 - 92
3/8" (9.5mm)	63	50 - 76
#4 (4.75mm)	40	35 - 45
#8 (2.36mm)	32	18 - 45
#16 (1.18mm)	23	10 - 36
#30 (0.6mm)	16	6 - 26
#50 (0.3mm)	10	2 - 18
#100 (0.15mm)	6	0 - 11
#200 (0.075mm)	2	0 - 4
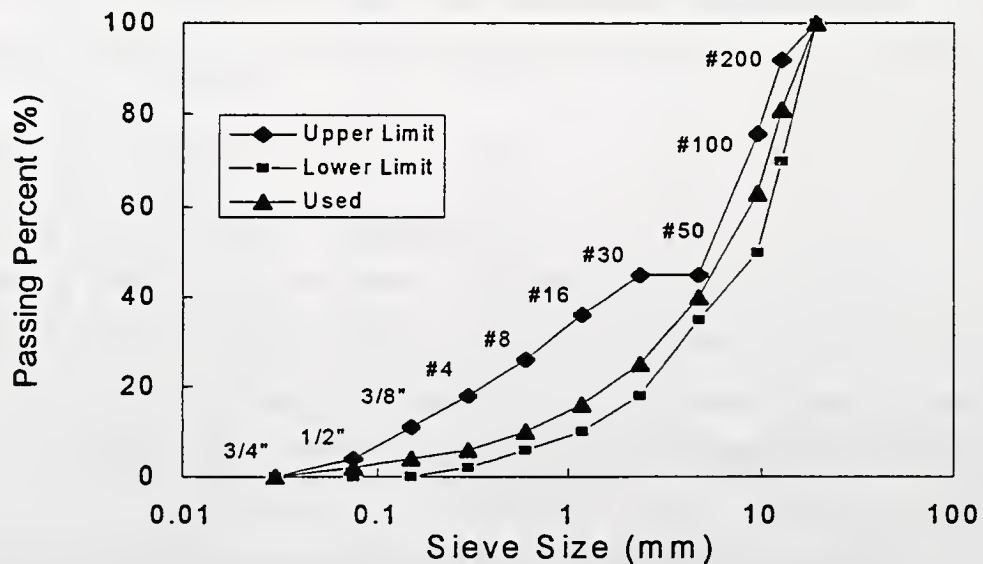
Figure 3.1 The Target Gradation Used

Table 3.5. The Physical Properties of AC-10 and AC-20 (Park, 1995)

Test	AC-10 (requirement of Specification)	AC-20 (requirement of Specification)
Penetration @ 77°F (25°C) (0.1mm), 100g, 5sec	87-106 (70-140)	63 - 65 (50 - 110)
Kinematic Viscosity @275°F (135°C), Centistokes, Min.	316 (250)	406 (300)
Absolute Viscosity @140°F (60°C), Poise, Max.	2670 (4000)	5497 (8000)
Flash Point, Cleveland Open Cup, °C, Min	231 (218)	260 (232)
Solubility in Organic Solvents, %, Min	99.9 (99.0)	99.95 (99.0)
Ductility @25°C, 5Cm/min Cm, Min.	60 (60)	60 (40)

3.3 Additive

3.3.1 Pyrolyzed Carbon Black (CB_p)

Vacuum pyrolysis is an established process. Pyrolysis of tires involves the application of heat to produce chemical changes and to derive various products such as oil and carbon black. Tire pyrolysis typically yields 55% of oil, 25% of carbon black, 9% of steel, 5% of fiber and 6% of gas. Vacuum pyrolysis minimizes secondary reactions such as thermal cracking and reduction and oxidation reductions (Roy et al., 1990).

There are several different methods of tire pyrolysis. The pyrolyzed carbon black (CB_p) used in this research is obtained from the most common process, reductive (retort) pyrolysis. The process schematic is given in Figure 3.2.

The CB_p, used in this research, was provided by Wolf Industries, Brazil, Indiana. It contains 9 % ash, 4% sulfur, 12% butadiene copolymer (nitride rubber), and 75% carbon black. This CB_p could partially replace commercial carbon black for the preparation of low-grade rubber parts. (Roy et al., 1990). More than 90% of CB_p passes through the # 200 sieve. According to test results provided by Wolf Industries, CB_p is insoluble in water. The particle size and surface area of CB_p passed through a mill grinder are given in Table 3.6.

The main characteristics of a representative carbon black sample produced under vacuum at 525°C are summarized in Table 3.7. Koch Materials, Indiana, is working with Wolf Industries to refine other methods for adding the black to asphalt, including thermal blending, blowing in the black, or pelletizing it to ease the addition.

The CB_p is mixed with asphalt. The particles of CB_p are much coarser than commercially available high structure HAF (High Abrasion Furnace) type carbon black, however, most of the coarse particles are easily broken down by normal pressure. The color is lighter black than HAF type carbon black.

Table 3.6 The Particle Size and Surface Area of Pyrolyzed Carbon Black (Mill Ground)

Type	$Rg(\overset{o}{A})$, Particle Size	Specific Surface Area, gm/cm^3	Large Scale df	Large Scale $Rg(\mu m)$
BC 100	430	157	1.9	0.87
BC 200	343	188	2.3	0.52
BC 500	439	159	2.4	0.70
WC 500	230	338	1.7	N/A
NC 339	304	187	N/A	(≥ 0.49)

Note : NC 399 is a pure carbon black and listed for comparing to pyrolyzed carbon black.

Table 3.7 General Properties of Carbon Black Produced during Vacuum Pyrolysis of Used Tires (Roy et al., 1990)

Property	Value
Iodine Index (mg/g)	144.2 - 151.4
DPB Adsorption (ml/100g)	84.6 - 93.0
Heat Loss at 105°C (%)	0.4 - 1.0
Tint Strength (% ITRB)	57.1 - 60.6
Ash (%)	15.5 - 17.0
Volatile Matter	3.3 - 4.9
S (%)	2.5 - 3.0

Note : Ultimate temperature was 525°C and total pressure varied between 1.5 and 4.5 kPa. (Feedstock included both regular and belt used tire samples.)
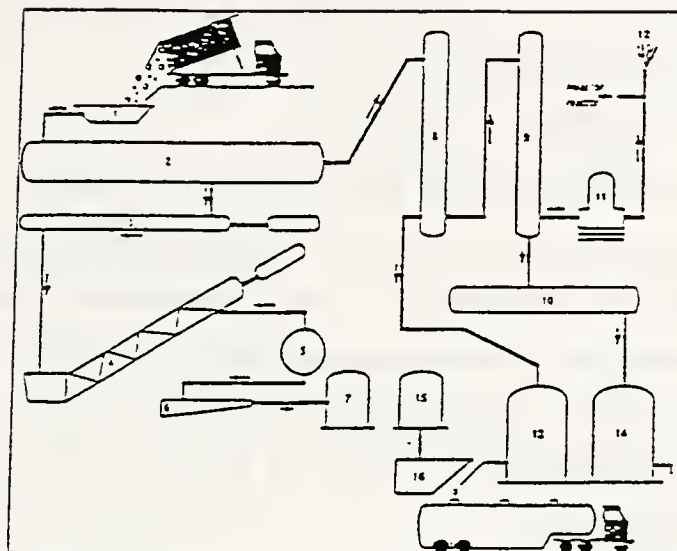
Note : 1=Feed Conveyor, 2=Vacuum Reactor, 3=Cooling Screw, 4=Discharge Screw, 5=Crusher, 6=Vibratory Screen, 7=Carbon Black Handling System, 8=Heavy Oil Quencher, 9=Light Oil Quencher, 10=Decanter, 11=Vacuum Pump, 12=Elare Stack, 13=Heavy Oil Storage, 14=Light Oil Storage, 15=Magnetic Seperator, 16=Steel Recovery Bin.

Figure 3.2 Schematic of the Operation Process of Pyrolyzed Carbon Black
       (Roy et al., 1990)

3.3.2 Carbon Black (CB)

Carbon black (CB) has been used as a reinforcing agent for rubber since about 1915, and has been used in many other applications such as ink, plastic, rubber, electronic wires, and so on. Among these, the rubber industry is the largest user and tire manufacture is one of the largest applications.

CB is the only one formed in the vapor phase from the decomposition of vaporized hydrocarbons. As defined by Powell (1968), CB is formed by incomplete

combustion of many organic substances such as solid, liquid, and gas. The major distinct characteristics are (Yao and Monismith, 1986):

- small particle size (100 to 500 nanometers, mean diameter) and large surface area (15 to over $100m^2/g$)
- hydrophobic materials
- irregular particle shapes (from clustered to branched forms).

In general, the quality of CB has been determined by surface area and particle size. The CB structure is measured by the absorption of liquid, such as dibutyl phthalate. Surface area is determined by nitrogen or iodine adsorption (Rostler et al., 1977).

There are more than 40 different types of CB. Each CB may be composed of several grades, as determined by the particle size and the specific area. CB is divided to four categories by Powell (1968);

- furnace carbon black (made in a furnace by partial combustion of hydrocarbons)
- channel black (manufactured by impingement of natural gas flames on channel irons)
- thermal black (produced by thermal decomposition of natural gas)
- lamp black (collected from soot lamps or burning candles).

Table 3.8 shows typical properties of several different types of CB. It can be noted from Table 3.8 that the particle size of all CB is orders of magnitude smaller than ground limestone. As the mean particle diameter increases, the surface area decreases. Typical performance characteristics of CB are given in Figure 3.3. As indicated in Figure 3.3, as the particle size becomes smaller, dispersibility becomes more difficult and electrical conductivity becomes higher. Also, as higher structure CB is used, dispersibility becomes easier, loading capacity becomes lower, and oil absorption and viscosity become higher.

The CB used in this research was purchased from CABOT Industry, Boston, Massachusetts (CABOT, 1994). The trade mark is REGAL 300R. The analytical specifications of this CB are given in Table 3.9. As can be seen Table 3.9, densities are

12.5 ± 3 lb/ft^3, ash content is a maximum of 1.0 percent, iodine index is 76 ± 5 mg/g, Dibutyl Phthalate absorption is 85 ± 5 cc/100g, and tint strength is $113 \pm 5\%$ ITRB.

Table 3.8 Summary of Typical Properties of Carbon Black (Rostler et al., 1977)

Symbol	Type	Mean Particle Diameter, mm	Surface Area m^2/g	DPB Adsorption cc/100g
SAF	Super Abrasion Furnace Black	19	145	115
HAF-HS	High Structure, High Abrasion Furnace Black	26	90	125
HAF	High Abrasion Furnace Black	29	80	103
FEF	Fast Extruding Furnace Black	42	40	120
SRF	Semi-Reinforcing Furnace Black	60	25	75
MT	Medium Thermal Black	500	7	33
MT	Kaolin Clay	100-5000	5 - 10	25
MT	Ground Limestone	35000	3.1	N/A

Note : 1. Mean particle size : Estimate of average "particle" or nodule size from electron micrographs.
2. Surface area : Measured by nitrogen adsorption, BET Method
3. DPB absorption : Measured of void volume of bulk carbon black using dibutyphthalate as absorpbate.

Table 3.9 Analytical Specifications for REGAL 300R Carbon Black
(CABOT Industries, 1994)

Property	Test Method	Specification
Density (lbs/ft^3)	ASTM D1513	12.5 ± 3.0
Ash (%)	ASTM D1506	1.0 max
Iodine Index (mg/g)	ASTM D1510	76 ± 5
Tint Strength (%ITRB)	ASTM D3265	113 ± 3.0
Dibutyl Phthalate Aborption (cc/100g)	ASTM D2414	85 ± 5
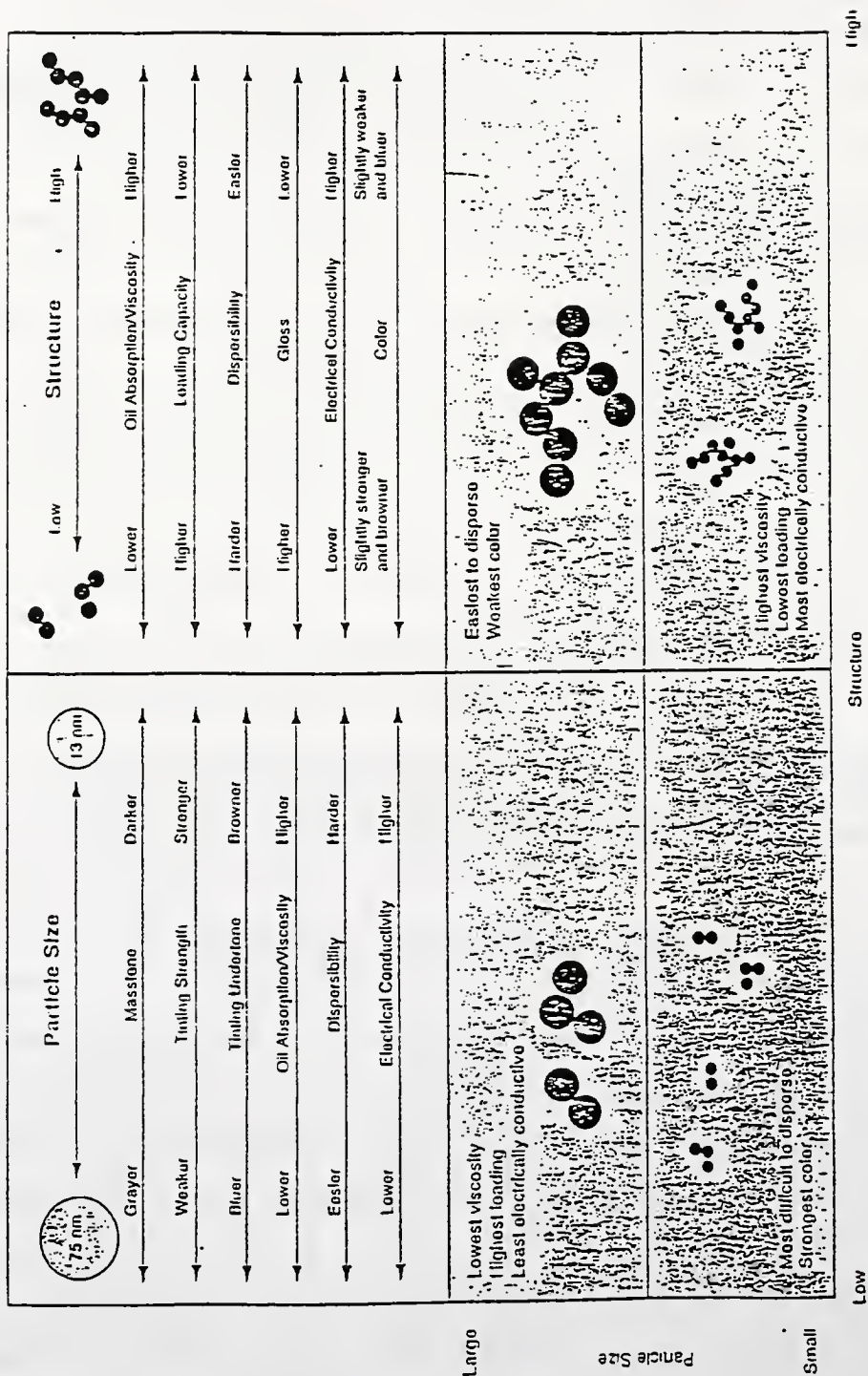
Figure 3.3 Typical Performance Characteristics of Carbon Black (CABOT, 1994)

CHAPTER 4

FUNDAMENTAL CHARACTERISTICS OF ASPHALT BINDER

4.1 Introduction

This chapter mainly provides a brief summary of asphalt binder study conducted by Zeng and Lovell (1995) and the results of bending beam rheometer tests. The properties of pure AC-10 grade asphalt and pure AC-20 grade asphalt are shown in Chapter 3. Modified asphalt binders are produced to alter and improve the properties of the asphalt to enhance the long term performance of pavements. While the modifier may affect many properties, the majority of modifiers attempt to reduce temperature dependency, oxidative hardening and the moisture susceptibility of asphalt mixtures. Therefore, the properties of asphalt modified by carbon black (CB) and pyrolyzed carbon black (CB_p) are introduced in this chapter.

4.2 Properties of Binder with CB and CB_p

4.2.1 Penetration Test

Penetration testing for bituminous materials has been used to measure the consistency of asphalt materials, expressed as the distance in tenths of a millimeter that a standard needle vertically penetrates a sample of the materials under known condition of loading, time and temperature (Zeng and Lovell, 1995).

At a testing temperature of 77°F, the penetration of AC-10 and AC-20 modified with commercial CB decreases steadily from 101 to 68 and 65 to 49, respectively, when the proportion of CB added increases from 0% to 20%. At 59°F, the penetrations decrease from 40 to 27 and 27 to 19.5, respectively, with the increase of CB added.

According to the results by King et al. (1993), the penetration increases at 4°C with additional polymer, up to some low and intermediate level of polymer.

In case of AC-10 and AC-20 modified with CB_p, the trends are essentially the same as those for CB on asphalt cements, i.e., the penetration at either temperature decreases steadily when the percentage of CB_p added increases. The most significant difference is that the difference of penetration between the top and bottom of the samples increases. Table 4.1 shows the effect of the inclusion of CB and CB_p on penetration value.

Table 4.1 Percent of Penetration Value Change due to the Inclusion of 15% of CB and CB_p (Zeng and Lovell, 1995)

Binder	AC 10		AC 20	
Temperature (°F)	59	77	59	77
CB	- 12 %	- 31 %	- 18 %	- 15%
CB_p	- 25 %	- 22 %	- 27 %	- 19 %

4.2.2 Softening Point

Softening point is measured by ring and ball (R&B) method in accordance with ASTM D36 -93. It is defined as the temperature at which an asphalt cement can not support the weight of a steel ball and starts flowing. Table 4.2 shows the test results for softening point. The inclusion of CB and CB_p causes an increase of softening point for AC-10 and AC-20 grade asphalt. Softening point for AC-10 with CB is larger than for AC-20 with CB_p.

Table 4.2 Summary for Softening Point (Zeng and Lovell, 1995)

Asphalt	Additive	0 %	5 %	10 %	15 %	20 %
AC-10	CB	123	126	128	132	137
AC-10	CB_p	123	124	126	128	131
AC-20	CB	126	126	130	133	136
AC-20	CB_p	126	126	127	130	132

4.2.3 Temperature Susceptibility

Temperature susceptibility is the rate at which the consistency of an asphalt cement changes with a change in temperature, and is a very important property of asphalt cement. There are currently three different approaches for determining temperature susceptibility, such as penetration index, penetration-viscosity number and viscosity-temperature susceptibility. Among them, penetration index was employed to calculate temperature susceptibility (Zeng and Lovell, 1995). Penetration index (PI) is defined as;

$$PI = \frac{20 - 500A}{1 + 50A}$$

$$A = \frac{\log P_1 - \log P_2}{T_1 - T_2}$$

where, P_1 and P_2 : penetration at T_1 and T_2

T_1 and T_2 : Temperature

PI for AC-10 with CB tends to increase slightly from 0.0 to about 1.8 and then drops to 1.2. For AC-20 with CB, PI increases from 0.38 to about 1.4 and drops to 0.0. PI for AC-10 with CB_p is approximately a straight line with a slight increase and for AC-20 with CB_p indicates a decrease of penetration index.

The lower the PI value of asphalt cement, the higher its temperature susceptibility. Most paving asphalt cements have a PI between + 1 and -1. Asphalt cements with a PI below -2 are highly temperature susceptible, and usually exhibit brittleness at low temperatures, and are very prone to transverse cracking in cold climates.

4.3 Bending Beam Rheometer

4.3.1 Test Equipment

The bending beam rheometer (BBR) is a simple specification tool that measures asphalt stiffness at low temperatures under controlled loading conditions (Bahia et al.,

1992). The bending beam rheometer system consists of the rheometer unit, a temperature controlled bath, and a data acquisition system using a personal computer. The BBR base unit, shown in Figure 4.1, is constructed entirely of stainless steel with a brushed finish cover, and adjustable feet for leveling the unit. The base houses the cooling fluid bath, a set of precision air regulators, a power switch, regulator control switch, and the signal conditioning electronics. The tank is constructed of stainless steel and has a two gallon capacity. The cooling fluid inlet and outlet plumbing is mounted at the rear of the unit (ATS, 1993). Load frame shown in Figure 4.2 is an independent three-point loading device that is designed to apply a load of up to 200 grams. The load frame may be operated in the supplied fluid bath or it may be used in ambient conditions.
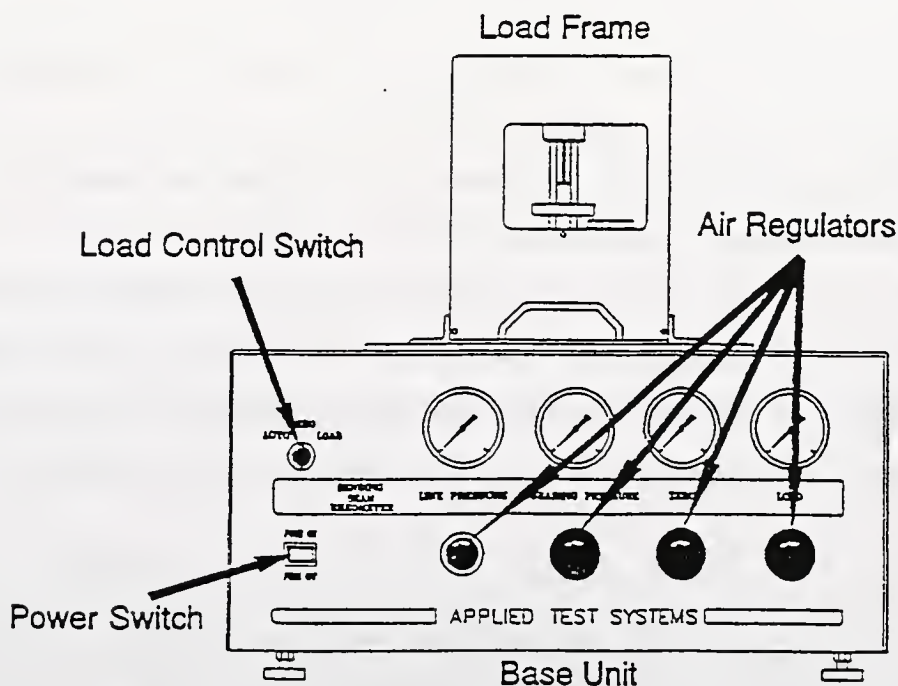
Figure 4.1 Bending Beam Rheometer Base for Front (ATS, 1993)
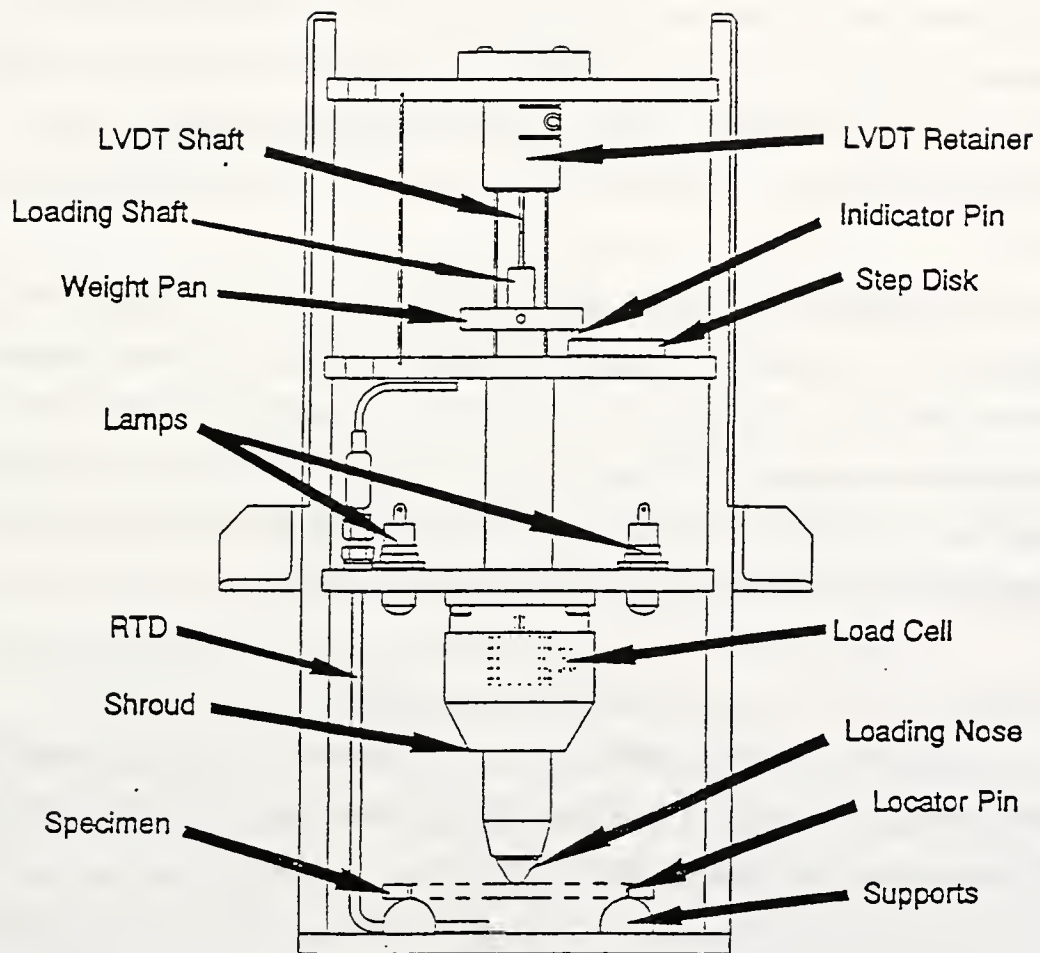
Figure 4.2 Bending Beam Rheometer Load Frame (ATS, 1993)

4.3.2 Specimen and Testing Program

In order to prepare the beam specimen, aluminum bars are assembled to create a mold. To isolate the beam specimen from the aluminum bars, polyethylene strips 0.1 mm thick were used to cover the inner sides of the mold. The mold set consists of two side bars, a base bar, two end pieces, and three polyethylene sheet strips. The mold is assembled using two O-rings around the end portion. The aluminum bars are covered with the polyethylene strips from the inside, the asphalt is then poured and cooled. During demolding the specimen, the mold is cooled down to the testing temperature, the aluminum sides are taken apart, and the specimen is left with the polyethylene sheets. The sheets, being flexible, can then be peeled off easily from the asphalt cement. The dimension of specimen is 127 mm long, 12.7 mm wide and 6.35 mm thick (Bahia et al., 1992).

The laboratory experiment was designed to test two different asphalt grades, AC-10 and AC-20, with 0 %, 10 %, and 20 % of CB or CB_p. The testing temperatures selected were 5°C, 0°C, -5°C, -10°C, and -15°C. A standardized loading time, 240 seconds, was employed. This loading time was selected as a compromise between shortening the testing time and having a time long enough to successfully perform the time-temperature superposition procedure (Bahia et al., 1992).

4.3.3 Theory of Analysis

Using the elementary bending theory the deflection for a prismatic beam, for an elastic material, in a three-point loading mode, is a maximum at the center of the span and can be determined using the following formula;

$$\delta = \frac{PL^3}{48EI}$$

where, δ = deflection of beam at midspan (mm)

P = load applied (N)

L = span length (mm)

E = elastic modulus (Pa)

$$I = \text{moment of inertia of section (mm}^4)$$

According to the elastic-viscoelastic correspondence principle, it can be assumed that if the viscoelastic beam is subjected to loads which are all applied simultaneously at time = 0 and held constant, the stress distribution is the same as that in an elastic beam under the same load. Its strains and displacements depend on time and are derived from those of the elastic problem by replacing E with 1/D(t), which is equivalent to S(t).

$$S(t) = \frac{PL^3}{4bh^3\delta(t)}$$

where, S(t) : time dependent flexural creep stiffness.

4.3.4 Test Results

Figure 4.3 shows a typical BBR test result, for AC-10 with 20% CB_p. The other results are shown in Appendix A. The reason for plotting the stiffness, calculated from the load and deflection, versus loading time on a log-log plot is to apply the time-temperature superposition principle (Bahia et al., 1992). The flexural creep stiffness at -5°C, -10°C, and -15°C shows a linear relationship as loading time increases. The result at 0°C particularly, shows a failure of the beam specimen, when the slope between stiffness and time is constant, then slightly increases, and then shows a large decrease.

The time at which the beam specimens failed on loading is shown in Table 4.3. All the cases except AC-20 with 10% of CB and CB_p show that the time to reach a failure increases about two times. This implies that the inclusion of CB and CB_p makes the flexural creep stiffness of the beam specimen increase, and can be used as a reinforcing additive in asphalt. Figure 4.4 shows how to use shift factors as follows;

- Select a reference temperature, for example -15°C.
- Shift the curve belonging to different temperatures with respect to the curve of -15°C.
- Determine the shift factor.
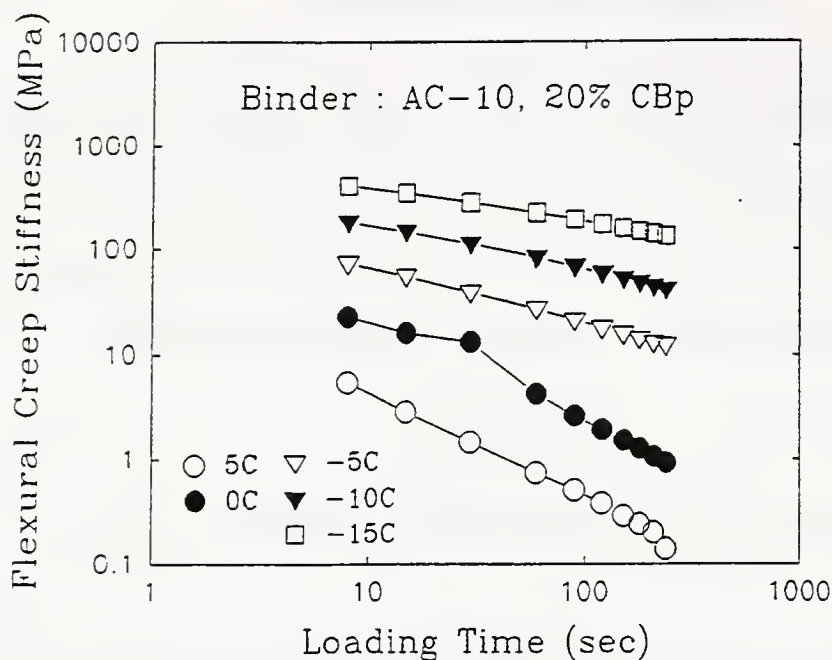
Figure 4.3 The Flexural Creep Stiffness for AC-10 with 20% CB$_p$

Table 4.3 Time (sec) to Reach at Failure at 0°C

Asphalt	Pure	10% CB	20% CB	10% CB$_p$	20% CB$_p$
AC-10	15	30	60	30	30
AC-20	60	60	120	60	120

The determined shift factors for each test are shown in Figure 4.5. In this research, only results at -5°C, -10°C, and -15°C were used to determine the shift factor, because the beam specimen failed at relatively high temperatures (0°C and 5°C). The shift function shown follows a simple linear relationship with temperature with the range of testing temperatures. This results indicate that asphalt are fairly similar in their temperature dependency at low temperatures.
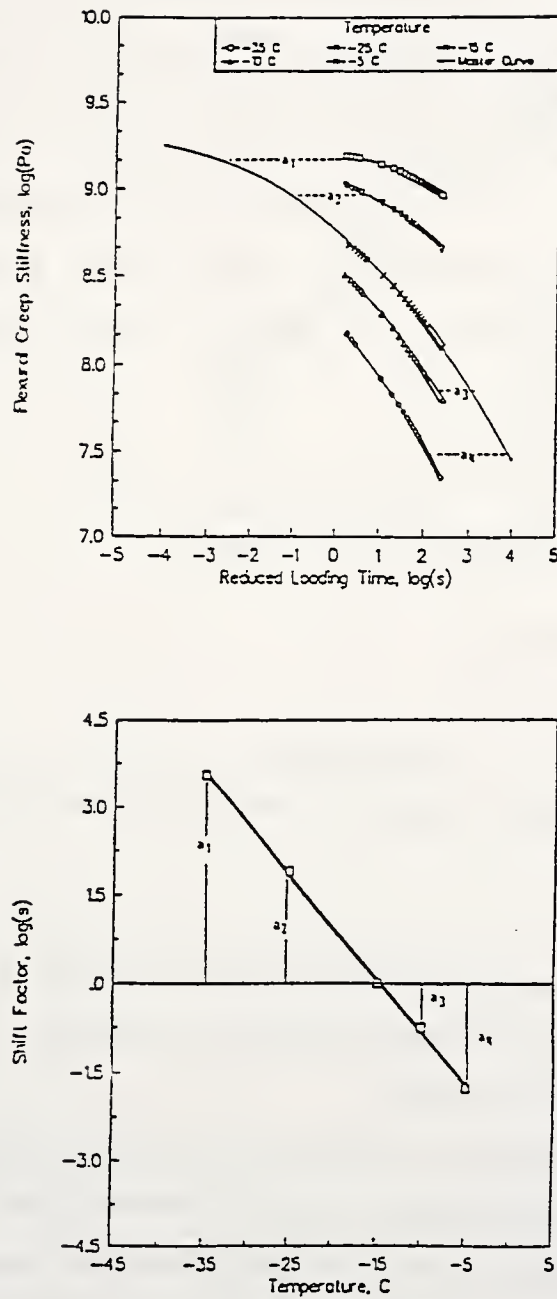
Figure 4.4 The Example to Determine the Shift Factor (Bahia et al., 1992)
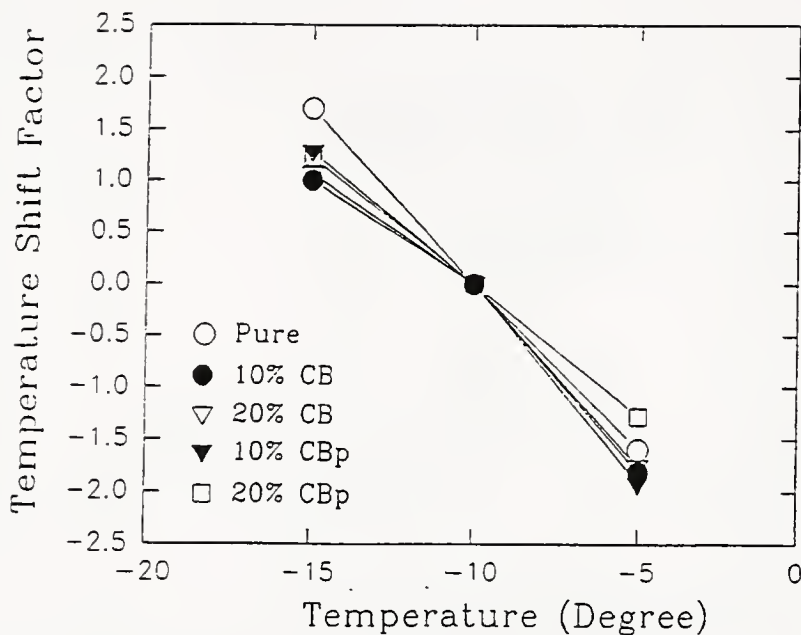
Figure 4.5 Summary for Shift Fctors

4.4 Conclusion

Within the limited laboratory testing in this study, the following principal conclusion can be drawn:

- The measured creep stiffness of AC-20 binder is higher than that of AC-10 bender at same testing temperature and loading time, because the viscosity of AC-20 asphalt is much higher than that of AC-10 asphalt.

- The inclusion of CB and CB_p for both asphalt, AC-10 and AC-20, makes an increase of creep stiffness at each testing temperature and increases the time to reach a failure (larger bending). This implies that the inclusion of CB and CB_p makes the flexural creep stiffness of the beam specimen increase, and the CB and CB_p can be used as a reinforcing additive in asphalt.

- The flexural creep stiffness at lower temperature (less than 0°C) show a linear relationship as the loading time increases. The change of the flexural creep stiffness become smaller as the testing temperature decreases.

- According to the recommendation by King et al. (1993), the asphalt stiffness should be less than 200 MPa at loading of 60 seconds to avoid a low temperature cracking. In this study, the temperature to meet King's recommendation is around -13°C for AC-10 binder and -10°C for AC-20 binder.

- The bending beam rheometer is a good testing tool to characterize the linear viscoelastic properties of asphalt as influenced by time of loading and testing temperatures.

CHAPTER 5

MARSHALL MIX DESIGN

5.1 Introduction

For many decades, two methods of asphalt paving mix design, the Marshall method and the Hveem method, have been used. According to a survey in 1984, approximately 75% of the state highway departments used methods related to the Marshall method (Kandhal and Koehler, 1985). The remaining 25 percent used methods related to the Hveem method. Figure 5.1 shows the results of the 1984 survey.
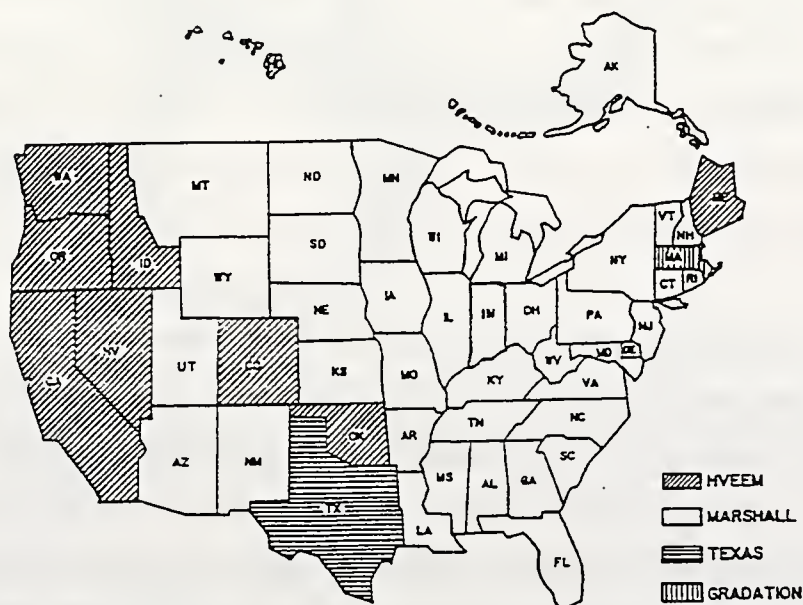
Figure 5.1 HMA Mixture Design Methods Used by States in the USA
(Kandhal and Koehler, 1985)

The Marshall method of designing paving mixtures was developed by Bituminous Engineer Bruce Marshall at the Mississippi Highway Department (Roberts et al., 1991). The earliest Marshall method was improved by the US Corps of Engineers through extensive research and experimental work. The Marshall test procedure has been standardized by the American Society for Testing and Materials (ASTM). The ASTM Standard D 1559, *Resistance to Plastic Flow of Bituminous Mixture Using Marshall Apparatus*, descrives the standard testing procedures (ASTM *Road*, 1993).

There are two major advantages for Marshall method. One is to show density and voids properties of asphalt materials. This analysis ensures that the important proportions of mix constituents are at their proper levels to achieve a durable HMA. Another advantage is that the required equipment is relatively inexpensive and highly portable (McGennis et al., 1995). On the other hand, the method has two major disadvantages. One is that this method does not simulate the mixture densification that occurs under traffic in a real pavement. Another is that Marshall stability as a strength parameter does not properly estimate the shear strength of HMA. The Marshall method also includes potential error sources, such as producing batch, temperature control, compacting efforts, non-uniformity of the aggregate, the degree of blending of aggregate and binders, the testing skills, and so forth. Although the Marshall test has its shortcomings, many state highway agencies have used this method due to its simplicity and economy.

5.2 The Fundamental Characteristics of Bituminous Mixtures

It is important to understand weight-volume relationships of compacted HMA. Mix design is recognized as a volumetric process to determine the volume of asphalt cement and aggregates which are required to make a mixture with the desired properties. In fact, it is very difficult to deal with the volume of aggregates and asphalt cement in the field. Due to this reason, mass is used instead of volume, and the specific gravity is used to change from weight to volume.

Figure 5.2 illustrates VMA, air voids, and effective asphalt content in compacted asphalt paving. Also, Figure 5.3 shows the representation of volumes in a compacted asphalt specimen.
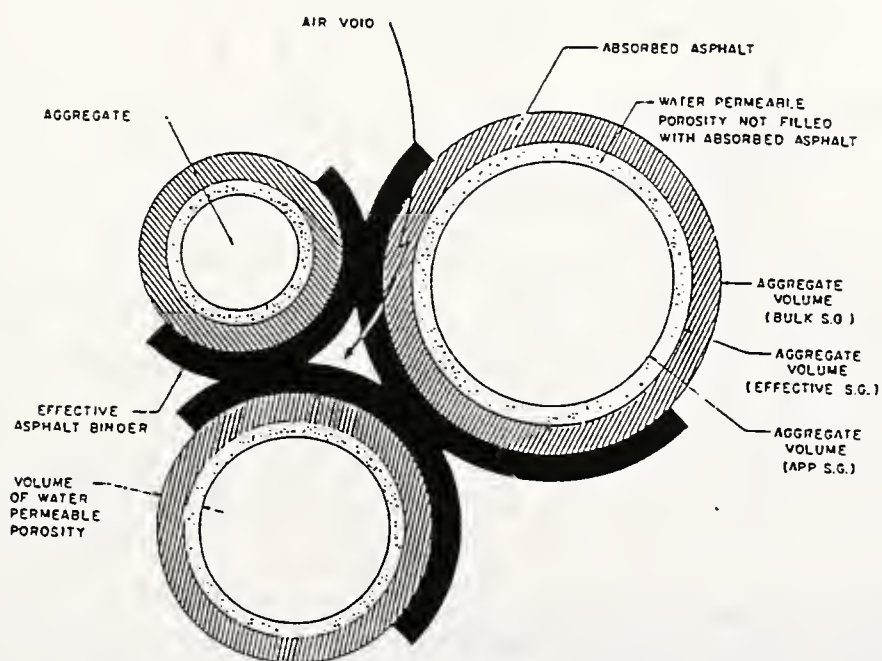
Figure 5.2 Illustration VMA, Air-Void and Effective Asphalt Content in Compacted Asphalt Paving Mixture (Aspahlt Institue, 1988)
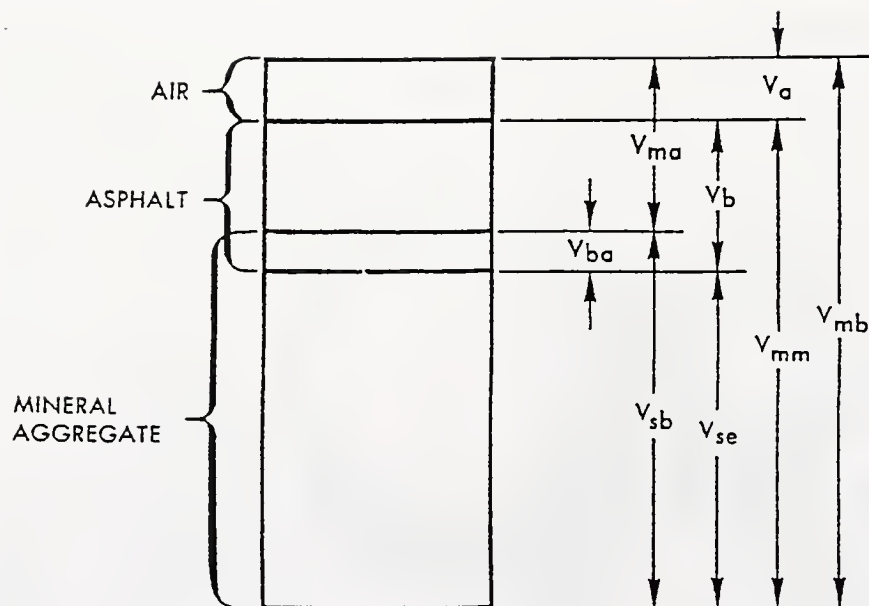
V_{ma} = Volume of voids in mineral aggregate
V_{mb} = Bulk volume of compacted mix
V_{mm} = Voidless volume of paving mix
V_a = Volume of air voids
V_b = Volume of asphalt
V_{ba} = Volume of absorbed asphalt
V_{sb} = Volume of mineral aggregate (by bulk specific gravity)
V_{se} = Volume of mineral aggregate (by effective specific gravity)

Figure 5.3 Representation of Volumes in a Compacted Asphalt Specimen
(Asphalt Institute, 1988)

5.2.1. Conventional Volumetric Design

In general, asphalt concrete mix design has a multi-step iterative process as follows;

step 1 : Aggregate stockpile fractions like coarse and fine are selected. The specific gravity and absorption of each fraction are determined by following ASTM C127 for coarse aggregate and ASTM C128 for fine aggregate. The blended aggregate bulk specific gravity, G_{sb}, is determined using equation 5.1.

$$G_{sb} = \frac{\sum_{i=1}^{i=k} P_i}{\sum_{i=1}^{i=k} \frac{P_i}{g_{sbi}}} \qquad (5.1)$$

where P_i : individual stockpile fraction ($\sum P_i = 100\%$)

g_{sbi} : individual stockpile bulk specific gravity

step 2 : The heated blended aggregate is mixed with proper amounts of asphalt binder, P_b, and placed in an oven to have enough absorption. The mixed samples are compacted using Marshall hammer, Gyratory machine, and so on.

step 3 : Check the bulk specific gravity of the sample mixtures, G_{mb}, in accordance with ASTM D2726.

$$G_{mb} = \frac{A}{C - B} \qquad (5.2)$$

where A : dry weigh in air

B : submerged weight in water

C : saturated-and-surface dry weight in air

step 4 : check the mix strength (Marshall stability) and plastic flow (permanent deformation).

step 5 : check the maximum theoretical specific gravity, G_{mm}, in accordance with ASTM D2041.

For each asphalt content, air void (VTM), voids in mineral aggregate (VMA), and void filled with asphalt cement (VFA) are determined as follows:

$$VTM = 100 * \left(1 - \frac{G_{mb}}{G_{mm}}\right)$$

$$VMA = 100 * \left[1 - \frac{G_{mb} * (1 - P_b)}{G_{sb}}\right] \qquad (5.3)$$

$$VFA = 100 * \frac{VMA - VTM}{VMA}$$

In order to perform a volumetric analysis, three different bulk specific gravities must be determined ;

G_{sb} : The bulk specific gravity of the blended aggregate

G_{mb} : The bulk specific gravity of the mixture, and

G_{mm} : The maximum theoretical specific gravity of the mixture.

Among them, G_{mb} and G_{mm} are determined directly on samples of the asphalt-aggregate mixture, while G_{sb} is determined indirectly from the each fractions of the blended aggregate using water as the immersant medium. There are some potential error sources in determining G_{sb}. : (i) any error made in the determination of G_{sb} of any fraction is carried through to the final determination of G_{sb}, (ii) the determination of the saturated-and-surface-dry condition is very subjective, and becomes difficult as the macrotexture and absorption of the aggregate increases, and (iii) the use of water instead of asphalt has an effect on the resulting specific gravity.

5.2.2 A Self-Consistent Volumetric Asphalt Design (Coree, 1995)

In order to overcome some potential error sources of conventional volumetric method, the following procedures are recommended by Coree (1995).

Step 1 : Select the aggregate components based upon their physical and mechanical characteristics. Blend them to meet a target gradation. It necessary, the specific gravity of the asphalt binder, G_b, may be determined at this stage.

Step 2 to **step 4** is the same as before.

Step 5 : Defending on the maximum aggregate size used in the mixtures tested, the samples at each asphalt content are softened, combined, and mixed into the following samples for theoratical maximum specific gravity test (ASTM D2041) :

Max. Agg. Size	Combined Sample Size	Number
≥ 12.5mm (1/2")	1800gm	2
≤ 9.5mm (3/8")	1200gm	3

Perform the maximum theoretical specific gravity test on all the samples produced above, thereby providing estimates of G_{mm} at each nominal asphalt content.

Figure 5.4 shows a summary of his conclusion. By considering the information provided at any asphalt content, the following conclusions may be drawn :

A. The volume represented between the $100/G_{mb}$ and $100/G_{mm}$ lines shows the air void volume of the sample.

B. The volume represented between the $100/G_{mm}$ and $100/G_{sc}$ lines shows the total volume of asphalt.

C. The volume represented between the $100/G_{mm}$ and $100/G_{sb}$ lines shows the volume of free asphalt.

D. The volume represented between the $100/G_{sb}$ and the $100/G_{sc}$ lines shows the volume of absorbed asphalt.

With these simple conclusions, the volumetric parameters may be obtained ;

$$VMA = 100 * \frac{\frac{100}{G_{mb}} - \frac{100}{G_{mm}}}{\frac{100}{G_{mm}}} = 100 * \left(1 - \frac{G_{mb}}{G_{mm}}\right)$$

$$(5.4)$$

$$VMA = 100 * \frac{\frac{100}{G_{mb}} - \frac{100}{G_{sb}}}{\frac{100}{G_{mb}}} = 100 * \left(1 - \frac{G_{mb}}{G_{sb}}\right)$$
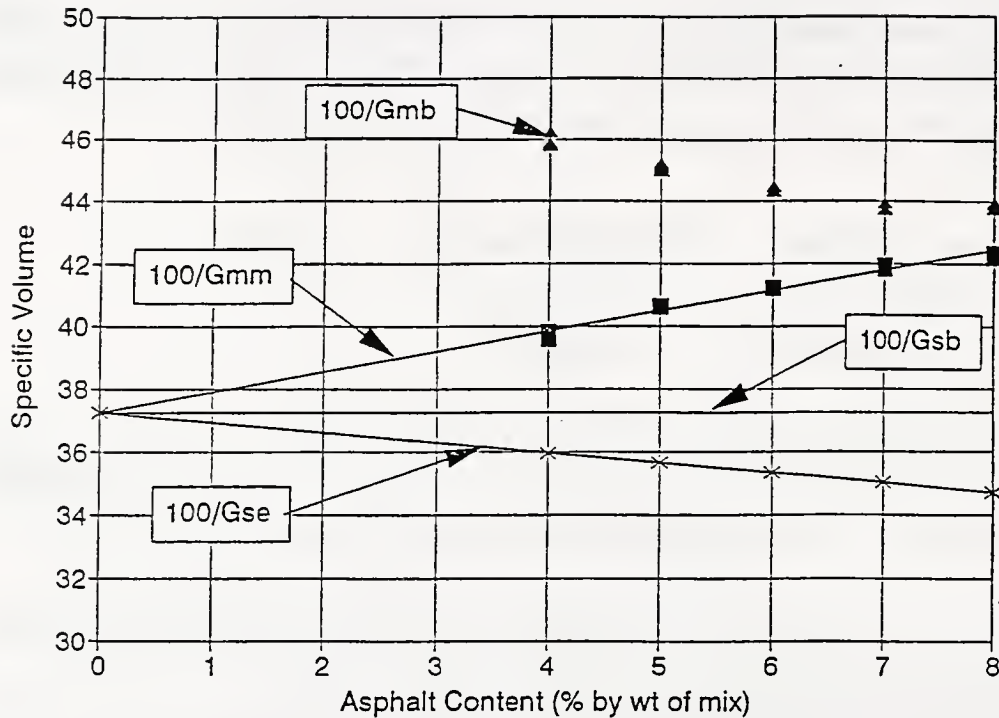
Figure 5.4 Conclusion for a Self-Consistent Volumetric Asphalt Design (Coree, 1995)

5.3 Test Procedures

5.3.1 Mix Preparation

The prepared asphalt cement in 5 quart cans was heated between 145°C and 150°C (290°F and 300°F) for an hour. The heating temperature is similar to that of a mixing plant. The Hobart mechanical mixer was used at the low speed setting. Enough mixing time was given to get a well-coated mixture.

The mass of 1200 grams of the blended aggregate for one batch was stored in a plastic bag. The aggregate in the plastic bag was transferred to the stainless bowl and heated more than 3 hours in the oven in order to remove the moisture in the aggregate. Three samples were prepared for each asphalt content with additives (CB and CB_p). About 4-5g of moisture was evaporated during heating. Therefore, the total dried weight of the blended aggregate is almost 1196.0 ± 1.0g. After mixing with asphalt and

aggregate, the mixtures were put into the oven for about 3 hours to permit absorption of asphalt cement. The compacting effort of 75 blows per side was used to simulate heavy traffic load. The other procedures followed were ASTM D1557-93 and Asphalt Institute (1988). After compacting the mixtures, the samples were cooled at room temperature for more than 12 hours, and then the cooled sample were pulled from the mold.

5.3.2 Bulk Specific Gravity of the Mixture

The height of mixtures extruded from the mold were measured. The bulk specific gravity of the mixtures were determined in accordance with ASTM D2726.

5.3.3 Marshall Stability and Flow

This test was conducted following ASTM D1559. A brief summary is shown below. The specimens were put into the water bath at 140°F for at least 30 min, removed from the water bath, and quickly placed in the Marshall testing head. The load was applied at 2 inch/minute until the maximum load was reached. When the load just began to decrease, test was stopped. Figure 5.5 shows a typical result of the Marshall test (McGennis et al., 1995). From the Figure Marshall stability is defined as the maximum load and the flow was recorded by the distance from origin at maximum load to the point at which load started to decrease. The initial stability should be corrected for specimen height using factors in Table 5.1, ASTM D1559-93.

5.3.4 Theoretical Maximum Specific Gravity of the Mixture

Standard procedure for theoretical maximum specific gravity (TMSG) is shown in ASTM D 2041. The theoretical maximum specific gravity can be calculated as follows;

$$TMSG = \frac{A}{E - D} \tag{5.5}$$

where A :   mass of oven dry sample in air (g)

D : mass of container filled with water at 25°C (77°F)

E : mass of container filled with sample and water at 25°C

5.4 Marshall Criteria for the Optimum Binder Content

Although the Marshall test method of asphalt paving mixture is standardized by ASTM D1559, the criterion for the optimum asphalt content is not standardized. Therefore, many different criteria are in use. In our project, the INDOT criterion (1993) was used to determine the optimum binder content, as shown in Table 5.1. Also, the US Army criteria (1987) shown in Table 5.2 and the Asphalt Institute criteria in Table 5.3 were used for the purpose of comparison.
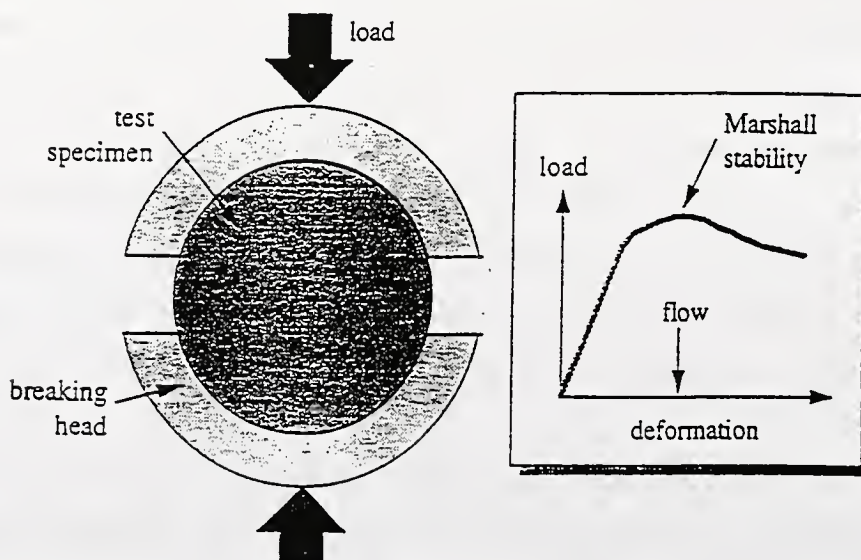
Figure 5.5 The Typical Result for the Marshall Stability and Flow (McGennis et al., 1995)

Table 5.1 INDOT Marshall Specifications (INDOT, 1993)

Mix Criteria	Min.	Max.
Compaction(No. of blows each side of specimen)	75	75
Stability (N)	5340	-
Flow (*0.01in)	6	16
Percent of Air Voids	4.0	8.0
Percent Voids in Mineral Aggregate(VMA) 3/8"(9.5mm) of Nominal Maximum Particle Size	16	-
• 1/2"(12.5mm) of Nominal Maximum Particle Size	15	-
• 3/4"(19.0mm) of Nominal Maximum Particle Size	14	-
• 1.0"(25.0mm) of Nominal Maximum Particle Size	13	-
Base 5D Mixtures	12	-

Note 1) The nominal maximum particle size is the largest sieve upon which any material will be permitted to be retained.
2) The percent air voids for base 5D mixture shall be 3.0 to 5.0.
3) The optimum bitumen content shall be the bitumen content that procedure 6.0% air voids for all mixtures except base 5D[401.04(b)].

Table 5.2 Marshall Criteria by U.S Army (U.S. Army TM 5-822-8, 1987)

Test Property	Type of Mix	Criteria for 100 psi tires
Stability(N)	All*	Min. 6680
Flow(*0.01in)	All*	Max. 20
Air Voids(%)	Asphalt Concrete	3 - 5
	Sand Asphalt	5 - 7
	Binders	4 - 6
VMA(%)	Asphalt Concrete	75 - 85
	Sand Asphalt	65 - 75
	Binder	65 - 75

* Asphalt concrete, sand asphalt, and binders
Note : The criteria shown above for 100psi tires are often used in the design of highway pavements, but they are subject to modification where subtstantial experience indicates the need for such a change.

Table 5.3 Marshall Mix Design Criteria for Asphalt Institute (1988)

	Light Traffic Surface & Base		Medium Traffic Surface & Base		Heavy Traffic Surface & Base	
Marshall Method[1]	Min	Max	Min	Max	Min	Max
Number of compaction	35		50		75	
Stability (N)	3336		5338		8006	
Flow (0.25 mm)	8	18	8	16	8	14
VFA	70	80	65	78	65	75
VMA	See	below	Table			

Notes

1. All criteria, not just stability value alone, must be considered in designing an asphalt paving mix. Hot mix asphalt bases that do not meet these criteria when tested at 60°C (140°F) are satisfactory if they meet the criteria when tested at 38°C (100°F) and are placed 100 mm or more below the surface. This recommendation applies only to regions having a range of climatic conditions similar to those prevailing throughout most of the United States. A different lower test temperature may be considered in regions having more extreme climatic conditions.

2. Traffic Conditions
    Light   Traffic conditions resulting in a design EAL $< 10^4$
    Medium   Traffic conditions resulting in a design EAL between 10^4 and 10^6
    Heavy   Traffic conditions resulting in a design EAL $> 10^6$

3. Laboratory compaction efforts should closely approach the maximum density obtained in the pavement under traffic.

4. The flow value refers to the point where the load begins to decrease.

5. the portion of asphalt cement lost by absorption into the aggregate particles must be allowed for when calculating percent air-voids.

6. Percent voids in the mineral aggregate is to be calculated on the basis of the ASTM bulk specific gravity for the aggregate.

Minimum percent voids in mineral aggregate (VMA)

Nominal Maximum Particle Size [1,2]		Minimum VMA (%) Design Air Voids (%)[3]		
mm	in.	3.0	4.0	5.0
1.18	No. 16	21.5	22.5	23.5
2.36	No. 8	19.0	20.0	21.0
4.75	No. 4	16.0	17.0	18.0
9.5	3/8	14.0	15.0	16.0
12.5	1/2	13.0	14.0	15.0
19.0	3/4	12.0	13.0	14.0
25.0	1.0	11.0	12.0	13.0
37.5	1.5	10.0	11.0	12.0
50	2.0	9.5	10.5	11.5
63	2.5	9.0	10.0	11.0

1. Standard specification for Wire Cloth Sieves for Testing Purposes. ASTM E11 (AASHTO M92)
2. The nominal maximum particle size larger than the first sieve to retain more than 10 %

3. Interpolate minimum voids in the mineral aggregate (VMA) for design air void values between those listed.

5.5 Results and Discussion

As previously mentioned, fundamental characteristics of the mixtures would be obtained from Marshall test method. In general, the analysis of test results is performed to get the relationship between binder content and the others as follows :

- Bulk Specific Gravity vs. Binder Content
- Air Voids (VTM) vs. Binder Content
- VMA vs. Binder Content
- VFA vs. Binder Content
- Stability vs. Binder Content
- Flow vs. Binder Content

One of the typical test results is shown in Figure 5.6 and the others are shown in Appendix B.

5.5.1 Unit Weight of the Mixtures

Unit weight vs. CB content

Figures 5.7 (a) and (b) show the relationship between bulk specific gravity of the mixture with AC-10 and AC-20 and CB content. The changes of unit weight of the mixtures are not significant with the increase of CB content. Rostler et al. (1977) reported the size of carbon black and asphalt cement. The size of carbon black is 100 to 150 nanometer and that of asphalt cement is about 5000 nanometer. This means that if the carbon black is dispersed very well in the asphalt cement, it becomes an integral part of the asphalt cement. The main reason to show the fluctuating results for each binder content is to demonstrate that carbon black is not fully and uniformly dispersed.

Unit weight vs. CB_p content

The relationship between the unit weight of the mixtures and CB_p content is shown in Figure 5.7 (c) and (d). The unit weight decreases as the percent of CB_p increases for AC-10 and AC-20. Considering the particle size of CB_p, this can be expected. In general, the particle size of CB_p is not uniform. The maximum size of CB_p
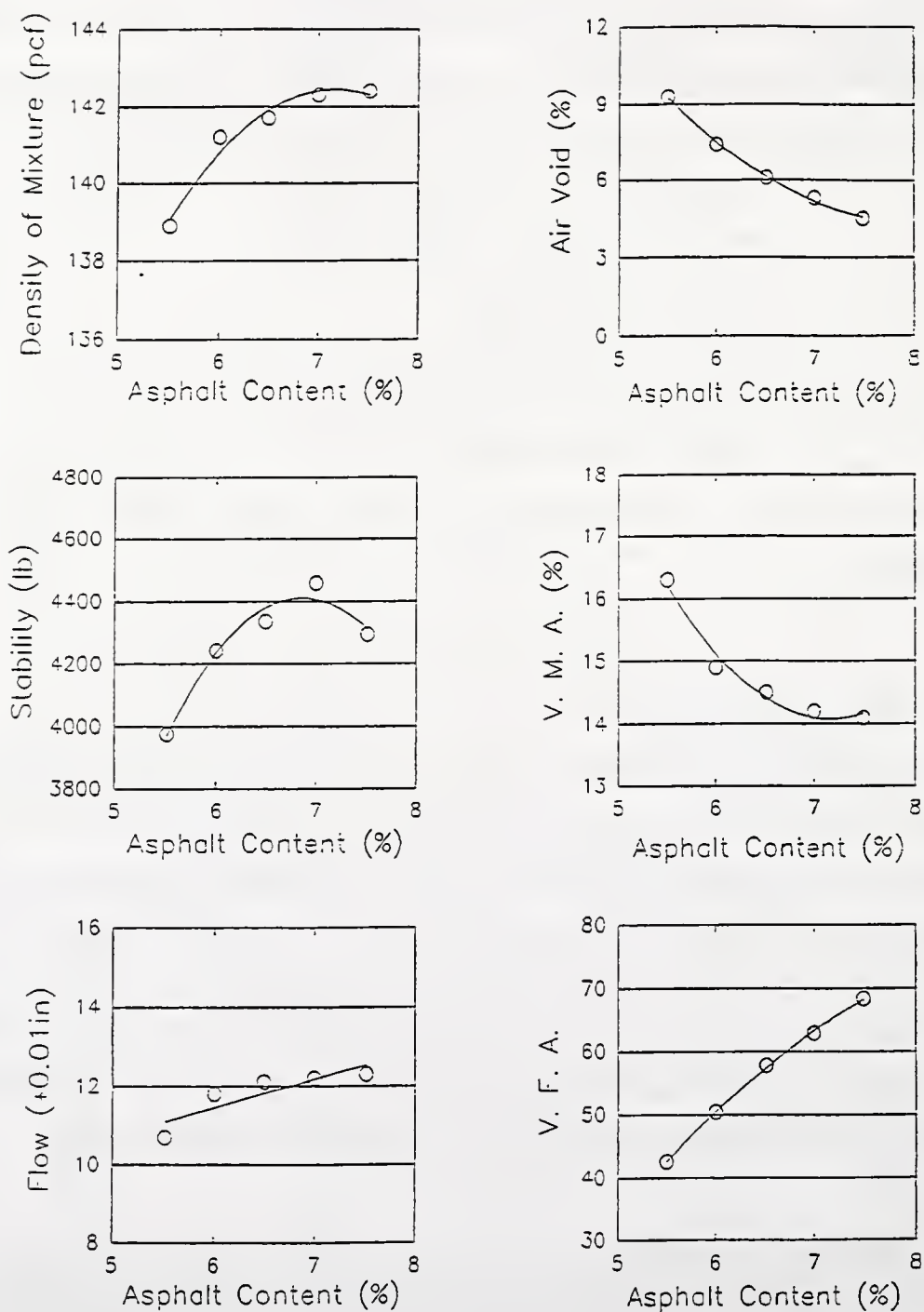
Figure 5.6 Typical Test Result for AC-10 with 10% CB

is about 0.3 mm. Also, the specific gravity of CB_p is heavier than that of asphalt. Due to these reasons, the unit weight of the mixture decreases as the content of CB_p increases. In general, the density of the mixture increases as the asphalt content increases. The main reason is that the hot asphalt cement lubricates the particles to allow the compacting effort to force the aggregate closer together.

Legend :　　○ 5.5% Binder　　▽ 6.5% Binder　　□ 7.5% Binder

　　　　　　　● 6.0% Binder　　▼ 7.0% Binder
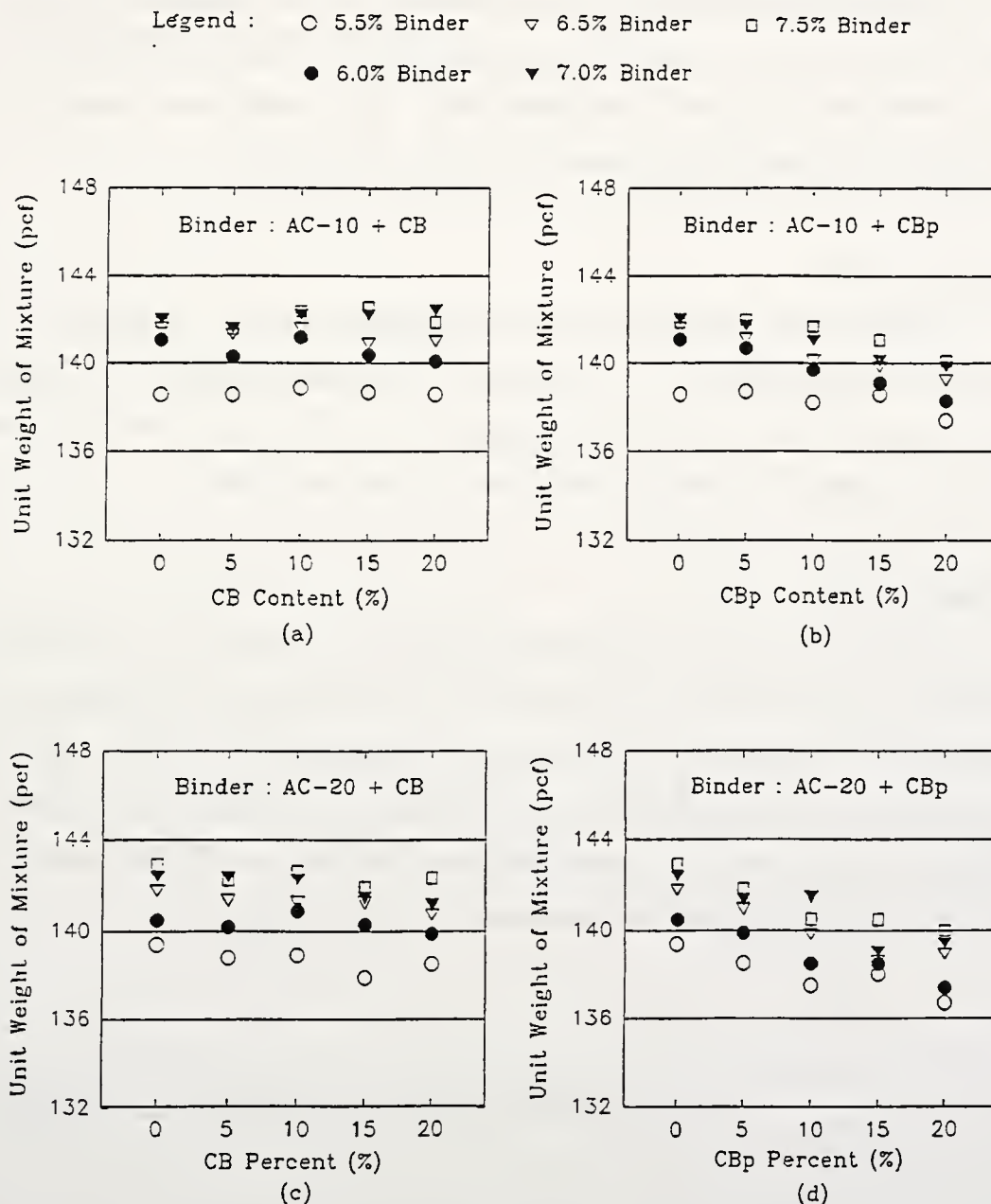
Figure 5.7 The Relationship between the Unit Weight of the Mixtures and Additives

5.5.2 Air Voids

The importance of air voids in the mixture has been discussed by many researchers, because the physical properties and performance of the mixture, such as stability and durability, are affected by air voids. If the air voids are higher than 8 percent, the mixture is susceptible to damage by water and air and the rate of oxidation of the binder is significantly increased and accelerated. On the other hand, the low air voids (less than 3 percent) produces a rutting problem due to large plastic flow (Brown et al., 1989). Many agencies recommended from 3 to 6 percent of air voids for the compacted dense-graded HMA specimen at optimum binder content.

Air Voids vs CB

Figure 5.8 (a) and (b) represent the relationship between air voids and CB content for AC-10 and AC-20. It is noted that air voids increases slightly as the carbon black content increases (for both bitumen grades) and as the binder content decreases. This is also reported by Khedaywi (1988) using oil shale ash in HMA.

Air voids vs CB_p

Figure 5.8 (c) and (d) represent the relationship between air voids and CB_p content for AC-10 and AC-20. The general trend is the same as for CB mixtures. But, the change of air voids in CB_p mixtures is larger than that of CB mixtures. As it was explained before, the main reason is the uniformity of CB_p and CB and the degree of dispersion in asphalt cement. The non-uniformity of particle size of CB_p has an effect on the large change of the air voids of the mixtures.

Legend : ○ 5.5% Binder   ▽ 6.5% Binder   □ 7.5% Binder

● 6.0% Binder   ▼ 7.0% Binder
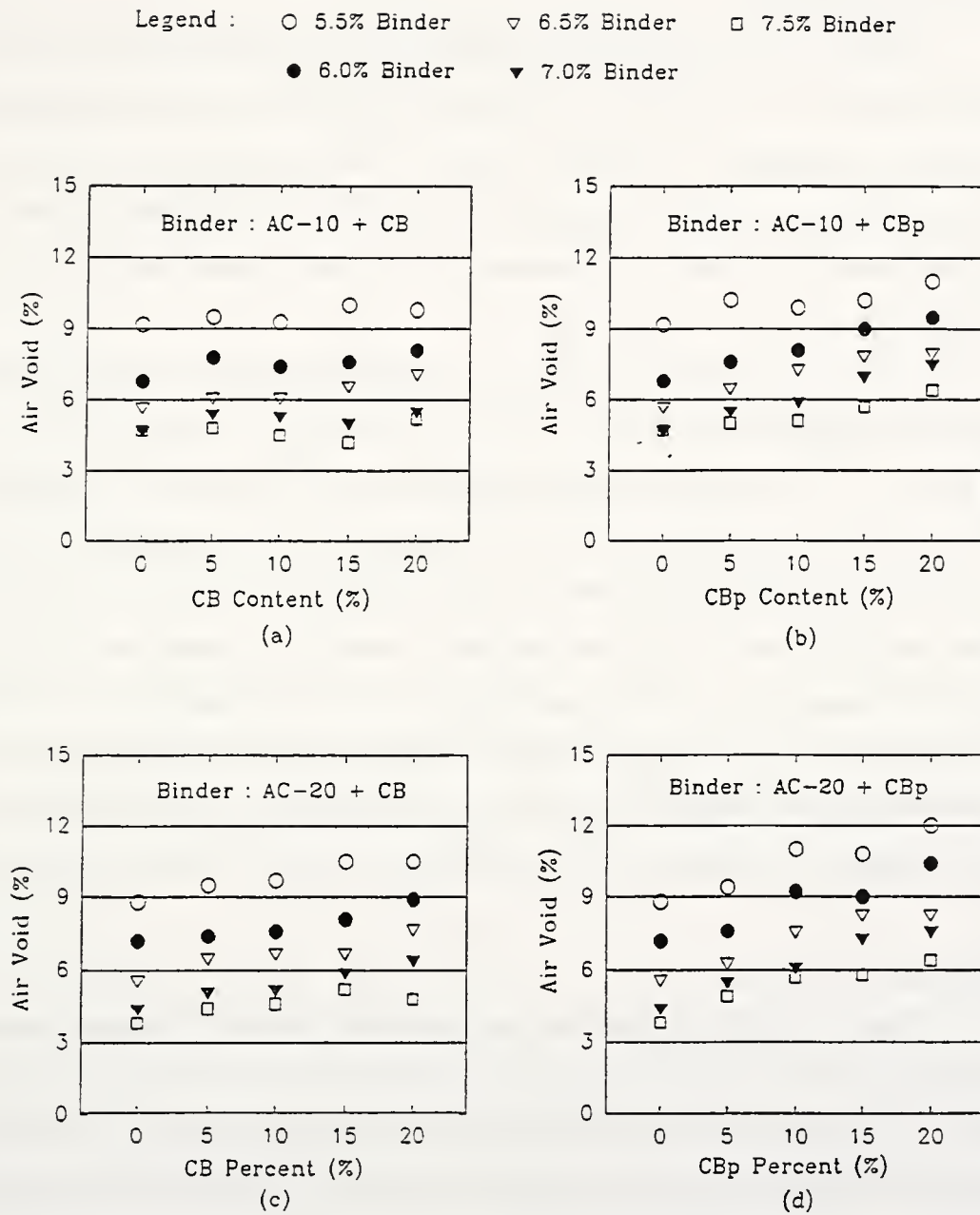
Figure 5.8 The Relationship between Air-Voids and Additives

5.5.3 Void in Mineral Aggregate (VMA)

VMA vs. CB Contents

Figure 5.9 (a) and (b) show the relationship between VMA of the mixture and CB contents for AC-10 and AC-20. In case of AC-20 with CB, VMA increases as the percent of CB increases. The VMA is a function of bulk specific gravity of mixture and bulk specific gravity of blended aggregate, shown in Eq. 5-3. Considering Figure 5.9, the result should be expected. The fluctuation of the results means that CB is not fully and uniformly dispersed into the AC-20.

The results for AC-10 with CB do not show a trend similar to AC-20 with CB. If we neglect the results for 10 % and 20 % of CB, results show a similar trend for AC-20 with CB. VMA increases slightly as the percent of CB increases. As mentioned before, VMA is a direct function of bulk specific gravity of blended aggregates for 10 % and 20 % of CB. If the traditional method using ASTM C-128 and C-129 (ASTM *Road*, 1993) were used in this project, the results would show a similar trend for AC-20 with CB, because only one bulk specific gravity of blended aggregate was used for determination of VMA. However, as shown in Figure 5.10, the bulk specific gravity of blended aggregates changes with CB and CB_p content due to the non-uniformity and non-homogeneity of aggregates, a different surface area, texture, and shape, and so on.

VMA vs. CB_p Contents

Figure 5.9 (c) and (d) show the results for AC-10 with CB_p. The results shows a similar trend for CB except for 5% of CB_p. The result for AC-10 with 5% CB_p shows a hump due to the large bulk specific gravity (2.707) of blended aggregates. The results for AC-20 with CB_p show a trend similar to the others. Except for 5% CB_p mixture, VMA for AC-20 with CB_p is significantly increased with increasing CB_p content. The result for 5% CB_p shows a low value of VMA due to the low bulk specific gravity of blended aggregates.

Legend : ○ 5.5% Binder   ▽ 6.5% Binder   □ 7.5% Binder

● 6.0% Binder   ▼ 7.0% Binder
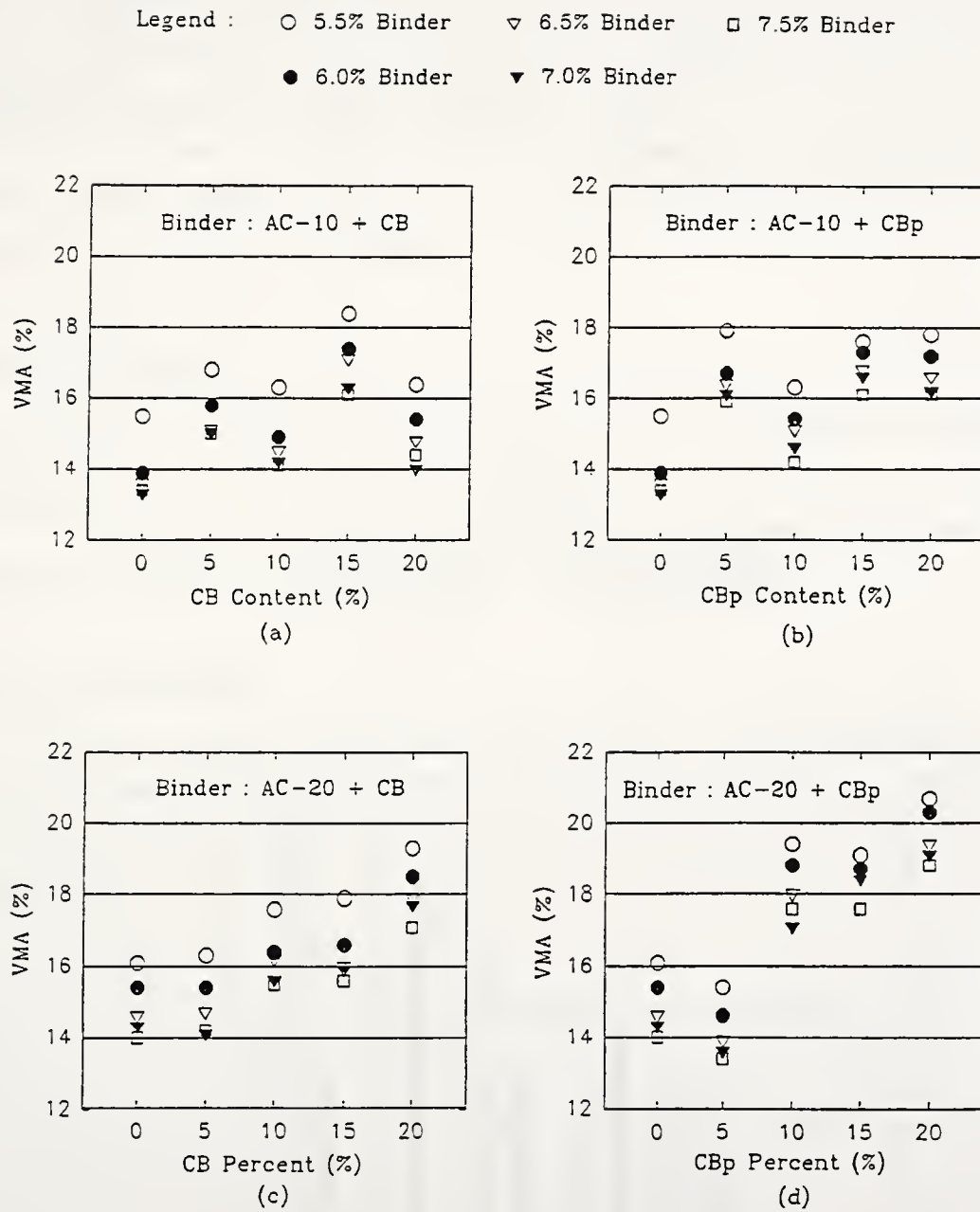
Figure 5.9 The Relationship between VMA and Additives

VMA is one of important parameters for HMA. VMA is defined as the total volume of voids within the compacted aggregate. The mixture performance is affected by VMA, durability problem due to low VMA, stability problem due to high VMA, and so on. From Figure 5-3, VMA consists of two major component, the volume of voids filled with asphalt and the air-void volume.
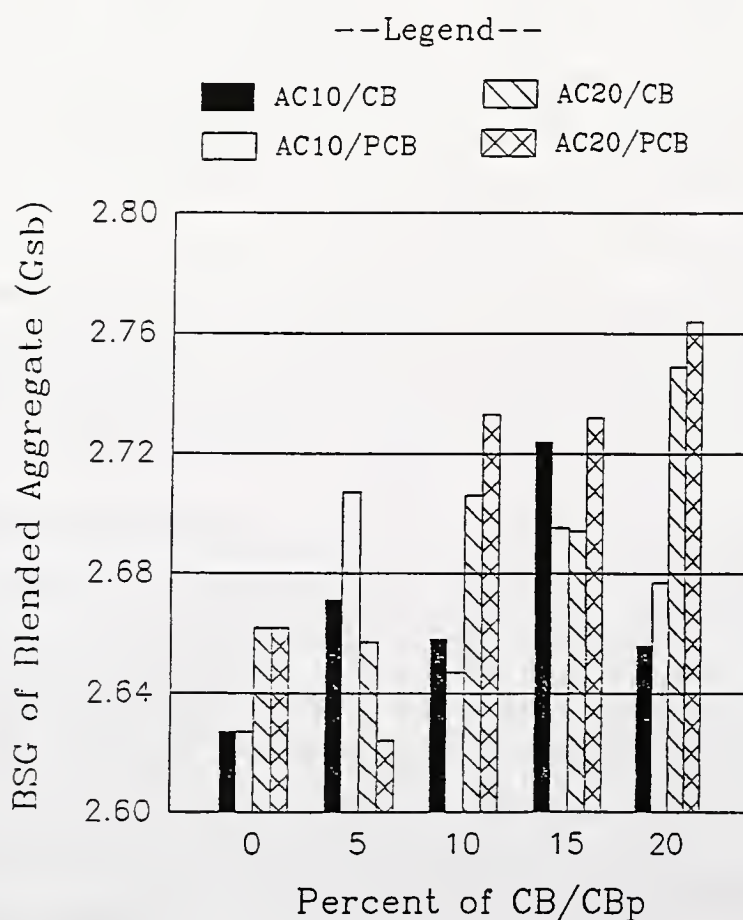
Figure 5.10 The Relationship between G_{sb} and Additive Content

5.5.4 Voids Filled with Asphalt Cement (VFA)

Voids filled with asphalt cement is a direct function of air void (VTM) and the voids in mineral aggregate (VMA). The VFA is an important parameter in the determination of the stability and the rutting of the asphalt mixtures. The low VFA can indicate a lack of asphalt cement, but the high VFA can indicate problems like rutting and poor stability. By U.S. Army (1987) and Asphalt Institute (1988), 65% to 78% of VFA is recommended for heavy traffic base.

VFA vs. CB Contents

Figure 5.11 (a) and (b) show the relationship between VFA and carbon black contents for AC-10 and AC-20 mixtures. VFA decreases slightly as the percent of carbon black increases for AC-10 and AC-20 mixtures. The fluctuations of the results are due to the results of VMA, because VFA is directly related to VMA.

VFA vs. CB_p Contents

Figure 5.11 (c) and (d) show test result for AC-10 and AC-20 mixtures with CB_p. In both case, VFA decreases as the percent of CB_p increases. The change of VFA for CB_p is larger than that of VFA for CB. In general, the trend of VFA is inverse to the trend of VMA.
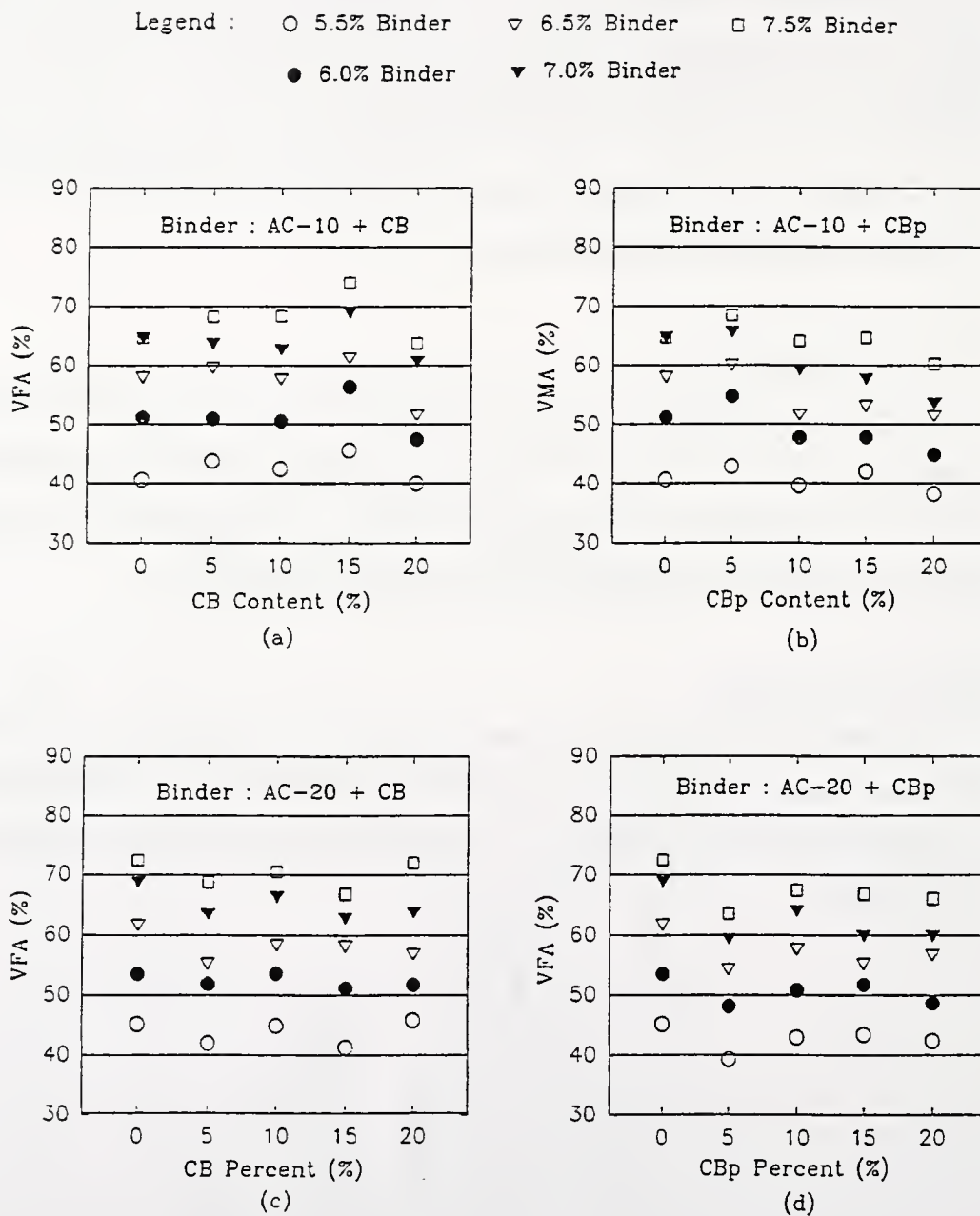
Figure 5.11 The Relationship between VFA and Additive Content

5.5.5 Marshall Stability

<u>Stability vs CB</u>

Figure 5.12 represents the relationship between stability and CB content for AC-10 and AC-20 mixtures. The measured stability for both cases is from about 16000 N to 22000 N. The recommended minimum stability is 5340 N by INDOT (1993), 6680 N by U.S. Army (1987), and 8010 N by AI (1994). The variation of stability is about 20% for AC-10 mixtures and about 10% for AC-20 mixtures. The stability increase by adding CB varies case by case, but the stability increase of AC-10 mixtures as CB content increases, is larger than that of AC-20 mixtures. Considering the binder content, 7.0% of binder content for AC-10 and AC-20 mixtures shows a good stability. Also, 10%, 15% and 20% of CB content for AC-10 mixtures shows some increase of stability. This result shows a trend similar to Rostler et al. (1977), and Vallerga and Gridley (1980). Although the increase of Marshall stability is not much (about 10-15%), the effect for inclusion of carbon black is positive.

The Marshall stability for slag mixtures is much higher, about two times, than the stability for limestone mixtures reported by Park (1995). There are two possible reasons. The first is that the strength of slag is higher than that of limestone. The second is the amount of asphalt used. In order to make a proper range of air-voids and VMA, the amount of asphalt for the slag mixture is higher than for limestone mixtures.

<u>Stability vs CB_p</u>

Figure 5.12 (c) and (d) show the relationship between stability and CB_p content for AC-10 and AC-20. The test results are a little bit random. The average stability is about 16000 N to 22000 N for AC-10 mixtures and about 18000 N to 23000 N for AC-20. The variation of stability for both cases is about 20%. Both 7.0% and 7.5% of binder content for both cases show relatively good results for both asphalts. The effect for inclusion of CB_p is more significant for AC-10 mixtures than for AC-20 mixtures. This is a reverse trend to that for CB. The increase of Marshall stability shows at 10%, 15%, and 20% of CB_p for AC-10 mixtures and at 15% and 20% of CB_p for AC-20 mixtures.

Legend :   O 5.5% Binder   ▽ 6.5% Binder   □ 7.5% Binder

● 6.0% Binder   ▼ 7.0% Binder
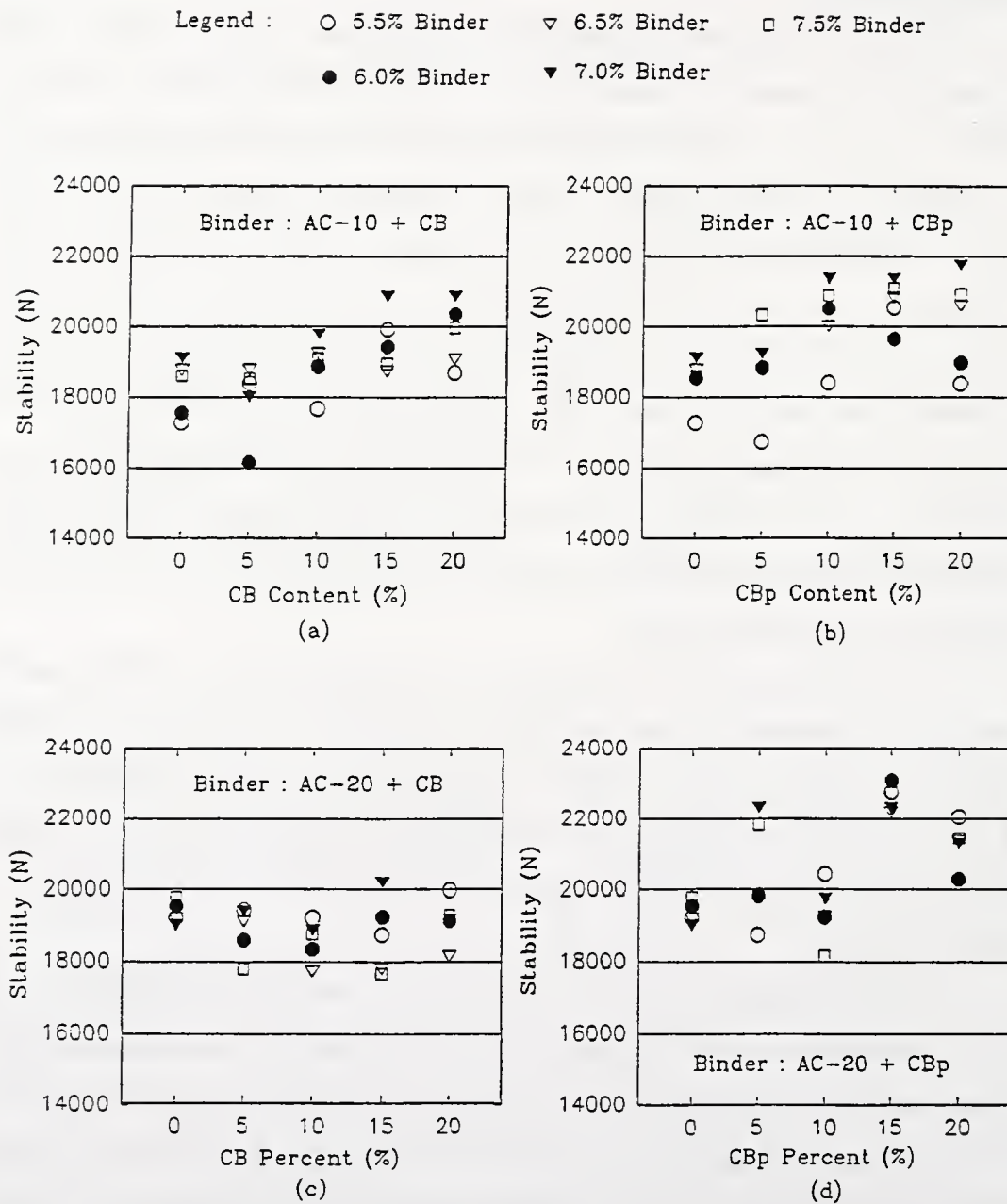
Figure 5.12 The Relationship between Marshall Stability and Additive Content

5.5.6 Flow

Flow vs. CB Content

Figures 5.13 (a) and (b) show the relationship between flow and CB content. The flow value increases with increasing CB content, up to 15 % , and then slightly decreases with increasing CB content for AC-10 mixtures. Also, the higher the binder content, the higher the flow values for every case. The ductility of asphalt modified CB and CB_p with short term aging increases with increasing additive content, up to 10 %, and then decreases with increasing additive content, up to 20 %. The compacted specimen using Marshall equipment experienced short term aging due to curing procedure in hot oven for 3 hours. Although the trend due to adding CB is slightly different, the inclusion of CB has an effect on the ductility of mixtures. For AC-20 mixtures, the trend for flow value is similar to that for AC-10 mixtures.

Flow vs. CB_p Content

The results are shown in Figure 5.13 (c) and (d). The trend for CB_p mixtures is similar to that for CB mixtures, however, the degree of change for CB_p mixtures is less than for CB mixtures. This trend is in reverse to the ductility test results by Zeng and Lovell (1995). In case of large binder contents, for example 7,5 % binder, the flow value for AC-20 mixtures is not related to the increase of CB_p content.
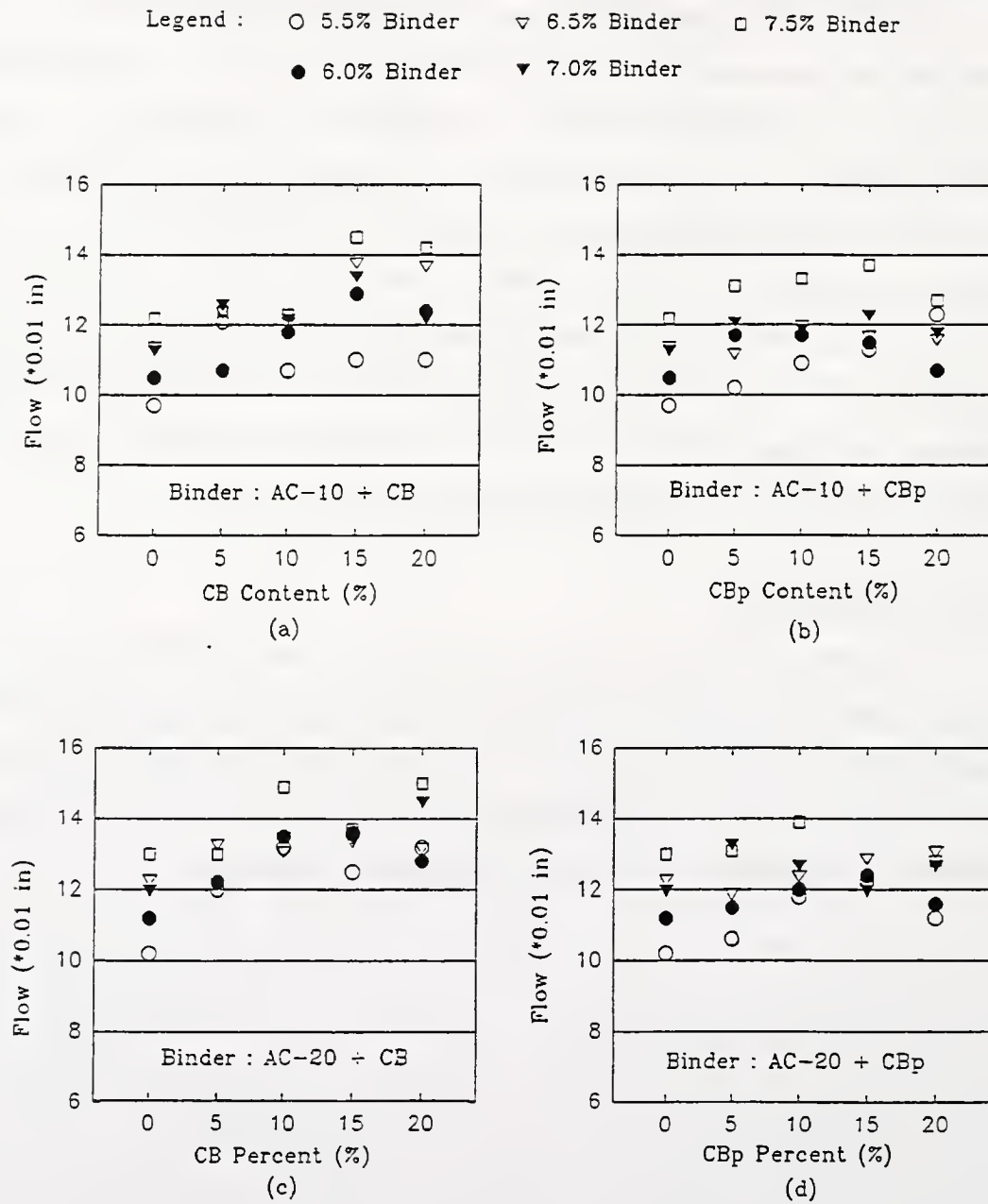
Figure 5.13 The Relationship between Flow Value and Additive Content

5.5.7 The Optimum Binder Content

The optimum binder content is one of important factors for the bituminous mixture design, because it affects the ability of the asphalt pavement to support traffic loads. The specification for the determination of the optimum binder content varies with each agency and state. The Indiana Department of Transportation specification (1993) was used to determine the optimum binder content.

Table 5.4 shows the results by INDOT specification, for the optimum binder content at 6% of air voids and the other characteristics at the optimum binder content. Figure 5.35 shows the trend of the optimum binder content by adding CB and CB_p for AC-10 and AC-20 mixtures. The optimum binder contents for AC-10 and AC-20 mixtures increase as the percent of CB and CB_p increase. The reason for increase of the optimum binder content is the absorption of asphalt by CB and CB_p and the replacement of asphalt by CB and CB_p.

For AC-10 mixtures, the optimum binder content with CB is smaller than that with CB_p at the same content. The main reason is the difference of the particle size and uniformity of CB and CB_p. In case of CB, carbon black would become a part of asphalt cement. On the other hand, some of CB_p should be a part of asphalt cement, and the others should act like the fine aggregate or mineral filler. The same phenomenon was noted for AC-20 mixtures. It is noted that the optimum binder content for AC-20 mixture is slightly larger than that for AC-10 mixtures at the same content of CB and CB_p.

Table 5.4 Summary of the Optimum Binder Content

Binder		Optimum Binder Content	Unit Weight (lb/in^3)	Stability (N)	Flow (0.01in)	VMA (%)	VFA (%)
AC-10 CB	0 %	6.3	141.5	18512	10.9	13.7	57
	5 %	6.6	141.5	18423	12.1	15.1	60
	10 %	6.6	142.1	19580	11.9	14.4	58
	15 %	6.7	141.6	19758	13.3	16.8	64
	20 %	6.87	141.9	20292	13.3	14.4	57.5
AC-10 CB_p	5 %	6.67	141.7	19269	12.0	16.2	63
	10 %	7.0	141.2	21138	12.5	14.6	58
	15 %	7.33	141.0	21223	13.1	16.3	60.3
	20 %	7.7	140.4	21223	12.3	16.0	61.5
AC-20 CB	0 %	6.4	141.6	19224	11.6	14.8	60
	5 %	6.6	141.6	19090	12.6	14.6	58
	10 %	6.7	142.0	18156	13.75	15.8	62
	15 %	6.85	141.7	18957	13.5	15.8	62
	20 %	7.1	141.7	18868	14.4	17.5	65
AC-20 CB_p	5 %	6.7	141.2	21004	12.8	13.7	57
	10 %	7.2	140.9	18779	13.2	17.4	66
	15 %	7.45	140.8	22962	12.3	17.7	65
	20 %	7.75	140.4	21271	13.4	18.7	67.5

5.6 Conclusion

Based on the laboratory test for Marshall mix design, the following principal conclusions can be drawn:

- As the inclusion of carbon black and pyrolyzed carbon black increases, air-voids of the mixtures tend to increase. The change of air-voids in CB_p mixtures is larger than CB mixtures, due to the non-uniformity of the particles.

- The bulk specific gravity of the blended aggregate is not a constant. It depends on the shape and surface texture of the aggregate, and the characteristics of the binder (asphalt+additive).

- A self-consistent volumetric asphalt design gives more reasonable values for voids in mineral aggregate (VMA) than a conventional volumetric design, because the latter has some possible error sources, such as the determination of the bulk specific gravity of each aggregate and the blended aggregate, the determination of the saturated-and surface-dry condition, and the use of water instead of asphalt cement.

- The use of iron blast furnace slag as an aggregate for binder courses of pavement produces a high Marshall stability, an average about 20000 N. Also, as the inclusion of CB or CB_p increase, the Marshall stability increases. However, the effect on the Marshall stability for AC-20 mixtures with carbon black (CB) is not as significant as in the other cases. The inclusion of CB and CB_p has an effect on increase of flow values which are within the acceptable ranges.

- The optimum binder content is inclined to increase as the content of CB and CB_p increases.

- There is no doubt that carbon black as a microfiller becomes as integral part of the asphalt cement due to its small particle size, about 100 to 150 nanometer. Pyrolyzed carbon black with a large particle size acts both as a mineral filler and with small particle size acts as a microfiller, due to the variation of particle size (up to 0.3 mm).

CHAPTER 6
GYRATORY TESTING

6.1 Background of the Gyratory Testing Machine

The gyratory testing machine was developed by the Texas Highway Department in 1939. The main purpose was to develop the methods and equipment that would simulate road conditions and to give accurate reproducible results. Different machine models were tested in the laboratory. The Gyratory Molding Machine was the ninth version; and, since been incorporated in a standard procedure by the Texas Highway Department (Ortolani and Sandberh, 1952).

The molding method employing "specimen shear" consisted of a mold having four equally spaced handles which were individually lifted in succession a prescribed number of times. The molding cylinder has two 60.96cm handles attached to act at an included angle of 75°, by which the gyratory motion is imparted to the specimen (Ortolani and Sandberh, 1952).

In 1957, the kneading compactor developed by the Corps of Engineers was introduced to the AAPT (Association of Asphalt Paving Technologist) at the annual meeting in Atlanta. There are four primary reasons to develop the kneading compactor (McRae and McDaniel, 1958):

- to produce the high density under channelized traffic of the wheel load
- to produce test specimens having stress-strain relationships corresponding to those of actual pavement samples of equivalent density and bitumen content
- to give an indication of how many repetitive load applications a pavement sample can take before flushing

- to give a new approach to overcome the limitations of current pavement mixture design tests.

Two different types of kneading compactor were developed:

- gyratory compactor with fixed gyration angle with variable gyratory stress (shown in Figure 6.1)

- gyratory compactor with variable gyration angle with variable gyration stress (shown in Figure 6.2)

The main differences of the second model from the first one are:

- to obtain its hydraulic pressure from an electrically operated hydraulic pump system

- to utilize the foot valve for vertical load application

- to measure and control the gyratory stress
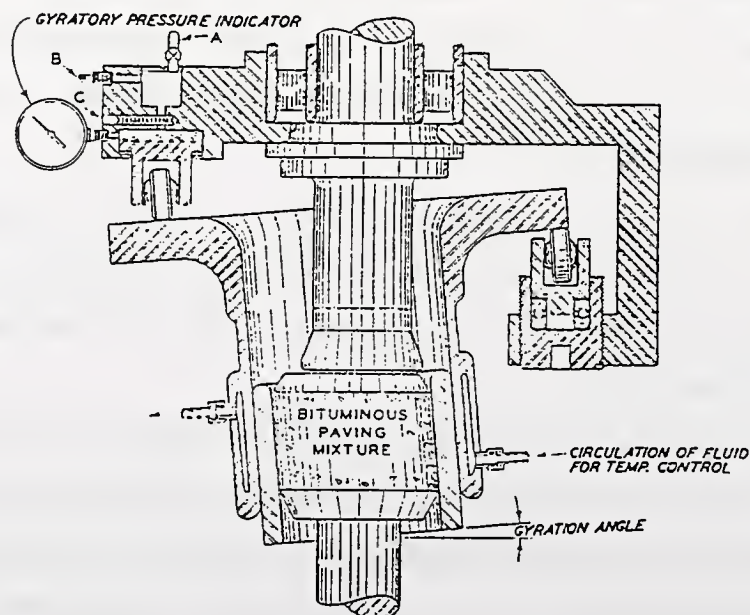
Figure 6.1 Kneading Compactor for Bituminous Paving Mixtures, First Model (McRae and McDaniel, 1958)
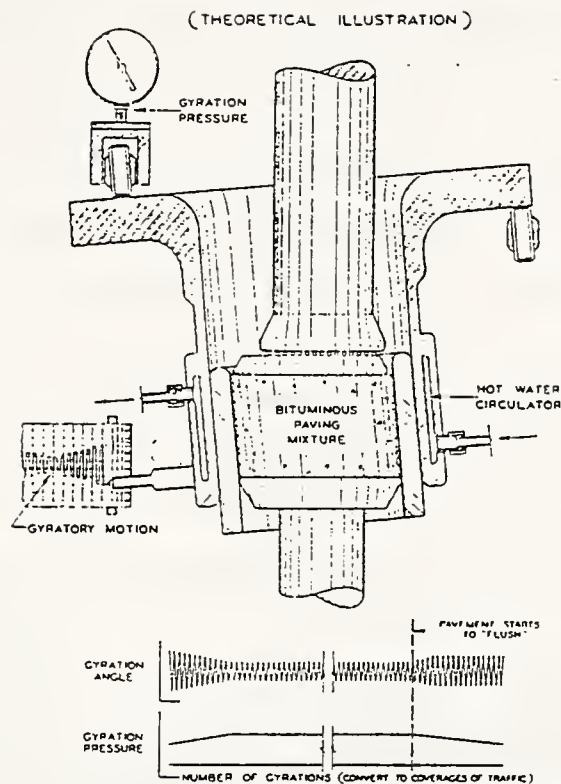
Figure 6.2 Kneading Compactor for Bituminous Paving Mixtures, Second Model
(McRae and McDaniel, 1958)

Two types of gyratory testing machine have been recently used: the U.S. Army Corps of Engineers gyratory and the SHRP (Strategic Highway Research Program) gyratory. The main difference is that the SHRP gyratory machine has a fixed plate, whereas the U.S. Army Corps of Engineers gyratory testing machine is freely rotated. The former is used only for the compaction of the specimen, but the latter is used for the compaction and shear testing of the specimen.

The GTM which has been most used was developed by the U.S. Army Corps of Engineers in 1962. Figure 6.3 shows the typical schematic of the GTM. Referring to the manual from the Engineering Developments Company Inc. (McRae, 1993), mold A containing a test specimen is clamped in position in the flanged mold chuck B. Vertical pressure on

UPPER ROLLER
(OIL-FILLED CHAMBER)

UPPER ROLLER
(AIR-FILLED CHAMBER)

TOP VIEW

TEST
SPECIMEN

A. Specimen Mold
B. Mold Chuck
C. Lower Roller
D. Upper Roller
E. Upper Ram Shaft
F. Lower Ram Shaft
G. Upper Head
H. Lower Head
I. Gyrograph
J. Pressure Gage
K. Filling Valve
L. Heating Element
M. Chuck Flange
N. Recorder Pen
O. Spring Support Sleeve
P. Helical Spring
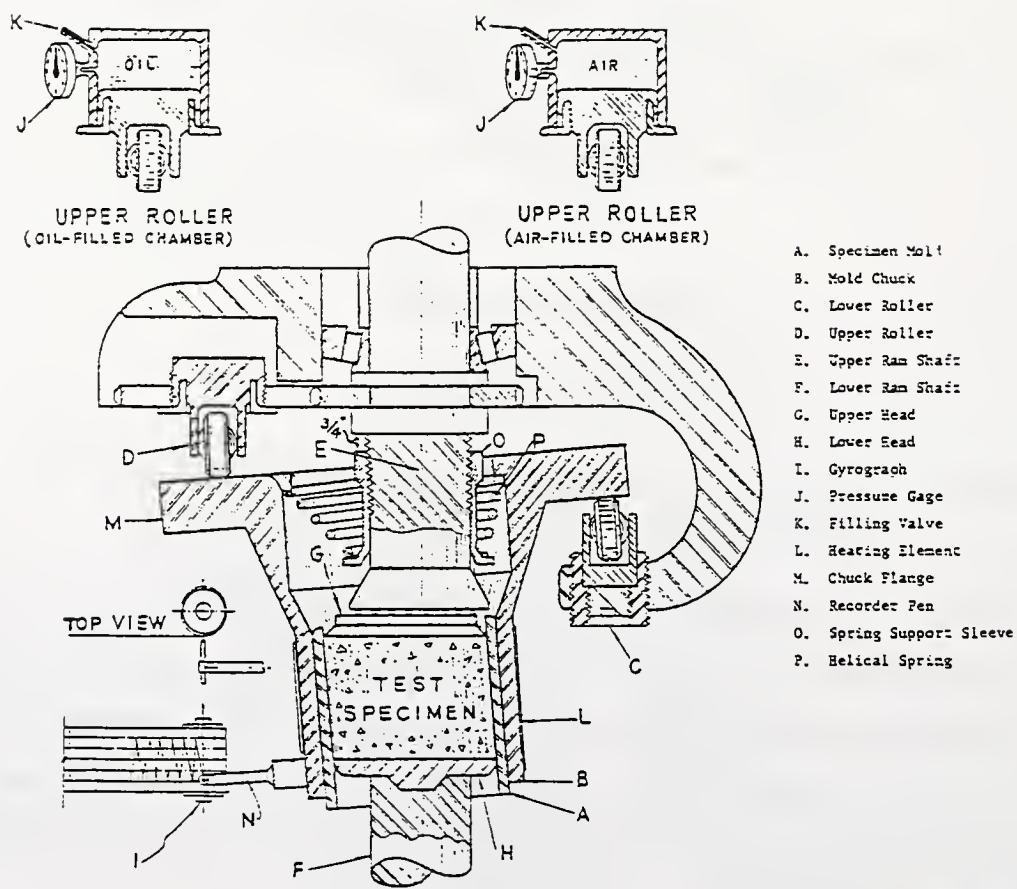
Figure 6.3 Schematic of U.S. Army Gyratory Testing Machine (U.S. Army Corps of
Engineers, 1962)

the test specimen is maintained by upper ram E and lower ram F acting against heads G and H, respectively. Head G acts against a roller bearing and is therefore free to slip while head H is fixed. Since the mold is securely held by the chuck a gyratory motion (shear strain) is imparted to mold chuck B by rollers C and D as they travel around the flanged portion of the chuck. These bearing surfaces are lubricated surfaces. Roller C is adjustable in elevation to permit setting any desired gyratory angle (shear strain) but is maintained at a fixed elevation when using the oil-filled cell. It may very slightly in elevation when using the air-filled cell. The oil-filled roller was used for this study. Upper rollers D, containing the pressure cell, emit signals that are transmitted by telemetry and digitized by the tall panel meter. The gyratory motion (shear strain) is sensed by angular transducer, and recorded by recorder I and N. This recording of shear strain is called a Gyrograph. Sample gyrographs are shown in Figure 6.4.
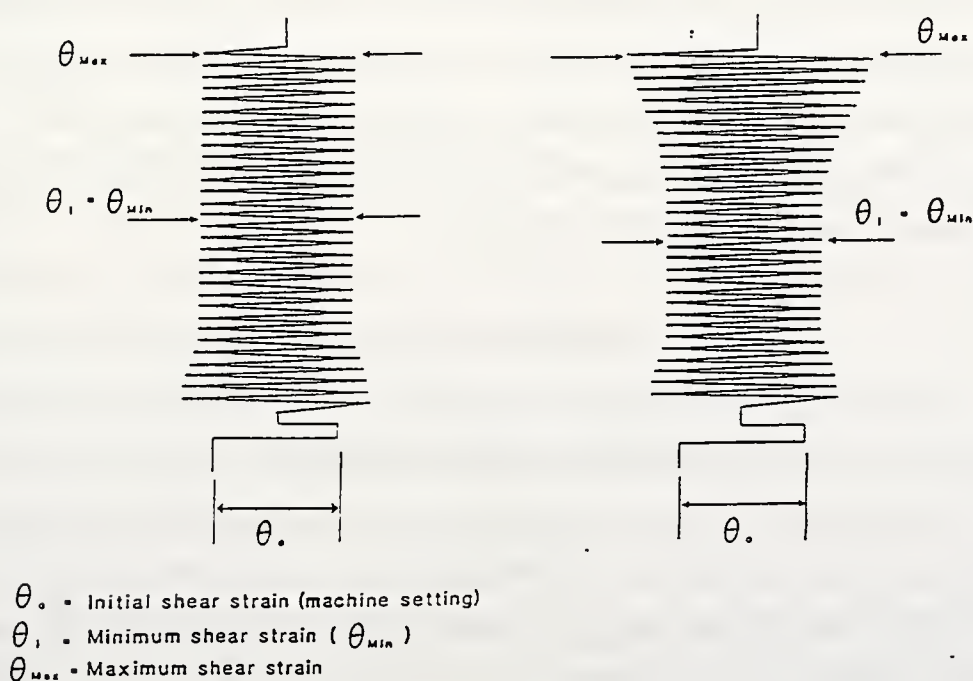
Figure 6.4 Typical Types of Gyrograph (McRae, 1993)

In a recent study of Asphalt-Aggregate Mixture Analysis System (AAMAS), (Von Quintus and Kennedy, 1988) supported by NCHRP, the Texas gyratory shear compactor proved to simulate field conditions, especially field particle orientation. The GTM accomplishes this through angle of gyration, vertical pressure, and number of gyrations. In France, the GTM is used to simulate density at the end of construction instead of during service (Blankenship et al., 1994). This means that the GTM can simulate two stages of compaction,

- during the construction with 8 percent of target air-voids
- after the construction with traffic load densification.

6.2 Testing Equipment and Procedures

6.2.1 Testing Equipment

The U.S. Army Corps of Engineers 8A/6B/4C model was used for our study. The model number represents a diameter of specimen size. This machine produces a shearing or kneading action in the sample by a gyratory motion of the sample mold while pressure is maintained on the sample at each end of the mold by means of loading plungers whose faces remain parallel to each other.

6.2.2 Mix Preparation

The mix preparation of gyratory compaction specimens followed ASTM D 3387-93 and the manual provided by the Engineering Developments Company Inc. (McRae, 1993). The masses of 1200 grams of aggregate and the optimum binder content which was determined from the Marshall mix design were used to make the size of specimen for 101.6mm (4 inch) diameter and approximately 68.6mm (2.7 inch) height. The chuck temperature was kept at $140^{\circ}C \pm 5^{\circ}C$.

6.2.3 Compaction

A 101.6mm (4 inch) diameter mold was used for the preparation of specimens. A 1.25° angle of gyration and a (120 psi) vertical pressure were employed. Although 1° is most commonly used, the angle of 1.25° was selected to simulate the worse condition. The vertical pressure (ram pressure) simulates the maximum anticipated time contact pressure, since the theoretical stress for compaction and maximum induced shear are based on the concept of simulating the field conditions for the test (Zhang et al., 1994).

A value of 500 revolutions was chosen for the ultimate compaction efforts, although SHRP (1994) recommended 230 revolutions as the ultimate traffic densification. According to McRae's recommendation (1993), compaction is completed as the variation in densification of the specimen is not greater than $0.157kN/m^3$ after an additional 100 revolutions

The variation of roller pressure and height of the sample were monitored and recorded at every 50 revolutions to check the effects of subsequent loads and inclusions of different ratios of pyrolyzed carbon black and carbon black. The roller pressure and the height of sample were measured at four positions differing by approximately 90°. The height of sample, gyratory angle, and applied pressure were recorded by the gyrograph. After the compaction was completed, the sample was extruded from the mold. The compacted samples cooled in the laboratory temperature (18°C to 20°C) for more than 24 hours prior to the bulk specific gravity test. The bulk specific gravity tests were performed in accordance with ASTM D 2727-93.

6.3 Testing Result and Discussion

6.3.1 Air Voids

The air voids in the mixture is one of the most important parameters in asphalt concrete, since the physical properties and performance of mixtures during the service life of the pavement can be predicated from the air voids. The relationships between air voids and GTM revolutions for each mixture are presented in Figure 6.5 and 6.6. The

air voids of 5 to 8 percent after construction and that of 3 to 5 percent after traffic densification have been found to be acceptable in most environments, both for surface and for binder courses (Von Quintus and Kennedy, 1988).

AC-10 Mixtures

Figures 6.5 (a) and (b) show the relationship between air voids and GTM revolutions for AC-10 mixtures. As the GTM revolutions increased, air voids, at the optimum binder content, correspondingly decrease. As can be seen in Figure 6.5 (a), the air voids at the same number of revolutions increases as the content of CB is increased. Considering the decreasing rate of air voids, the initial compaction would be completed in less than about 100 GTM revolutions and the traffic densification would start after about 100 GTM revolutions.

The results for AC-10 CB_p mixtures are shown in Figure 6.5 (b). The inclusion of CB_p had the effect of increasing the air voids of the mixtures. The same trend for initial compaction and traffic densification was obtained.

AC-20 Mixtures

Figures 6.6 (a) and (b) present the relationship between air voids and GTM revolutions for AC-20 mixtures. The variation of the air voids at the same value of GTM revolutions is less than that in AC-10 mixtures. Also, there is no general trend of the change of air voids due to the inclusion of CB and CB_p. Judging from Figure 6.6, the traffic densification might occur near the 100 GTM revolution value. Considering the whole testing result, the final air voids were about 2 percent to 4 percent. The decreasing rate of air voids after 100 GTM revolutions was relatively small. The main reason is the high strength of the slag as a coarse aggregate. The aggregate provided a strong, stone skeleton to resist the applied loads. The compaction using Gyratory Testing Machine should minimize crushing of the aggregate during the compaction. Both grades of asphalt mixtures might be permeable to air and water due to high air voids in the initial stage of construction (Brown and Cross, 1989; Santucci et al., 1985).

The potential for premature cracking, raveling, and freezing and thawing of the AC-10 mixtures with CB or CB_p might be more significant than that in AC-20 mixtures with CB or CB_p. In the case of the AC-10 mixture, the inclusion of CB or CB_p will decrease the rutting potential, because when the air voids of the in-place mixture are less than 3 percent, permanent deformation is likely to occur due to plastic flow (Brown and Cross, 1989).

6.3.2 Gyratory Compactability Index

The Gyratory Compactibility Index (GCI) defines the compactibility of the mixture and can be determined as follows:

$$GCI = \frac{\gamma_{30}}{\gamma_{60}}$$

where γ_{30}: unit weight at 30 GTM revolutions

γ_{60} : unit weight at 60 GTM revolutions

The closer this index approaches unity, the easier the mix is to compact (ASTM, 1993). Table 6.1 gives the summary of gyratory compactibility index for each mixture. As can be seen in Table 6.1, the range of GCI value is 0.963 to 0.971. In the case of AC-10 mixtures, the inclusion of CB slightly decreased GCI. The GCI value slightly increased as the amount of CB increased. In AC-10 CB_p mixtures, except for 15 percent of CB_p, a trend similar to AC-10 CB mixtures was demonstrated. In the case of AC-20 mixtures, the inclusion of CB_p slightly increased GCI, but the inclusion of CB showed a slight decrease in GCI. There is no significant difference between the different asphalt grade and content of CB. The only significant difference is between CB and CB_p. However, this difference is insignificant from a practical point of view.

Table 6.1 Summary of GCI for Each Mixture

Asphalt	Additive	0 %	5 %	10 %	15 %	20 %
AC-10	CB	0.97	0.964	0.965	0.968	0.968
AC-10	CB_p	0.970	0.968	0.970	0.966	0.971
AC-20	CB	0.967	0.966	0.967	0.963	0.964
AC-20	CB_p	0.967	0.966	0.970	0.970	0.971
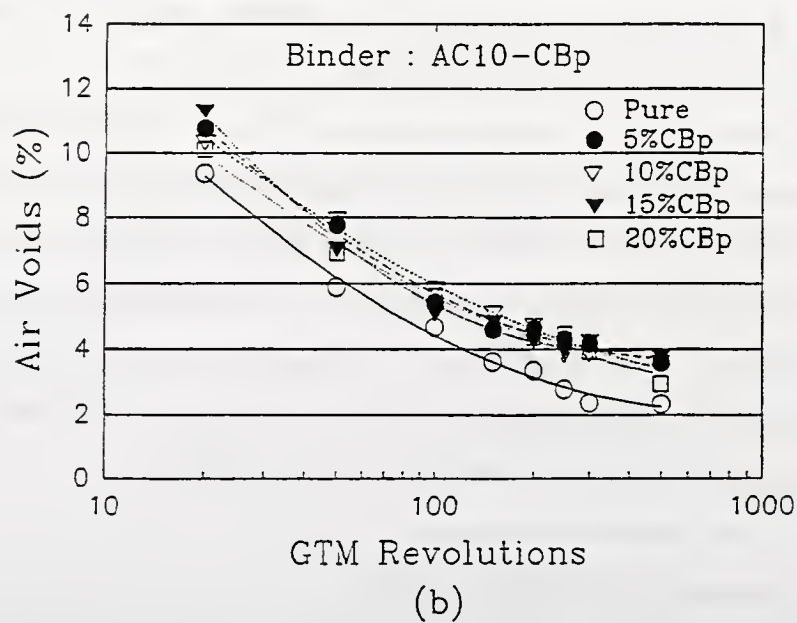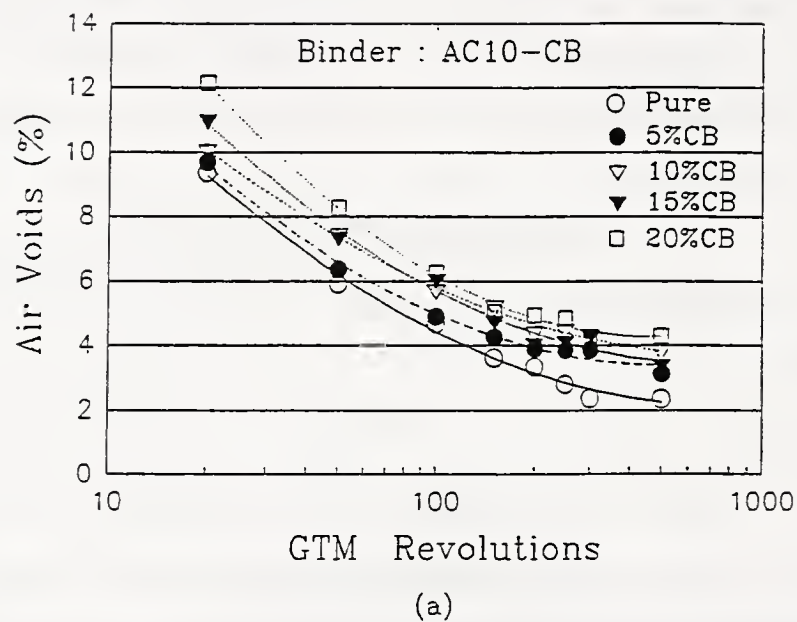
Figure 6.5 Air-Voids and GTM Revolutions for AC-10 Mixtures
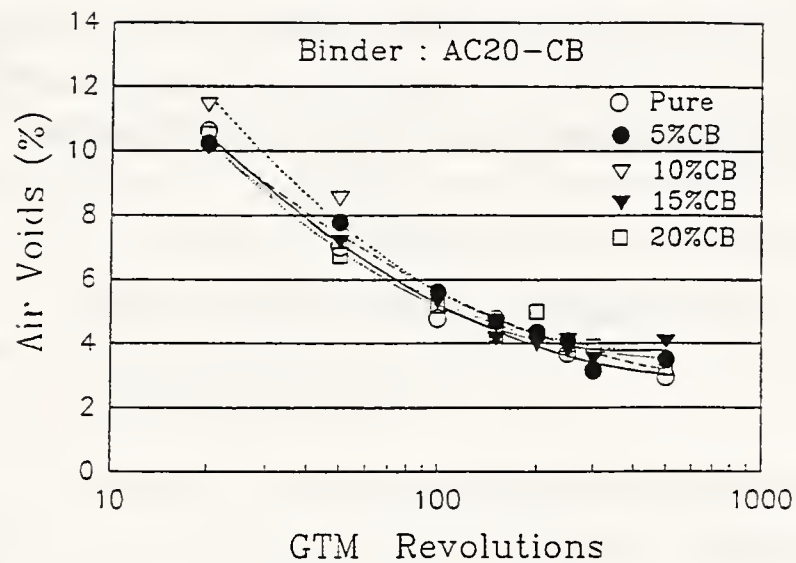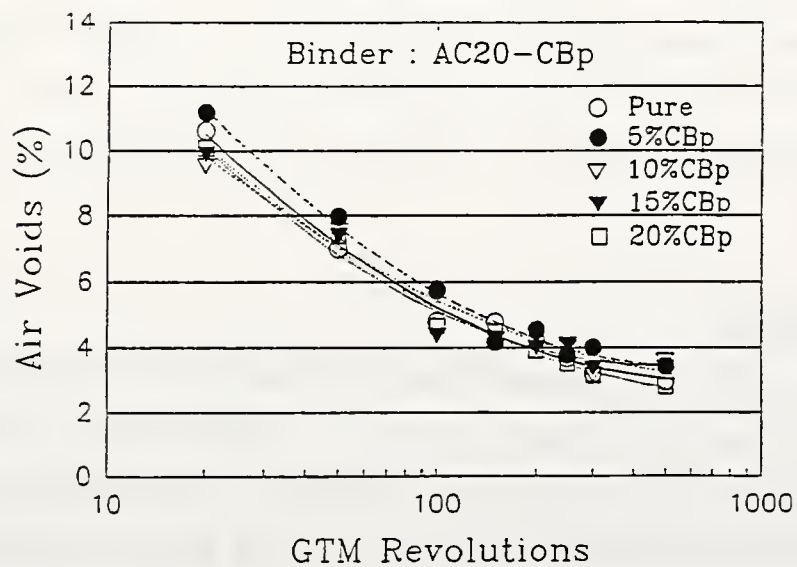
Figure 6.6 Air-Voids and GTM Revolutions for AC-20 Mixtures

6.3.3 Gyratory Stability Index

The Gyratory Stability Index (GSI) is an important parameter used to predict the stability of a mixture, and is related to the potential for the mixture to experience plastic deformation. As the GSI value is closer to unity, the mixture becomes more stable, and less plastic deformation is likely to occur. The GSI is defined as follows:

$$GSI = \frac{\theta_{max}}{\theta_{min}}$$

where θ_{max} : the maximum gyratory angle

θ_{min} : the minimum gyratory angle

An official criterion for GSI has not been determined. According to the recommendation of McRae (1993), a GSI close to unity implies a stable mix. According to NAPA (1991), a value significantly above 1.1 usually indicates unstable mixtures. Research conducted by the Maine DOT suggests that "GSI should be less than 1.15 after 300 revolutions to prevent rutting", and Illinois DOT (1991) studies suggested that GSI should be less than 1.25 after 300 revolutions (Zhang et al., 1994). Based on the previous research on GSI value, a GSI value of 1.15 was selected as a criterion in this study.

AC-10 Mixtures

The relationship between GSI and GTM revolution for AC-10 mixtures with CB and CB_p is provided in Figure 6.7 (a) and (b). The inclusion of CB showed positive results except for the inclusion of 20 percent of CB. Most of GSI values were less than 1.1, which indicates stability. After long loading duration, more than 400 GTM revolutions, the GSI value is apt to increase slightly. Judging from Figure 6.7 (a), the mixture with a large amount of CB might be unstable.

In case of CB_p mixtures, the GSI value was significantly uniform, (between 1.00 to 1.05) which indicates reasonable stability. The inclusion of CB_p as a microfiller and mineral filler should have an effect on the stability of mixtures. The large particles of

CB_p may be compensating for the lack of aggregate grading. This means that the inclusion of CB_p might impart an increased friction angle to the mixtures.

AC-20 Mixtures

The relationship between GSI and GTM revolution for AC-20 mixtures with CB and CB_p is shown in Figure 6.8 (a) and (b). Considering the selected criterion of GSI, the mixtures with CB or CB_p were reasonably stable, except mixtures with 20 percent of CB. Large amounts of CB or CB_p (more than 15 percent) are inclined to be unstable after long loading duration, although mixtures with 15 percent of CB, and 15 and 20 percent of CB_p remained within the criterion.
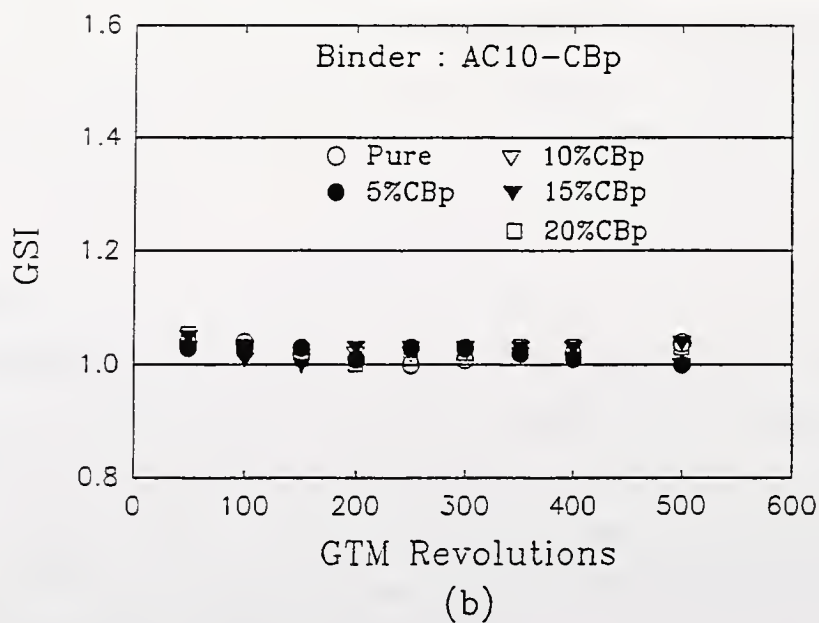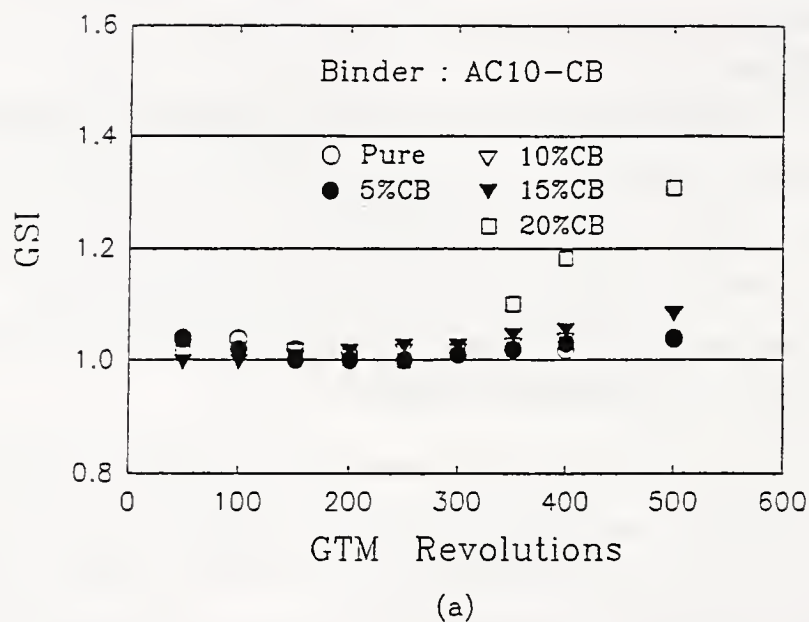
Figure 6.7 GSI and GTM Revolutions for AC-10 Mixtures
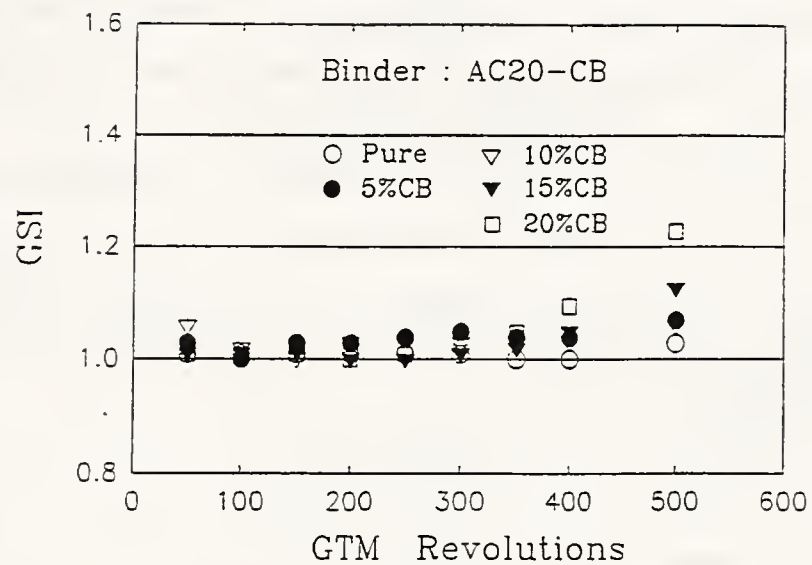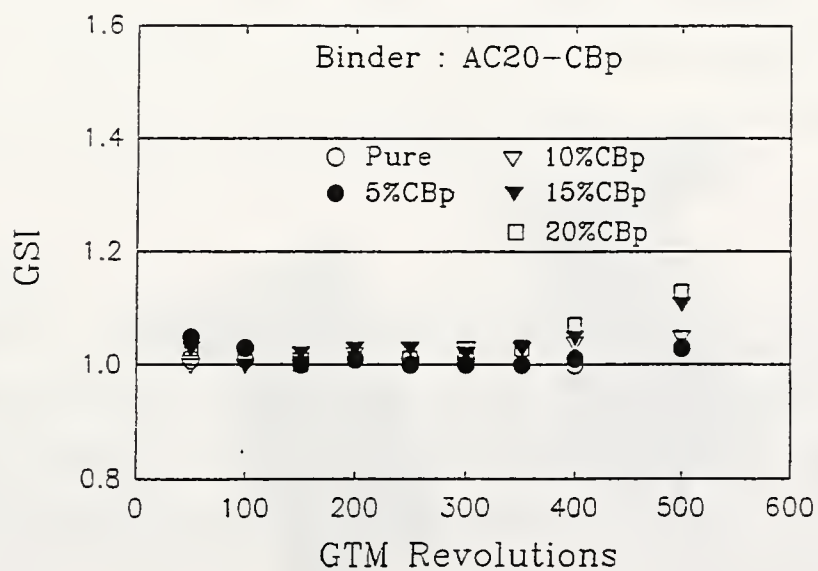
Figure 6.8 GSI and GTM Revolutions for AC-20 Mixtures

6.3.4 Gyratory Shear

Gyratory shear represents the shear resistance of mixture which is a function of the imposed vertical pressure and degree of strain. A decrease of this value during compaction and densification indicates a loss of stability. There is no official criterion for gyratory shear, S_g. According to the recommendation of the Maine DOT (1992), 241.3 kPa (35 psi) after 300 revolutions is the minimum S_g value (Zhang et al., 1994). A value of 275.8 kPa (40 psi) after 300 revolutions has been selected for the S_g criteria.

Figure 6.9 shows the force diagram of GTM. Taking the moments about o, while neglecting wall friction and moment, N*b, the formula for gyratory shear is developed as follows;

$$2WL = \int_0^h S_g A \, dh$$

$$\therefore S_g = \frac{2WL}{Ah}$$
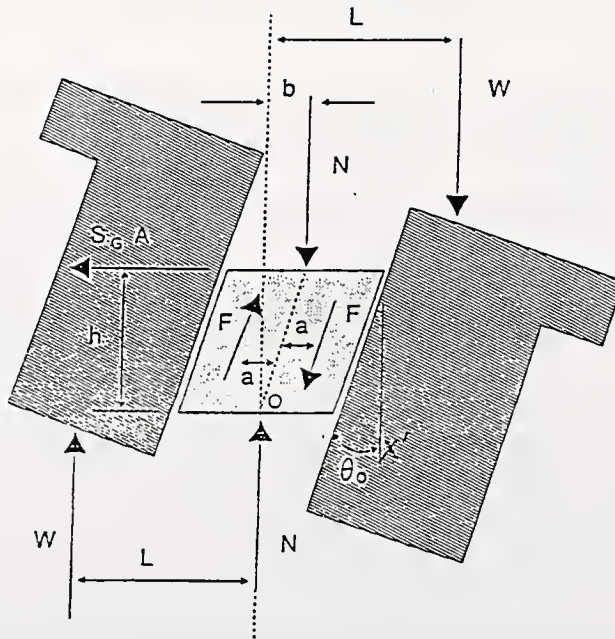
Figure 6.9 The Force Diagram of GTM (McRae, 1993)

Using this formula, gyratory shear, S_g, for GTM model 8A/6B/4C can be obtained as follows :

$$S_g = \frac{8.27 * P}{h}$$

where P: vertical roller pressure (psi)

h : height of specimen (in).

AC-10 Mixtures

Figure 6.10 (a) and (b) show the relationship between gyratory shear and GTM revolutions. In the case of mixtures with CB, as the GTM revolutions increased, S_g value of mixtures without CB increased, however, S_g of the others decreased slightly. The range of S_g value was between 275.8 kPa to 413.7 kPa (40 psi to 60 psi). Considering the selected criterion, only the mixtures with 15 percent of CB are not acceptable.

In the case of CB_p mixtures, the range of S_g value was 344.8 kPa to 413.7 kPa (50 psi to 60 psi) and the values were almost uniform, except the values at 500 GTM revolutions. The variation of the S_g value of CB_p mixtures as the number of GTM revolutions increased was less than that of CB mixtures.

AC-20 Mixtures

Figure 6.11 (a) and (b) represent the relationship between gyratory shear and GTM revolutions for the AC-20 mixtures. Both cases, CB mixtures and CB_p mixtures, show slightly decreased S_g values, as the GTM revolutions increased. Only AC-20 mixtures with 10 percent CB_p and 20 percent CB were not acceptable.

(a)

(b)
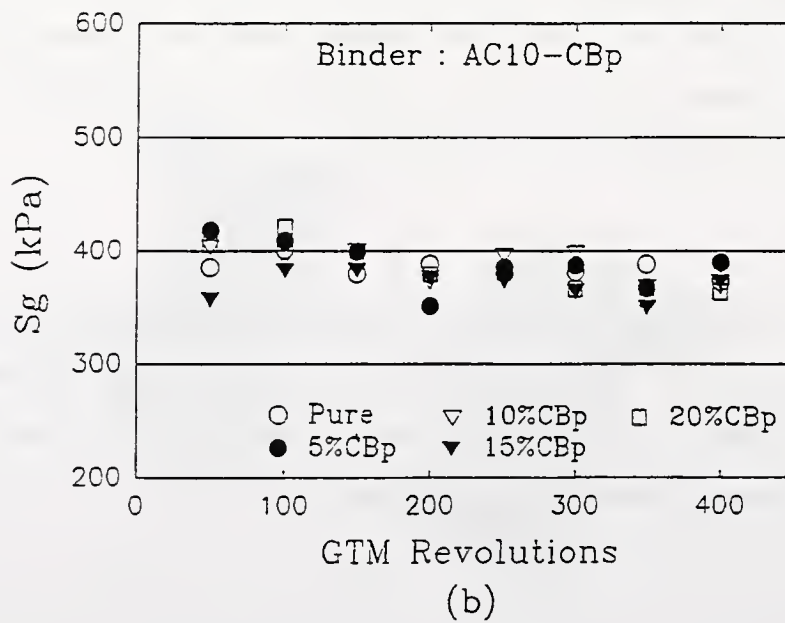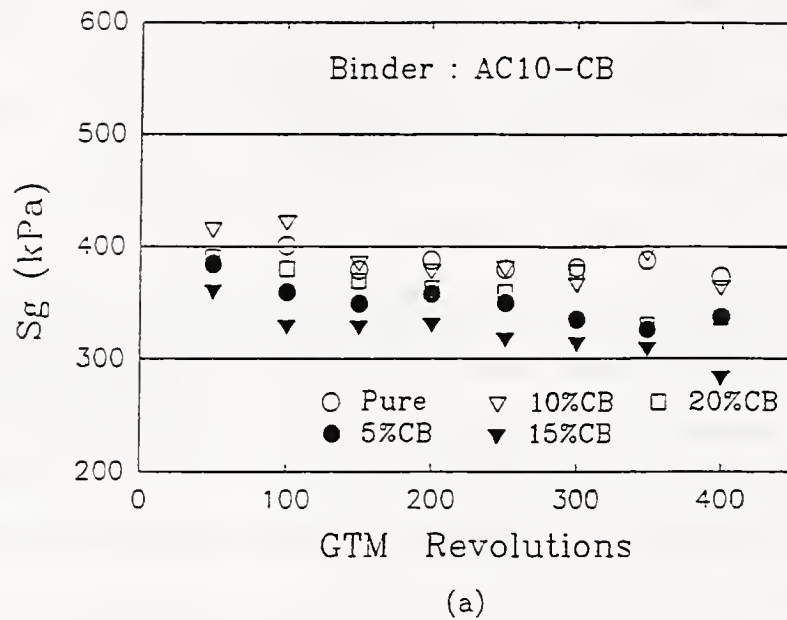
Figure 6.10 Gyratory Shear and GTM Revolutions for AC-10 Mixtures
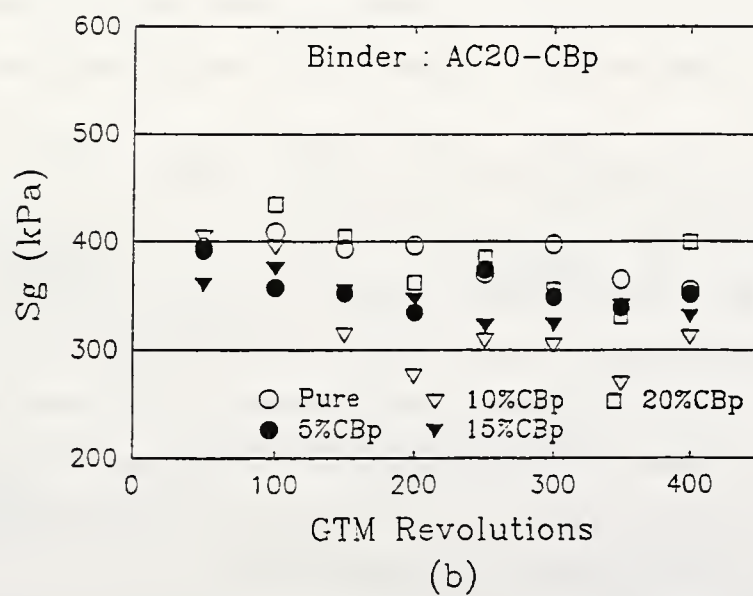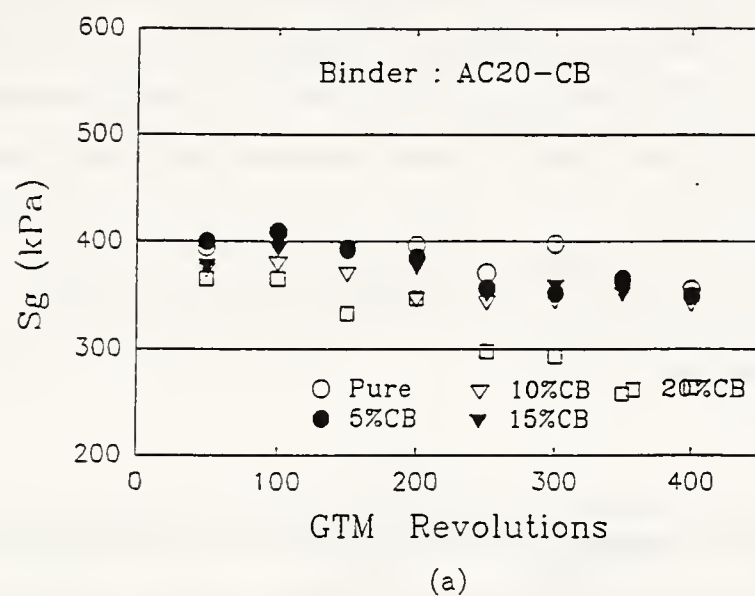
Figure 6.11 Gyratory Shear and GTM Revolutions for AC-20 Mixtures

6.3.5 Gyratory Shear Factor

Gyratory shear factor is defined as the ratio of the measured gyratory shear strength to the approximate theoretical maximum induced shear stress (ASTM, 1993). This is similar to a safety factor; when the GSF value is less than unity, the mixture might fail in simple shear for the defined loading conditions. The theoretical maximum induced shear stress (τ_{max}) for a strip load on a homogeneous elastically isotropic mass is defined as follows:

$$\tau_{max} = \frac{Vertical..Pressure}{\pi} = \frac{120psi}{3.1415} = 38.2psi \ (263.4 \ kPa)$$

and the GSF is calculated:

$$GSF = \frac{S_g}{\tau_{max}}$$

The GSF should be considered with the GSI at the same time, because pavement design should limit the amount of deformation. The value of GSI is a function of plastic deformation of the mixture, and GSF is related to the shear strength of the mixture. If the mixture meets these two criteria, less plastic deformation and higher shear resistance can be expected.

Table 6.2 and Table 6.3 show the summary of GSI and GSF at 100 GTM revolutions and 500 GTM revolutions, respectively. As can be seen in Table 6.2, all mixtures passed the design criteria. As mentioned before, the main reason is the high strength and high friction angle of slag. It is difficult to find the general trend of GSI and GSF of AC-10 mixtures with CB or CB_p, with the increase of GTM revolutions.

At 500 revolutions, all mixtures, except AC-10 mixture and AC-20 mixture with 20 percent of CB, met the criteria. As the GTM revolution increased, both, CB and CB_p mixtures showed an increase of GSI and a decrease of GSF.

Considering the effect of CB or CB_p as an additive, both acted favorably, except for large amounts of CB with AC-20 asphalt.

Table 6.2 The Summary of GSI and GSF at 100 GTM Revolutions

Type	AC10+CB		AC10+CB$_p$		AC20+CB		AC20+CB$_p$	
Percent	GSI	GSF	GSI	GSF	GSI	GSF	GSI	GSF
0	1.038	1.523	1.038	1.523	1.009	1.553	1.009	1.553
5	1.020	1.367	1.029	1.554	1.000	1.548	1.029	1.359
10	1.000	1.461	1.010	1.503	1.019	1.446	1.000	1.506
15	1.000	1.252	1.010	1.459	1.010	1.498	1.000	1.429
20	1.018	1.445	1.031	1.600	1.009	1.388	1.020	1.651

Criteria : GSI ≤ 1.15 and GSF ≥ 1.0

Table 6.3 The Summary of GSI and GSF at 500 GTM Revolutions.

Type	AC10+CB		AC10+CB$_p$		AC20+CB		AC20+CB$_p$	
Percent	GSI	GSF	GSI	GSF	GSI	GSF	GSI	GSF
0	1.038	1.788	1.038	1.788	1.028	1.214	1.028	1.214
5	1.039	1.349	1.000	1.548	1.069	1.189	1.029	1.240
10	1.086	1.833	1.000	1.374	1.058	1.387	1.048	1.312
15	1.084	1.021	1.040	1.406	1.125	1.277	1.108	1.107
20	1.309	1.613	1.031	1.705	1.226	1.264	1.127	2.057

Criteria : GSI ≤ 1.15 and GSF ≥ 1.0

6.3.6 Marshall Stability and Flow

<u>Marshall Stability</u>

The summary of Marshall stability for AC-10 mixtures and AC-20 mixtures is shown in Figure 6.12 and 6.13. As can be seen in the Figures, Marshall stability increased as the GTM revolutions increased. The relationship between Marshall stability and logarithmic GTM revolutions was almost linear.

The results by regression for each mixture are shown in Table 6.4. As can be seen in the Table, the slope of the mixtures without CB or CB_p showed larger values indicating that unmodified mixtures may be more sensitive. The slope of the mixtures with CB_p was larger than that of the mixtures with CB. In the case of CB mixtures, the dispersion velocity during the mixing is very important. When the CB is properly dispersed, the microsize and the hydrophobic property of CB particles, saturated by the asphalt cement, makes CB a part of the asphalt cement. This is called "microfiller action of CB", and is in contrast to conventional mineral fillers. Vallerga and Gridley (1980) recommended the use of pelletized CB to improve the dispersing effect and high speed mixing, approximately 15000 rpm, in order to achieve the full development of the dispersing effects in the asphalt mixtures. In our research, relatively lower mixing velocity, about 8000 rpm, was used. This might be the main reason that lower values occur, although the high performance CB was used. However, the differences observed between the slopes are relatively insignificant in engineering terms, and any conclusions drawn should be treated only as indicative rather than definitive.

Table 6.4 The Result for the Slope between Marshall Stability and GTM Revolutions

Asphalt Cement		AC -10		AC-20	
Additive		Slope	R^2	Slope	R^2
	0 %	15438	0.991	15526	0.966
CB	5 %	15289	0.988	15109	0.987
	10 %	14489	0.945	12907	0.980
	15 %	14805	0.929	15323	0.967
	20 %	13822	0.989	12966	0.979
CB_p	5 %	16120	0.991	16403	0.980
	10 %	15882	0.969	13372	0.978
	15 %	14710	0.942	14083	0.943
	20 %	14214	0.966	14123	0.966
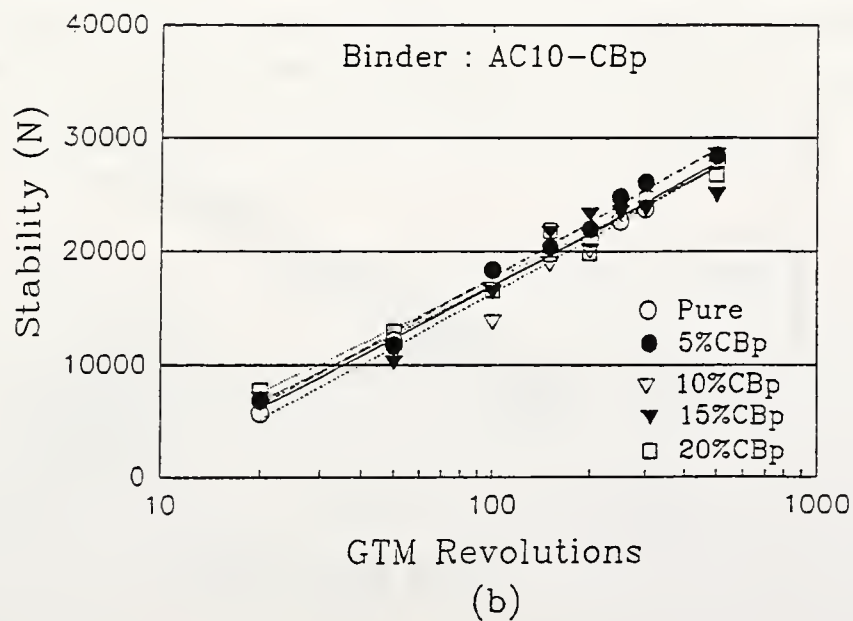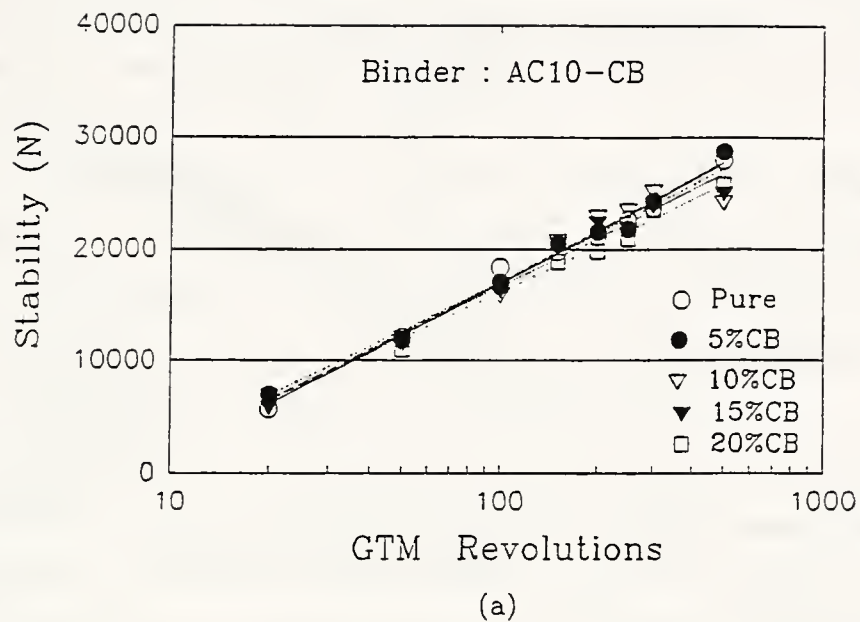
Figure 6.12 Marshall Stability and GTM Revolutions for AC-10 Mixtures
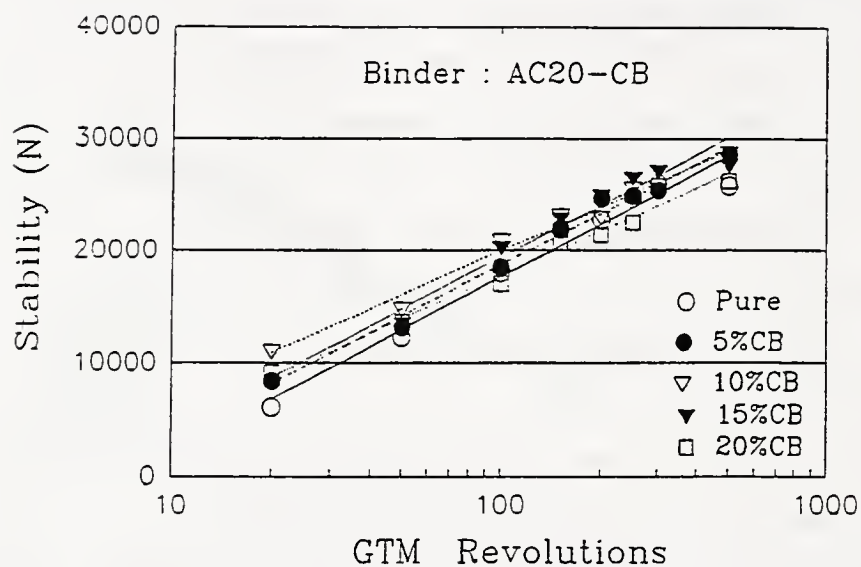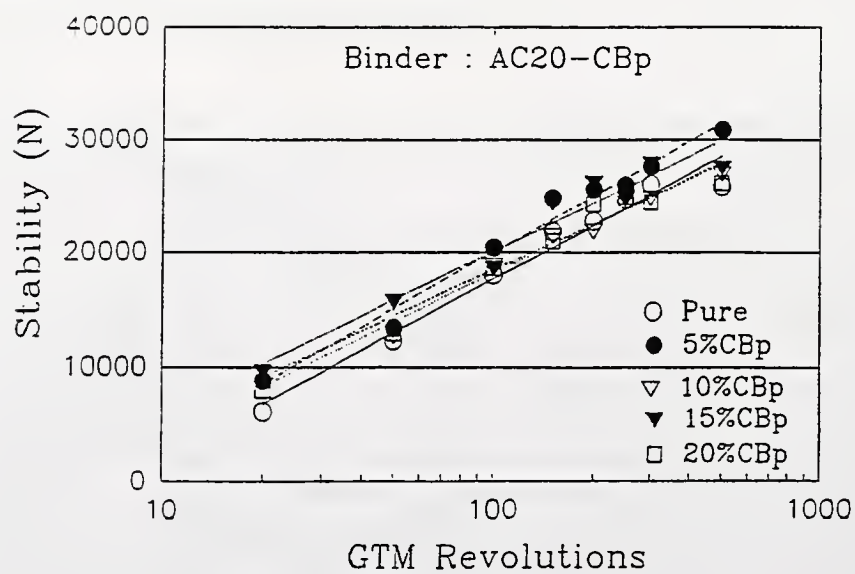
Figure 6.13 Marshall Stability and GTM Revolutions for AC-20 Mixtures

Flow

Figure 6.14 and 6.15 showed the summary of flow for AC-10 and AC-20 mixtures. According to ASTM criteria, the range of acceptable flow is 0.2032cm to 0.4064cm, in the range 3% < VIM < 5%. As the GTM revolutions increased, the flow value tended to stabilize.

In the case of AC-10 CB mixtures, mixtures without CB showed a lower bound and mixtures with 20 percent of CB represented the higher bound. On the other hand, mixtures with 20 percent CB_p indicated a lower bound and mixtures with 5 percent of CB_p showed the upper bound. After a long loading duration, the flows for AC-10 mixtures with CB or CB_p were within the criteria.

In the case of AC-20 mixtures, the flow values of CB mixtures were higher than that of CB_p mixtures at the initial stage of compaction. At the final stage of compaction, the range of flow values for both mixtures were almost identical, about 0.35cm to 0.45cm. In both cases, the mixtures without CB and CB_p represented a lower bound, while the mixtures with 20 percent of CB and with 10 percent of CB_p represented the upper bound. Judging from the INDOT criteria, only mixtures without CB and CB_p and with 15 percent of CB_p were acceptable. The others did not meet the criteria.
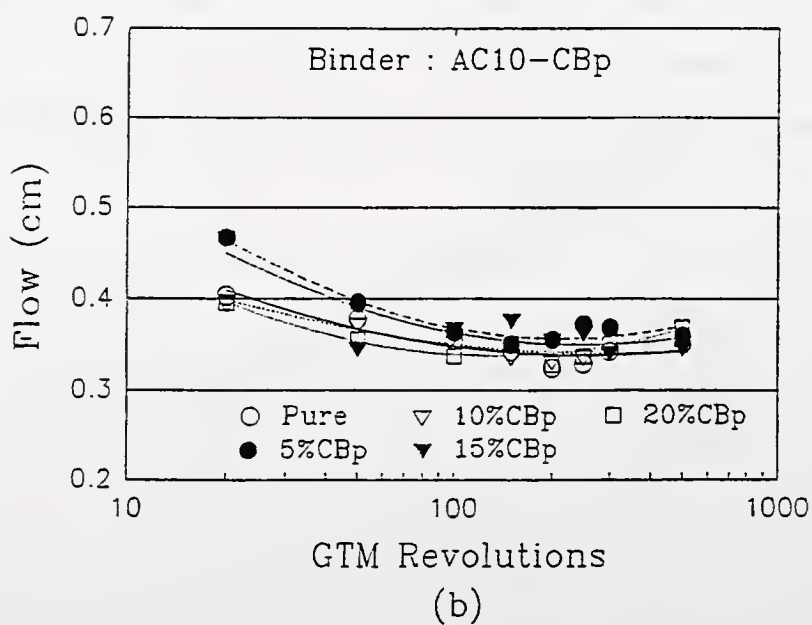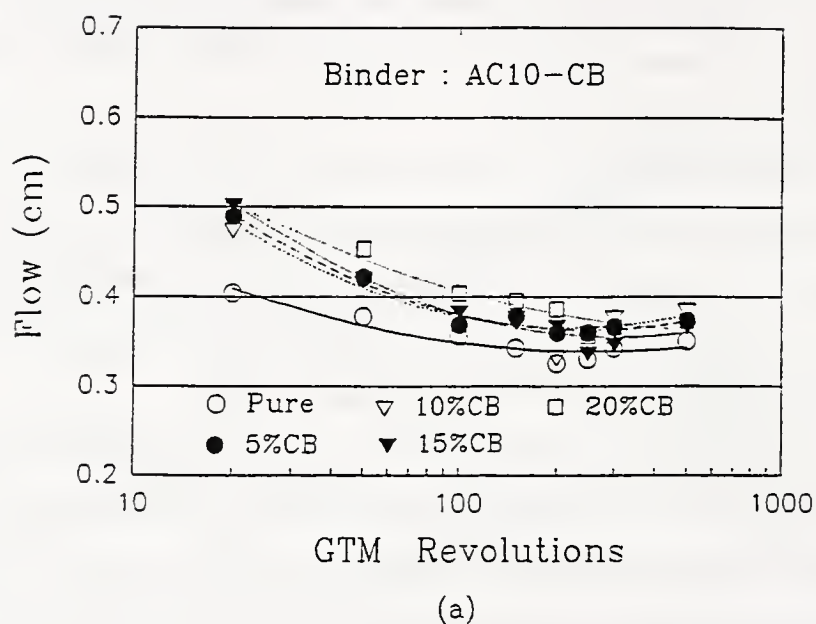
Figure 6.14 Flow and GTM Revolutions for AC-10 Mixtures
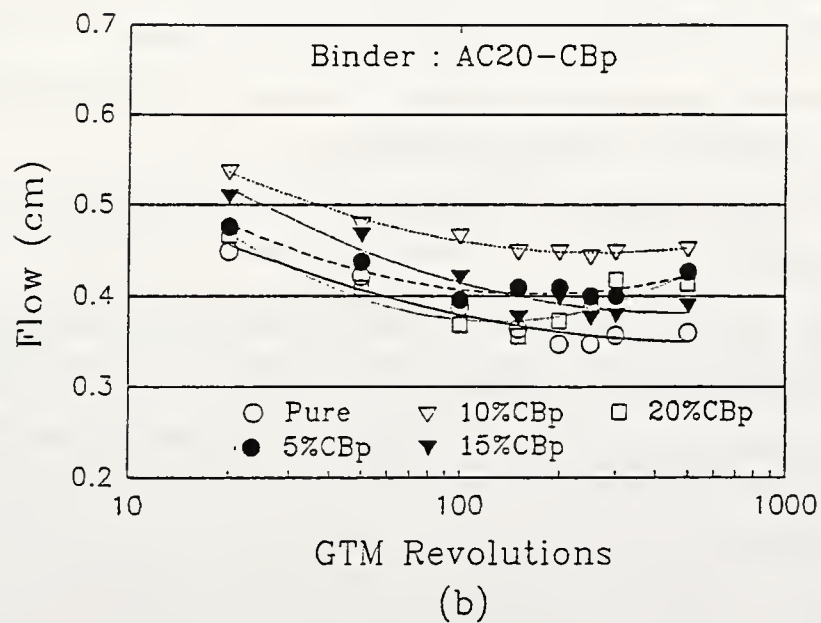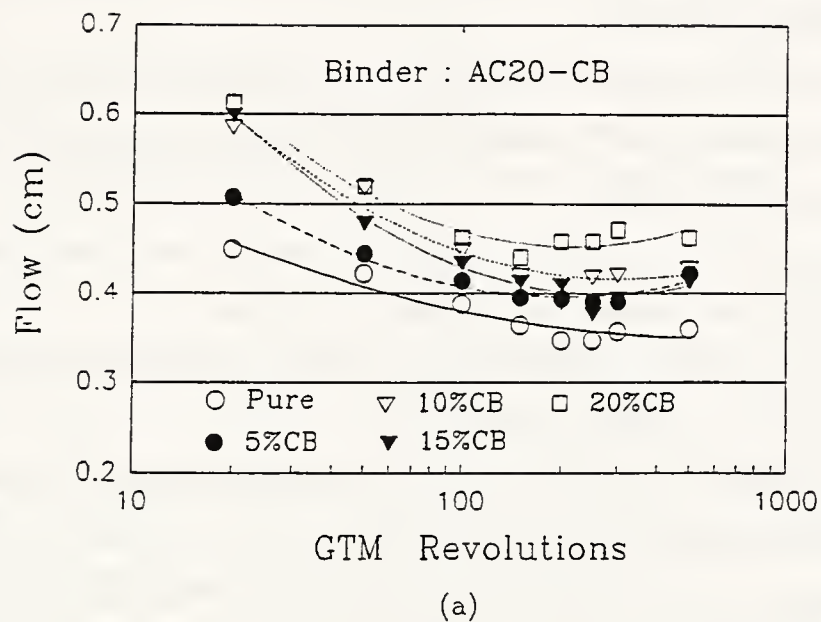
Figure 6.15 Flow and GTM Revolutions for AC-20 Mixtures

6.4 Conclusion

Within the limited laboratory testing in this study, the following principal conclusions can be drawn:

- As the GTM revolutions increased, air voids deceased. The air voids of AC-10 mixture increased with increasing percent of CB and CB_p, but AC-20 mixtures did not show a similar trend.

- Judging from the change of air voids, about 100 GTM revolutions divided the initial compaction and the traffic densification of the mixtures.

- The range of GCI value for all the mixtures was 0.963 to 0.971, which indicates little difficulty in compacting the mixtures.

- Considering the value of GSI, AC-10 CB_p mixtures represented very stable mixtures. The inclusion of CB_p had the effect of producing a very stable mixture during long loading application. Only AC-10 mixtures and AC-20 mixtures with 20 percent of CB indicated instability for long loading application due to the flushing of binder.

- The AC-10 CB_p mixtures represented the best performance of retaining the shear resistance for long loading applications. The others showed a slight decrease of the shear resistance for long loading applications.

- The Marshall stability and logarithm of GTM revolutions showed a linear relationship.

- The flow of AC-10 mixtures with CB and CB_p remained in an acceptable range after long loading application, but that of AC-20 mixtures with CB and CB_p was out of range. In all the mixtures, the flow stabilized after long loading applications.

CHAPTER 7

RESILIENT MODULUS AND INDIRECT TENSILE TEST

7.1 Background

The stress induced by a wheel load on a typical asphalt concrete surface layer is illustrated in Figure 7.1. Four general stress conditions are existed:

- triaxial compression at the surface and immediately underneath the wheel
- longitudinal and transverse tension combined with vertical compression at the bottom of the asphalt concrete layer and immediately underneath of load
- longitudinal or transverse tension at the surface at some distance from the load
- logitudinal or transverse compression at the bottom of the asphalt layer at some distance from the load.

The critical location for load-induced cracking is generally considered to be at the bottom of the asphalt concrete layer and immediately underneath the load, where the stress state is logitudinal and transverse tension combined with vertical compression (Roque and Buttlar, 1992). This is the reason why resilient modulus test and indirect tensile test have been used to determine the potential tension cracking using indirect tensile test mode.

The resilient modulus (M_R) test has been used very widely with many laboratories due to its simplicity and ability to test asphalt specimens similar in size to those used for the widely known Marshall and Hveem tests. This is one of the common methods to measure the stiffness modulus for hot mix asphalt (HMA). The M_R is a dynamic test response defined as the ratio of the repeated axial load to the recoverable deformation:

$$M_R = \frac{P * (0.27 + v)}{t * H}$$ (7.1)

where P : applied load (kN)

v : Poisson's ratio

t : specimen height (mm)

H : horizontal deformation (mm)

The M_R test may be conducted on all types of pavement materials ranging from cohesive to stabilized materials. However, test conditions affect M_R responses for different materials in different ways (Yoder and Witczak, 1975). The M_R provides the stiffness of the mixtures, since it has been found that the M_R at low temperature is somewhat related to cracking potential of pavement (Park, 1995). The stiffer mixtures at low temperatures tend to crack earlier than the more flexible mixtures (Roberts et al., 1991).
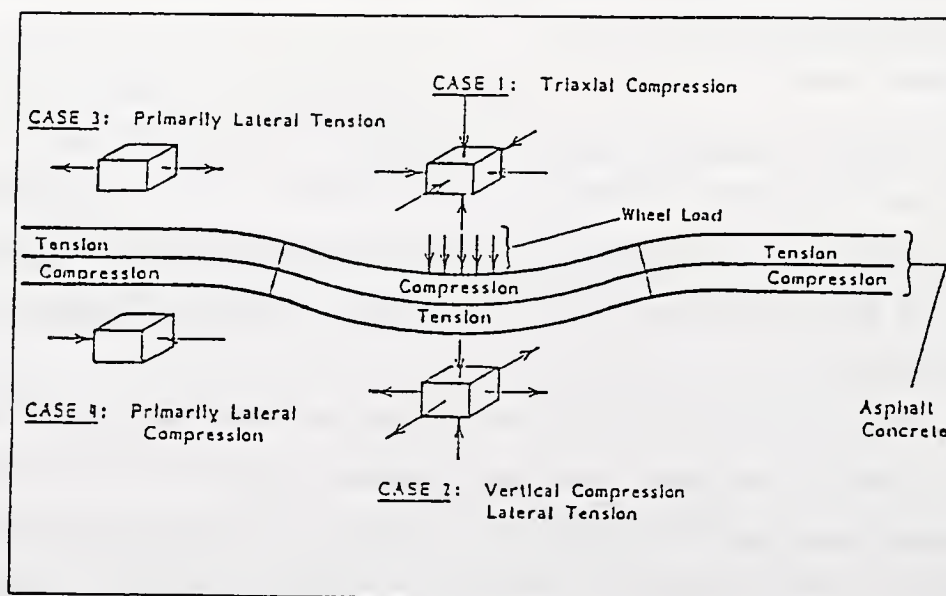
Figure 7.1 Typical Stress States in Asphalt Concrete Layer with Wheel Load Applied (Roque and Buttlar, 1992)

The indirect tensile test is conducted by loading a cylindrical specimen with a single or repeated compressive load which acts parallel to and along the vertical diametral plane (Figure 7.2, ASTM D4123-82). This loading configuration develops a relatively uniform tensile stress perpendicular to the direction of the applied load and along the vertical diametral plane, which ultimately causes the specimen to fail by splitting along the vertical diameter (Kennedy et al., 1975). This test provides two mixture properties, tensile strength and tensile strain at failure, which are useful in characterizing hot mix asphalt. It has many advantages, the most obvious being simplicity of test procedure. The theoretical distribution of stresses for a concentrated load is shown in Figure 7.3 (Yoder and Witczak, 1975).

where P = applied load
        t = thickness of specimen
        D = diameter of specimen
        a = width of the loading strip
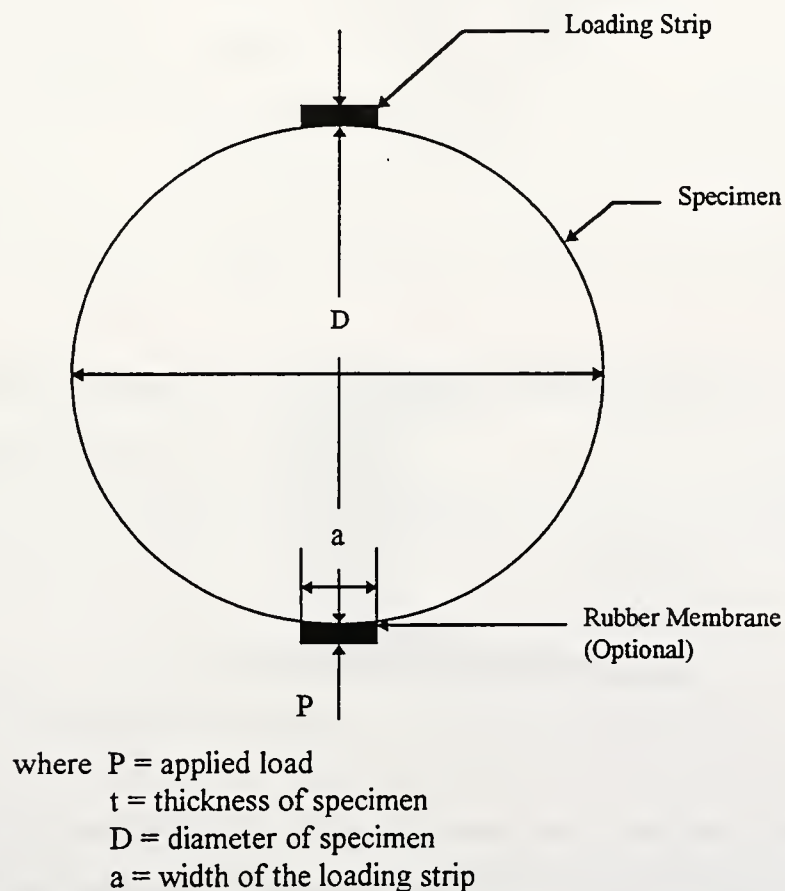
Figure 7.2 The Typical Loading Condition for Indirect Tensile Test (ASTM, 1993)
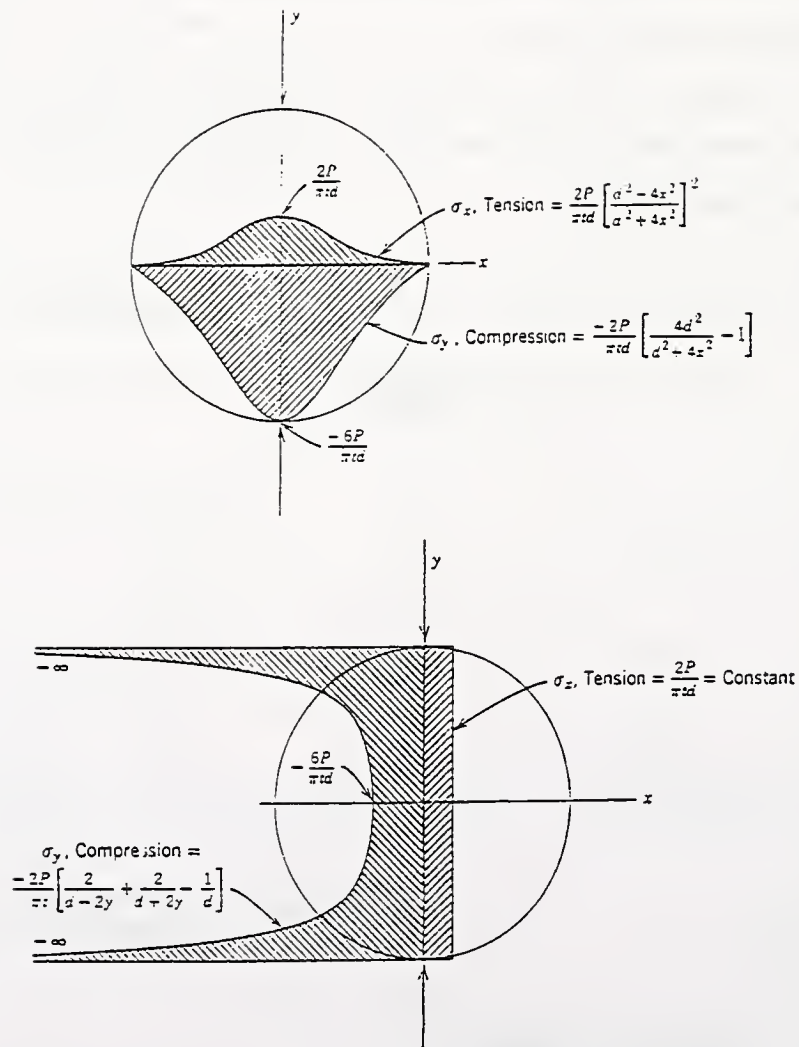
Figure 7.3 Theoretical Stress Distribution on Horizontal and Vertical Diametral Planes
for Indirect Tensile Test (Yoder and Witczak, 1975)

The equation of stress for each plane is given by equation 7.2 to 7.7:

horizontal :
$$\sigma_x = \frac{2P}{\pi dt}\left(\frac{d^2 - 4x^2}{d^2 + 4x^2}\right)^2 \qquad (7.2)$$

$$\sigma_y = -\frac{2P}{\pi dt}\left[\frac{4d^2}{d^2 + 4x^2} - 1\right] \qquad (7.3)$$

$$\tau_{xy} = 0 \qquad (7.4)$$

vertical :
$$\sigma_x = \frac{2P}{\pi dt} = \text{constant} \qquad (7.5)$$

$$\sigma_y = -\frac{2P}{\pi t}\left[\frac{2}{d - 2y} + \frac{2}{d + 2y} - \frac{1}{d}\right] \qquad (7.6)$$

$$\tau_{xy} = 0 \qquad (7.7)$$

where P : total applied load (kN)

t : specimen thickness (mm)

d : specimen diameter (mm)

x and y : coordinate values from center of specimen

These equations are presented by Frocht for idealized elastic solid (1957). The tensile strength, S_t, of the materials is determined by:

$$S_t = \frac{2P_{max}}{\pi dt} \qquad (7.8)$$

7.2 Testing Set-up and Procedures

Figure 7.4 represents an example of the installation of a specimen for a resilient modulus test. A closed loop, servo-hydraulically controlled loading system was used for the test. The MTS model 643.01 A, resilient modulus fixture, was used to determine the modulus. The specimens with 4 inch diameter and 2.5 inch height, which are compacted at the optimum binder content by Marshall equipment and Gyratory Testing Machine (GTM), were conditioned at two different testing temperature, 5°C (41°F) and 25°C

(77°F) for 24 hours prior to the test. The tests were carried out on diametrical specimens in the indirect tension mode at both testing temperatures. About 10 percent of the indirect tensile strength, 3.9 kN, was employed as an applied load. The one second repeated loading cycle (0.1 second loading and 0.9 second unloading) was applied along the vertical diameter of the test specimen for 200 seconds. The test procedures followed are in accordance with ASTM D4123-82.
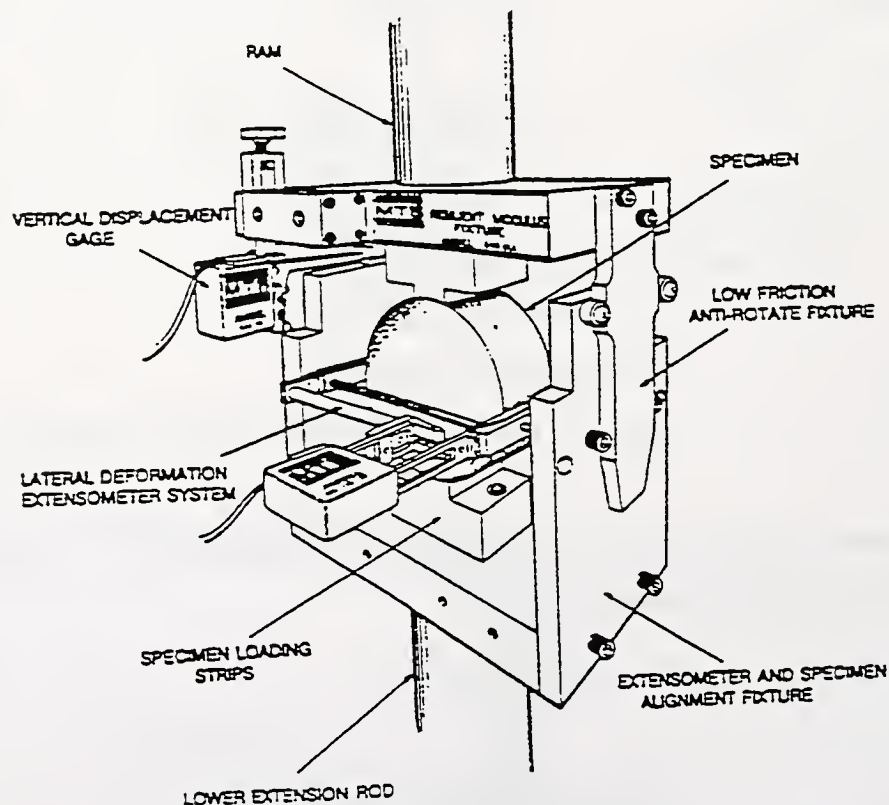
Figure 7.4 Typical Set-Up for Resilient Modulus Test (MTS, 1994)

The 810 Material Testing System (MTS) was employed to determine the indirect tensile strength. Figure 7.5 shows the detailed testing set-up. Testing was performed at 5°C, because the tensile strength at low temperature represents the cracking potential of the mixtures. A constant 1 second repeated loading cycle with 0.1 second loading and 0.9

second unloading was applied to the specimen for 50 seconds for the initial condition. The compressive loading was applied to the conditioned specimens until failure occured. The loading stroke rate of 13 mm/min (0.5 in/min) was used in accordance with SHRP recommendation (SHRP-A-379, 1994, Park, 1995). The data sampling frequency of 20 Hz was employed.
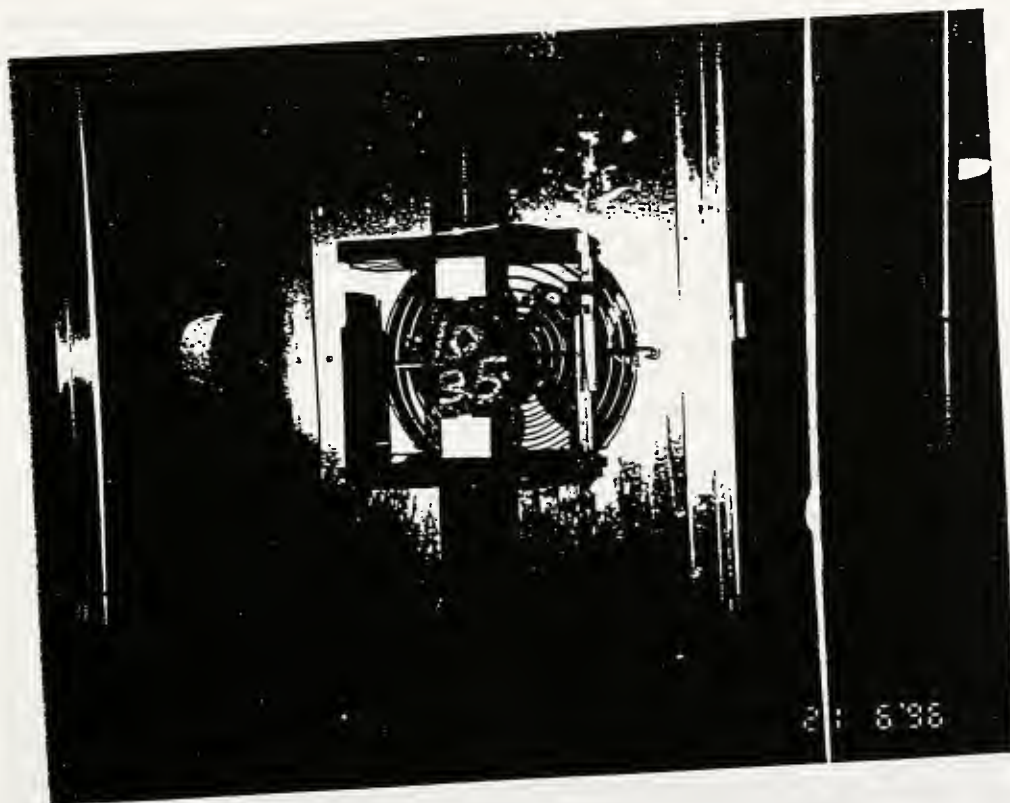
Figure 7.5 Set-Up for Indirect Tensile Test

7.3 Test Results and Discussion

7.3.1 Resilient Modulus Test

The results of the resilient modulus test for AC-10 mixtures and AC-20 mixtures are summarized in Table 7.1 and 7.2.

Table 7.1 Summary of M_R Test for AC-10 Mixtures (Unit : MPa)

Compaction		Marshall Compaction				Gyratory Compaction			
Temperature		5°C		25°C		5°C		25°C	
Addi.	%	M_R	Std.	M_R	Std.	M_R	Std.	M_R	Std.
CB	0	11.4	2.5	4.4	0.6	12.8	3.8	4.2	1.2
	5	10.8	2.6	5.2	0.6	13.2	8.4	4.2	1.5
	10	12.7	2.3	5.2	1.0	13.3	3.8	5.2	0.7
	15	14.8	7.0	7.1	1.0	13.3	8.5	5.3	0.8
	20	11.0	2.6	4.2	0.8	11.8	4.7	5.4	1.7
CB_p	5	13.9	5.7	5.2	1.0	12.3	3.8	2.7	0.6
	10	14.3	4.7	5.1	0.9	11.1	3.1	4.3	1.1
	15	15.9	5.8	5.0	0.7	14.6	3.8	3.5	0.9
	20	12.4	2.8	4.8	0.9	14.0	2.8	3.9	1.2

Table 7.2 Summary of M_R Test for AC-20 Mixtures (Unit : MPa)

Compaction		Marshall Compaction				Gyratory Compaction			
Temperature		5°C		25°C		5°C		25°C	
Addi.	%	M_R	Std.	M_R	Std.	M_R	Std.	M_R	Std.
CB	0	9.2	3.0	5.3	1.9	13.9	6.2	4.4	1.6
	5	13.8	6.5	5.7	1.9	14.5	5.0	5.8	1.6
	10	14.0	6.4	6.3	1.2	13.1	1.8	4.9	1.9
	15	15.6	7.2	5.5	16	12.5	1.9	4.9	2.3
	20	12.2	5.0	6.3	1.2	14.9	7.0	6.7	2.1
CB_p	5	11.1	4.7	6.3	2.6	14.5	6.4	5.0	1.5
	10	14.4	9.4	6.2	1.5	14.8	6.1	5.5	1.2
	15	15.8	7.5	8.7	1.2	13.9	6.5	5.3	1.9
	20	10.9	2.0	6.2	1.4	12.9	5.9	4.8	1.7

Temperature

In this study, two different testing temperature, 5°C and 25°C, were employed. The M_R at 5°C for both compacted specimens increases up to 15%, and then decreases, as the content of CB or CB_p increases. The M_R at 25°C shows a similar trend to M_R at 5°C. The measured M_R for all the cases at both temperatures is around 13 MPa and 5 MPa, respectively. As was expected, the M_R at low temperature is regularly 3 times larger than at high temperature. Figure 7.6 shows an example for the M_R as the testing temperature change. The Marshall compacted samples show larger rates of changes for M_R than the gyratory compacted specimens.

Asphalt Grade

Table 7.3 shows the comparison of the effect of asphalt grade for M_R with same testing temperature, additives, and compaction method. The M_R for AC-20 mixtures is always higher than for AC-10 mixtures. The main reason should be that AC-20 asphalt is harder than AC-10 asphalt. According to the results of the binder study conducted by Zeng and Lovell (1995), AC-20 asphalt showed lower penetration value, higher softening point, and ductility than AC-10 asphalt. If the other testing conditions are same, the grade of asphalt should have a significant effect on the M_R of the mixtures.

Table 7.3 Summary of the Effect of the Asphalt Grade

Additive	Marshall Compaction		Gyratory Compaction	
	5°C	25°C	5°C	25°C
CB	AC10 < AC20	AC10 < AC20	AC10 < AC20	AC10 < AC20
CB_p	AC10 < AC20	AC10 < AC20	AC10 < AC20	AC10 < AC20
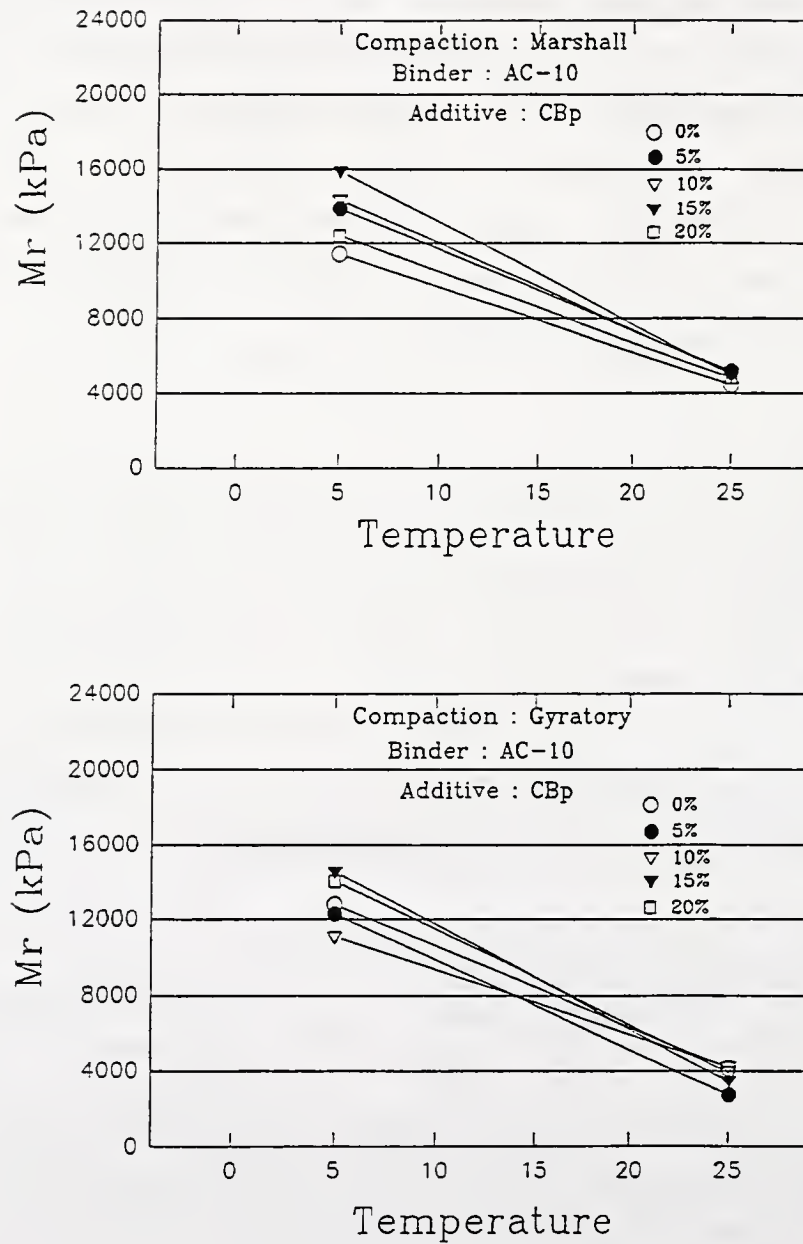
Figure 7.6 Temperature Susceptibility for AC-10 CB$_p$ Mixtures

Compaction Method

Table 7.4 shows the effect of different compaction method for M_R. The M_R for Marshall compacted specimens is higher than the gyratory compacted specimens at high temperature, 25°C. The possible reason would be the effect of crushed aggregate, which can make higher friction in the mixtures, during the compaction. On the other hand, the M_R for gyratory compacted specimens, except AC-10 CB_p mixtures, is higher than for Marshall compacted specimens. The possible reason would be the orientation of aggregate particles, which can make for tighter mixtures, during the compaction. As was seen in Table 7.1, the standard deviation of M_R for gyratory compacted specimens is less than that for Marshall compacted specimens. According to a recent study of Asphalt-Aggregate Mixture Analysis System (AAMAS), (Von Quintus and Kennedy, 1988), the gyratory compaction proved to simulate field condition, especially field particle orientations. Considering these results, the use of M_R for Marshall compacted specimens is overestimated at high temperature and underestimated at low temperature.

Table 7.4 Summary of the Effect of the Compaction Method

Additive	AC-10		AC-20	
	5°C	25°C	5°C	25°C
CB	M* < G**	M > G	M < G	M > G
CB_p	M > G	M > G	M < G	M >G

* Marshall compaction and ** gyratory compaction

Additives

Table 7.5 shows the effect for different additives, CB and CB_p. For AC-10 mixtures, the M_R for CB_p mixtures is higher at low temperature than for CB mixtures, however, it is less at high temperature than for CB mixtures. For AC-20 mixtures, there is no general trend.

Table 7.5 Summary of the Effect of the Additives

Binder	AC-10		AC-20	
Temperature	5°C	25°C	5°C	25°C
Marshall	$CB < CB_p$	$CB > CB_p$	$CB > CB_p$	$CB < CB_p$
Gyratory	$CB < CB_p$	$CB > CB_p$	$CB < CB_p$	$CB > CB_p$

7.3.2 Indirect Tensile Test

Applied force (kN) and vertical displacement (mm) were measured during the testing. The testing data were automatically collected by Automatic Testing System (ATS, Ver. 3.12). An example of the results of indirect tensile test, including raw data at failure and failure mode, is shown in Figure 7.7. The failure of the asphalt mixtures occurred within 10 seconds after test began in all the cases. The tensile strength of the asphalt mixtures were calculated by using Equation 7.8. Table 7.6 and 7.7 summarize the results for tensile strength of the mixtures.
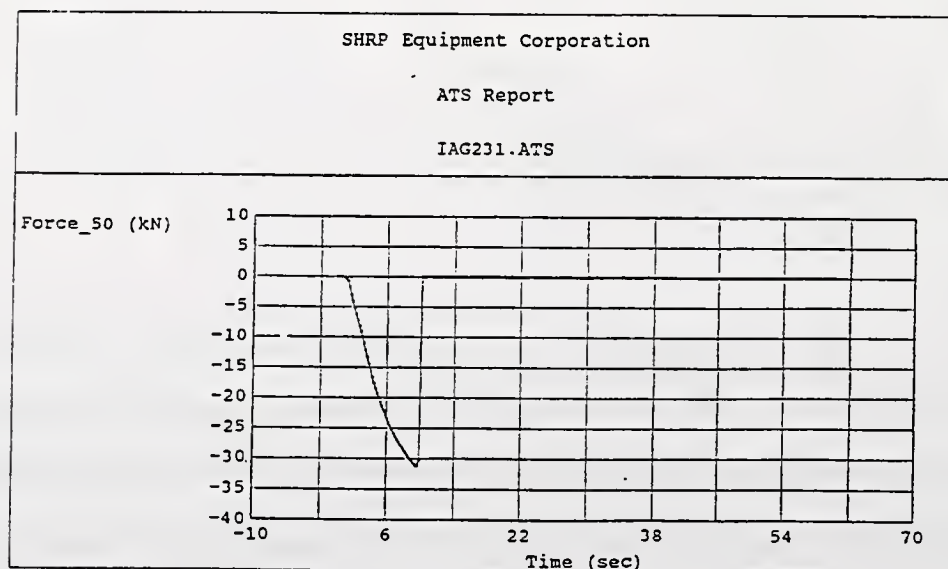
Figure 7.7 Result of AC-20 + 10 % CB_p Mixtures

Table 7.6 Summary of the Tensile Strength for AC-10 Mixtures

Compaction		Marshall Compaction			Gyratory Compaction		
Add.	%	Load (kN)	S_t (kPa)	Std.	Load (kN)	S_t (kPa)	Std.
CB	0	28.0	2506	438	31.2	272	39
	5	31.5	2827	95	33.0	2905	63
	10	31.9	2848	89	36.2	3234	301
	15	37.9	3422	42	37.9	3368	126
	20	36.8	3290	201	38.2	3390	138
CB_p	5	31.0	2766	115	33.8	2992	39
	10	34.3	3048	189	35.8	3172	204
	15	34.7	3051	202	35.2	3059	173
	20	35.2	3086	281	33.0	2827	82

Table 7.7 Summary of the Tensile Strength for AC-20 Mixtures

Compaction		Marshall Compaction			Gyratory Compaction		
Add.	%	Load (kN)	S_t (kPa)	Std.	Load (kN)	S_t (kPa)	Std.
CB	0	35.2	3120	375	35.0	3109	303
	5	33.5	3004	360	36.6	3262	193
	10	36.7	3293	216	36.4	3231	330
	15	39.6	3550	106	36.4	3209	381
	20	39.2	3509	80	37.7	3302	331
CB_p	5	37.2	3328	153	37.6	3344	111
	10	37.2	3309	304	38.2	3379	126
	15	36.6	3241	177	37.4	3253	157
	20	39.1	3446	195	34.8	2987	169

Asphalt Grade

As can be seen in Figure 7.8, the tensile strength of AC-20 mixtures are higher than those of AC-10 mixtures at low temperature. This is the same relation as for resilient modulus tests.

Compaction Method

The variation of tensile strength for the gyratory compacted specimens is less than that for the Marshall compacted specimens. This relation is similar to resilient modulus tests. It means that gyratory compaction shows better reproducibility than the Marshall compaction. For AC-10 mixtures, the tensile strength for the gyratory compacted specimens is slightly higher than that for the Marshall compacted specimens. However, in the case of AC-20 mixtures, the tensile strength is not significantly different for either compaction method.

Additives

The tensile strength of CB_p mixtures for both asphalt grade and compaction method is higher than that of CB mixtures at relatively low additive content, up to 10 %. On the other hand, the tensile strength of CB mixtures is higher than that of CB_p mixtures at high content of additives. The possible reason would be that a large amount of CB_p could reduce the effective asphalt film thickness in the mixtures, because CB_p with large particle size acts like mineral filler and fine aggregate. However, CB become a part of asphalt cement due to its small particle size when it added into asphalt cement. Therefore, the inclusion of CB does not make any change of the effective asphalt film thickness.
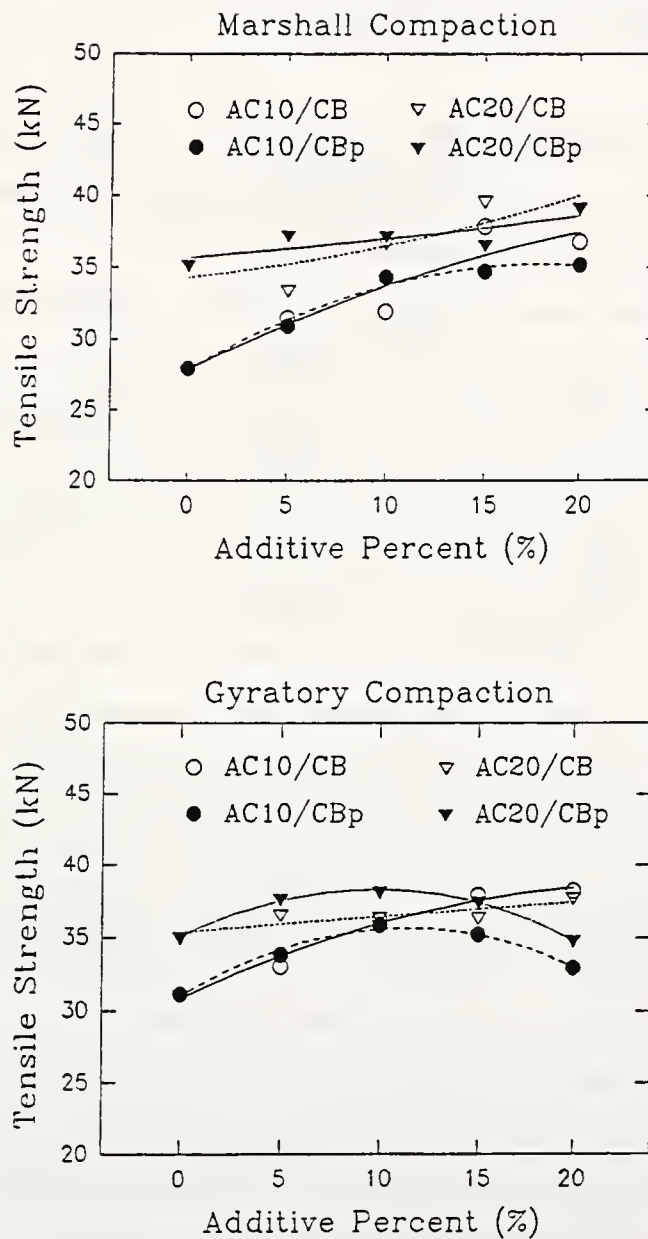
Figure 7.8 Summary of the Tensile Strength

7.4 Conclusions

Based on the laboratory test for resilient modulus and indirect tensile strength, the following principal conclusions can be drawn:

- The M_R at low temperature, 5°C, is around 2 to 3 times larger than at high temperature, 25°C. The rate of change of M_R is larger for Marshall compacted specimens than for gyratory compacted specimens.

- The grade of asphalt cement has a significant effect on the M_R and tensile strength of the mixtures. The higher asphalt grade, the higher M_R and tensile strength.

- The effect of compaction method for the M_R is relatively significant. The Marshall compaction shows relatively poor reproducibility, however, gyratory compaction does not. The use of M_R for Marshall compacted specimens is overestimated at high temperature and underestimated at low temperature.

- The inclusion of CB and CB_p produces an increase of M_R and tensile strength. In the case of AC-10 mixtures, CB_p can produce a more dominant difference than CB at low temperature, however, CB is better than CB_p at high temperature.

- Tensile strength of CB_p mixtures up to 10 %, is better than CB mixtures. However, that of CB mixtures, larger than 10 %, is better than CB_p mixtures. The tensile strength of the mixtures would depend on the effective asphalt film thickness of the mixtures.

CHAPTER 8
DYNAMIC CONFINED CREEP TEST

8.1 Introduction

The main purpose of the creep test is to evaluate the susceptibility for deformation and to determine the creep modulus at long loading duration for use in thermal cracking and rutting analysis (Von Quintus and Kennedy, 1988). Rutting or permanent deformation has long been recognized as one of major failure modes that are associated with channelized traffic. The types of rutting are rigorously divided into four categories:

- shear failure

- consolidation rutting (due to poor compaction)

- plastic flow rutting (due to squeezing material under the load)

- pavement surface wear (due to abrasion of the surface under traffic)

Overall stress conditions and mix composition are the major reasons for permanent deformation of asphalt mixes. Permanent deformation in the form of rutting should become more significance for heavy duty highway pavements due to the increased number of repetitions of heavy axle loads and increased tire pressure up to 830 kPa (120 psi). There are many factors which influence the creep modulus, such as thermal cracking, fatigue cracking, permanent deformation, and moisture damage (Von Quintus and Kennedy, 1988). Figure 8.1 shows the importance rating for the effect of the creep modulus on pavement distress. Among them, thermal cracking and permanent deformation are highly dominant effects for creep modulus on pavement distress.
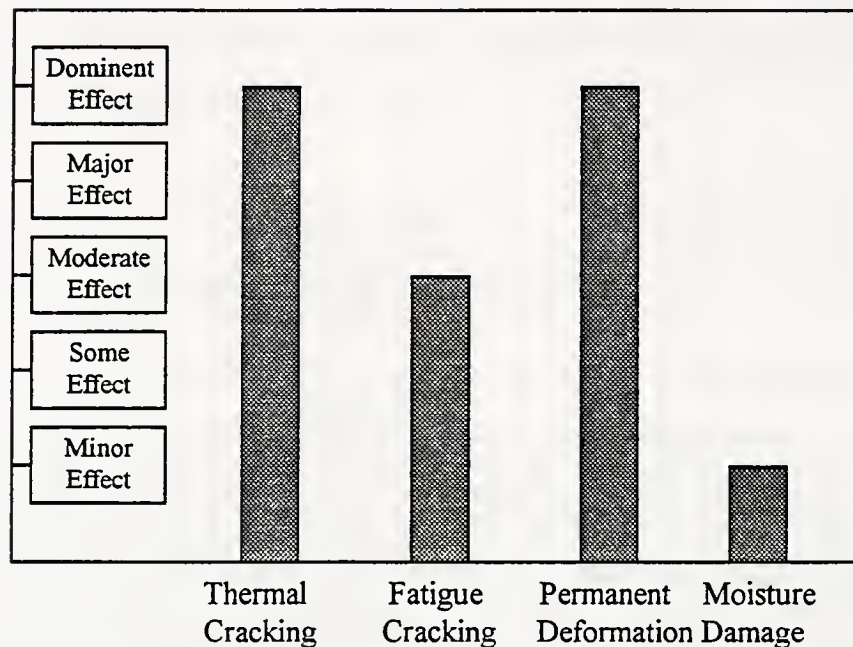
Figure 8.1 Effect of the Creep Modulus on Pavement Distress (Von Quintus and
Kennedy, 1988)

8.2 Concept of the Creep Deformation in Asphalt Concrete

The continuous time-dependent deformation under constant stress or load is
called creep (Bolk, 1981). Inherent to engineering materials is the characteristic to
undergo some level of deformation when subjected to an externally applied load, and the
deformation continues indefinitely as the load remains. A popular generalized form used
to illustrate the various stages of creep is shown in Figure 8.2. Creep strain for a given
stress level is plotted versus elapsed time and the creep strain is devided into three
stages. In the primary stage the rate of deformation increases very rapidly. In steady
state region, the deformation rate is constant, as are the angle of slope and rate of
deformation. The third region is the failure stage, in which the deformation again
increases rapidly (Little et al., 1994).
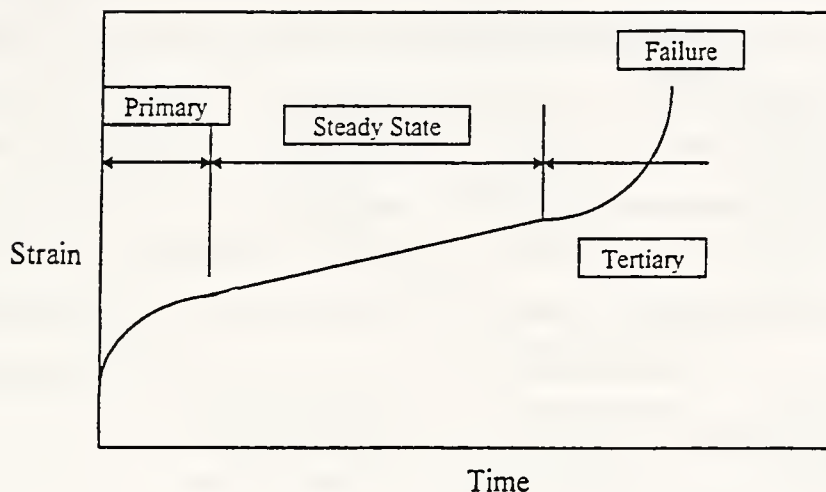
Figure 8.2 A Popular Generalized Form of Creep Behavior (Little et al., 1994)

Asphalt concrete is composed of a three-dimensional particle skeleton (solid), a viscous mortar matrix (fluid), and air-filled voids (gaseous) (Huschek, 1985). The principle of the internal structure, a three-phase system, is illustrated in Figure 8.3. Asphalt concrete is usually defined as a viscoelastic material. With viscoelastic materials, the longer the time to reach the final value of stress (lower stress rate), the large is the corresponding strain. In order to explain the viscoelastic material, a number of different models have been suggested, such as linear viscoelastic model, mathematical models, Maxwell model, Kelvin model, Van der Poel model, Brugers model, and so on. Among them, the Burgers model is considered as the best representation for the behavior of asphalt concrete. Figure 8.4. shows the behavior of the Burgers model. The creep behavior in the Burgers model is described in equation 8.1.

$$\varepsilon(t) = \frac{\sigma_0}{E_1} + \frac{\sigma_0 * t}{\eta_1} + \frac{\sigma_0}{E_2}\left(1 - e^{\frac{-E_2 * t}{\eta_2}}\right) \tag{8.1}$$

where σ_0 : applied stress

E_1 and E_2 : spring constant

η_1 and η_2 : Newtonian dashpot

possible shear plane
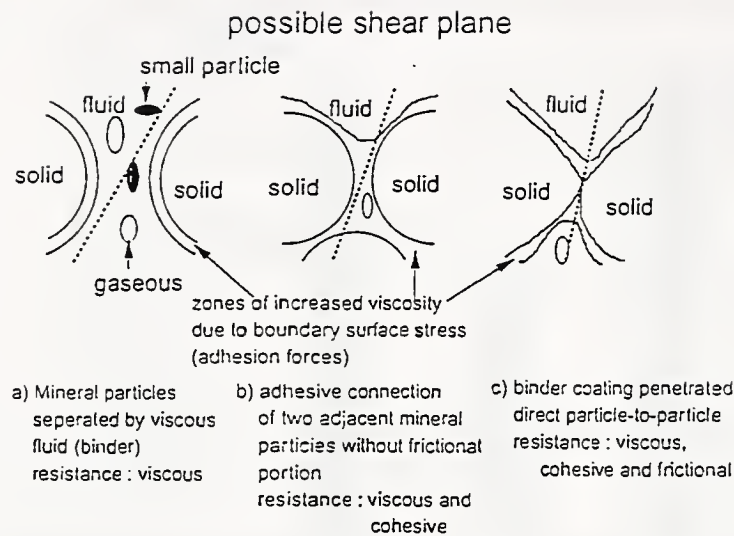
Figure 8.3 Illustration for the Internal Structure of a Three-Phase System (Huschek, 1985)

Equation 8.1 shows that the application of a stress, σ_0, induces an instantaneous elastic strain, σ_0/E_1, followed by an additional retarded elastic strain and an indefinite viscous flow. If the stress is released at some time t_1, an immediate elastic recovery equal to σ_0/E_1 takes place, followed by gradual decrease in the strain to a permanent value of $(\sigma_0 t_1/\eta)$. The Brugers model shown in Figure 8.4 is thought to give the best model representation for the behavior of sol-gel asphalt (Gabrielson, 1992).

With the Burgers model as a background, Perl et al. (1983) suggested that the total strain (ε_t) of asphalt concrete is composed of four components;

- ε_e : elastic strain
- ε_p : plastic strain
- ε_{ve} : viscoelastic strain
- ε_{vp} : viscoplastic strain.

Elastic and plastic strain are time independent, however, viscoelastic and viscoplastic plastic strain are time dependent. While elastic and viscoelastic strain are recoverable, plastic and viscoplastic strain are irrecoverable. Figure 8.5 illustrates the creep behavior

of asphalt concrete. The quantity t_1 is referred to as the loading duration and $t_2 - t_1$ is referred to as the rebounding duration. When the load is applied at $t = t_0$, a strain (ε_0) is generated immediately. This strain consists of the elastic and plastic components as shown in Figure 8.5. During the loading duration ($t_0 < t < t_1$), the strains containing viscoelastic and viscoplastic are incurred. If the load is removed ($t = t_1$), the elastic strain is recovered immediately. In the rebound period ($t_1 < t < t_2$), the viscoelastic strain is recovered. It can be observed from Figure 8.5 that at the end of the rebound period, the permanent creep strain consists of the irrecoverable plastic and viscoplastic strain.
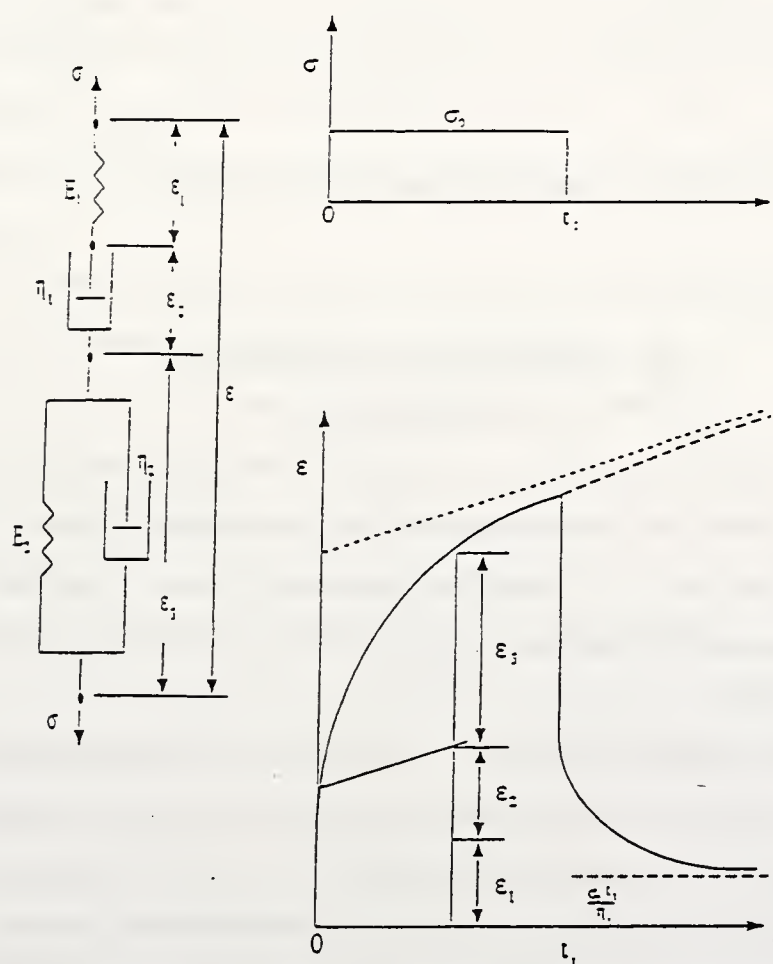
Figure 8.4 Behavior of the Burgers Model (Gabrielson, 1992)
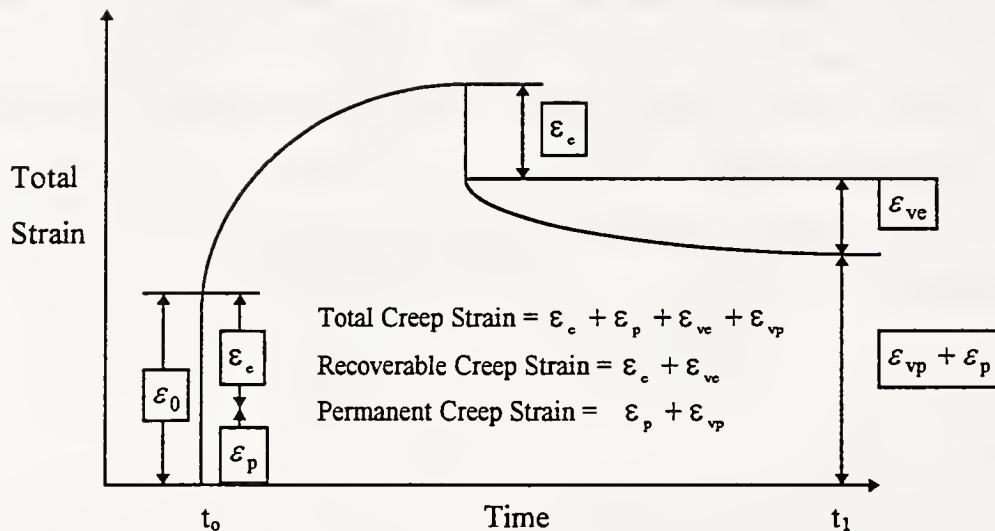
Figure 8.5 Creep Behavior of Asphalt Concrete (Perl et al., 1983)

8.3 Testing Equipment and Procedure

8.3.1 Testing Equipment

Creep testing was carried out on a Material Test System (MTS), feed back control hydraulic tester with a temperature controlled environmental chamber. A MTS model 810 was employed as a loading and measuring device. Automated Testing System (ATS) software collected and analyzed the testing data. Figure 8.6 shows the schematic of the Material Test System.

The front panel of the MTS is composed of four different panels; the oscilloscope, the temperature controller, the analog chassis, the hydraulic control, as can be seen in Figure 8.6. The oscilloscope, Tektronix 2225, 50 Mhz oscilloscope provides a visual check that the appropriate test frequency is applied throughout the test.

The temperature controller is described in the MTS manual (1994) as, "the microprocess based MTS 409.80 temperature controller is used for controlling the

environmental chamber. The control module for the temperature controller receives a thermocouple input and process as the heating or cooling so that the environmental chamber supplies the necessary temperature for testing. A block diagram of the temperature controller and the environmental chamber are shown in Figure 8.7. A 497.01 analog chassis with the 497 modulus installed is shown in Figure 8.8. The chassis contains 16 user slots and two dedicated bud board slots. The module provides interlock control, communication, transducer conditioning, and valve drive. The interlock controller allows test stations to have independent interlock and hydraulic status signals. The microprocessor based communication module provides data conversion between the system host and module residing on the 497 parallel bus. The function provided by the transducer conditioning are transducer excitation and output signal amplification. Both low and high level transducers can be used by the installation of AC/DC conditioners. Valve drivers provide drive current for servovalves according to command inputs received from each channel. Critical parameters are programmed through the 497 chassis bus.

The 497.05 hydraulic control panel is used to control hydraulic power supply. The functions provided by the hydraulic control panel are below:

- control of up to four independent hydraulic service manifolds
- hydraulic power supply control
- interlock shutdown and latched indicators to show interlock status
- programmable interlock station assignment
- electrical power outputs to the hydraulic service manifolds and a 497.01 analog chassis.

The hydraulic control panel functions are controlled by its front panel controls or by the host computer."
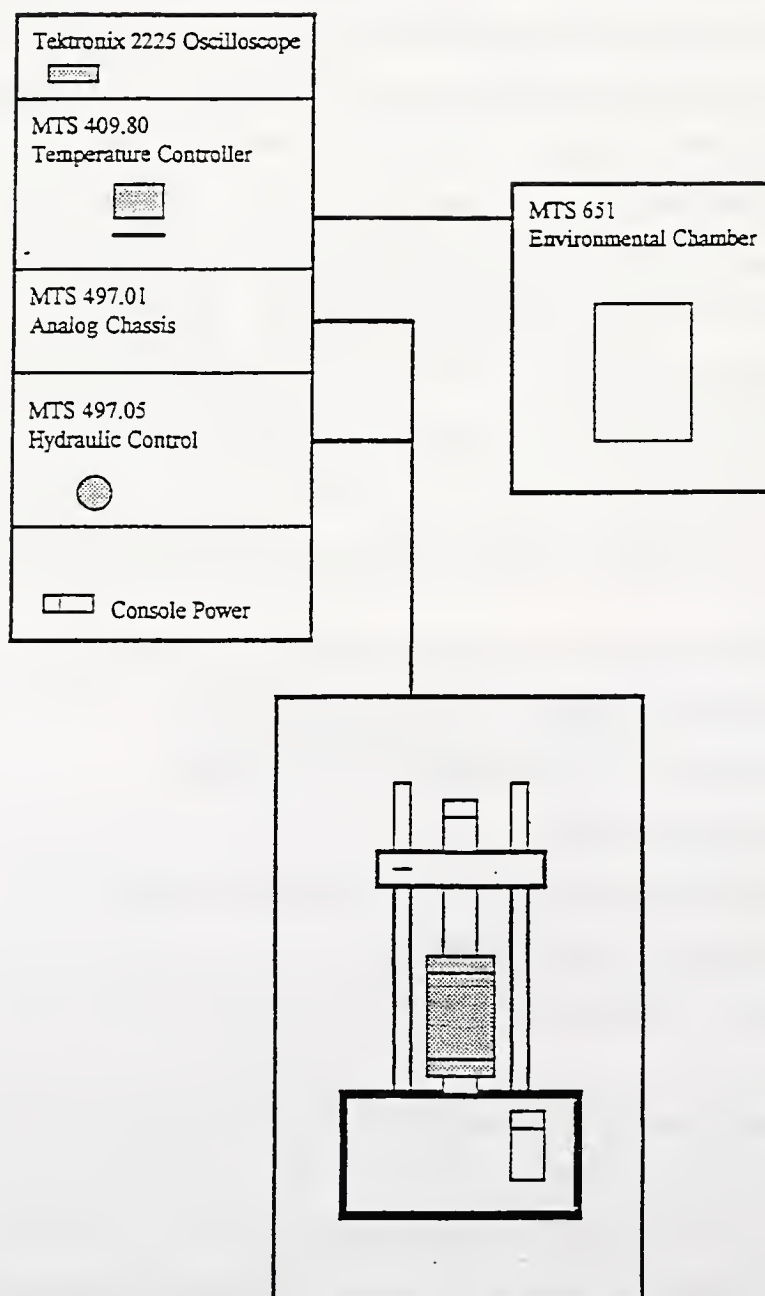
Figure 8.6 Schematic of the Material Test System (Park, 1995)
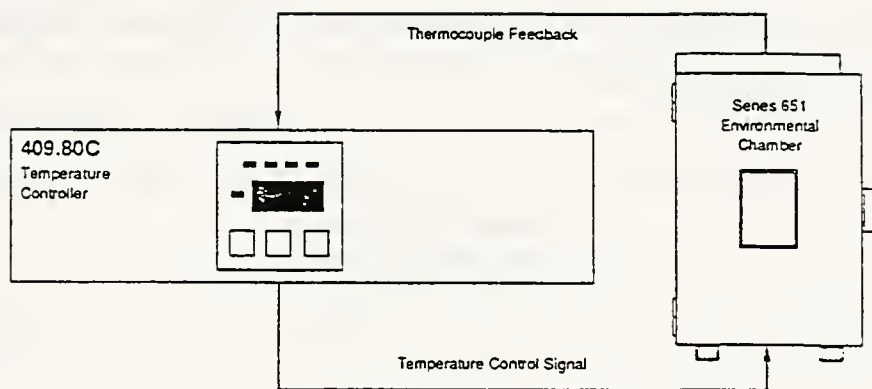
Figure 8.7 A Block Diagram of the Temperature Controller and the Environmental Chamber (MTS, 1994)
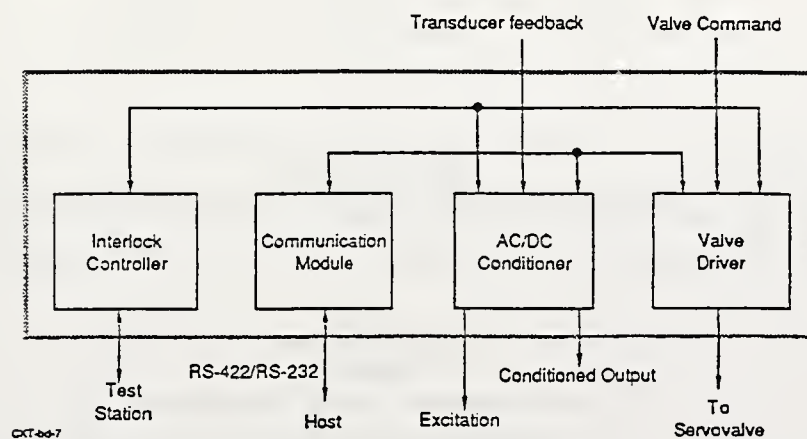
Figure 8.8 A 497.01 Analog Chassis with the 497 Modulus (MTS, 1994)

8.3.2 Testing Procedure

An extensive study on various creep tests has been conducted by Gabrielson (1992). According to the recommendation by Gabrielson, a dynamic confined creep test can simulate the field condition fairly well. The test procedure employed in this study was followed in accordance with recommendations by Gabrielson, although some modification were made as needed.

```
┌─────────────────────────────────┐
│      Sample Dimensions          │
│      Diameter : 10.16 cm        │
│       Height : 6.80 cm          │
└─────────────────────────────────┘
                │
                ▼
┌─────────────────────────────────┐
│         Sample Setup            │
│   Testing Temperature : 50°C    │
│  Heat sample in oven for 2.5 hours │
└─────────────────────────────────┘
                │
                ▼
┌───────────────────────────────────────────────┐
│            Initial Conditioning               │
│  Apply 137.9 kN/m² confining pressure         │
│  Apply 0.084 kN normal resistance load        │
│  Apply 30 cycles at 0.559 kN axial (0.1 sec load +0.9 sec unload) │
│  Rest 10 seconds at resistance load (0.084 kN) │
└───────────────────────────────────────────────┘
                │
                ▼
┌───────────────────────────────────────────────┐
│               Main Loading                    │
│ Apply 3600 cycles at 6.701 kN axial (0.1 sec load +0.9 sec unload) │
└───────────────────────────────────────────────┘
                │
                ▼
┌───────────────────────────────────────────────┐
│                 Unloading                     │
│  Rest 15 minutes at 0.084 kN resistance load  │
└───────────────────────────────────────────────┘
                │
                ▼
        ┌───────────────────┐
        │    End of Test    │
        └───────────────────┘
```

8.3.3 Testing Specimen

According to the Marshall testing results, the testing specimens were prepared at each optimum asphalt content and at 6% of air voids. The testing specimens with 4 inch diameter were compacted with 75 blows per face, which simulates high traffic volume. However, it was very difficult to make specimens with exactly 6% of air voids due to the relatively poor reproductibiity of Marshall method. The deviation of voids was limited to ± 1.0%. Table 8.1 shows the air-voids of each specimen prepared for the test. Every value shown in Table 8.1 is the average of three mixtures for each binder content.

Table 8.1 The Summary of Air-Voids of Testing Specimens

Compaction		Marshall				Gyratory			
Binder		AC-10		AC-20		AC-10		AC-20	
Additive		VTM	Std.	VTM	Std.	VTM	Std.	VTM	Std.
	0%	6.16	0.29	6.42	0.17	7.03	0.21	6.51	0.28
CB	5%	5.53	0.24	6.21	0.61	6.76	0.52	6.65	0.20
	10%	6.03	0.10	6.09	0.27	5.93	0.38	6.29	0.35
	15%	5.50	0.12	5.88	0.79	6.18	0.31	6.85	0.12
	20%	5.70	0.51	5.53	0.05	6.43	0.41	6.66	0.29
CB_p	5%	6.58	0.62	5.87	0.50	6.69	0.18	5.86	0.82
	10%	5.56	0.43	5.48	0.08	5.92	0.29	5.88	0.12
	15%	6.45	0.24	5.81	0.15	6.65	0.17	6.19	0.25
	20%	5.55	0.35	5.28	0.12	6.89	0.12	6.64	.021

8.4 Creep Strain of Mixtures

The creep strains of mixtures were measured at 1-hour increments. The summarized creep strains for each mixture are shown in Table 8.2 and Table 8.3, and from Figure 8.9 to 8.14.

Table 8.2 Summary of Creep Strains for Mixtures at 50°C

Compaction		Marshall		Gyratory	
Binder		AC-10	AC-20	AC-10	AC-20
	0 %	0.0168	0.0174	0.0466	0.0228
CB	5 %	0.0108	0.0163	0.0295	0.0212
	10 %	0.0135	0.0083	0.0157	0.0145
	15 %	0.0092	0.0117	0.0123	0.0167
	20 %	0.0102	0.0090	0.0111	0.0112
CB$_p$	5 %	0.0140	0.0104	0.0294	0.023
	10 %	0.0112	0.0078	0.0292	0.0210
	15 %	0.0073	0.0082	0.0276	0.0210
	20 %	0.0128	0.0078	0.0161	0.0138

Table 8.3 Summary of Creep Strains for Mixtures at 25°C

Compaction		Marshall		Gyratory	
Binder		AC-10	AC-20	AC-10	AC-20
	0 %	0.0077	0.0062	0.0069	0.0058
CB	10 %	0.0051	0.0050	0.0079	0.0076
	20 %	0.0041	0.0041	0.0058	0.0050
CB$_p$	10 %	0.0058	0.0048	0.0079	0.0077
	20 %	0.0042	0.0037	0.0076	0.0040
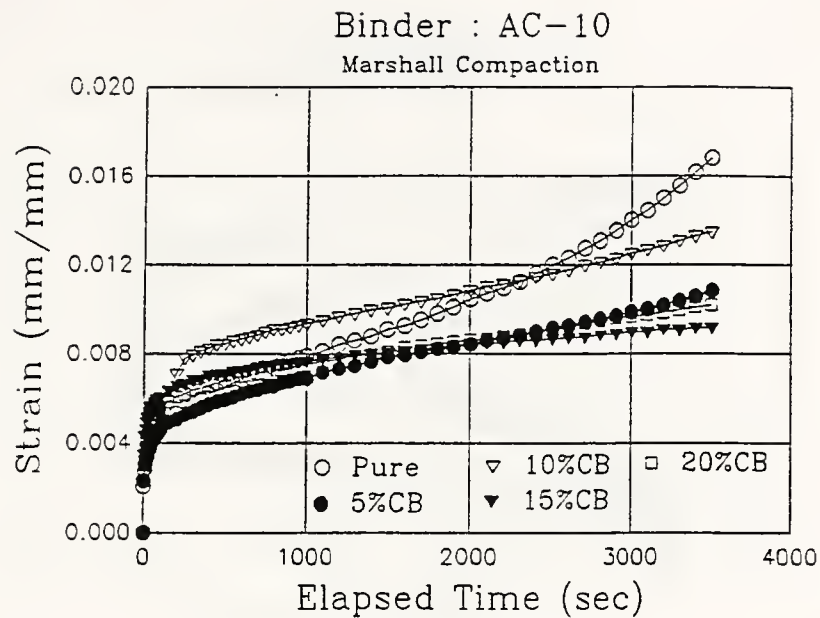
Figure 8.9 Summary for AC-10 Mixture Compacted Marshall Compactor at 50°C

Binder : AC-10
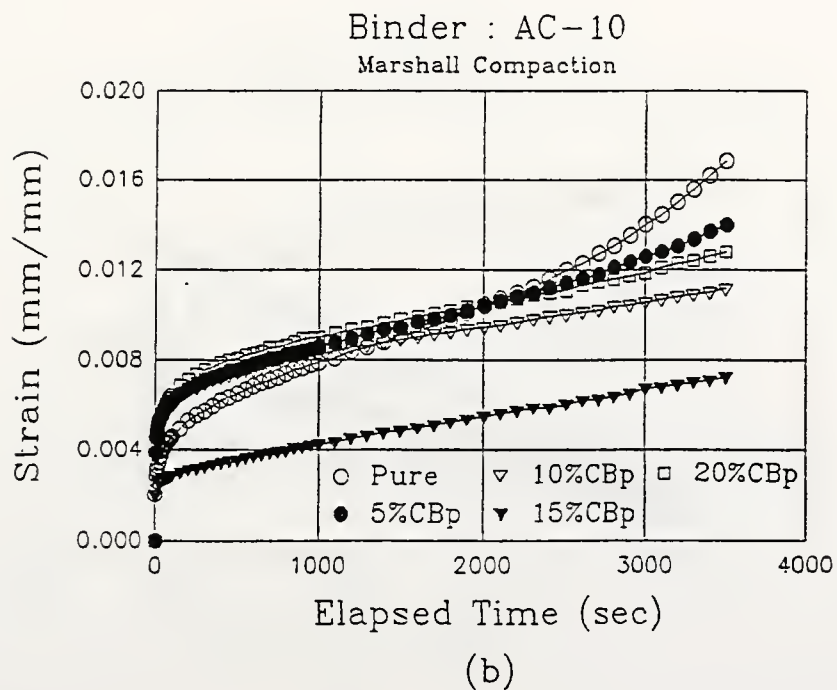Gyratory Compaction

(a)

Binder : AC-10
Gyratory Compaction
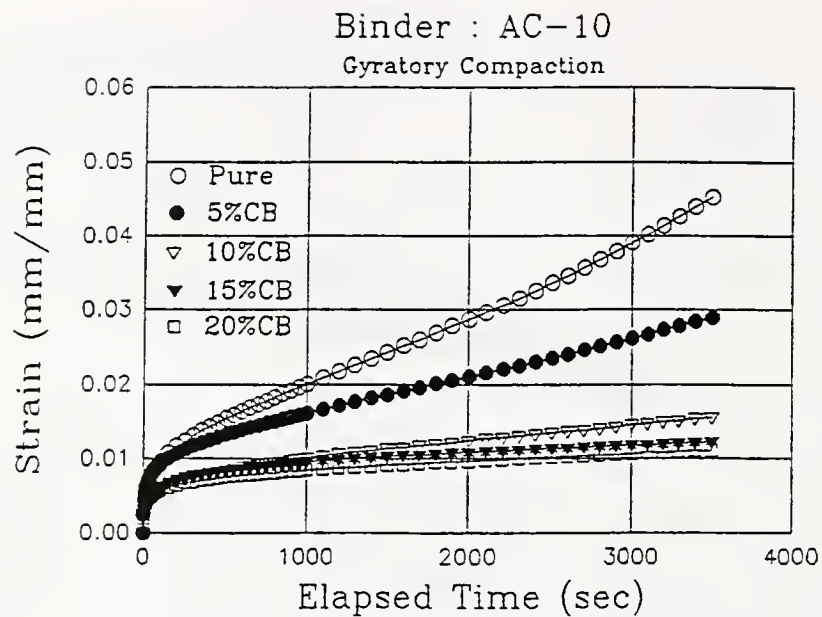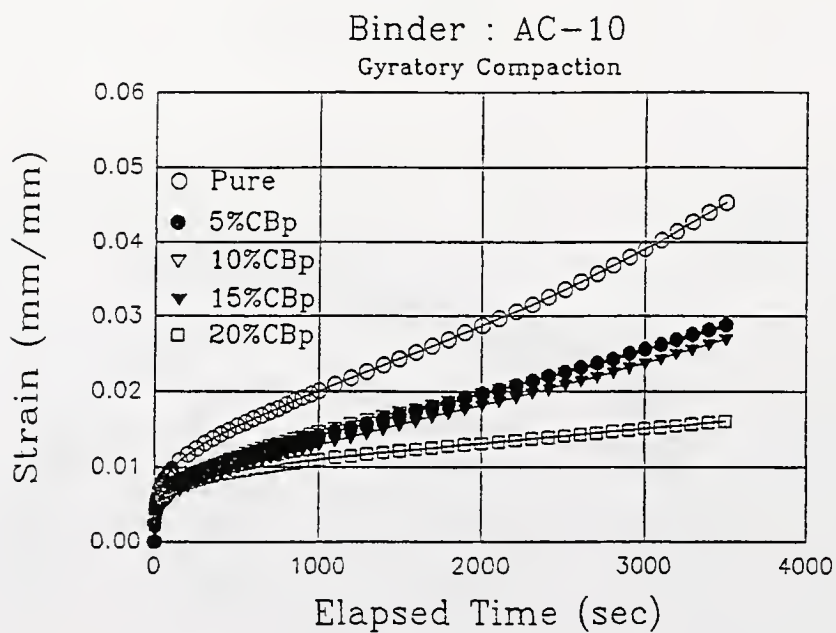
(b)

Figure 8.10 Summary for AC-10 Mixture Compacted Gyratory Compactor at 50°C

Figure 8.11 Summary for Creep Strain at 25°C

Figure 8.12 Summary for AC-20 Mixture Compacted Marshall Compactor at 50°C

Binder : AC−20

Gyratory Compaction

(a)

Binder : AC−20

Gyratory Compaction

(b)
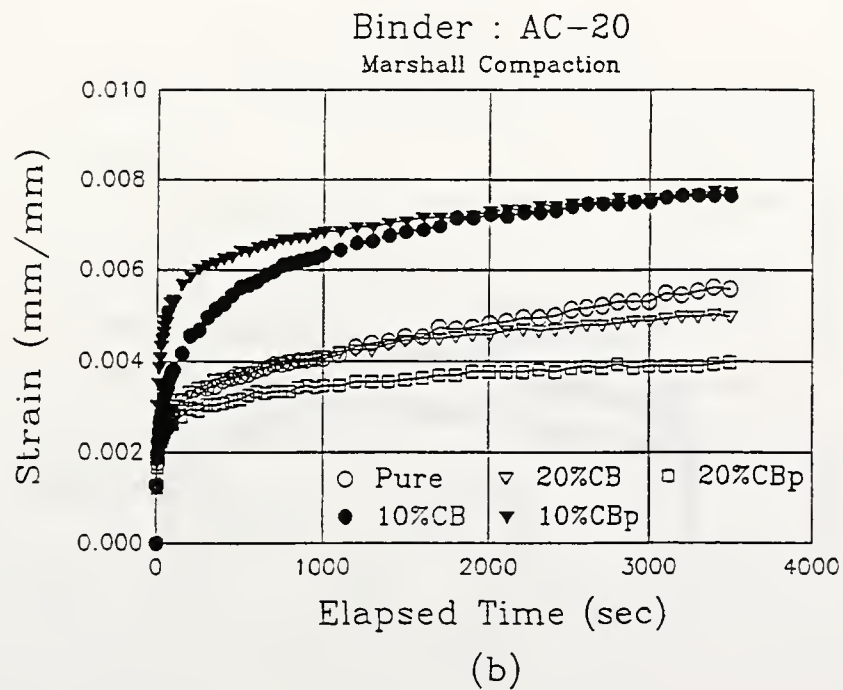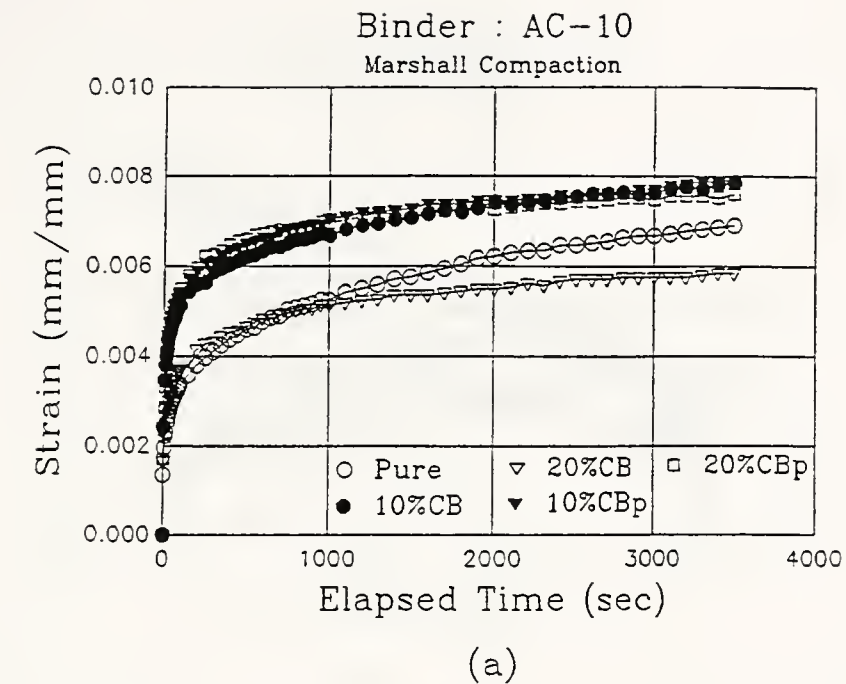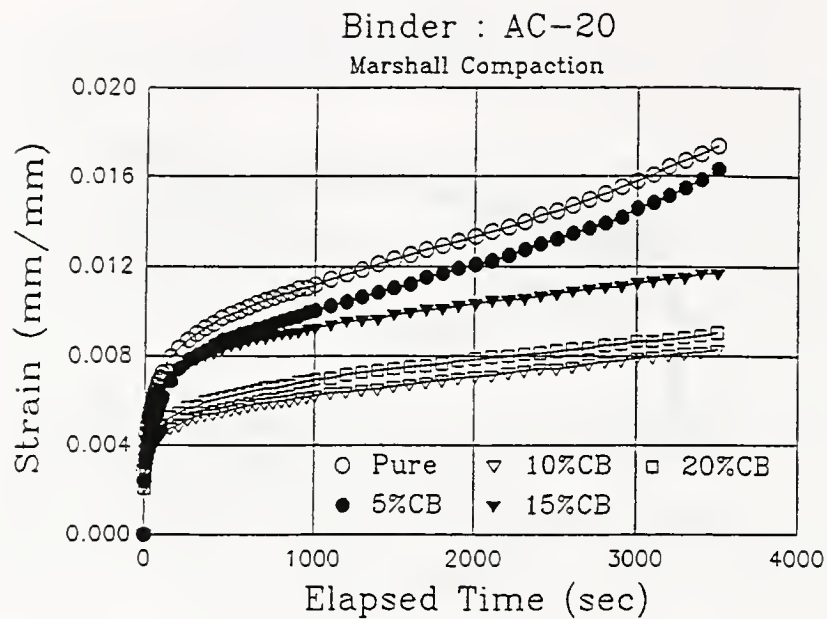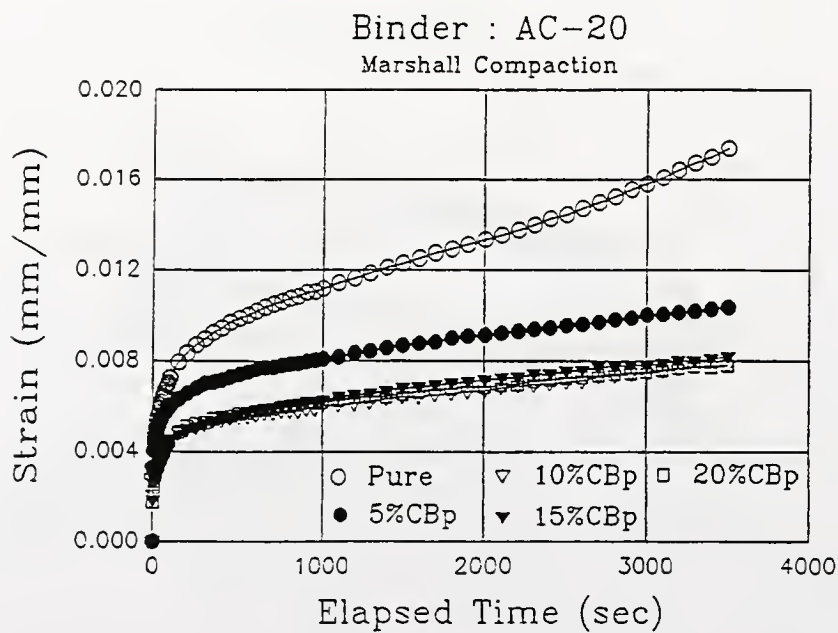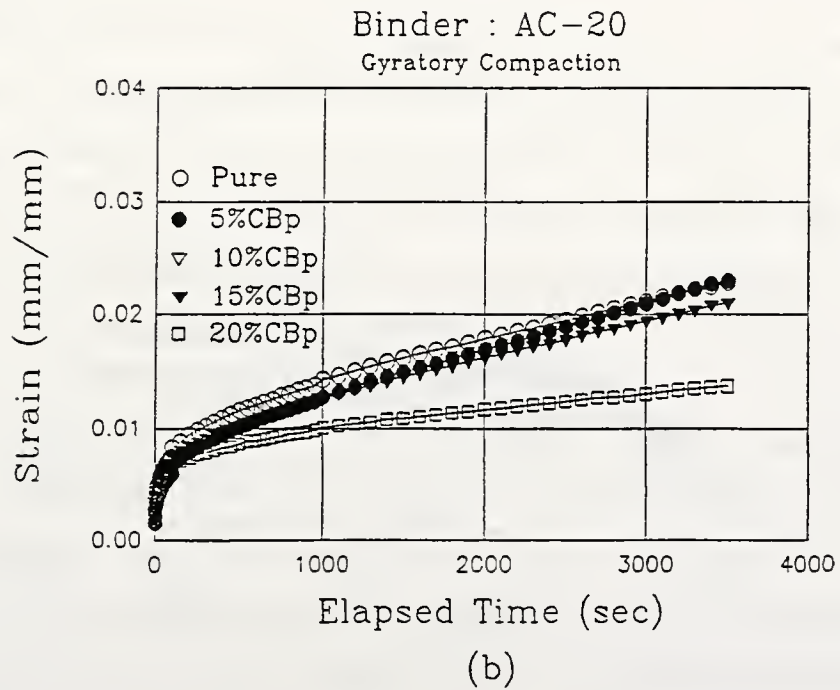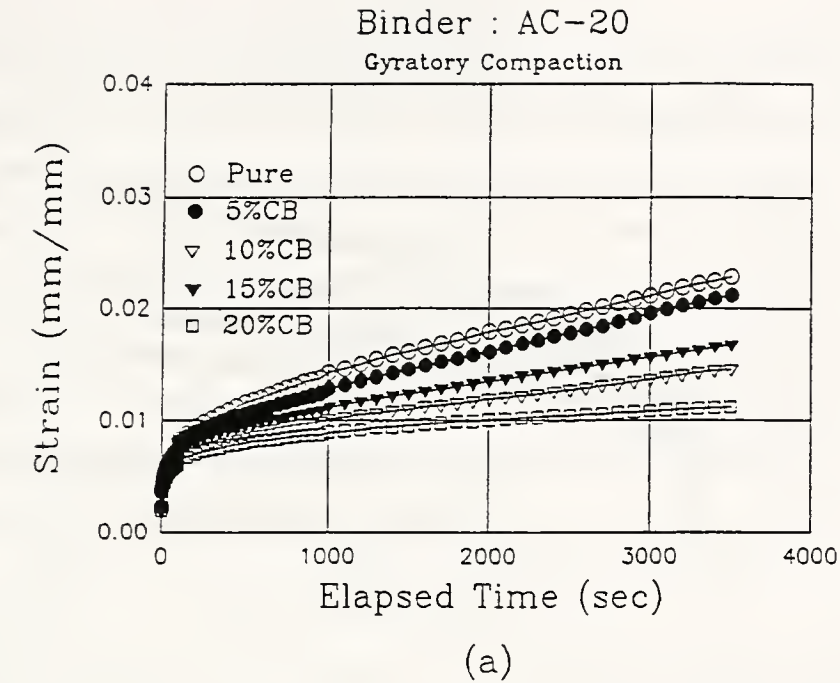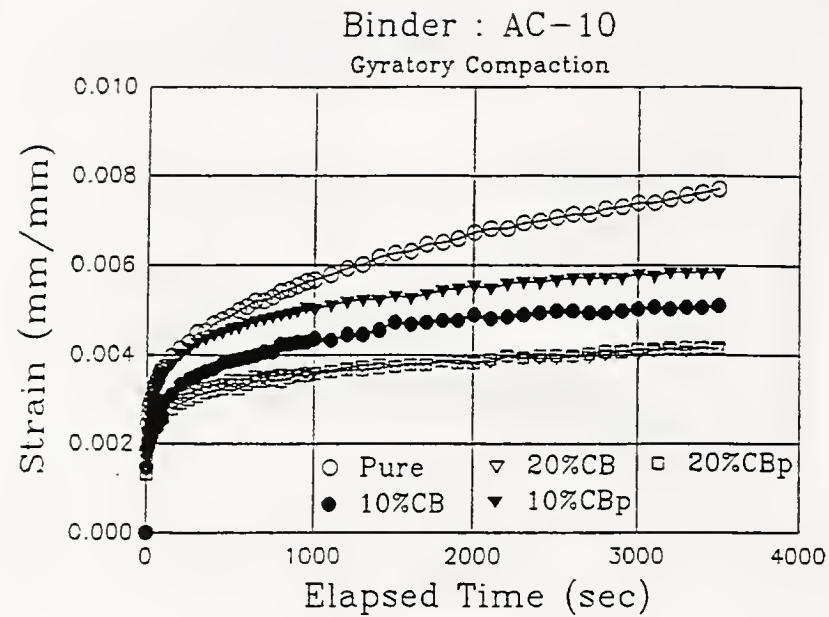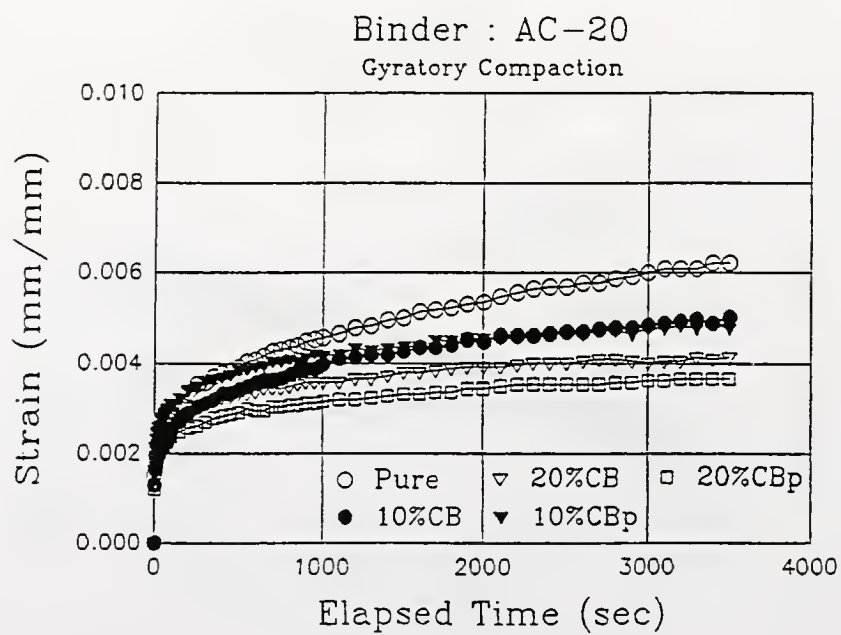
Figure 8.13 Summary for AC-20 Mixture Compacted Gyratory Compactor at 50°C

Figure 8.14 Summary for Creep Strain at 25°C

8.4.1 Effect of Binder

In this study, two types of asphalt (AC-10 and AC-20) modified by CB and CB_p were employed. The creep strain of AC-10 mixtures is generally larger than that of AC-20 mixtures if the testing temperature and compaction method are same. This is the same trend as for resilient modulus tests and indirect tensile tests. This means that the viscosity of asphalt is a dominant factor for creep strain if the other testing conditions are the same. The inclusion of CB and CB_p except the mixtures compacted by the Marshall compactor at 25°C, decreases the creep strain of mixtures. Among them, 15 % and 20 % of additive show better performance, although a 20 % of additive made a workability problem during mixing with binder and aggregates.

AC-10 Mixtures

The creep strains for AC-10 mixtures with CB compacted by Marshall at 50°C are summarized in Figure 8.9 (a). The testing results showed two different types of strain curve. The creep strain for AC-10 mixtures compacted by Marshall follows an almost ideal behavior of the viscosity material shown in Figure 8.2, which can be simplified and classified into primary stage, steady state region, and failure stage. The other results represent only first two stages. This means that the inclusion of CB delays of failure of mixtures. The amount of CB is not significant for the trend of creep strain of mixtures experienced. According to Gabrielson (1992), the creep strain less than 0.1 mm/mm predicts a rutted pavements. Considering this criterion, all of the AC-10 mixtures showed a good quality and performance, although the testing results indicated some variations.

The creep strain for AC-10 mixtures compacted by gyratory compactor at 50°C is shown in Figure 8.10 (a). The trend is similar to Marshall compacted mixtures, although there are some different magnitudes of creep strains.

As can be seen in Figure 8.9 (b) and 8.10 (b), the results for AC-10 mixtures with CB_p showed almost similar trends, although the initial shifts of creep strains for Marshall

compacted mixtures are shown. The strains at 1 hour experienced by the specimens are small, from 0.0073 to 0.0466 mm/mm. Judging from the recommendation by Gabrielson (1992), those mixtures with CB_p can be considered as mixtures with good quality and performance.

AC-20 Mixtures

The summary of the creep strain for AC-20 mixtures modified with CB and with CB_p is shown in Figure 8.13 (a) and Figure 8.14 (a). As can be seen in Figure 8.13, the results for AC-20 mixtures without additives (compacted by Marshall compactor) represents a ideal behavior for a viscoelatic material, however, mixtures compacted by gyratory compactor shows only the first two stages, primary and steady state. For both compactions, mixtures modified by 10 % and 20 % of CB show the lower creep strain, around 0.01 mm/mm at 50°C. The inclusion of a small amount of CB (5 %) did not have a significant effect on reducing the creep strain. The results for AC-20 mixtures modified by CB_p at 50°C are shown in Figure 8.13 (b) and 8.14 (b). A 20 % CB_p mixture show the most significant decrease of the creep strain after long loading duration. The creep strain of mixtures experienced is around 0.008 mm/mm for Marshall compaction and 0.004 mm for gyratory compaction. In the results for gyratory compacted specimens, only 20 % of CB_p decreases the creep strain at 50°C. On the other hand, all the CB_p amounts acts on reducing the creep strain of Marshall compacted specimens.

At 25°C, the AC-20 mixtures represent very similar creep strain as AC-10 mixtures, when the mixtures are not modified with CB_p. In the case of Marshall compaction, low amount of CB_p (10 %) do not reduce the creep strains. However, all the mixtures compacted by the gyratory machine show lower creep strains than unmodified mixtures.

8.4.2 Effect of Compaction Method

The effect of different compaction methods on the creep strain are summarized in Table 8.3. The creep strains of Marshall compacted specimens are lower than those of gyratory compacted specimens at 50°C except AC-20 mixtures modified by CB_p. However, at low temperature, 25°C, the creep strains of Marshall compacted specimens are higher than those of gyratory compacted specimens.   As pointed out in the introduction of this Chapter, gyratory compaction is currently the best one to simulate the field condition.   Therefore, the creep strain for Marshall compacted specimens may underpredict at high temperature (50°C) and overpredict at low temperature (25°C).   In case of unmodified mixtures, the Marshall compacted specimens followed a trend typical of the ideal viscoelastic materials. However, gyratory compacted specimens experienced only primary and steady state stages. This means that gyratory compaction can produce more stable mixtures than Marshall compaction, although gyratory compacted specimens showed higher creep strain at 1 hour than Marshall compacted specimens.

Table 8.4 Summary for the Effect of Compaction Method

Temperature	50°C		25°C	
Binder	AC-10	AC-20	AC-10	AC-20
CB	M* < G**	M < G	M > G	M > G
CB_p	M < G	M > G	M > G	M > G

* Marshall Compaction and **Gyratory Compaction

8.5 Creep Strain Rate

The permanent deformation is an important parameter for the analysis of rutted asphalt pavement. Due to the variable of construction, the permanent deformation may highly depend on the deformation after short-term loading condition. Therefore, more well-defined analysis should be needed to characterize the phenomena of pavement deformation. The creep strain rate (mm/mm/sec) is defined as the slope of the strain curve with time in the steady state region. In this study, a linear regression method was

employed to determinate the creep strain rate of the mixtures. The ranges of steady state are rigorously from 200 seconds to 4000 seconds. The creep strain rates are summarized in Table 8.5.

The inclusion of additive for AC-10 mixtures and AC-20 mixtures decreased the creep strain rate, except for the shaded area in Table 8.5. As can be seen in the Table, the effects of additives, CB and CB_p, are better for AC-10 mixtures than for AC-20 mixtures, due to the high viscosity of AC-20 binder. This trend is similar to the creep strain and resilient modules test. In case of AC-20 mixtures, a small amount of additives, CB and CB_p, about 5% by asphalt weight, did not show a significant effect on reducing the creep strain rate at high temperature, 50°C. Judging from the effect of different compaction methods, the Marshall compacted mixtures represent better creep strain rates, which means lower values, than the gyratory compacted mixtures. The possible reason may be the crushing of aggregate during compaction and the different particle orientations.

Table 8.5 The Summary of Creep Strain Rate ($*10^{-6}$ mm/mm/sec)

Temp.	50°C				25°C			
Comp.	Marshall		Gyratory		Marshall		Gyratory	
Binder	AC-10	AC-20	AC-10	AC-20	AC-10	AC-20	AC-10	AC-20
0 %	3.01	2.26	9.30	3.50	0.70	0.61	0.85	0.70
CB 5%	1.43	2.23	4.90	3.30				
10%	1.09	0.82	2.20	1.70	0.48	0.60	0.35	0.45
15%	0.63	1.00	1.10	2.20				
20%	1.05	0.83	1.10	0.99	0.32	0.39	0.22	0.24
CB_p 5%	1.95	0.92	9.80	4.00				
10%	1.13	0.73	5.50	3.30	0.37	0.39	0.37	0.28
15%	1.18	0.77	5.30	2.10				
20%	1.41	0.65	2.00	1.60	0.27	0.22	0.27	0.23

8.6 Creep Modulus

8.6.1 Creep Modulus Criteria

The creep modulus is calculated, based on the recorded deformation and applied stress, as a function of loading time using the following equation (Hills et al., 1974) :

$$S_{mix}(T,t) = \frac{\sigma}{\varepsilon_t} \tag{8.2}$$

where S_{mix} (T,t): creep modulus at a specified temperature (T) and loading time (t)

σ : applied stress (psi), and

ε_t : axial strain at t= Δ h/h where Δ h is change in height of specimen,

and h is original height of specimen.

The creep modulus criterion has been developed by several agencies. The 1-hour loading for creep testing is very common, because it seems to be long enough to be applicable to the loading conditions during which rutting occurs in the pavement, yet short enough to be practicable (Little et al., 1994). The minimum required creep modulus at 1-hour loading from the creep modulus charts developed by Mahboub and Little (1988) are shown in Table 8.6. All these criteria are for testing for 1-hour at 40°C and at a stress level that approximates a realistic average vertical compressive stress within the pavement layer.

Table 8.6 The Minimum Required Creep Modulus (Mahboub and Little, 1988)

Pavement Type	Minimum Required Creep Modulus (MPa)	
	Low Rut Potential	Moderate Rut Potential
Asphalt concrete over rigid base	69.0	34.5
Full depth asphalt concrete (intermediate layers)	55.2	20.7
Full depth asphalt concrete (lower layers)	27.6	17.2
Surface asphalt concrete layer	55.2	27.6

Similar criteria from the creep test have been developed by other researchers. Table 8.7 summarizes these criteria. The creep modulus measured in this study are from 20 MPa to 110 MPa and the average value of creep modulus is about 70 MPa. The vertical pressure used was 827 kPa (120 psi) to simulate current heavy traffic load; the testing temperature was 50°C to simulate more severe field conditions; and the loading duration was 1-hour. Although some of the creep modulus measured are less than the recommendations shown in Table 8.7, testing conditions were more severe. One of test results for creep modulus is shown in Figure 8.15 and the others are shown in Appendix C.

Table 8.7 The Summary of Minimum Required Creep Modulus (Little et al., 1994)

Researcher	year	Temp.	Loading Time	Stress Level (kPa)	Min. Req. Creep Mod.
Viljeon and Meadows	1981	40°C	100 min.	207	82.7 MPa
Khedr	1986	40°C	60 min.	207	137.9 MPa
Kronfuss et al.	1984	40°C	60 min.	103	max 45.3
This Study	1996	50°C	60 min.	827	70 MPa

8.6.2 Creep Modulus Rate

As was pointed out in previous section, time and temperature are dominant factors on creep behavior of asphalt pavement. The creep modulus rate is defined as the slope of creep modulus with time in log-log scale. The summary for creep modulus rate is shown in Table 8.7. The inclusion of additives, CB and CB_p, decreases creep modulus rate, which means that the mixtures modified by CB and CB_p are less sensitive than the unmodified mixtures with time. Except are shown as shaded area in Table 8.8. At testing temperature of 50°C, the AC-20 mixtures indicate lower creep modulus rate than AC-10 mixtures for both compactions. However, at a relatively low testing temperature

(25°C), both mixtures show similar results. This shows that the viscosity of asphalt is the major factor to control the creep modulus rate, as the testing temperature increases.

Table 8.8 The Summary of Creep Modulus Rate (*10^{-4} kPa)

Temp.	50°C				25°C			
Comp.	Marshall		Gyratory		Marshall		Gyratory	
Binder	AC-10	AC-20	AC-10	AC-20	AC-10	AC-20	AC-10	AC-20
0 %	-1.70	-1.30	-2.30	-1.80	-1.30	-1.10	-1.20	-1.20
CB 5%	-1.30	-1.50	-1.70	-1.60				
10%	-1.10	-0.97	-1.50	-1.30	-0.75	-1.30	-1.00	-1.20
15%	-1.10	-0.95	-1.10	-1.40				
20%	-0.93	-1.00	-1.10	-1.00	-0.85	-0.90	-0.67	-0.74
CB_p 5%	-1.10	-0.88	-2.40	-2.10				
10%	-0.92	-0.85	-3.10	-1.80	-0.68	-0.67	-0.89	-0.81
15%	-1.30	-0.98	-2.30	-1.40				
20%	-1.00	-1.00	-1.30	-1.30	-0.65	-0.72	-0.83	-0.79

8.7 Conclusions

Within the limited laboratory testing in this study, the following principal conclusions can be drawn :

- The unmodified mixtures followed a ideal creep behavior of viscoelastic materials, including primary stage, steady state region, and failure stage. However, the modified mixtures followed only the first two stages, primary and steady state. This means that the inclusion of CB and CB_p can produce more stable mixtures which can require longer times to reach failure.

- Although some of mixtures reached the failure mode, the mixtures used showed relatively good quality and performance in accordance with the recommendation of Gabrielson, i.e., less than 0.1 mm/mm of permanent strain.

- The viscosity of asphalt should be the major factor at high testing temperature (50°C) to control the creep strain, creep strain rate, creep modulus, and creep modulus rate.

- The Marshall compacted mixtures represent better creep strain rates (lower values) than the gyratory compacted mixtures due to the crushing of aggregates and different particle orientations during compaction.

- The creep strain for Marshall compacted specimens may underpredict at high temperature (50°C) and overpredict at low temperature (25°C), because gyratory compaction simulates the field construction better than Marshall compaction.

- Although some of the creep modulus measured are less than the recommended value, the testing conditions were more severe.

CHAPTER 9

HAMBURG WHEEL TRACKING TEST

9.1 Background of the Equipment

The wheel tracking device has been used in the Hamburg, Germany area since 1974 for research on asphalt binder course mixes. In 1984, the Hamburg Load Authority began using wheel tracking tests as a specification tool to determine the resistance to moisture damage and permanent deformation (Elf Industries, 1992)

The Hamburg wheel tracking device was introduced to the United States in 1990 after the representatives of the American Association of State Highway and Transportation Officials (AASHTO), Federal Highway Administration (FHWA), National Asphalt Pavement Association (NAPA), Strategic Highway Research Program (SHRP), Asphalt Institute (AI) and Transportation Research Board (TRB) made a two week research tour of six European countries (Aschenbrener, 1993). After the European pavement study tour, the Colorado Department of Transportation (CDOT) and the FHWA Turner-Fairbank Highway Research Center demonstrated the Hamburg wheel. The tracking device used in this study was purchased in May 1990, from Helmut Wind Inc. of Hamburg, Germany by Koch Materials, Terre Haute, Indiana.

The Hamburg Wheel Tracking Device used is shown in Figure 9.1 and the schematic sketch for Hamburg Wheel Tracking Device is shown in Figure 9.2. The detail information for this device is shown in Table 9.1.
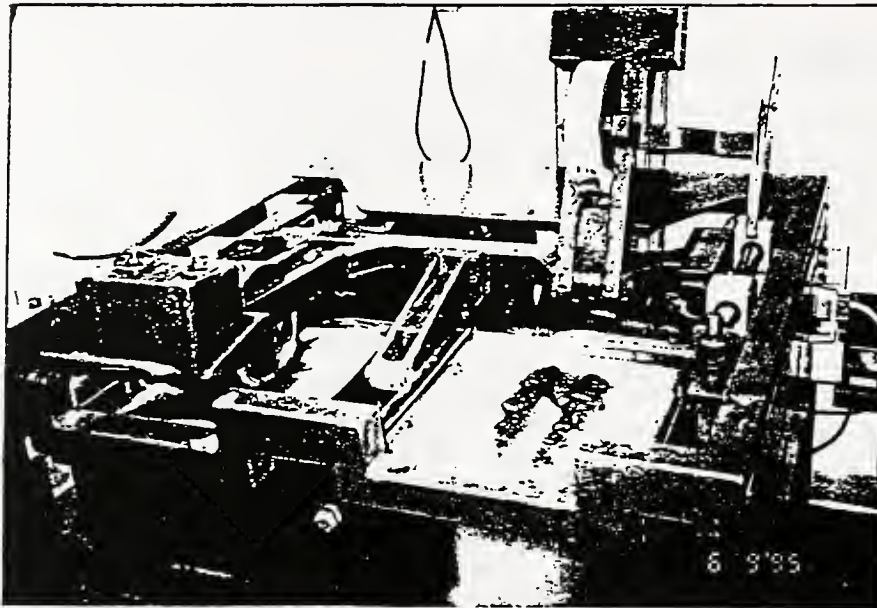
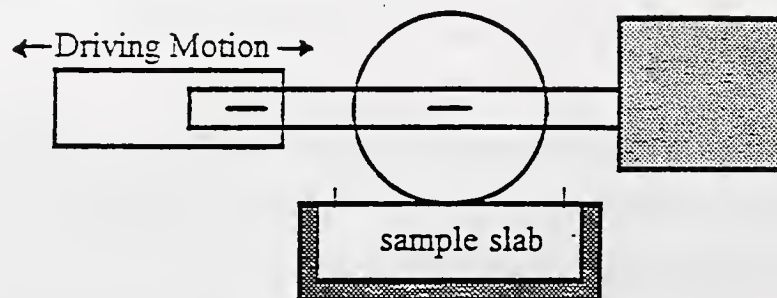Figure 9.1 The Hamburg Wheel Tracking Device

Figure 9.2 The Principal Sketch for Hamburg Wheel Tracking Device (Park, 1995)

Table 9.1 Information of the Hamburg Wheel Tracking Device

Type		Subject
Materials of steel wheel		V2A steel, rust resistant
Dimension of wheel	diameter	203.5 ± 1 mm
	width	47.0 ± 0.02 mm
	surface	plane
Wheel load		71 ± 0.1 kg
Side play of each bearing of the load arms		≤ 0.2 mm
Length of the rolling section		230 ± 10 mm
Rolling frequency		$53 \pm 2 \text{ min}^{-1}$
Time duration of load pressure		0.1 sec

9.2 Test Procedure

A total of 8800 grams of aggregate was used to make duplicate slabs. Based upon the results of Marshall and gyratory tests, conventional mixtures and mixtures modified with 10 % and 15 % of CB and CB_p were tested. A linear kneading compactor was used for the preparation of sample slabs at 6 percent of targeted air voids. Figure 9.3 shows the linear kneading compactor (Elf Industries, 1992). The compacted slab has a length of 320 mm (12.6 in.), width of 260 mm (10.2 in.), and depth of 40 mm (1.6 in.). The bulk specific gravity test according to ASTM D2726-93 was followed. The range of measured air voids is around 8 to 9 percent which is different from the targeted air voids, 6 %. Table 9.2 shows measured air voids of the prepared slab.

Table 9.3 shows the detail testing conditions for the wheel tracking test. A pair of specimens was tested simultaneously and was submerged under water at 50°C for 30 minutes in order to ensure thermal stability. The deformations at the center of the slab were measured by LVDT automatically. Each sample slab is subjected 20,000 passes of the wheel, unless 20 mm of deformation occurs earlier.

Table 9.2 The Air-voids of Prepared Specimens (Elf Industries, 1992)

		AC-10		AC-20	
	content	air voids	std.	air voids	std.
CB	0 %	6.0	0.06	7.9	0.08
	10 %	9.0	0.27	8.5	0.39
	15 %	9.1	0.91	9.0	0.12
CB_p	10 %	---	---	8.6	0.02
	15 %	8.9	0.21	8.6	0.08

Table 9.3 Testing Conditions

Type	Subject
Sample	duplicated specimens, fully immersed in water
Wheel	moving steel wheel
Speed	sinusoidal speed reciprocation
Weight	705 N (158.3 lb)
Contact Pressure	1490 kPa (216.9 psi)
Loading Cycle	0.1 sec load, 0.9 sec rest
Temperature	50°C
Deformation	up to 20 mm ± 0.01 mm
Test duration	20,000 cycles, unless 20 mm deformation is reached first

9.3 Test Results and Discussions

9.3.1 Testing Parameters

The results from the Hamburg wheel tracking test include post compaction consolidation, creep slope, stripping inflection point and stripping slope as shown in

Figure 9.3. The post compaction is defined as the range that the wheel rapidly deforms the pavement. For example, about 1000 passes in Figure 9.3 is called post compaction consolidation. A low value for post compaction consolidation would indicate that the compaction process during laboratory fabrication or field construction is near optimum levels. After the consolidation effect of the wheel occurs, we are concerned with the rate of permanent deformation in the mix, which is defined as the creep slope. The more rapid the rate of deformation, the more sensitive the mix is to rutting. The unit of creep slope is passes per mm. The stripping inflection point is defined as the number of passes where the curve changes shape and plunges downward. The lower the stripping inflection point, the lower the mechanical energy to make stripping damage occur. The stripping slope is defined as the rate of deformation after the stripping inflection point. In the field, a combination of stripping and rutting failure is seen often, particularly in the southeastern part of the U.S.
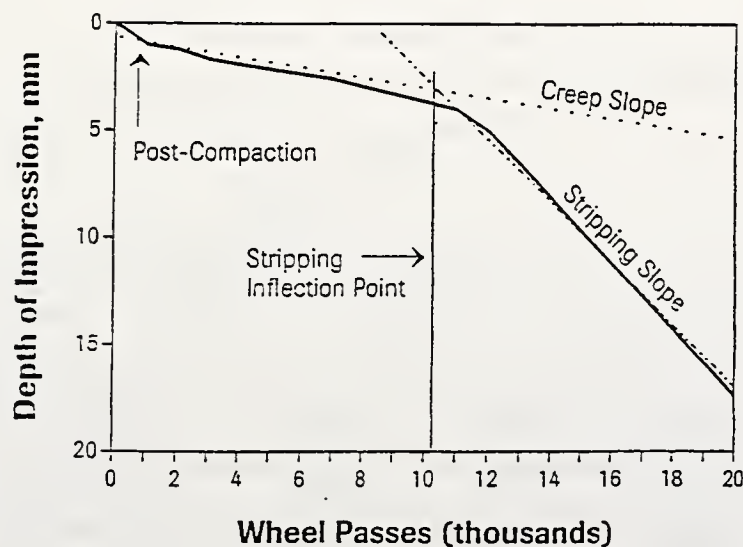
Figure 9.3 Testing Parameters for Hamburg Wheel Tracking (Elf Industries, 1992)

9.3.2 Test Results

<u>Creep Slope</u>

　　　　One of test results is shown in Figure 9.4 and the other test results for Hamburg wheel tracking are shown in Appendix D. Table 9.4 shows each testing parameter for Hamburg wheel tracking. The higher value of the creep slope means a lower potential for permanent deformation. The creep slope of pure AC-10 mixtures and AC-20 mixtures is 3195 passes/mm and 5208 passes/mm, respectively. The inclusion of CB into AC-10 mixtures produces a significant effect on increasing the creep slope. On the other hand, AC-10 modified CB_p decreases the creep slope. The inclusion of CB and CB_p for AC-20 mixtures indicate the decrease of creep slope of the mixtures. Based on the result from Chapter 8, dynamic confined creep test, the inclusion of CB and CB_p decreases permanent deformation of the mixtures at high testing temperature. Although the testing temperature for the dynamic confined creep test and the Hamburg wheel tracking test is same (50°C), the effect of the inclusion of additives is different. The effect of the water is very significant for rutting of the pavement.
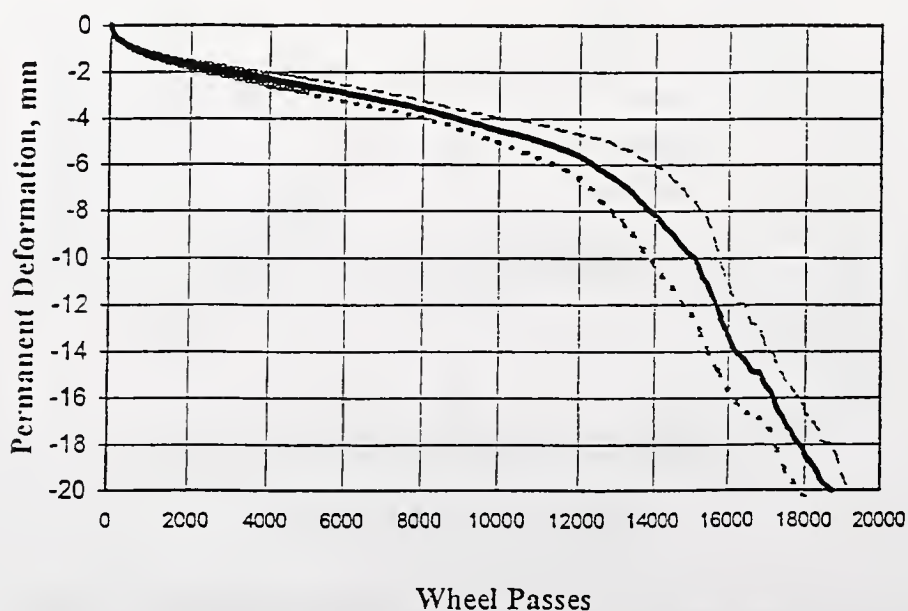
Figure 9.4 Test Result for AC-10 Mixture with 15% CB_p

Table 9.4 Testing Parameters

Aspahlt		AC-10				AC-20			
Add.	Cont.	Creep slope	Strip. In. Po.	Strip. slope	Poten. resis.	Creep slope	Strip. In. Po.	Strip. slope	Poten. resis.
CB	0 %	3195	7200	235	93	5208	15600	645	87
	10 %	409	10200	267	93	3817	14500	885	77
	15 %	5263	14500	437	92	3003	9600	375	88
CB_p	10 %	2000	7200	364	82	3185	8600	617	80
	15 %	3096	13300	361	88	4132	15300	505	88

Stripping Inflection Point

In the case of AC-10 mixtures, the inclusion of CB and CB_p increases the stripping inflection points of the mixtures. The CB mixtures are slightly better for stripping resistance than CB_p ones. This is similar to the results in Park's study (1995). Table 9.5 shows the comparison of stripping inflection point between slag mixtures and limestone mixtures. The stripping inflection point of slag mixtures is higher than that of limestone mixtures. In the case of AC-20 mixtures, the inclusion of CB and CB_p decreases the stripping inflection point of the mixtures. The possible reason would be the high viscosity of AC-20 asphalt.

Table 9.5 Comparison of Stripping Inflection Point

Binder		AC-10		AC-20	
Aggregate		Slag	Limestone	Slag	Limestone
Additive	0 %	7200	2800	15600	7100
CB	10 %	10200	6500	14500	< 20000
	15 %	14500	8000	9600	< 20000
CB_p	10 %	7200	3000	8600	7200
	15 %	13300	3500	15300	8800

Stripping Slope

The stripping slope of AC-10 mixtures increases very much due to the inclusion of CB and CB_p, however, for AC-20 mixtures the response varies. Only 10 % CB_p mixture shows the increase of stripping slope. The potential resistance is defined as the loss of its original rutting resistance. The higher the potential resistance, the higher the loss of its original rutting resistance after the mixtures are stripping. In the case of AC-10, CB_p mixtures are better than CB mixtures in keeping the original rutting resistance after the mixtures are stripping. In the case of AC-20 mixtures, low contents of CB and CB_p produce better results than high contents.

9.4 Conclusion

Within the limited laboratory testing in this study, the following principal conclusions can be drawn:

- AC-10 mixtures modified with CB produce higher creep slopes than with CB_p. However, the inclusion of CB and CB_p in AC-20 mixtures reduces the creep slope, which means that AC-20 mixtures modified by CB and CB_p are more sensitive to rutting than unmodified AC-20 mixtures.

- The additives, CB and CB_p, for AC-10 mixtures increase the stripping inflection point. However, for AC-20 mixtures a poor effect is produced, because AC-20 asphalt has a high viscosity.

- The inclusion of CB_p in AC-10 mixtures and AC-20 mixtures shows better performance than that of CB for retaining its original rutting resistance after the mixtures are stripping.

- The slag mixtures shows better performance than the limestone mixtures, including much higher resistance to stripping.

CHAPTER 10

SUMMARY, CONCLUSIONS AND RECOMMENDATIONS

10.1 Summary

This study, which is based on various laboratory tests and evaluations, investigates the usefulness and potential of using pyrolyzed carbon black (CB_p) from scrap tires as an additive, and air-cooled furnace slag as a coarse aggregate in hot mix asphalt. The fundamental characteristics and performance of asphalt mixtures modified with pyrolyzed carbon black are determined and compared to asphalt mixtures modified with carbon black (CB) and unmodified asphalt mixtures.

The optimum binder content and the relationship of density and voids were determined from Marshall mix design. The range of the optimum binder content was 6.3 % to 7.8 %. The Marshall stability as a strength value and flow at 140°F increased within the accepted ranges due to the inclusion of CB_p. The gyratory tests were conducted following the U.S. Army Corps of Engineers 8A/6B/4C model. The resilient modulus and indirect tensile tests were conducted to determine the stiffness of the mixtures at low temperatures, which is related to the cracking potential of the pavement. The inclusion of CB and CB_p produced an increase of M_R and tensile strength. Dynamic confined creep tests were carried out to check the rutting potential of pavements prepared with additions of CB, CB_p, and slag at high temperatures, which is one of the important problems associated with pavements. The mixtures modified by CB_p showed lower creep strain than the unmodified mixtures.

10.2 Conclusions

Within the limits of the laboratory testing done in this study, the following principal conclusions can be drawn:

- The measured flexural creep stiffness of AC-20 binder from the bending beam rheometer test is higher than that of AC-10 binder at the same testing temperature and loading time, because the viscosity of AC-20 asphalt is much higher than that of AC-10 asphalt.

- The inclusion of CB and CB_p for both asphalts, AC-10 and AC-20, increases flexural creep stiffness at each testing temperature and increases the time to reach failure (larger bending). This implies that the inclusion of CB and CB_p causes the flexural creep stiffness to increase, and CB and CB_p can be used as reinforcing additives in asphalt.

- The flexural creep stiffness at lower temperature (less than $0^{\circ}C$) shows a linear relationship as the loading time increases. The change of the flexural creep stiffness becomes smaller as the testing temperature decreases.

- As the inclusion of carbon black and pyrolyzed carbon black increases, air-voids of the mixtures tend to increase. The change of air-voids in CB_p mixtures is larger than in CB mixtures, due to the non-uniformity of the particles. The bulk specific gravity of the blended aggregate is not a constant. It depends on the shape and surface texture of the aggregate, and the characteristics of the binder (asphalt+additive).

- A self-consistent volumetric asphalt design gives more reasonable values for voids in mineral aggregate (VMA) than a conventional volumetric design, because the latter has some possible error sources, such as the determination of the bulk specific gravity of each aggregate and the blended aggregate, the determination of the saturated-and surface-dry condition, and the use of water instead of asphalt cement.

- The use of iron blast furnace slag as an aggregate for binder courses of pavement produces a high Marshall stability: an average of about 20000 N. Also, as the inclusion amounts of CB or CB_p increase, the Marshall stability increases. However, the effect on the Marshall stability for AC-20 mixtures with carbon black (CB) is not

as significant as in the other cases. The inclusion of CB and CBp increases flow values, but these remain within acceptable ranges. The optimum binder content tends to increase as the content of CB and CB_p increases.

- Carbon black acts as a microfiller and becomes an integral part of the asphalt cement, due to its small particle size, about 100 to 150 nanometers. Pyrolyzed carbon black, with larger particle sizes, acts both as a mineral filler and as a microfiller, due to the variation of particle size (up to 0.3 mm).

- Judging from the change of air voids, about 100 GTM revolutions divided the initial compaction and the traffic densification of the mixtures. The range of GCI value for all the mixtures was 0.963 to 0.971, which indicates little difficulty in compacting the mixtures. The Marshall stability and logarithm of GTM revolutions showed a linear relationship.

- Considering the value of GSI, AC-10 CB_p mixtures represented very stable mixtures. The inclusion of CB_p had the effect of producing a very stable mixture during long loading applications. Only AC-10 mixtures and AC-20 mixtures with 20 percent of CB indicated instability for long loading application due to the flushing of binder.

- The AC-10 CB_p mixtures represented the best retention of shear resistance for long loading applications. The others showed a slight decrease of the shear resistance for long loading applications.

- The flow of AC-10 mixtures with CB and CB_p remained in an acceptable range after long loading application, but that of AC-20 mixtures with CB and CB_p was out of the acceptable range. In all the mixtures, the flow stabilized after long loading applications.

- The M_R at low temperature, 5°C, is around 2 to 3 times larger than at high temperature, 25°C. The rate of change of M_R is larger for Marshall compacted specimens than for gyratory compacted specimens.

- The grade of asphalt cement has a significant effect on the M_R and tensile strength of the mixtures. The higher the asphalt grade, the higher the M_R and the tensile strength.

- The inclusion of CB and CB_p produces an increase of M_R and tensile strength. In the case of AC-10 mixtures, CB_p can produce a greater difference than CB at low temperatures. However, CB is better than CB_p at high temperature.

- Tensile strength of CB_p mixtures up to 10 %, is better than CB mixtures. However, that of CB mixtures, larger than 10 %, is better than CB_p mixtures. The tensile strength of the mixtures would depend on the effective asphalt film thickness of the mixtures.

- The unmodified mixtures follow the ideal creep behavior of viscoelastic materials, including primary stage, steady state region, and failure stage. However, the modified mixtures followed only the first two stages, primary and steady state. This means that the inclusion of CB and CB_p lead to more stable mixtures, which take a longer time to reach failure.

- The viscosity of asphalt should be the major factor at high testing temperature (50°C) to control the creep strain, creep strain rate, creep modulus, and creep modulus rate.

- The Marshall compacted mixtures represent better creep strain rates (lower values) than the gyratory compacted mixtures, due to the crushing of aggregate and different particle orientations during compaction. The creep strain for Marshall compacted specimens maybe underpredicted at high temperature (50°C) and overpredicted at low temperature (25°C), because gyratory compaction simulates the field construction better than Marshall compaction.

- AC-10 mixtures modified with CB produce higher creep slopes than with CB_p, however, the inclusion of CB and CB_p in AC-20 mixtures reduces the creep slope. This means that AC-20 mixtures modified with CB and CB_p are more sensitive to rutting than unmodified AC-20 mixtures.

- The additives, CB and CB_p, for AC-10 mixtures increase the stripping inflection point. However, for AC-20 mixtures a poor effect is illustrated, because AC-20 asphalt has a high viscosity.

- The inclusion of CB_p in AC-10 mixtures and AC-20 mixtures is better than that of CB in retaining the original rutting resistance after the mixtures start stripping.

- The slag mixtures show better performance than the limestone mixtures, including much higher resistance to stripping.

10.3 Recommendations

- Even though various types of conventional binder tests, including the penetration test, softening point test, ductility test, and aging test, were conducted by Zeng and Lovell (1995), more laboratory tests recommended by SHRP are needed. These include: bending beam rheometer (BBR); direct tension test (DTT); dynamic shear rheometer (DSR); rotational viscometer test; as well as rolling thin film oven (RTFO) test for short-term aging, and pressure vessel test for long-term aging, which should be added in order to characterize the complex rheological properties of binders.

- There are problems in using the pyrolyzed carbon black. There are handling difficulties associated with the powder forms of pyrolyzed carbon black. A possible alternative is to use pelletized pyrolyzed carbon black with a proper mixing agent. Another is the settlement or segregation of pyrolyzed carbon black after mixing with asphalt due to its relatively heavy weight. In the field, the time from mixing with asphalt to mixing with aggregate should be minimized.

- Although asphalt mixtures modified by pyrolyzed carbon black have shown relatively good performance, the long-term performance should be monitored. Therefore, test sections should be constructed and monitored for a long time, using the mixtures which have been shown to be most effective in the laboratory.

- The use of waste materials in hot mix asphalt may induce unexpected environmental problems. Although undesirable effects due to the use of pyrolyzed carbon black and iron slag have not been identified, long-term monitoring should be conducted.

LIST OF REFERENCES CITED

Ahmed, I, (1991), "Use of Waste Materials in Highway Construction", Report No. FHWA/IN/JHRP-91/3, School of Civil Engineering, Purdue University, West Lafayette, Indiana, 112 pp.

American Society for Testing and Materials (1993), Road and Paving Materials; Paving Management Technologies, Section 4, Vol. 4.03.

Applied Test System (ATS, 1993), "Bending Beam Rheometer", Instructor Manual, pp. 6-10.

Aschenbrener, T. (1993), "Influence of Testing Variables on the Results from the Hamburg Wheel Tracking Device", Colorado Department of Transportation, CDOT-DTD-R-93-22, Final Report, December 7, 35 pp.

Asphalt Institute Manual Series No. 2 (MS-2) (1988), Mix Design Methods for Asphalt Concrete and Other Hot-Mix Types, pp. 70-71.

Bahia, H. U., Anderson, D. A., and Christensen, D. W. (1992), "The Bending Beam Rheometer; A Simple Device for Measuring Low-Temperature Rheology of Asphalt Binders", AAPT, Vol. 61, pp. 117-153.

Blankenship, P. B., Mahboub, K. C., and Huber, G. A. (1994), "Rational Method for Laboratory Compaction of Hot-Mix Asphalt", TRB, Transportation Research Records, No. 1454, pp. 144-153.

Bolk, H.J.N.A. (1981), "The Creep Test", Study Centre for Road Construction, The Netherlands, February.

Brown, E. R., Collins, R. and Brownfield, J. R. (1989), "Investigation of Segregation of Asphalt Mixtures in the State of Georgia", TRB, Transportation Research Record, No. 1217, National Council, Washington, D.C.

Brown, E. R. and Cross, S. (1989), " A Study of In-Place Rutting of Asphalt Pavements", Proceeding AAPT, Vol. 58.

CABOT Industries (1994), "Carbon Black for Specialty Applications", CABOT Corporation Special Blacks Division, Catalogue.

Ciesielski, S. K. and Collins, R. J. (1993), "Current Nationwide Status of the Use of Waste Materials in Hot Mix Asphalt Mixtures and Pavements", Use of Waste Materials in Hot-Mix Asphalt, ASTM STP 1193, H. Fred, Eds.

Coree, B. J. (1995), "A Self-Consistent Volumetric Asphalt Concrete Design Method", Personnal Communication.

Dodds, J., Domenico, W. F., Evans, D. R., Fish, L. W., Lassahn, P. L. and Toth, W. J. (1983), "Scrap Tyres: A Resource and Technology Evaluation of Tyre Pyrolysis and Other Selected Alternative Technologies", US Department of Energy Report EGG-2241.

Elf Industries (1992), "Hamburg Wheel Tracking Device", Technote, Catalogue.

Elliot, D. (1990), *The Recycling and Disposal of Tyres*, KPMG, Peat, Marwick, McLintock, Salisbury, London.

Emery, J. J. (1982), "Slag Utilization in Pavement Construction", Extending Aggregate Resources, ASTM STP 774, American Society for Testing and Materials, pp. 95-118.

EPA (1991), "Market for Scrap Tires", Report No. EPA/530-SW-90-074A, United States Environmental Protection Agency, Office of Solid Waste, Washington, D.C., 115 pp.

Gabrielson R. J. (1992), "Evaluation of Hot Mix Asphalt (HMA) Static Creep and Repeated Load Tests", Ph. D Dissertation, Auburn University, Alabama, December 16.

Hills, J. F., Brein, D., and Van de Loo, P. J. (1974), "The Correlation of Rutting and Creep Tests and Asphalt Mixtures", Paper IP, 74001, Institute of Petroleum, London, England, January.

Huang, Y. H. (1993), Pavement Analysis and Design, Prentice Hall, New Jersey, pp. 36-39.

Huschek S. (1985), "The Performance Behavior of Asphalt Concrete under Triaxial Compression", AAPT, Vol. 54, pp. 407-431.

Indiana Department of Highway Specifications (1993), Indiana Department of Highways, Indianapolis, Indiana.

Kaminsky, W. and Sinn, H. (1980), "Pyrolysis of Plastic Waste and Scrap Tyres Using a Fluidised Bed Process", In *Thermal Conversion of Solid Wastes and Biomass* (Eds. L. Jones and S. B. Radding), ACS Symposium Series 130 (American Chemical Society Publishers, Washington, D.C.)

Kandhal, P. S. and Koehler, W. S. (1985), "Marshall Mix Design Method : Current Practices", Proceedings, AAPT, Vol. 54.

Kawakami, S., Inoue, K., Tanaka, H. and Sakai., T. (1980), "Pyrolysis of Plastic Waste and Scrap Tyres Using a Fluidised Bed Process", In *Thermal Conversion of Solid Wastes and Biomass* (Eds. L. Jones and S. B. Radding), ACS Symposium Series 130 (American Chemical Society Publishers, Washington, D.C.)

Kennedy, T. W., Hass, R. and Meyre, F. R. (1975), "Characterization of Pavement Materials for Fundamental Structural Analysis", Inter-American Conference on Materials Technology, Caracus, Venezuela, pp. 694-708.

Khedaywi, T. S. (1988), "Effect of Inclusion of Oil Shale Ash on Behavior of Asphalt Concrete", TRB, Transportation Research Record 1171, Washington D.C., pp. 1-7.

Khedr, S. A. (1986), "Deformation Mechanism in Asphaltic Concrete", *Journal of Transportation*, ASCE.

Kronfuss, R., Krzemien, R., Nievelt, G, and Putz, P. (1984), "Verformungsfestigkjeit von Asphalten Ermittlung in Kriechtest", Bundesministerim fur Bauten and Technik, Strassenforschung, Heft 240, Wein, Austria.

Lesueur, D., Dekker, D. L., and Planche, J. P. (1995), "Comparison of Carbon Black from Pyrolyzed Tires to Other Fillers as Asphalt Rheology Modifiers", TRB, Transportation Research Record 1515, Washington D.C., pp. 47-55.

Lewis, D. W. (1982), "Resource Conservation by Use of Iron and Steel Slags", Extending Aggregate Sources, ASTM STP 774, American Society for Testing and Materials, pp. 31-42.

Little, D. N., Button, J. W. and Youssef, H. (1994), "Development of Criteria to Evaluate Uniaxial Creep Data and Asphalt Concrete Pavement Deformation Potential", TRB, Transportation Research Record 1417, Washington D.C., pp. 49-57.

Mahboub, K. and Little D. N. (1988), "Improve Asphalt Concrete Mixture Design", Research Report 2474-1F, Texas Transportation Institute.

McGennis, R. B., Anderson, R. M., Kennedy, T. W., and Solaimanian, M. (1995), "Background of SUPERPAVE Asphalt Mixture Design and Analysis", FHWA, No. FHWA-SA-95-003, pp. 159.

McRae, J. L. (1993), "Gyratory Testing Machine Technical Manual", Engineering Developments Co. Inc., Mississippi, 103 pp.

McRae, J. L. and McDaniel, A. R. (1958), "Progress Report on the Corps of Engineer's Kneading Compactor for Bituminous Mixtures", Proceeding, AAPT, Vol. 27, pp. 357-382.

Miller, R. H. and Collins, R. J. (1976), "Waste Materials as Potential Replacements for Highway Aggregates", NCHRP, Report No. 166, TRB, NRC, Washington D.C., 94 pp.

MTS Corporation (1994), "Operation Manual for Material Testing System", Material Testing System Incorporation, Minnesota, Minneapolis.

Noureldin, A. S. and McDaniels, R. S. (1991), "Performance Evaluation of Steel Furnace Slag-Natural Sand Asphalt Surface Mixtures", AAPT Vol. 60, pp. 276-303.

Ogasaware, S., Kuroda, M. and Wakao, N. (1987), "Preparation of Activated Carbon by Thermal Decomposition of Used Automotive Tires", Industrial & Engineering Chemistry Research, Vol. 26, No. 12, pp. 2552-2555.

Ortolani, L. and Sandberh, H. A. (1952), "The Gyratory-Shear Method of Modeling Asphaltic Concrete Test Specimens; Its Development and Correlation with Field Compaction Methods", Proceeding, AAPT, Vol. 21, pp. 280-297.

Pakdel, H., Roy, C., Aubin, H. and Coulombe, S. (1991), "Formation of *dl*-limonene in Used Tyre Vacuum Pyrolysis Oils", *Environ. Sci. Technol.,* pp. 1646-1649.

Park, T. S. (1995), "Application of Pyrolyzed Carbon Black from Scrap Tires in Pavement Design", Ph.D Thesis, Purdue University, W. Lafayette, Indiana. and FHWA/IN/JHRP 95/12.

Perl, M., Uzan, J. and Arieh, S. (1983), "Visco-Elasto-Plastic Constitute Law for a Bituminous Mixture under Repeated Loading", TRB, Transportation Record 911, Washington D.C., pp. 20-27.

Powell, R. (1968), "Carbon Black Technology Recent Developments", Chemical Process Review, No. 21, Park Ridge, N.J., Noyles Development Corp.

Roberts, F. L., Kandhal, P. S., Brown, E. R., Lee, D., and Kennedy, T. W. (1991), Hot Mix Asphalt Materials, Mixture Design, and Construction, NAPA Research and Education Foundation, Maryland, pp. 137-250.

Roque, R. and Buttlar, W. (1992), "The Development of a Measurement and Analysis System to Accurately Determine Asphalt Concrete Properties Using the Indirect Tensile Mode", AAPT, Vol. 61, pp. 304-332.

RostLer, F. S., White, R. M. and Dannenbery, E. M. (1977), "Carbon Black as a Reinforcing Agent for Asphalt", AAPT, Vol. 46, pp. 376-401.

Roy, C., Labrecque, B., and Caumia de, B. (1990), "Recycling of Scrap Tires to Oil and Carbon Black by Vacuum Pyrolysis", Resources, Conservation and Recycling, No. 4, pp. 203-213.

Roy, C and Unsworth, J. (1989), "Pilot Plant Demonstration of Used Tyres Vacuum Pyrolysis", In Pyrolysis and Glasification (Eds. G. L. Ferrero, K. Maniatis, A. Buekens and A. V. Bridgwater), Elseveier Applied Science, London.

Santucci, L. E., Allen, D. D. and Coats, R. L. (1985), "The Effects of Moisture and Compaction on Quality of Asphalt Pavements", Proceeding , AAPT, Vol. 54.

SHRP (1994), "The SUPERPAVE Mix Design System Manual of Specifications, Test Methods and Practices", Strategic Highway Research Program, SHRP-A-379, National Research Council, Washington, DC., pp 125.

U. S. Army TM 5-822-8 (1987), Bituminous Pavements Standard Practice, Technical Manual, Department of the Army.

U. S. Army Corps of Engineers (1962), "Development of the Gyratory Testing Machine and Procedures for Testing Bituminous Paving Mixtures", Technical Report No. 3-595, U.S. Army Engineer Waterways Experiment Station, Vicksburg, Mississippi, 34 pp.

Vallerga, B. A. and Gridley, P. F. (1980), "Carbon Black Reinforcement of Asphalt in Paving Mixtures", Asphalt Pavement Construction, New Materials and Techniques, ASTM STP 724, J. A. Scherocmen, Ed., American Society for Testing and Materials, pp. 100- 128.

Viljeon, A. W. and Meadows, K. (1981), "The Creep Test - A Mix Design Tool to Rank Asphalt Mixes in Terms of Their Resistance to Permanent Deformation under Heavy Truck", National Institute of Road Research, Pretoria, South Africa.

Von Quintus, H. and Kennedy, T. W. (1988), "AAMAS Mixture Properties Related to Pavement Performance", AAPT, Vol. 57, pp. 553-570.

Williams, P. T., Besler, S. and Taylor, D. T. (1993), "The Batch Pyrolysis of Tyre Waste-Fuel Properties of the Derived Pyrolytic Oil and Overall Plant Economics", Journal of Power and Energy, Vol. 207, No. A1, pp. 55-63.

Williams, P. T., Besler, S. and Taylor, D. T. (1990), "The Pyrolysis of Scrap Automotive Tyres", *Fuel*, 1990, **69**, pp. 1474-1482.

Yao, Z. and Monismith, C. L. (1986), "Behavior of Asphalt Mixtures with Carbon Black Reinforcement", AAPT, Vol. 55, pp. 564-585.

Yodar, E. J. and Witczak, M. W. (1975), Principles of Pavement Design, 2nd Edition, John Wiley & Sons, Inc.

Zeng, Y. and Lovell, C. W. (1995), "Effect of Pyrolyzed Carbon Black on Asphalt Cement", Report No. FHWA/IN/JHRP 95/12, School of Civil Engineering, Purdue University, West Lafayette, Indiana, 142 pp.

Zhang, X., Gress, D. and Eighmy, T. (1994), "Bottom Ash Utilization as an Aggregate Substitute in Hot Mix Asphalt", Proceedings of the 2nd Annual Great Lakes, Geotechnical/Geoenvironmental Conference, May 20, 1994, Purdue University, West Lafayette, Indiana.

Other References

Anderson, D. A., Bahia, H. U., and Dongre, Raj (1992), "Rheological Properties of Material Filler-Asphalt Mastics and Their Relationship to Pavement Performance", Effects of Aggregates and Mineral Filler on Asphalt Mixture Performance, ASTM STP 1147, Richard C. Meininger, Editor, American Society for Testing and Materials, Phiadelphia.

Brown, E. R. and Cross, S. A. (1992), "A National Study of Rutting in Hot Mix Asphalt (HMA) Pavements", AAPT, Vol. 61, pp. 535-582.

Brown, S. F., Preston, J. N., and Copper, K. E. (1991), "Application of New Concepts in Asphalt Mix Design", AAPT, Vol. 60, pp. 264-286.

Brule, B., Brion, Y., and Tauguy, A. (1988), "Paving Asphalt Polymer Blends : Relationship between Composition, Structure and Properties", AAPT, Vol. 57, pp. 41-64.

Christensen, D. W. and Anderson, D. A. (1992), "Interpretation of Dynamic Mechanical Test Data for Paving Grade Asphalt Cement", AAPT, Vol. 61. pp. 67-116.

Coomarasamy, A. and Walzak, T. L (1995), "Effect of Moisture on Surface Chemistry of Steel Slags and Steel Slag-Asphalt Paving Mixes", TRB, Transportation Record 1492, Washington D.C., pp. 85-95.

Dangelo, J. A., Paugh, C.. Harman, T. P., and Bukowski, J. (1995), "Comparison of the SUPERPAVE Gyratory Compactor to the Marshall for Field Quality Control", AAPT, Vol. 64, pp. 611-635.

Decker, D. S. (1994), "Evaluating the Use of Waste Materials in Hot Mix Asphalt", AAPT, Vol. 63, pp. 12-21.

Frocht, M. M. (1957), Photoelasticity, Vol. 2, John Wiley & Sons, Inc., New York.

Harris, B. M. and Stuart, K. D. (1995), "Analysis of Mineral Fillers and Mastics Used in Stone Matrix Asphalt", AAPT, Vol. 64, pp. 54-95.

Hines (1991), "The Hamburg Wheel Tracking Device", Proceeding of the Twenty Eight Paving and Transportation Conference, Civil Engineering Department, The University of New Mexico, Albuquerque, New Mexico.

Jung, D. and Vinson, T. S. (1994), "Thermal Stress Restrained Specimen Test to Evaluate Low Temperature Cracking of Asphalt Aggregate Mixtures", TRB, Transportation Record 1417, Washington D.C., pp. 12-20.

Kandhal, P. S., Mellott, D. B., and Hoffman, G. L. (1983), "Laboratory and Field Characterization of Sulphlex as a Paving Binder", Properties of Flexible Pavement Materials, ASTM STP 807, J. J. Ermery, Ed., American Society for Testing and Materials, pp. 102-117.

Khatri, M. A., Martinez, D. F., Bayomy, F. M., Salter, J. A., and Tang, W. J. (1993), " Performance Evaluation on Asphalt Mixtures with Gasifier Slag as Fine Aggregate", Use of Waste Materials in Hot Mix Asphalt, ASTM STP 1193, H. Fred Waller, Ed., American Society for Testing and Materials, pp. 276-292.

Khosla, N. P. (1991), "Effect of the Use of Modifiers on Performance of Asphaltic Pavements", TRB, Transportation Record 1317, Washington D.C., pp. 10-22.

Kim, Y., Khosla, N. P., and Kim, N. (1991), "Effect of Temperature and Mixture Variables on Fatigue Life Predicted by Diametral Fatigue Testing", TRB, Transportation Record 1317, Washington D.C., pp. 128-138.

Krutz, N. C. and Gardiner, M. (1990), "Relationship Between Permanent Deformation of Asphalt Concrete and Moisture Sensitivity", TRB, Transportation Record 1259, Washington D.C., pp. 169-177.

Krutz, N. C., Siddharthan, R., and Gardiner, M. (1991), "Investigation of Rutting Potential Using Static Creep Testing on Polymer-Modified Asphalt Concrete Mixtures", TRB, Transportation Record 1317, Washington D.C., pp. 100-108.

Lenoble, C. and Nahas, N. C. (1994), "Dynamic Rheology and Hot-Mix Performance of Polymer Modified Asphalt", AAPT, Vol. 63, pp. 450-480.

McDaniel, R. S. (1994), "A State Prospective on the Use of Waste Materials in Asphalt Mixtures", AAPT, Vol. 63, pp. 2-11.

Mohammad, L. N. and Paul, H. R. (1994), "Evaluation of Indirect Tensile Test for Determining Structural Properties of Asphalt Mix", TRB, Transportation Record 1417, Washington D.C., pp. 58-63.

Sulaiman, S. J. and Stock, A. F. (1995), "The Use of Fracture Mechanics for the Evaluation of Asphalt Mixes", AAPT, Vol. 64, pp. 500-533.

West, R. C. and Ruth, B. E. (1995), "Compaction and Shear Strength Testing of Stone Matrix Asphalt Mixtures in the Gyratory Testing Machine", AAPT, Vol. 64., pp. 32-53.

APPENDICES

APPENDIX A

THE SUMMARY OF FLEXURAL CREEP STIFFNESS
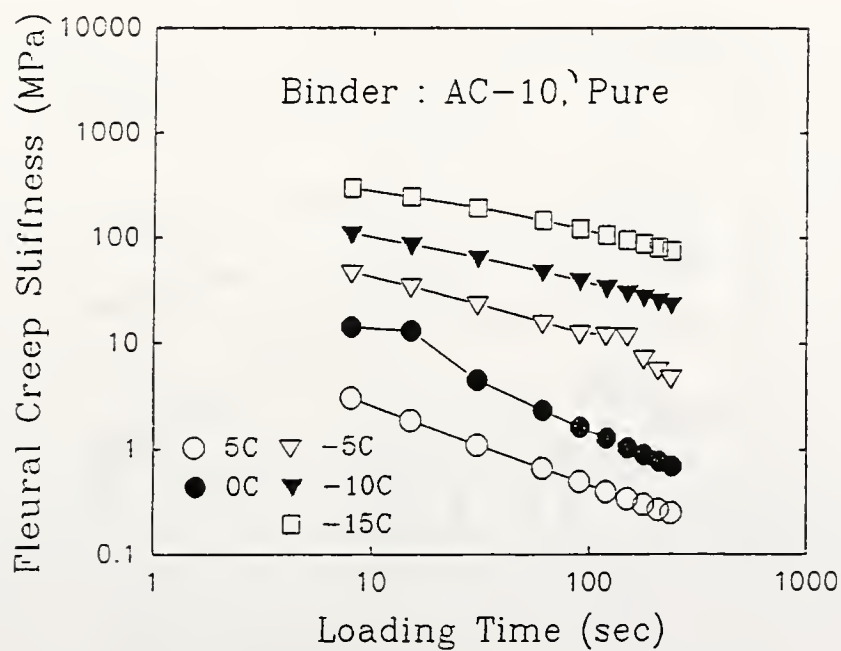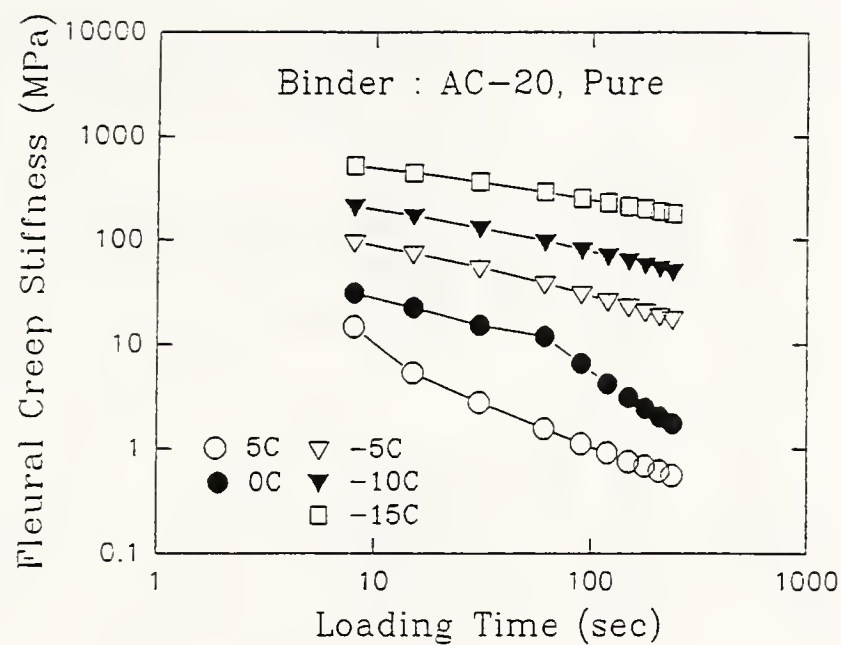
Figure A-1 The Flexural Creep Stiffness for Pure AC-10 and AC-20 Mixtures
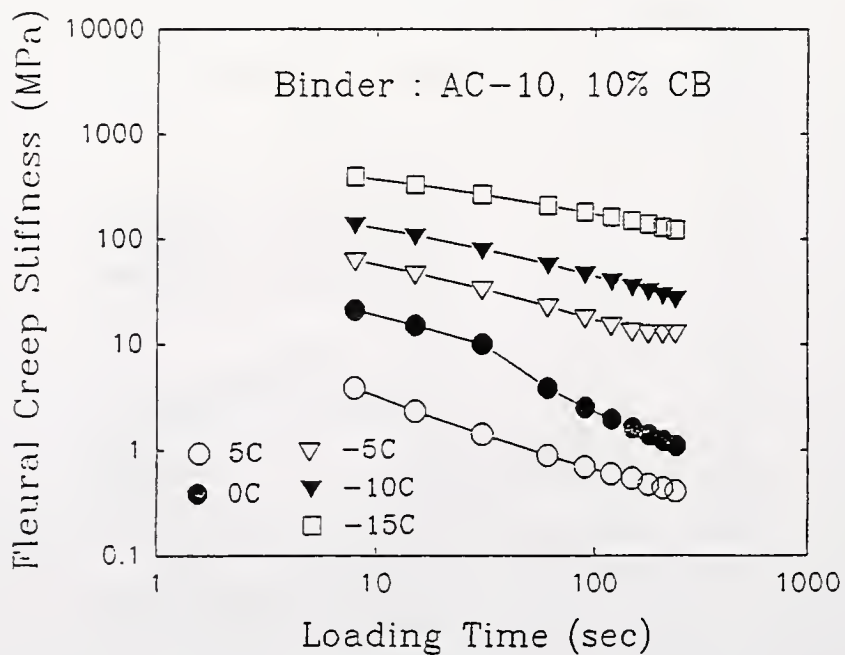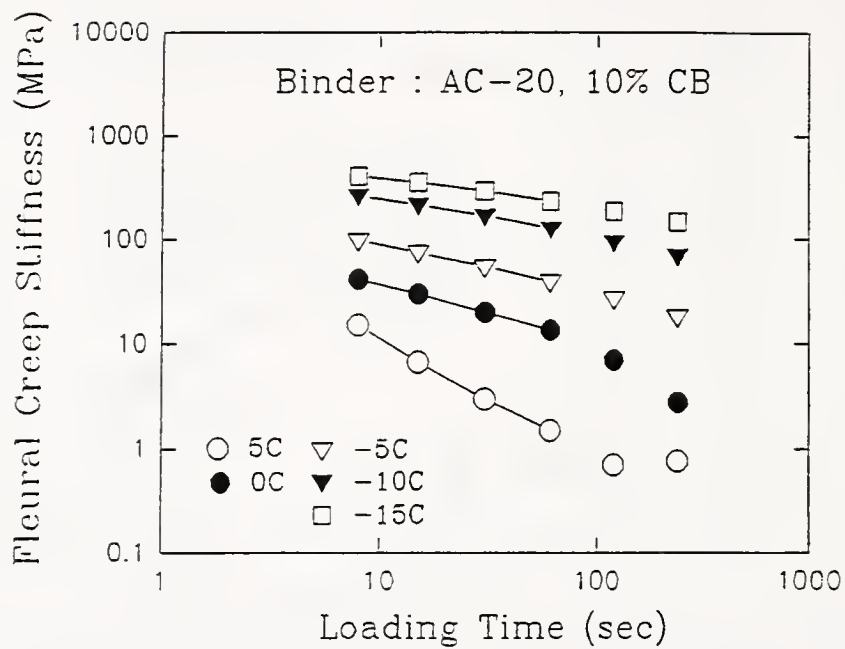
Figure A-2 The Flexural Creep Stiffness for AC-10 and AC-20 Mixtures Modified by 10% CB
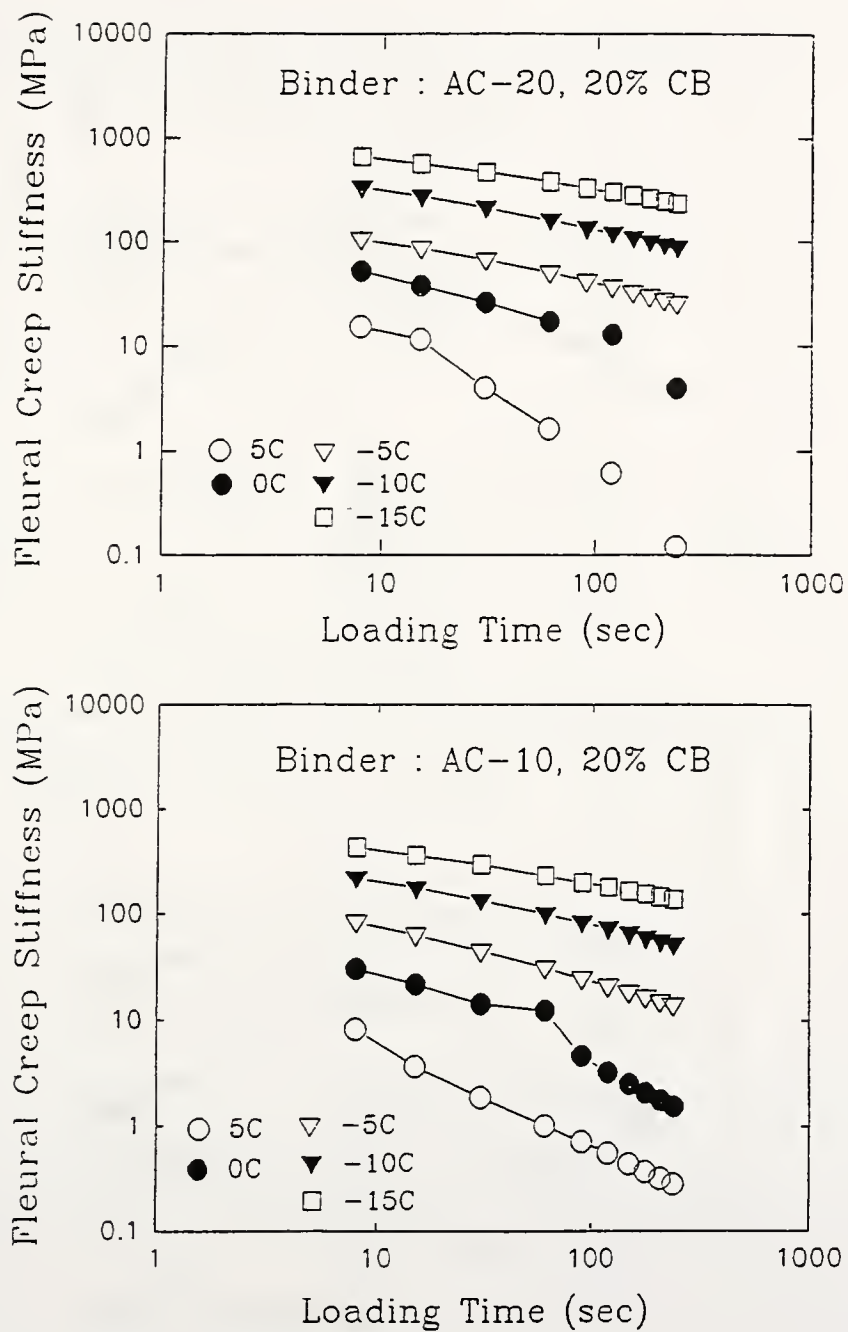
Figure A-3 The Flexural Creep Stiffness for AC-10 and AC-20 Mixtures Modified by 20% CB
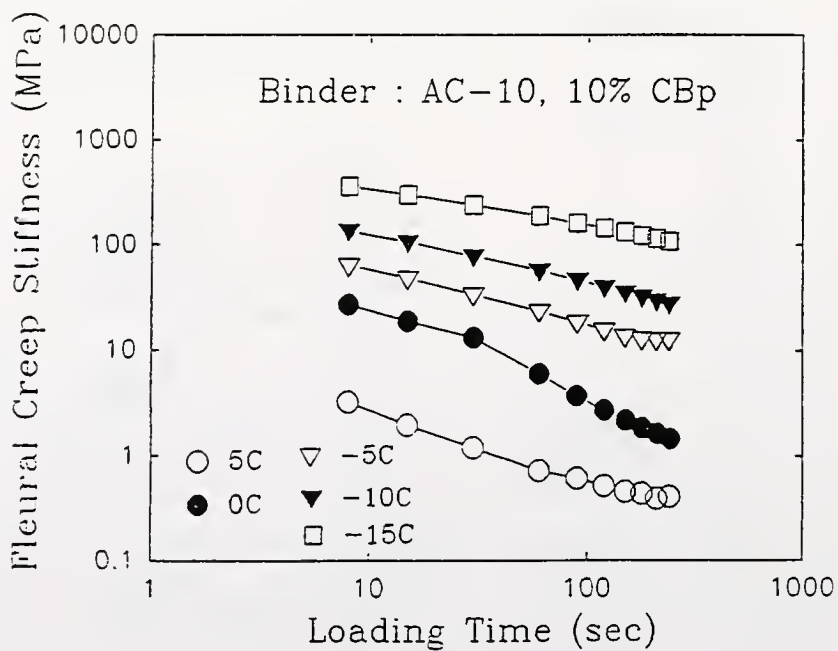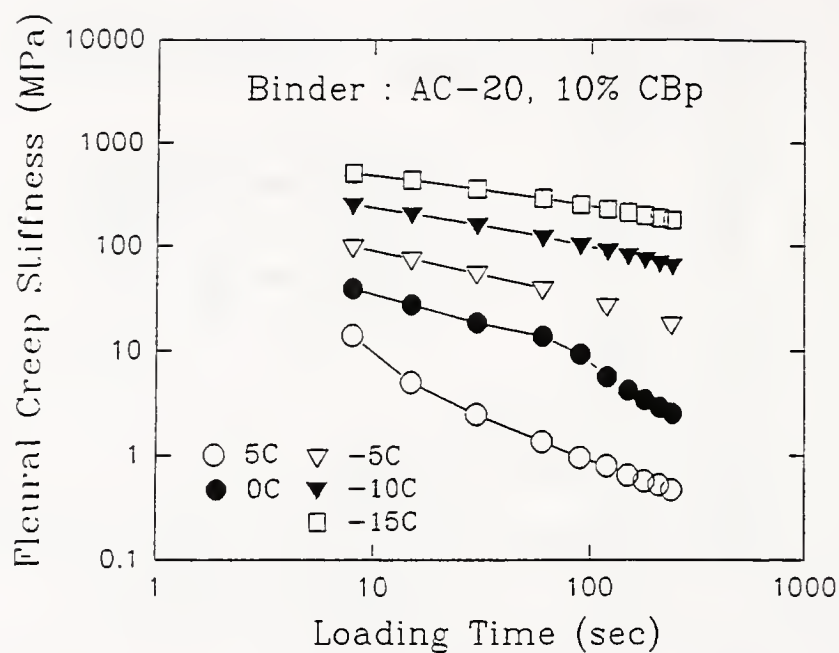
Figure A-4 The Flexural Creep Stiffness for AC-10 and AC-20 Mixtures Modified by 10% CB_p
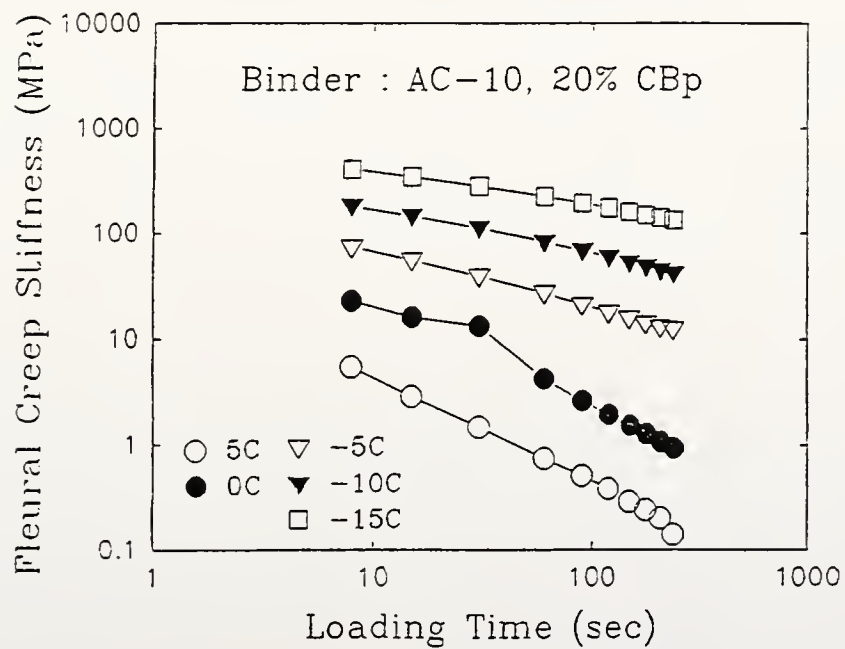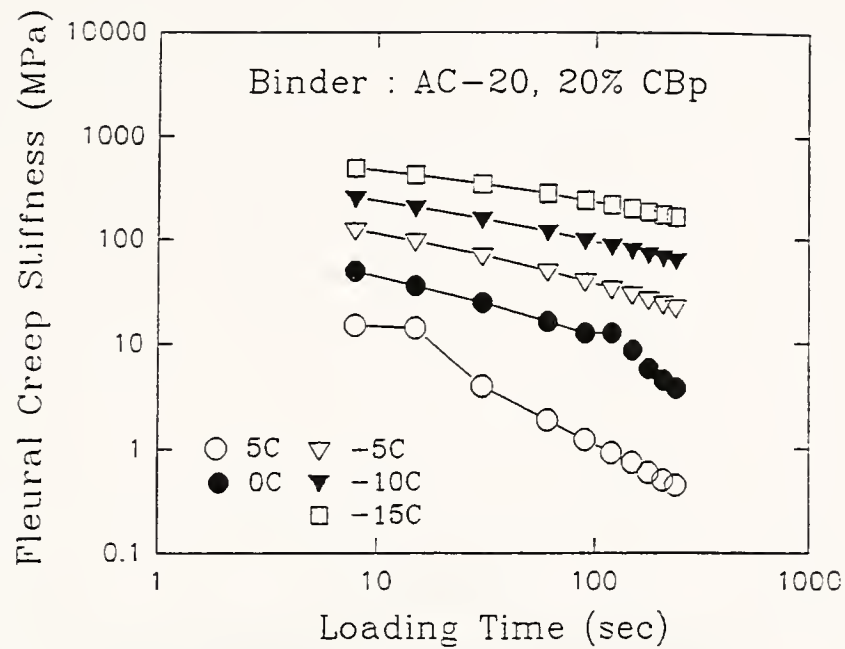
Figure A-5 The Flexural Creep Stiffness for AC-10 and AC-20 Mixtures Modified by 20% CB$_p$

APPENDIX B.

THE SUMMARY OF MARSHALL MIX DESIGN
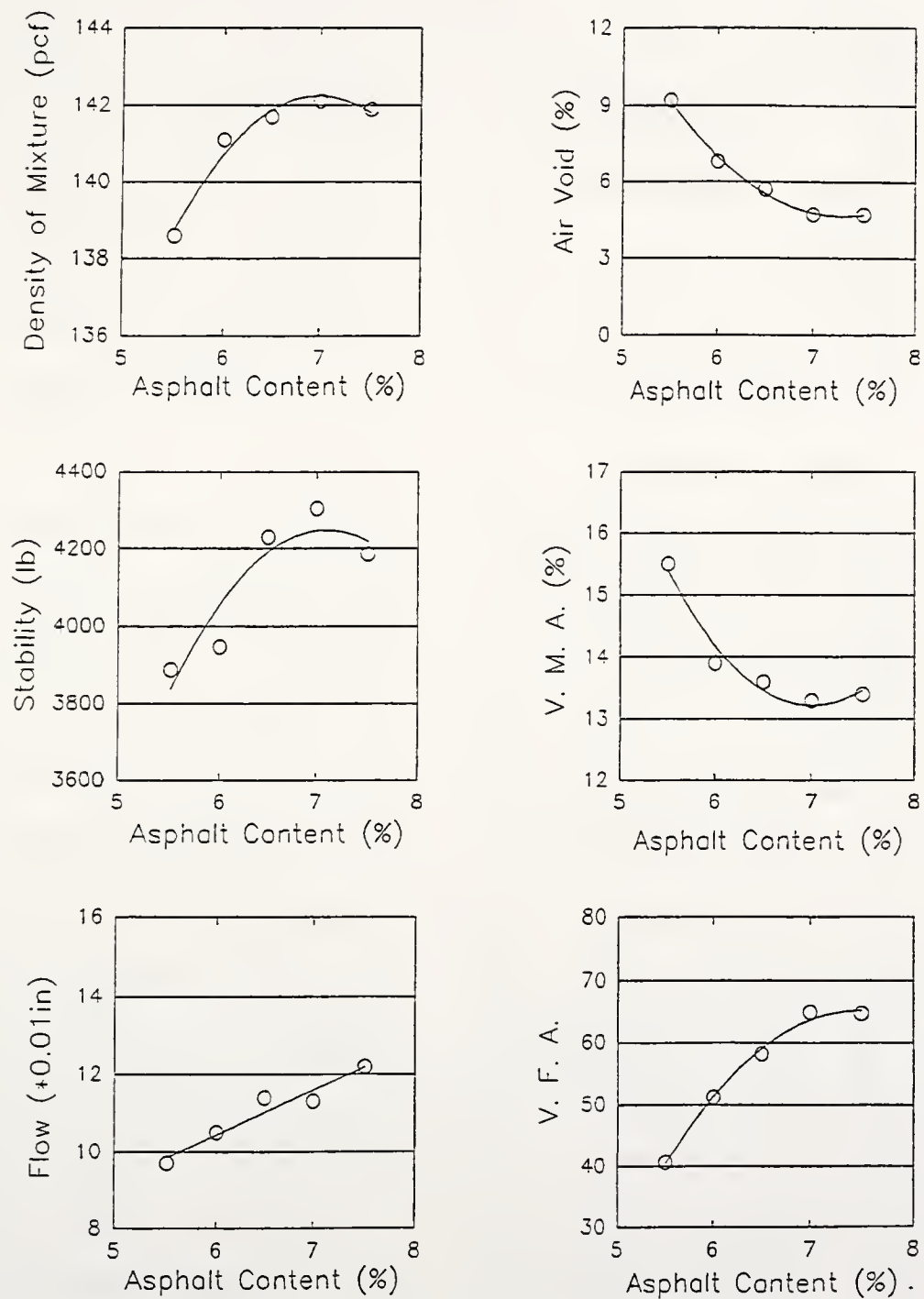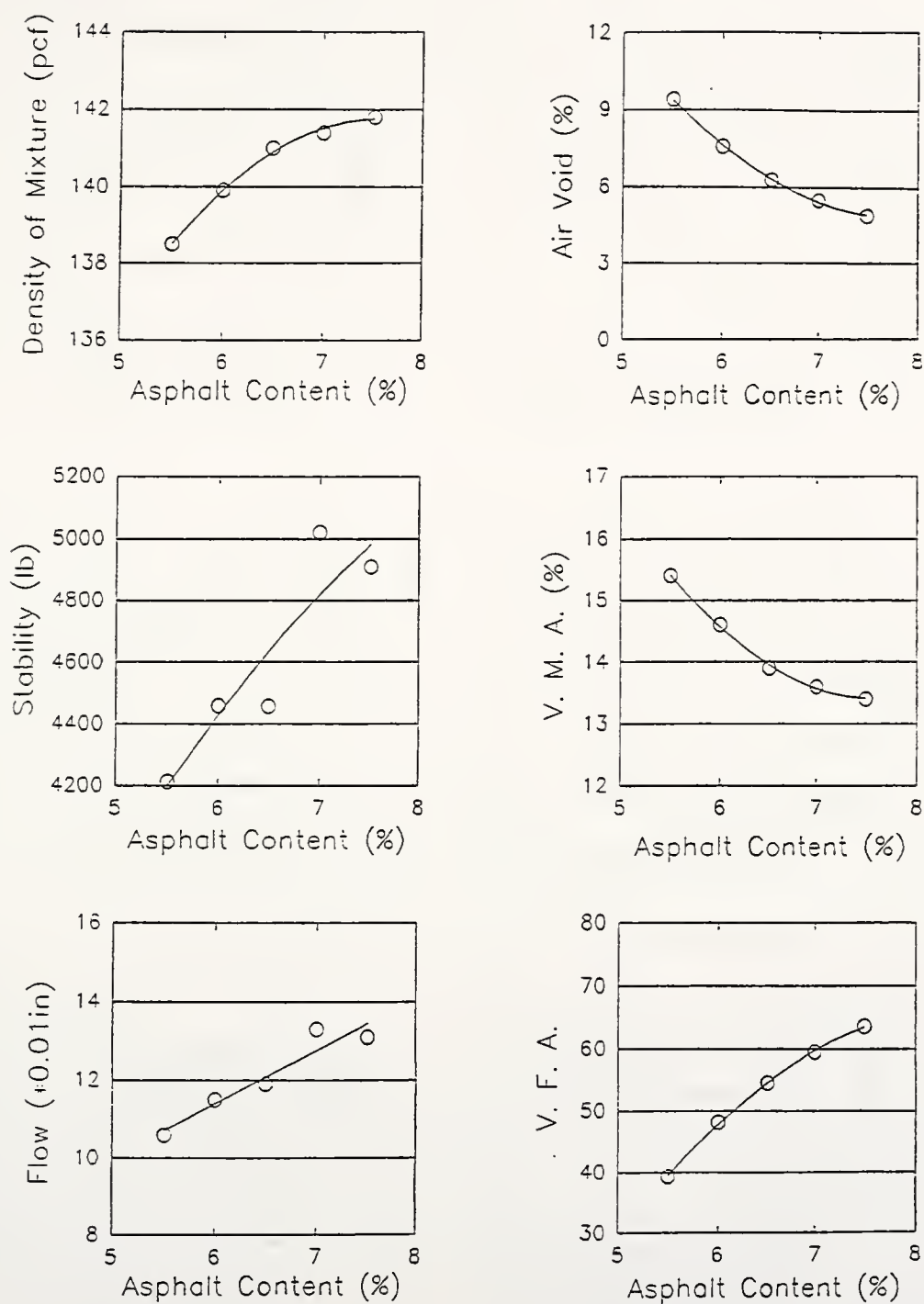
Figure B-1 The Summary of Test Results for AC-10 Mixtures
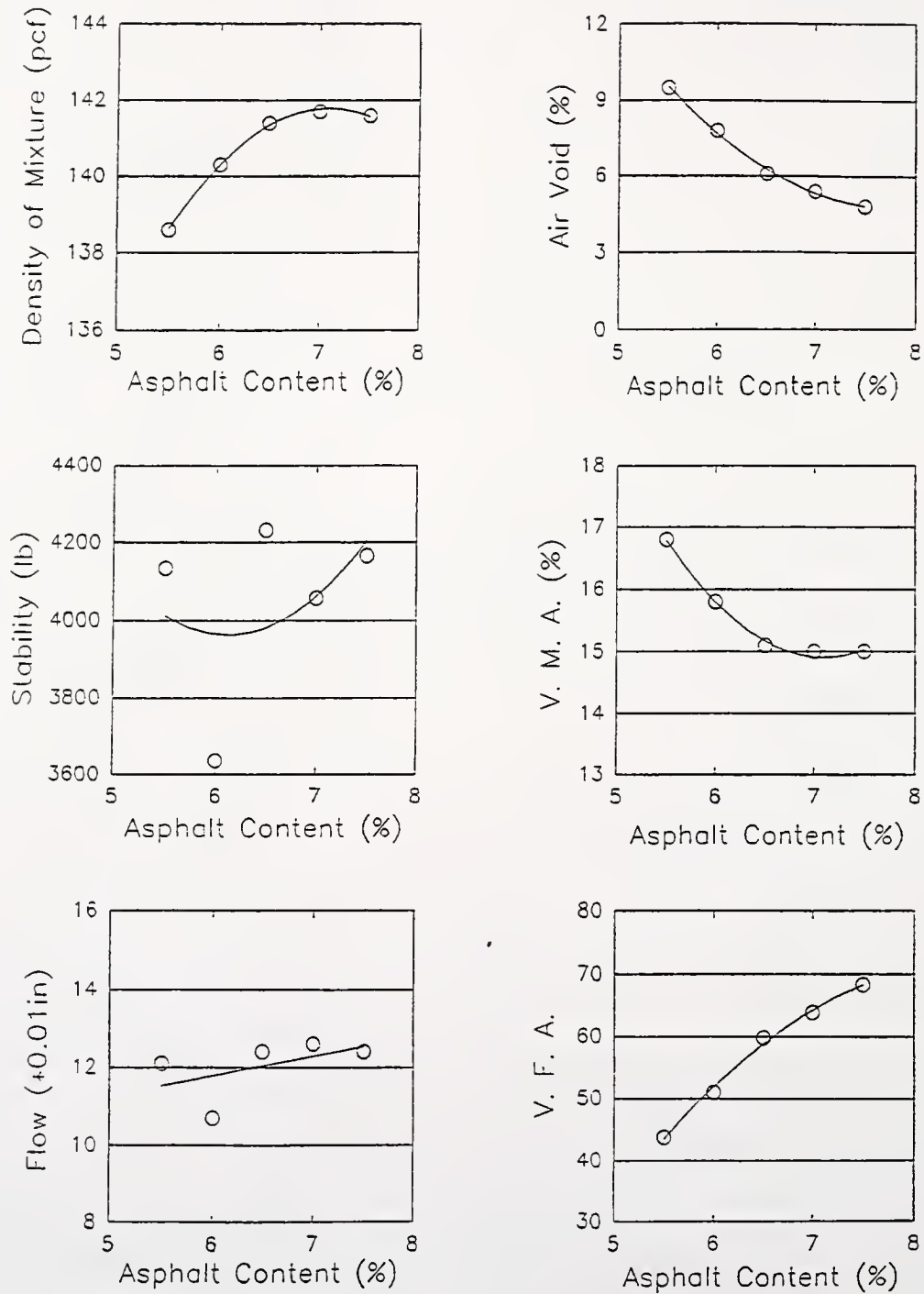
Figure B-2 The Summary of Test Results for AC-10 Mixtures Modified by 5% CB
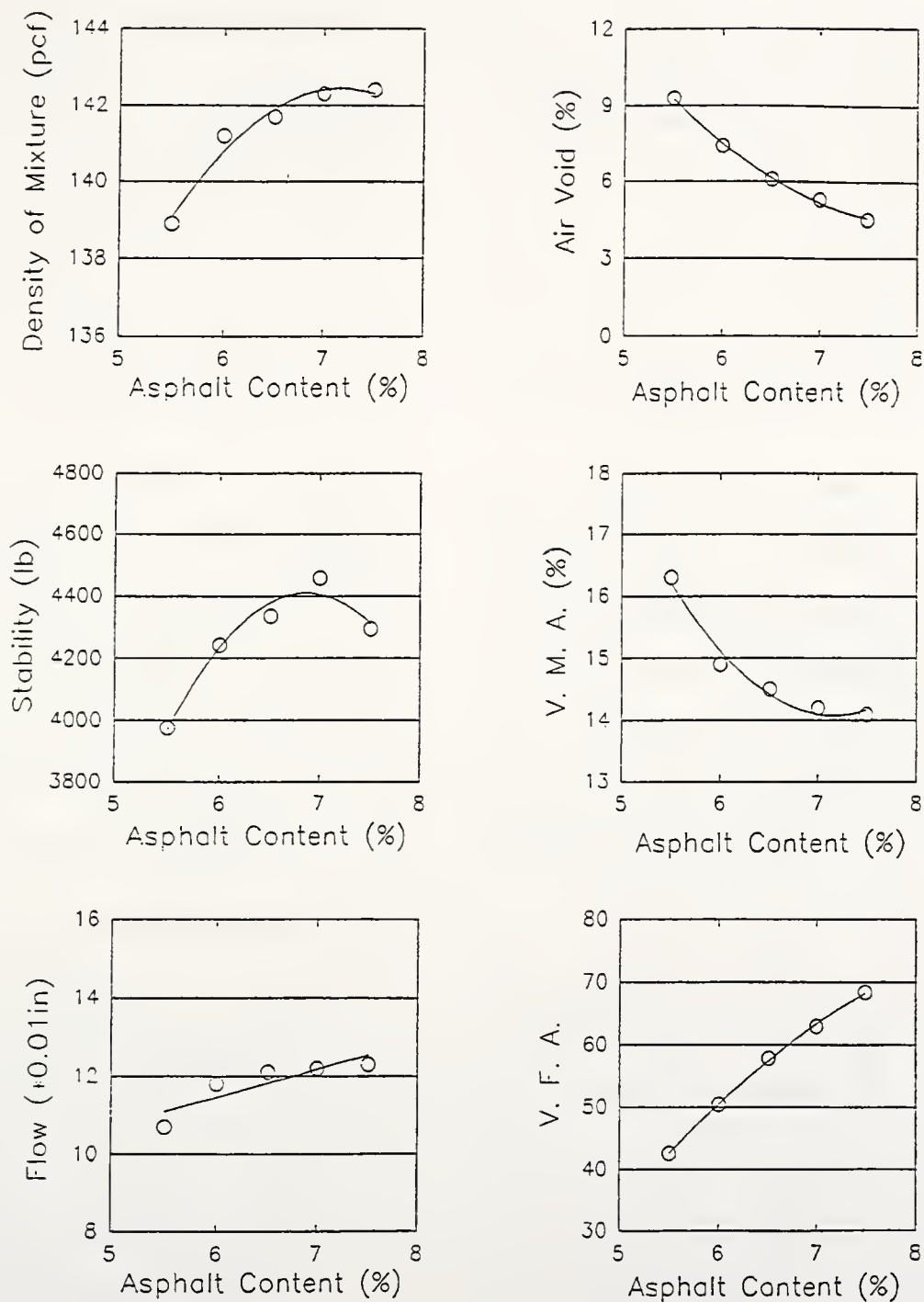
Figure B-3 The Summary of Test Results for AC-10 Mixtures Modified by 10% CB
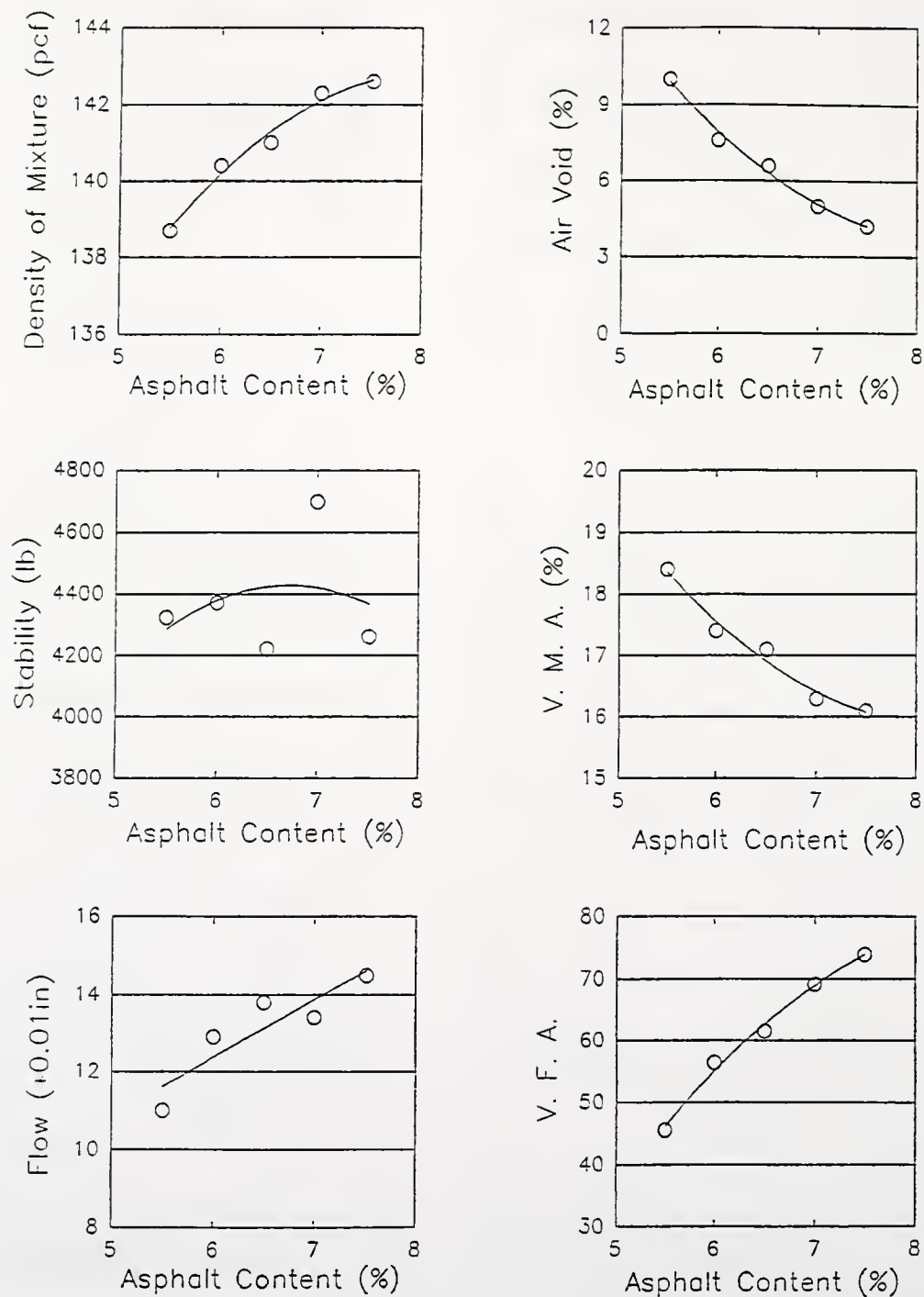
Figure B-4 The Summary of Test Results for AC-10 Mixtures Modified by 15% CB
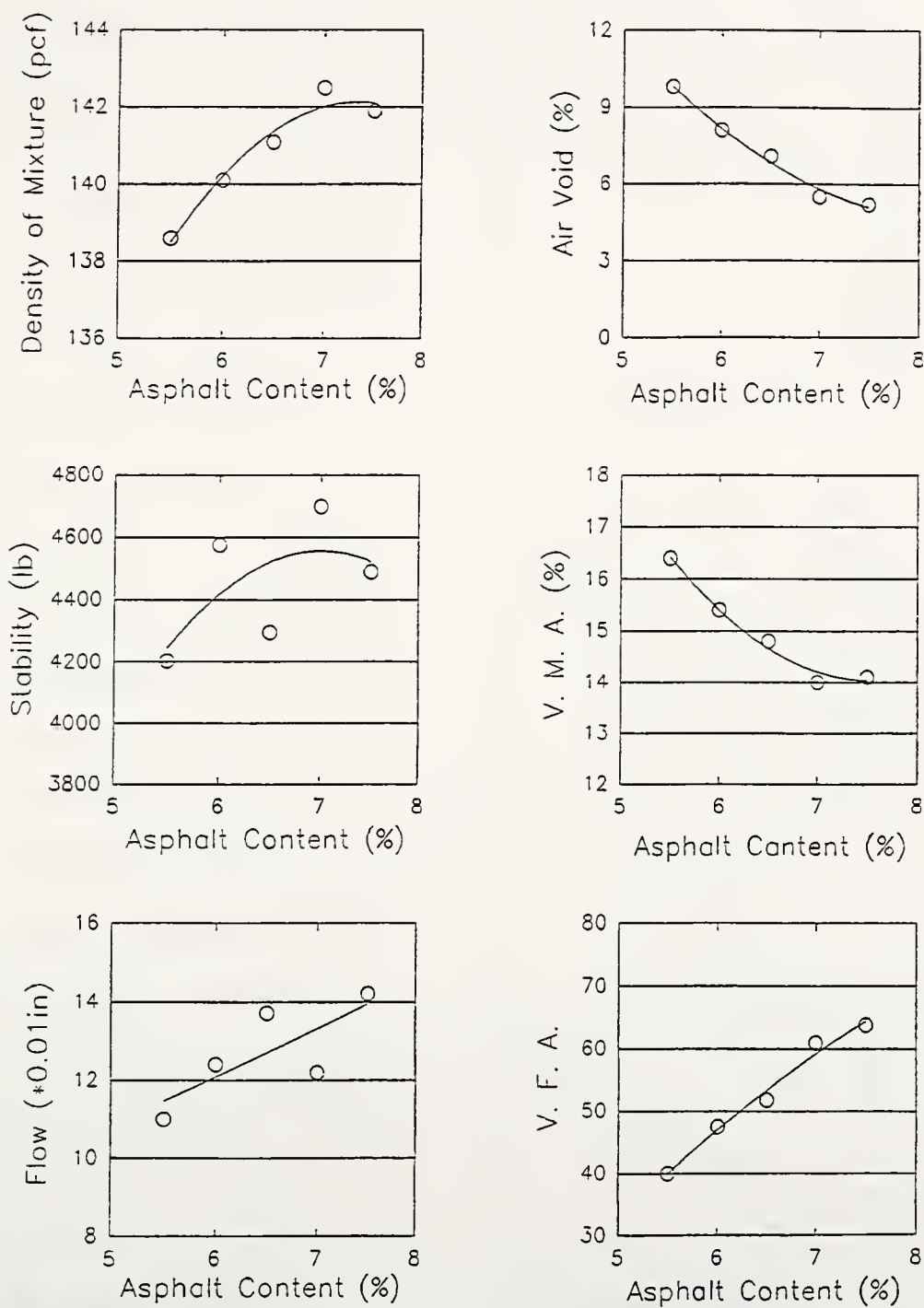
Figure B-5 The Summary of Test Results for AC-10 Mixtures Modified by 20% CB
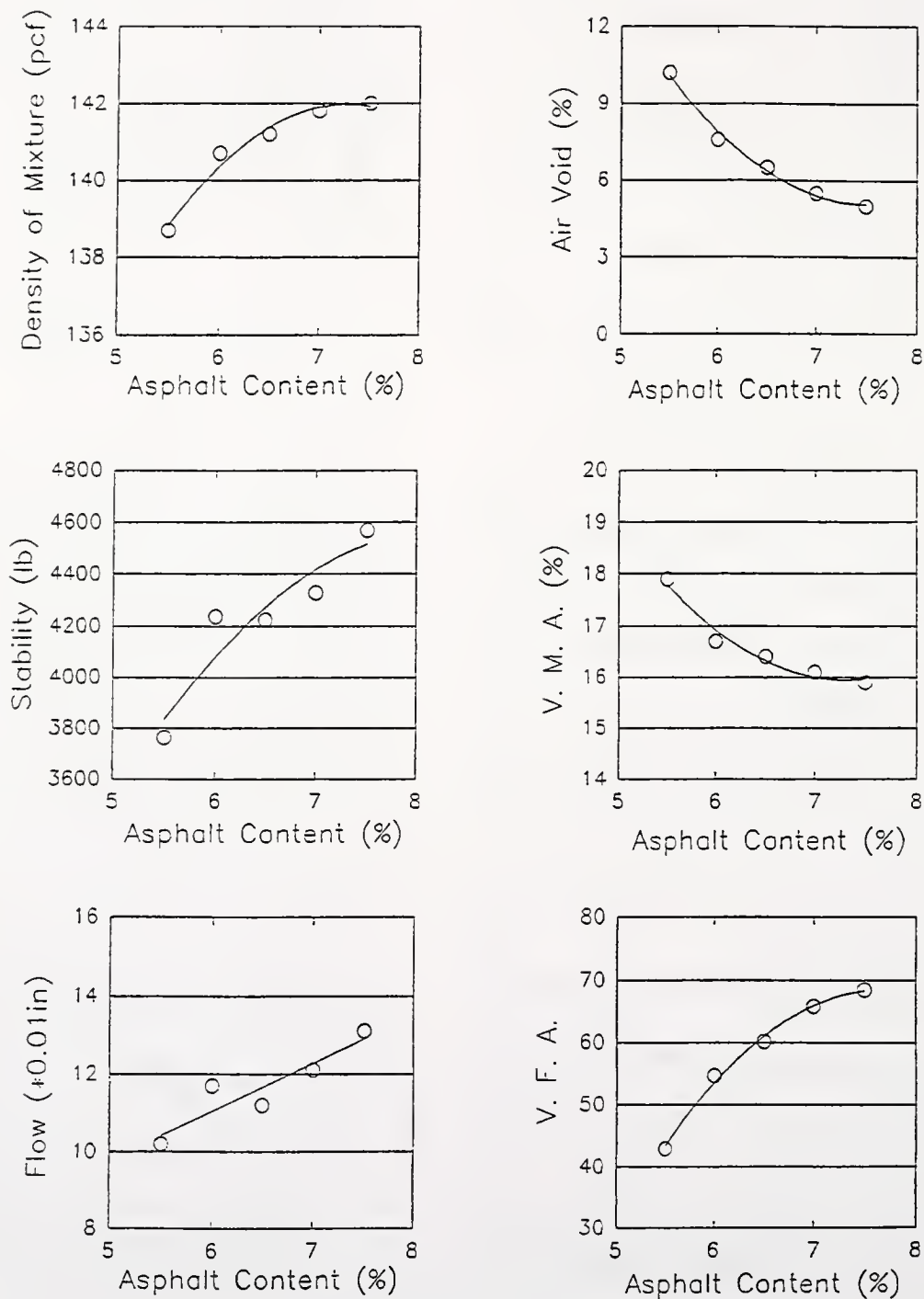
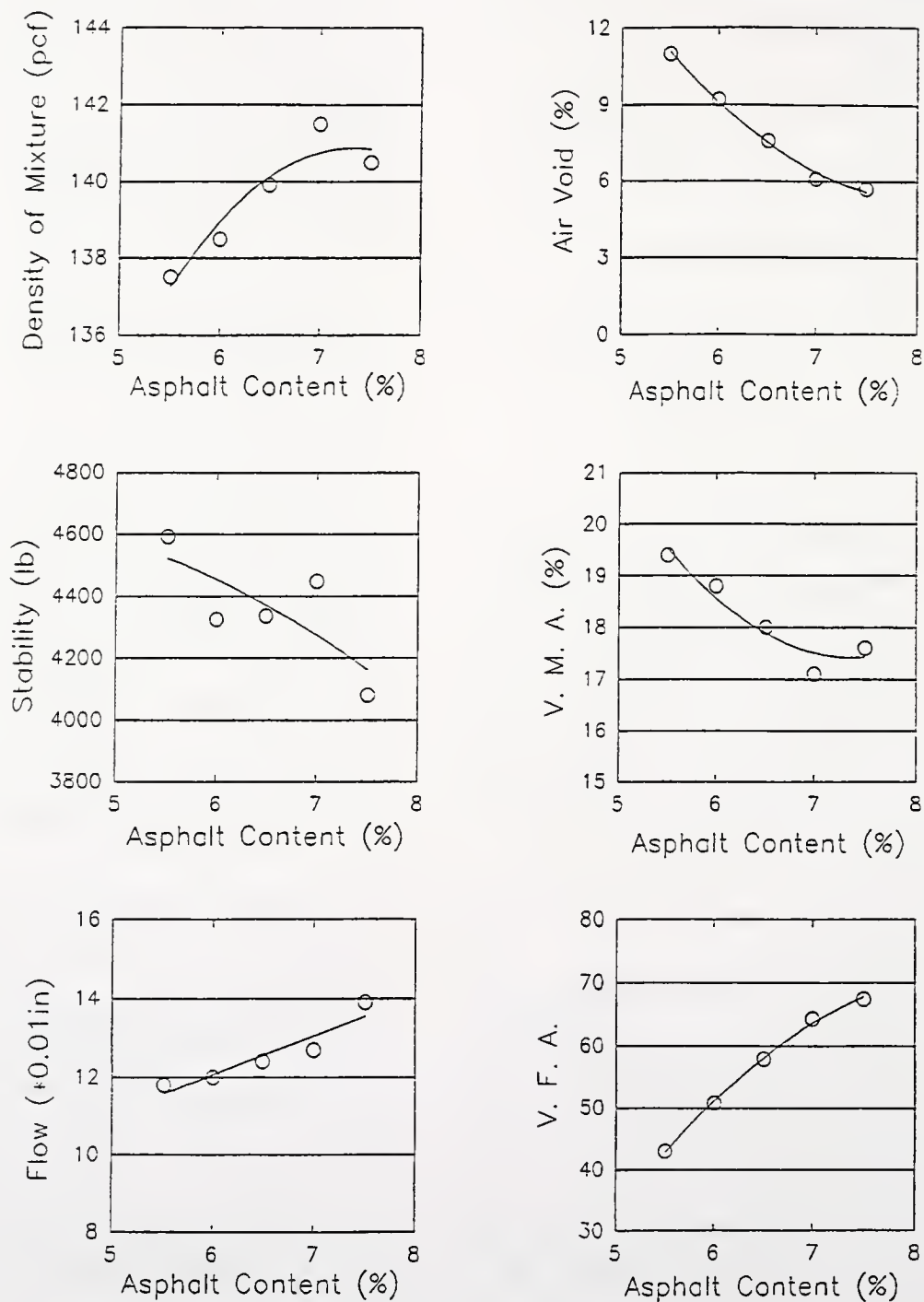Figure B-6 The Summary of Test Results for AC-10 Mixtures Modified by 5% CB$_p$
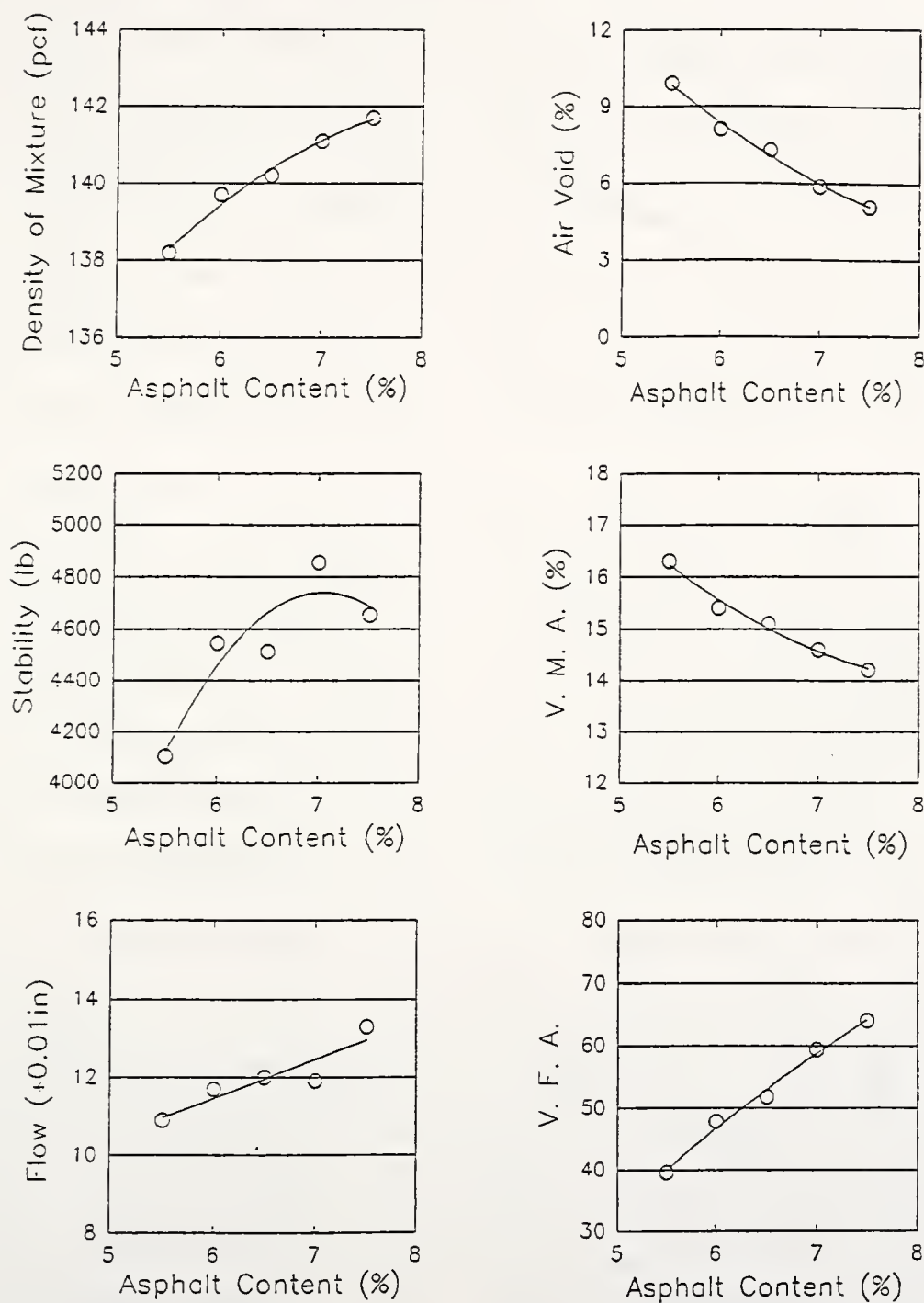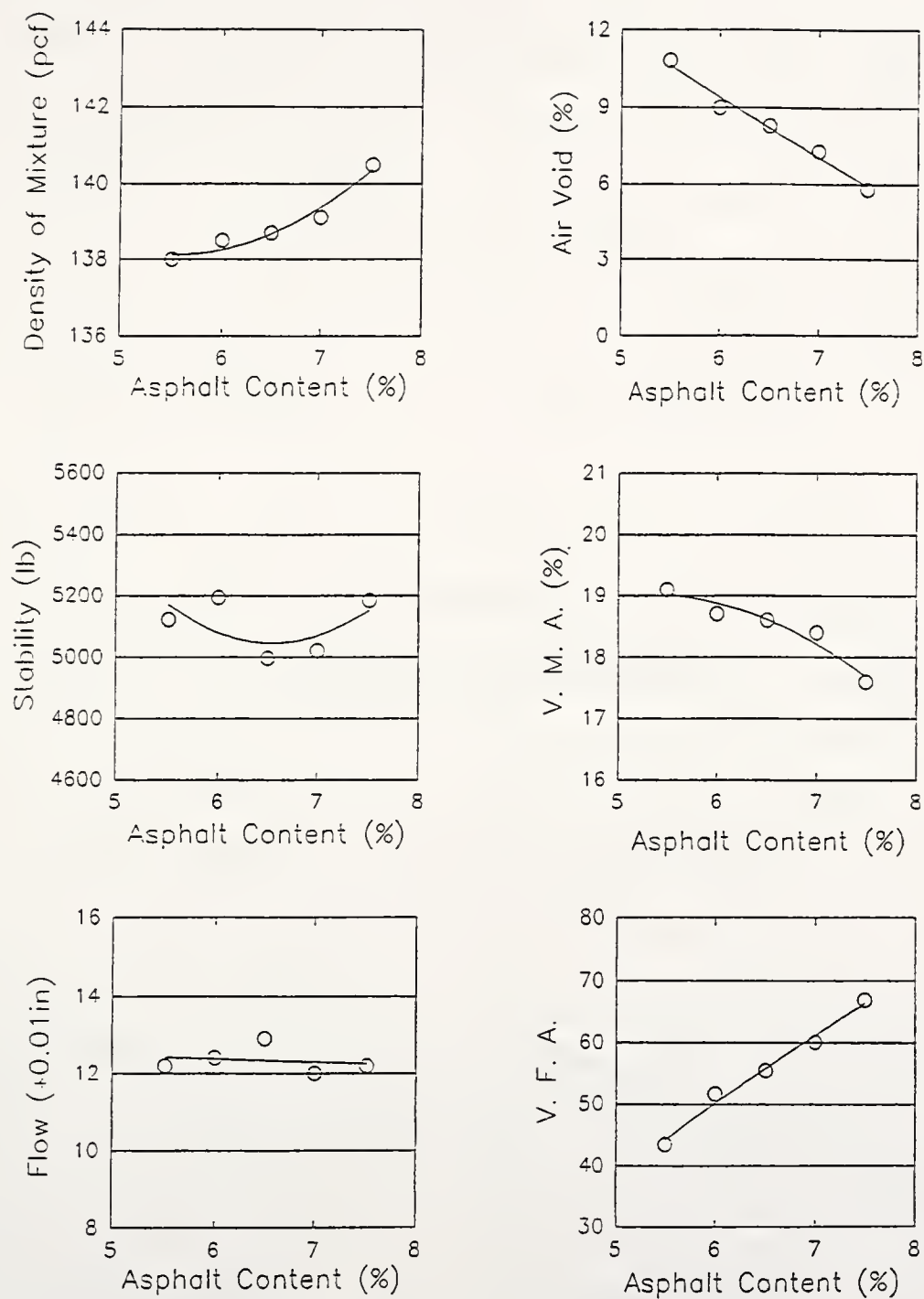
Figure B-7 The Summary of Test Results for AC-10 Mixtures Modified by 10% CB$_p$
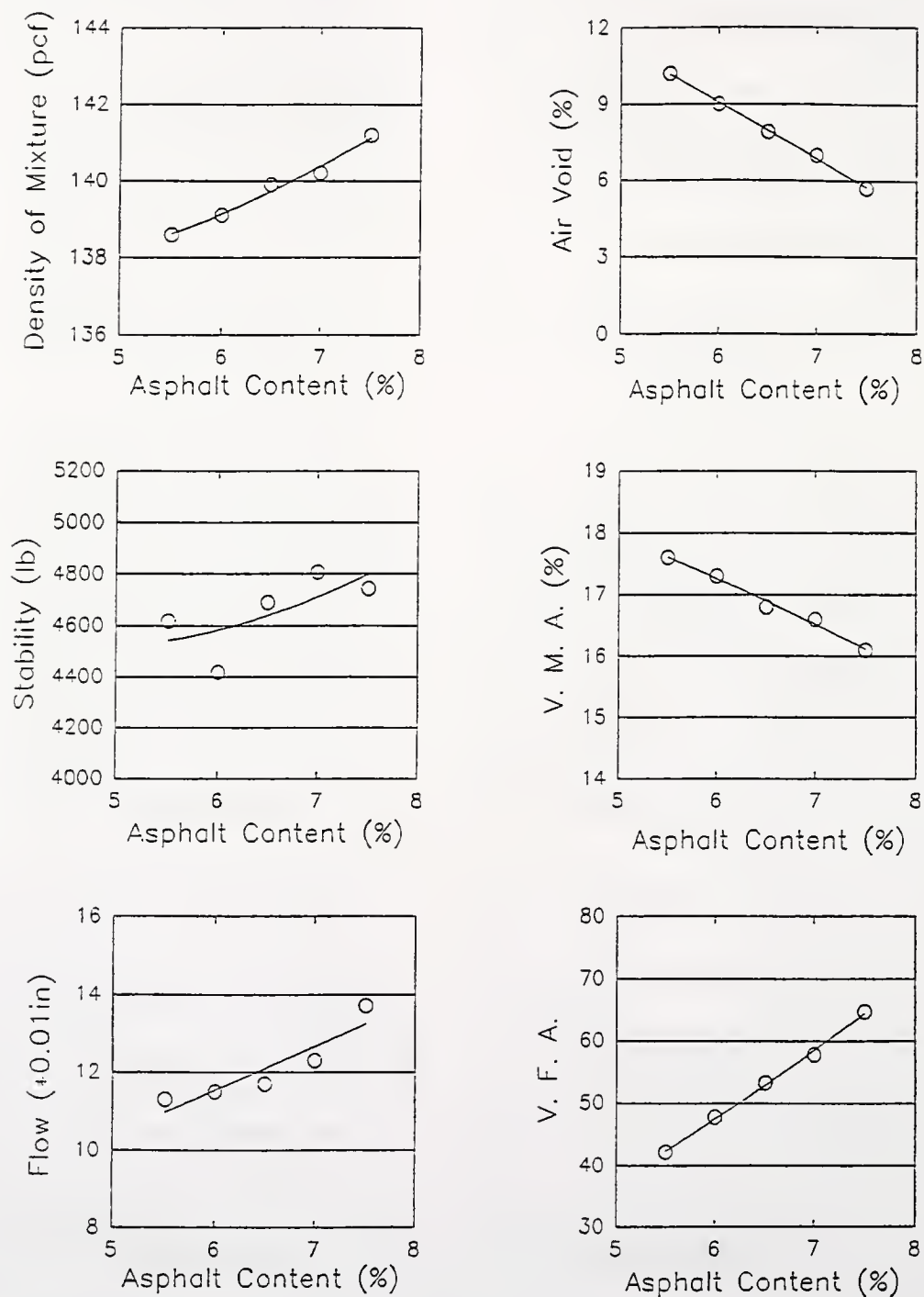
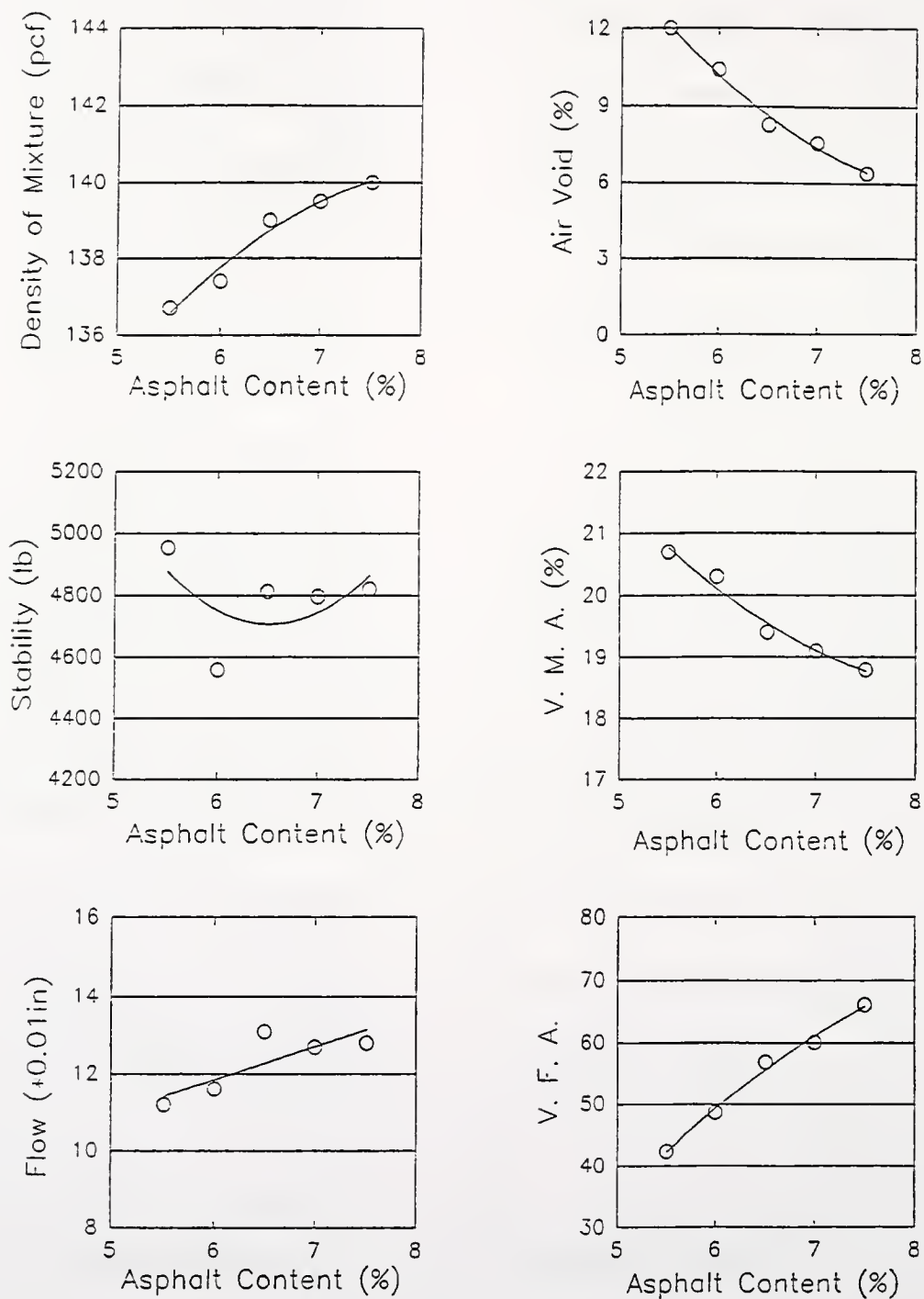Figure B-8 The Summary of Test Results for AC-10 Mixtures Modified by 15% CB_p
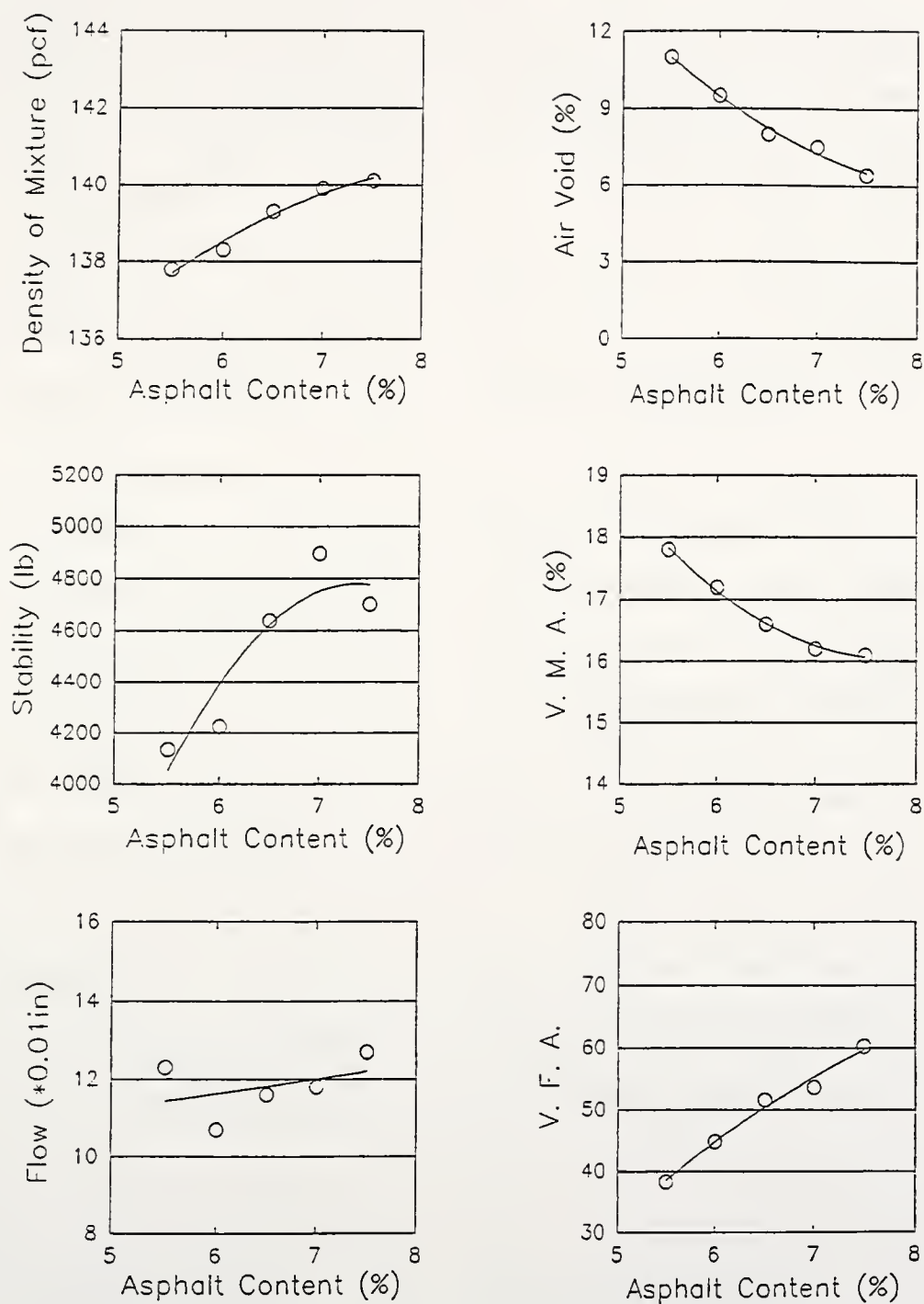
Figure B-9 The Summary of Test Results for AC-10 Mixtures Modified by 20% CB$_p$
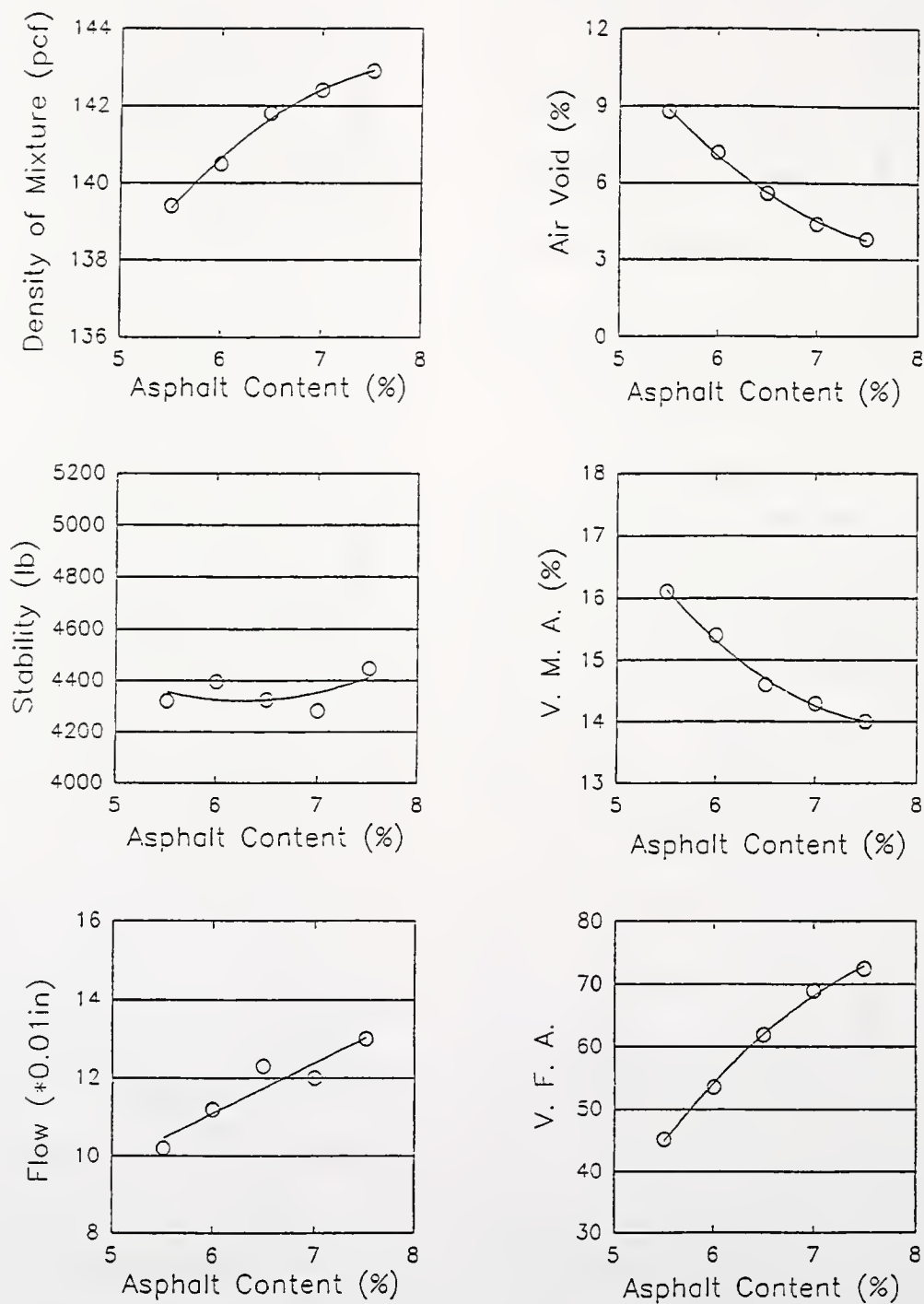
Figure B-10 The Summary of Test Results for AC-20 Mixtures
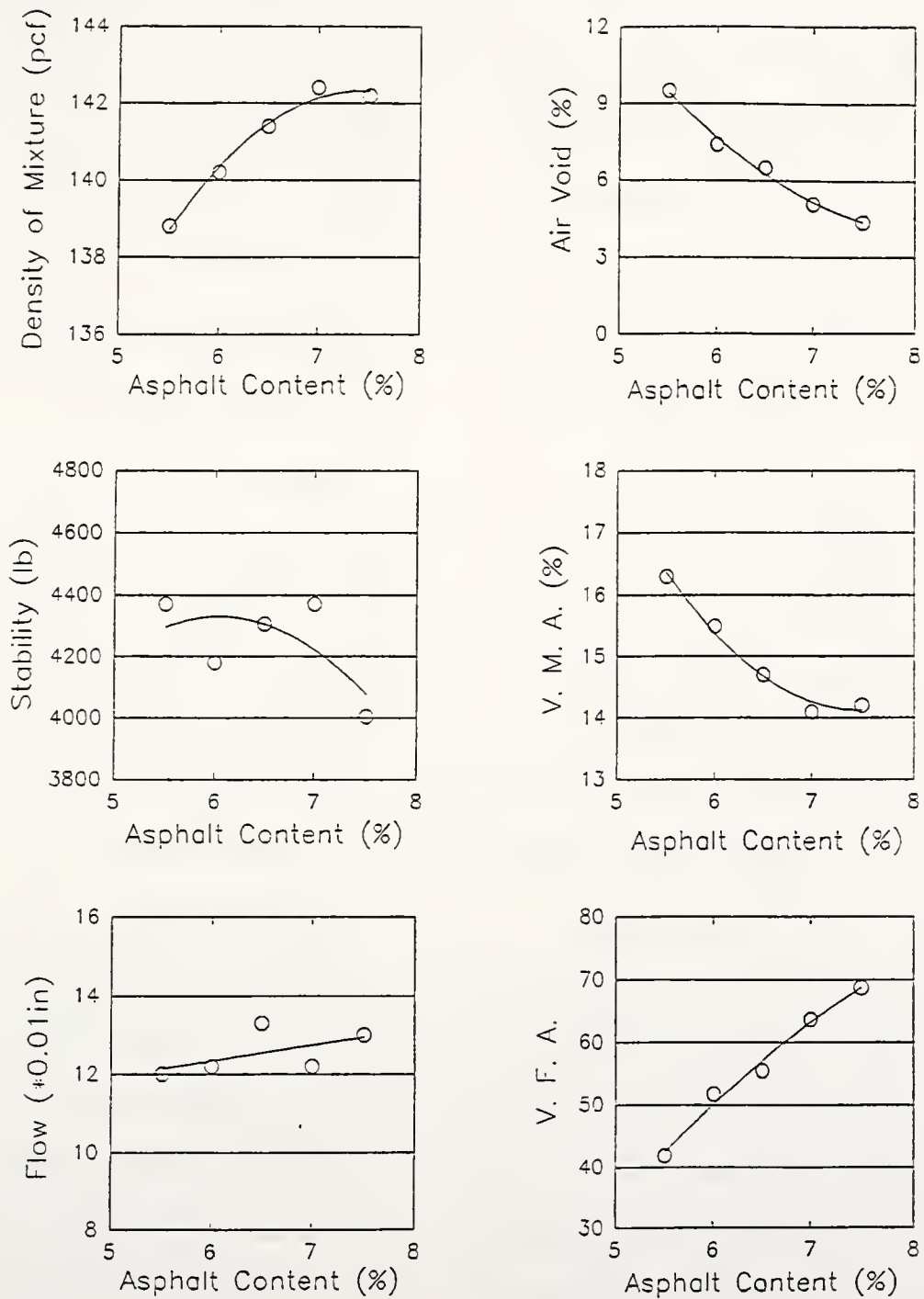
Figure B-11 The Summary of Test Results for AC-20 Mixtures Modified by 5% CB
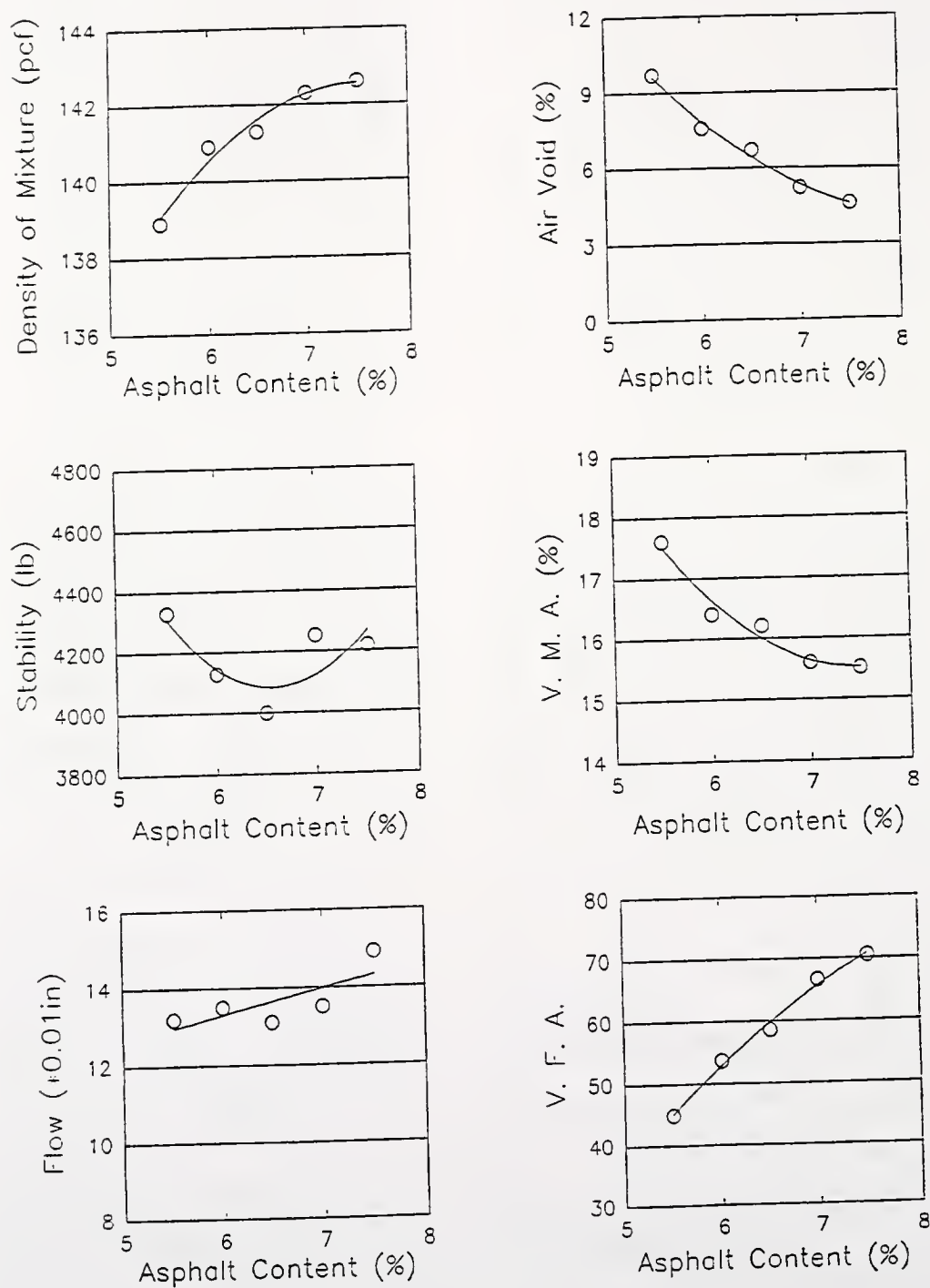
Figure B-12 The Summary of Test Results for AC-20 Mixtures Modified by 10% CB
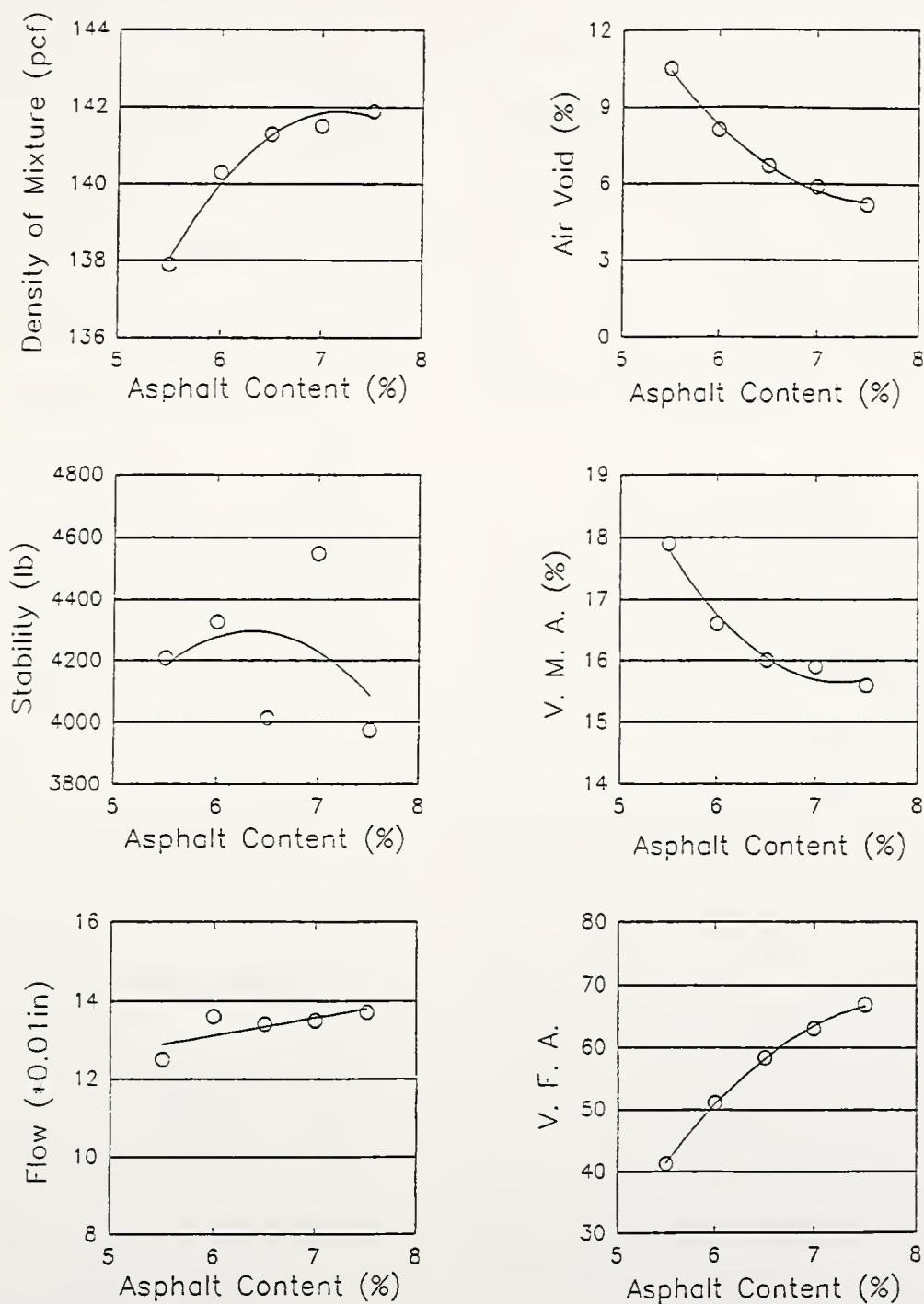
Figure B-13 The Summary of Test Results for AC-20 Mixtures Modified by 15% CB
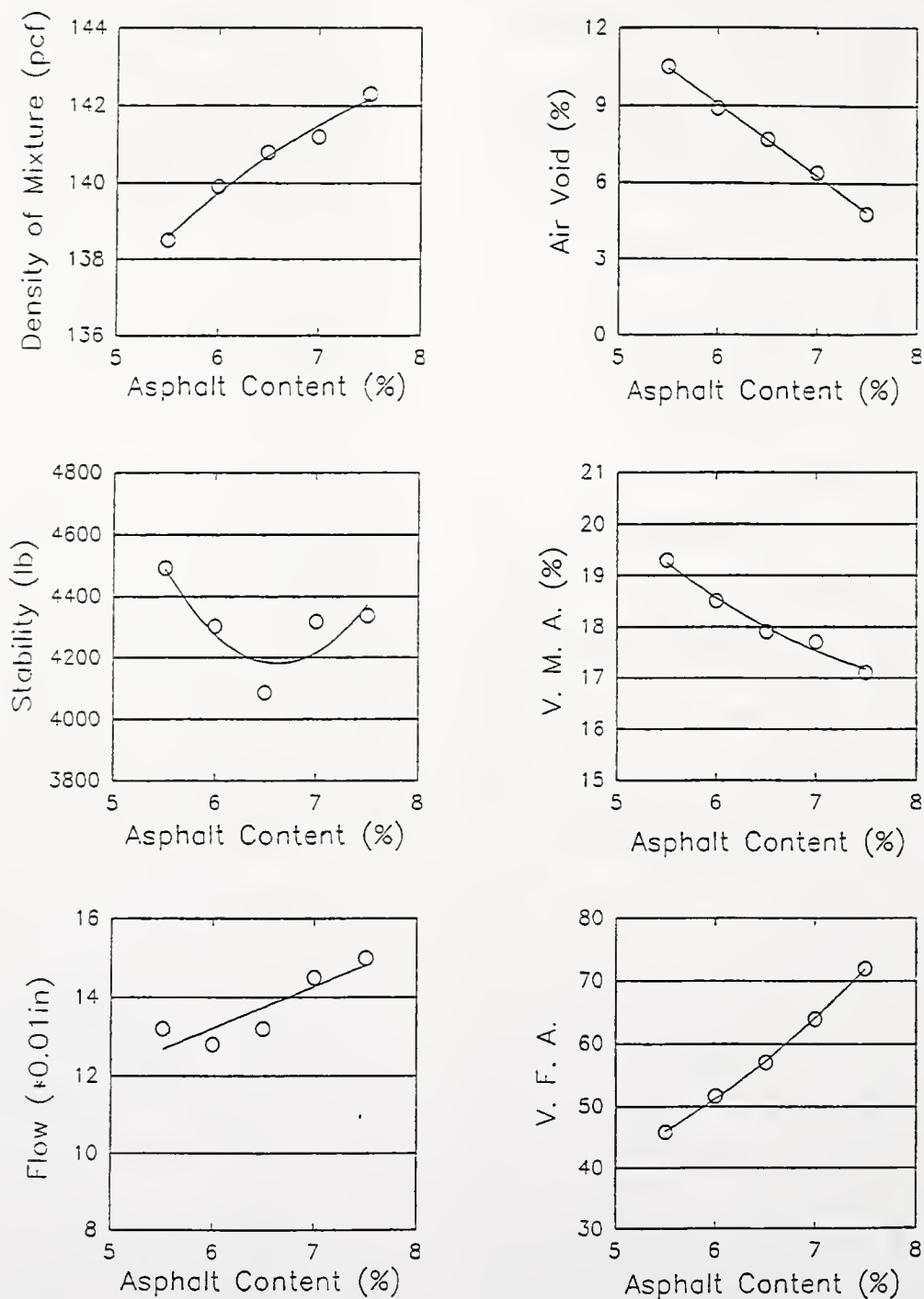
Figure B-14 The Summary of Test Results for AC-20 Mixtures Modified by 20% CB

Figure B-15 The Summary of Test Results for AC-20 Mixtures Modified by 5% CB$_p$

Figure B-16 The Summary of Test Results for AC-20 Mixtures Modified by 10% CB$_p$

Figure B-17 The Summary of Test Results for AC-20 Mixtures Modified by 15% CB$_p$

Figure B-18 The Summary of Test Results for AC-20 Mixtures Modified by 20% CB_p
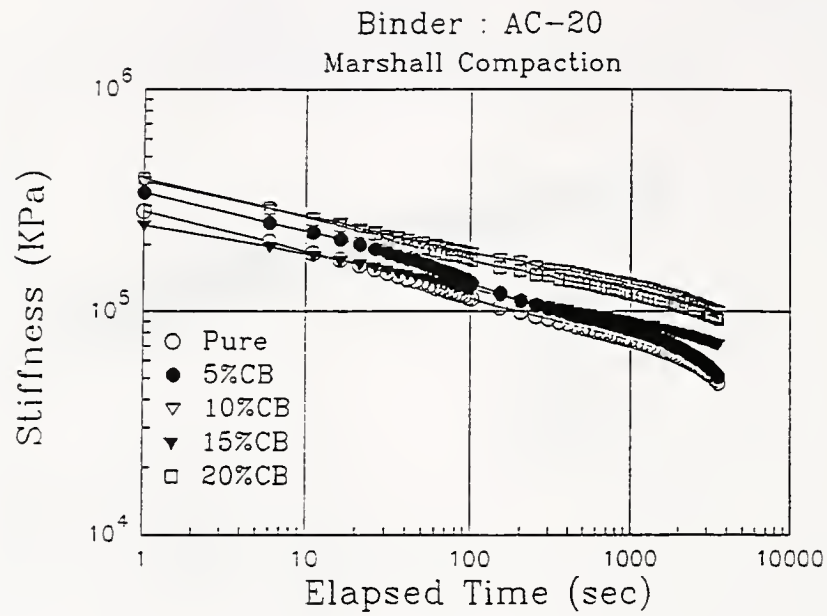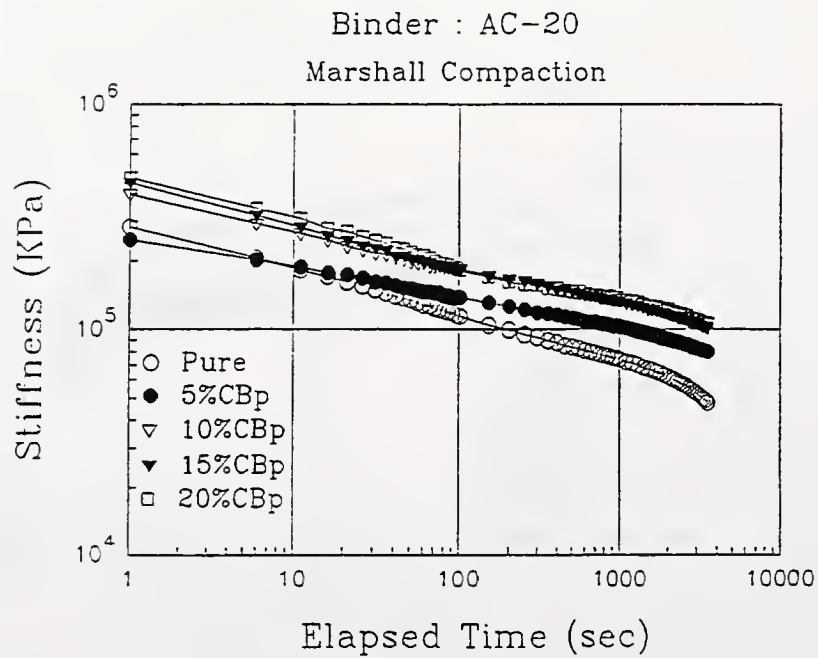
APPENDIX C.

THE SUMMARY OF CREEP MODULUS
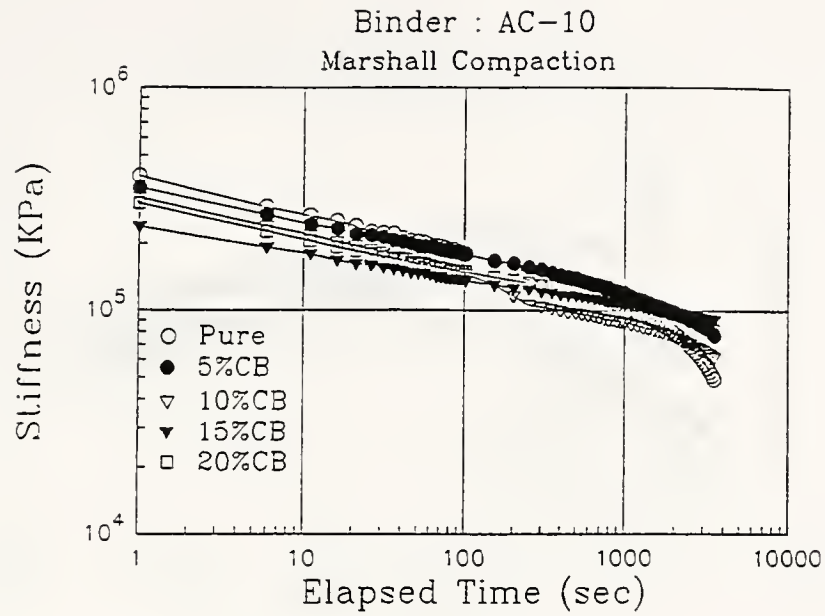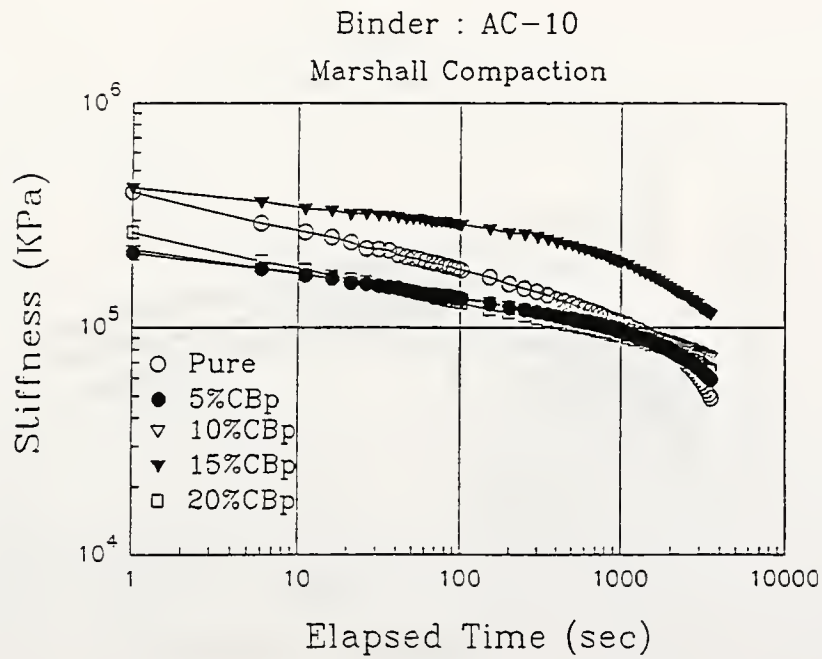
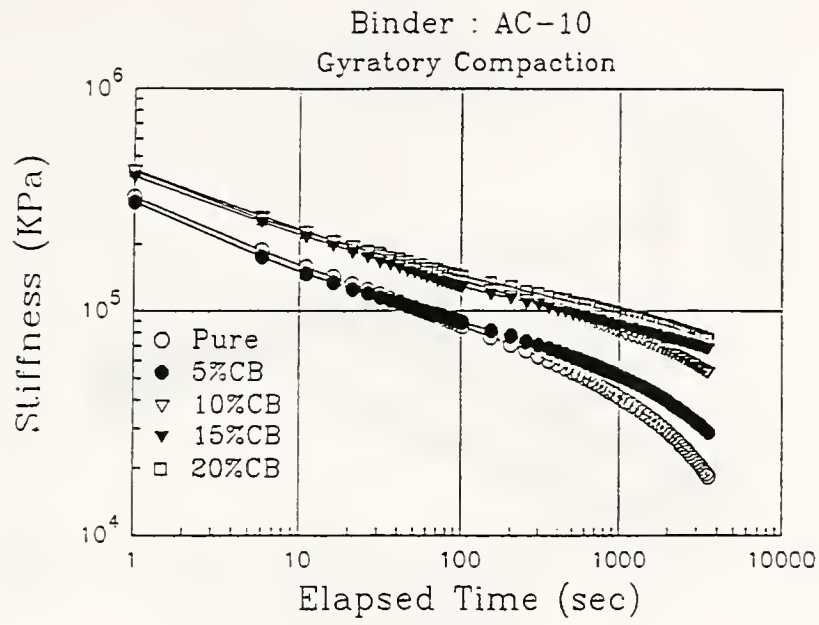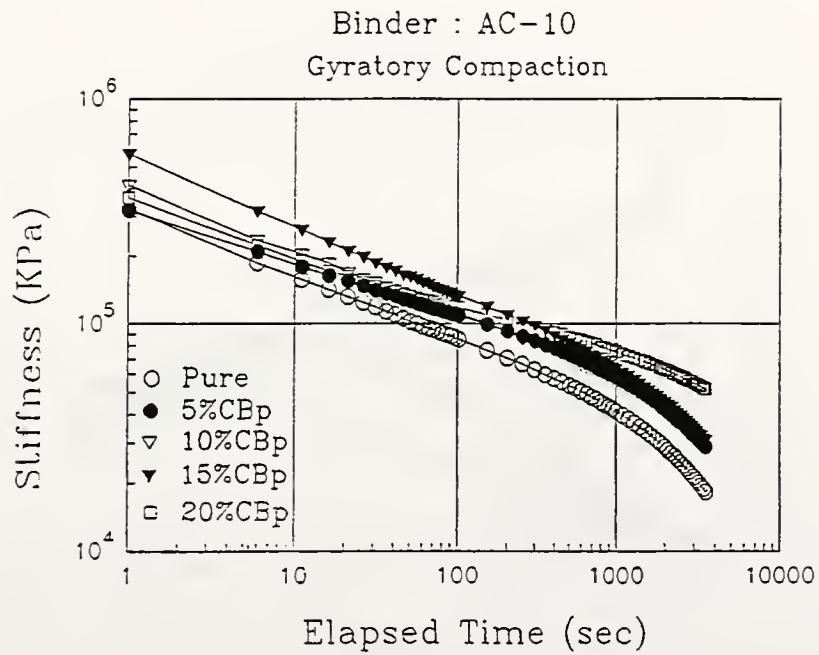Figure C-1 Creep Modulus for AC-10 Mixtures Compacted by Marshall Compactor
         at 50°C

Figure C-2 Creep Modulus for AC-20 Mixtures Compacted by Marshall Compactor at 50°C

Binder : AC-10
Gyratory Compaction

(a)

Binder : AC-10
Gyratory Compaction

(b)

Figure C-3 Creep Modulus for AC-10 Mixtures Compacted by Gyratory Compactor
at 50°C

Binder : AC−20
Gyratory Compaction
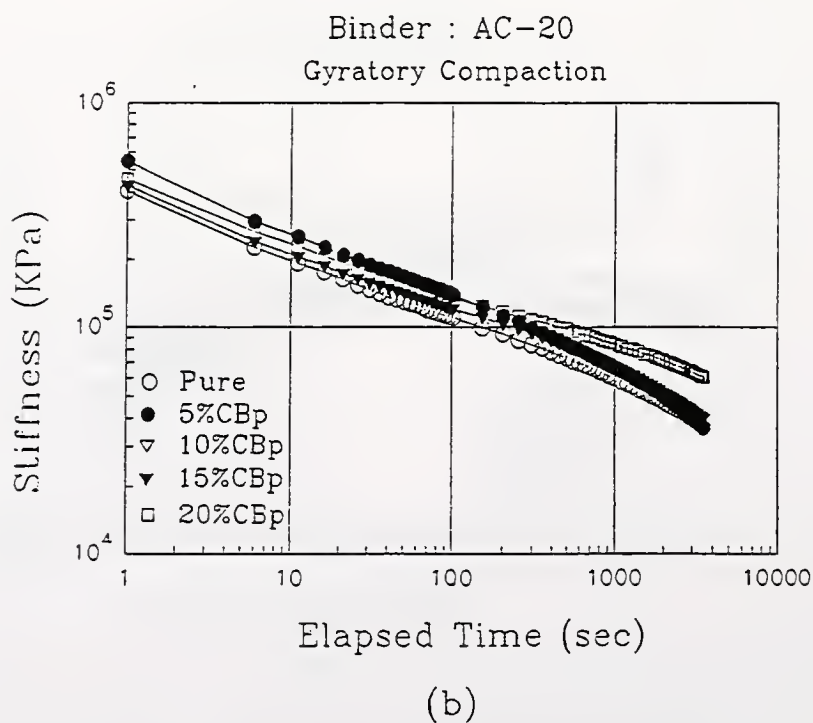

(a)

Binder : AC−20
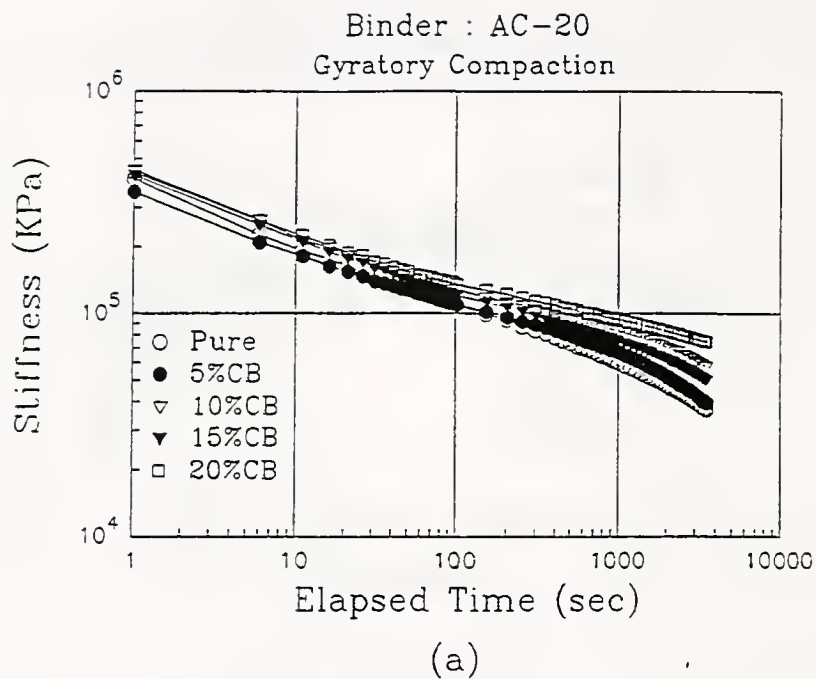Gyratory Compaction

(b)

Figure C-4 Creep Modulus for AC-20 Mixtures Compacted by Gyratory Compactor at 50°C

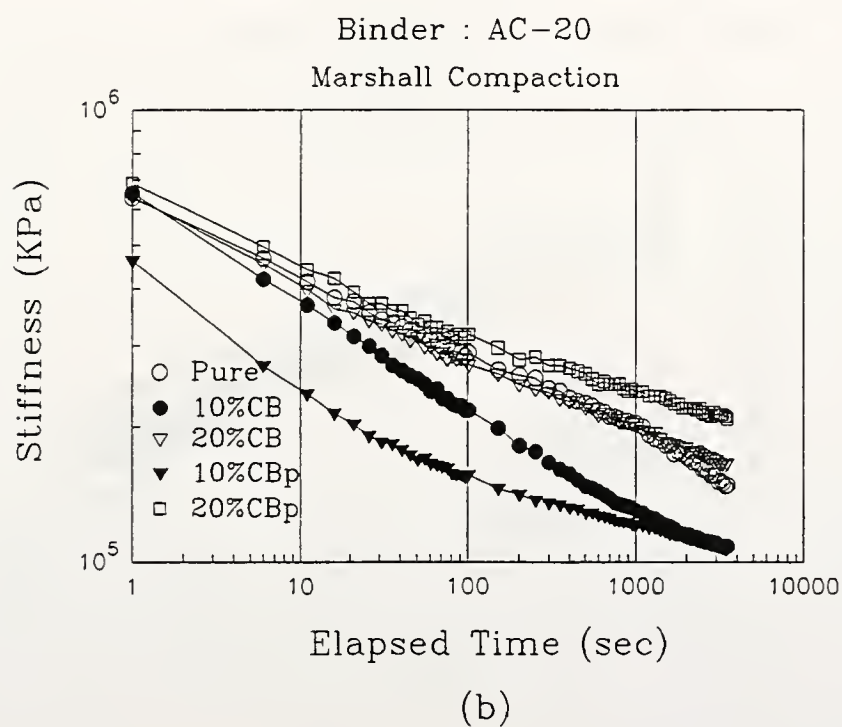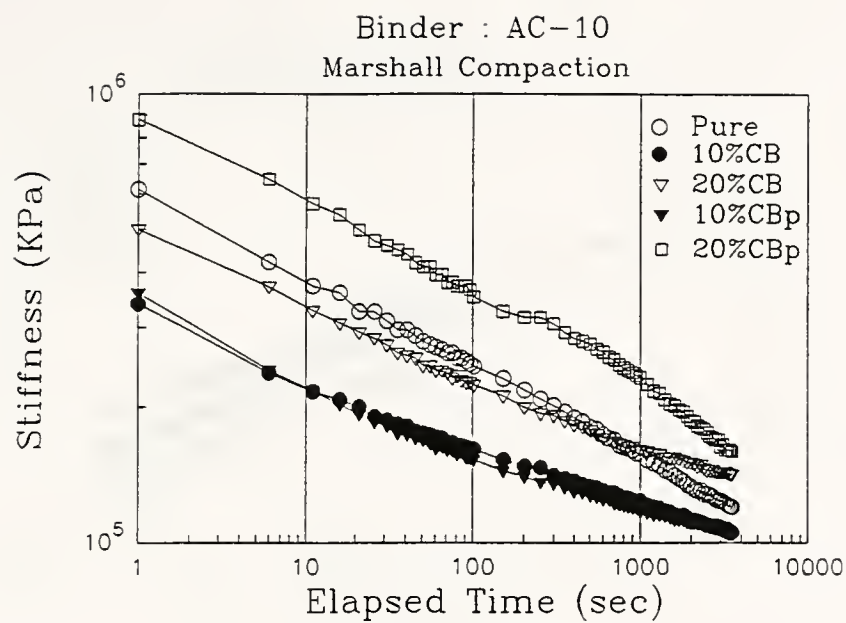Figure C-5 Creep Modulus for Mixtures Compacted by Marshall Compactor at 25°C
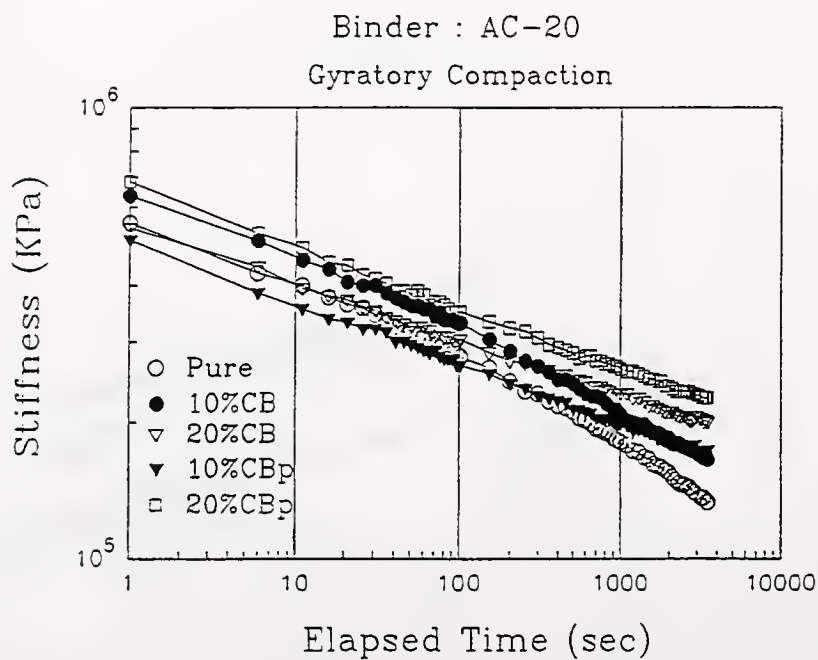
Figure C-6 Creep Modulus for Mixtures Compacted by Gyratory Compactor at 25°C
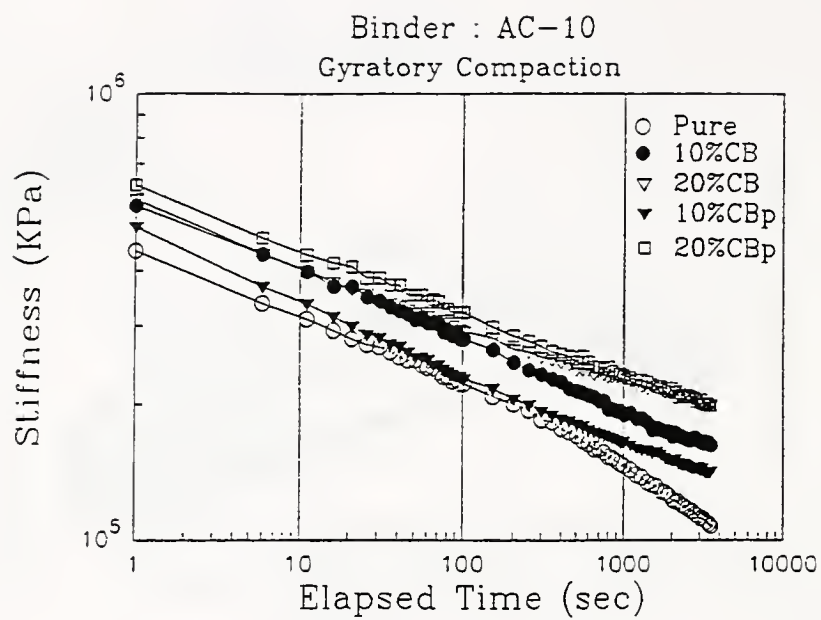
APPENDIX D.

THE SUMMARY OF HAMBURG WHEEL TRACKING TEST

Figure D-1 The Results for AC-10 Mixtures

Fgiure D-2 The Results for AC-10 Mixtures with 10% CB

Figure D-3 The Results for AC-10 Mixtures with 15% CB

Figure D-4 The Results for AC-10 Mixtures with 10% CB_p

Figure D-5 The Results for AC-10 Mixtures with 15% CB$_p$

Figure D-6 The Results for AC-20 Mixtures

Fgiure D-7 The Results for AC-20 Mixtures with 10% CB

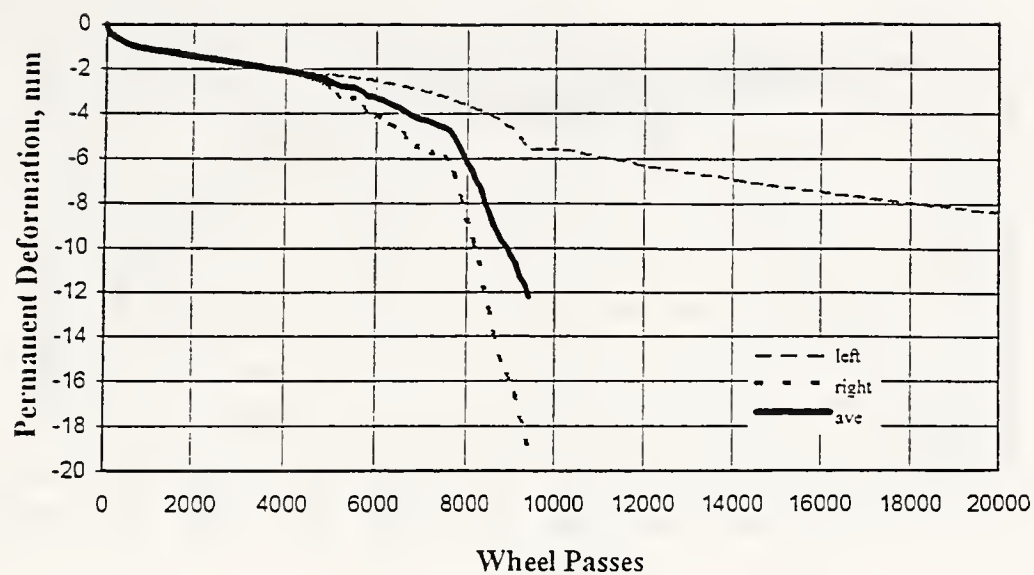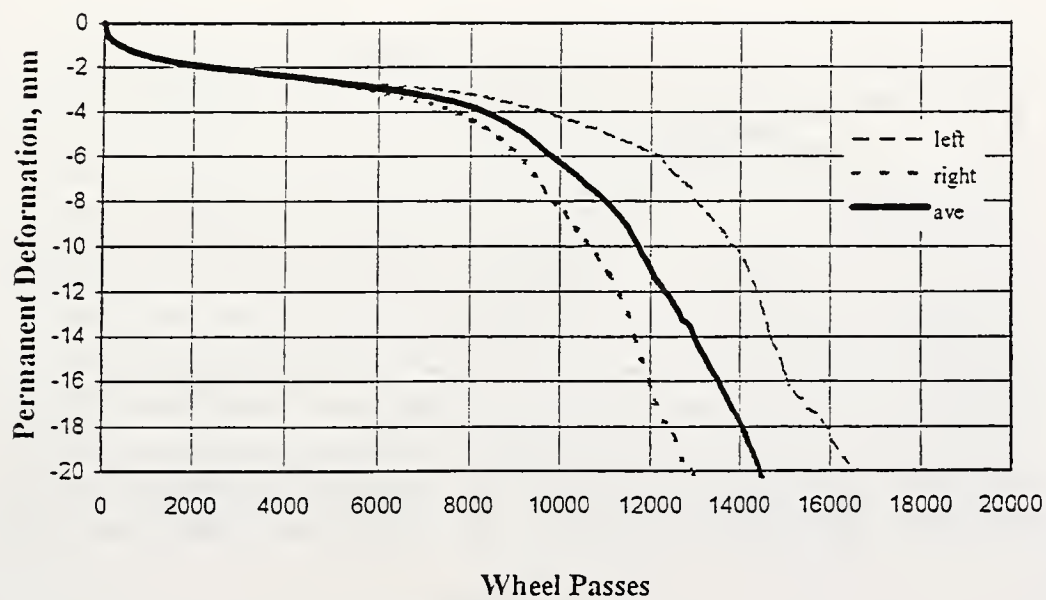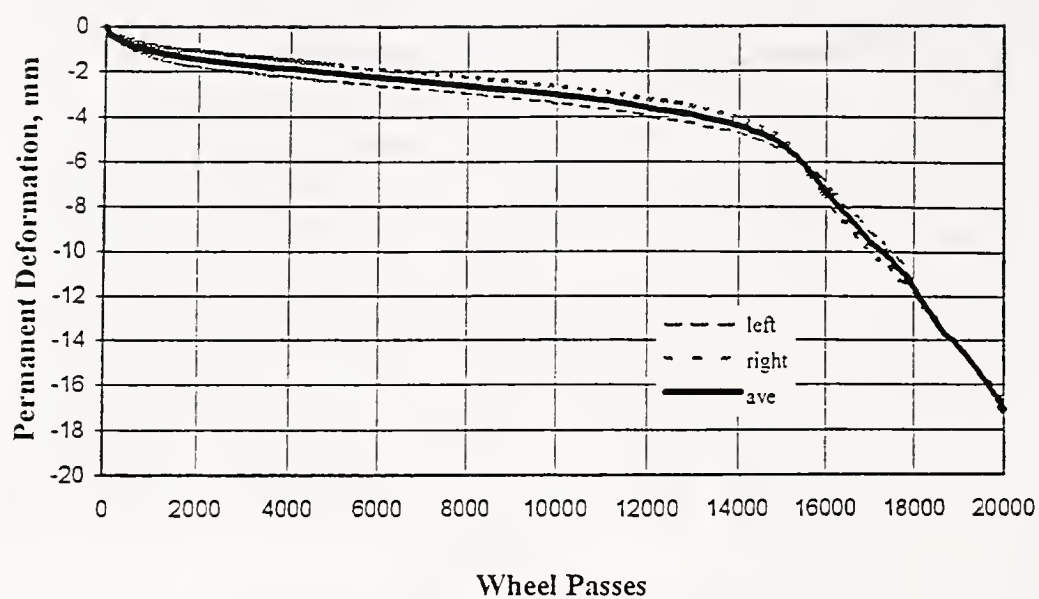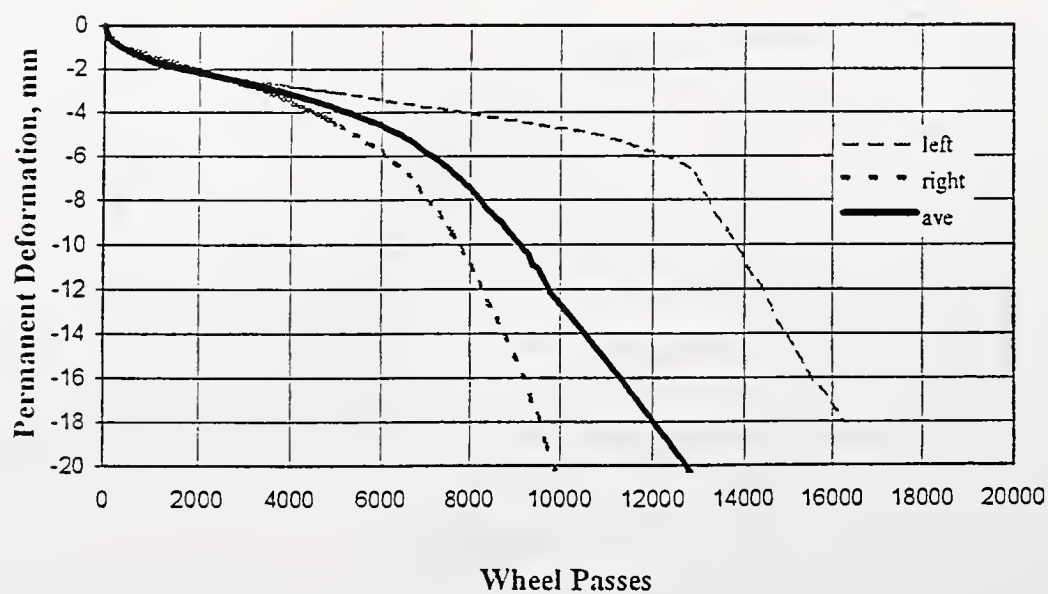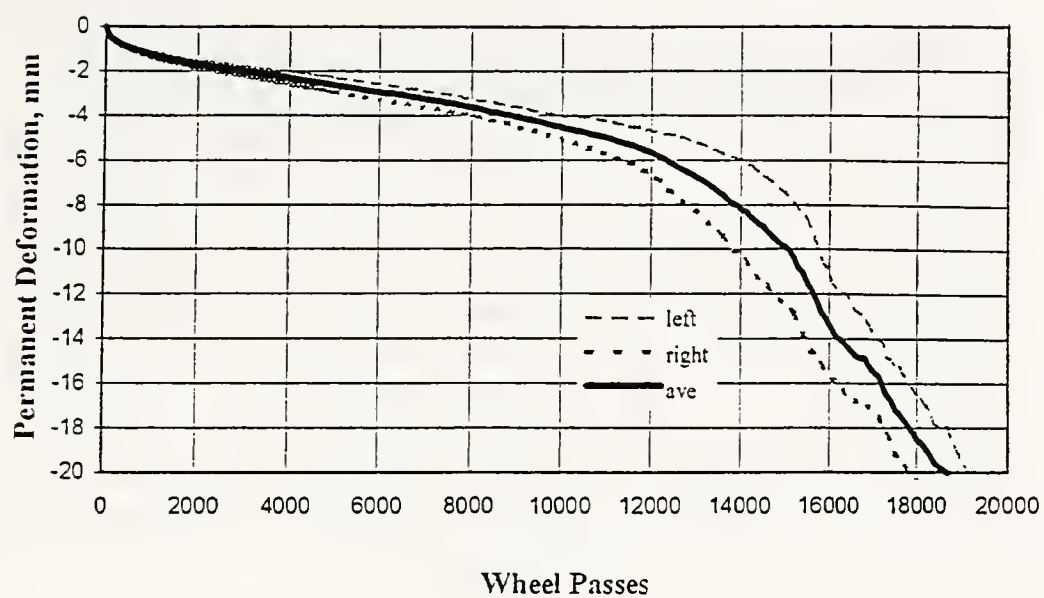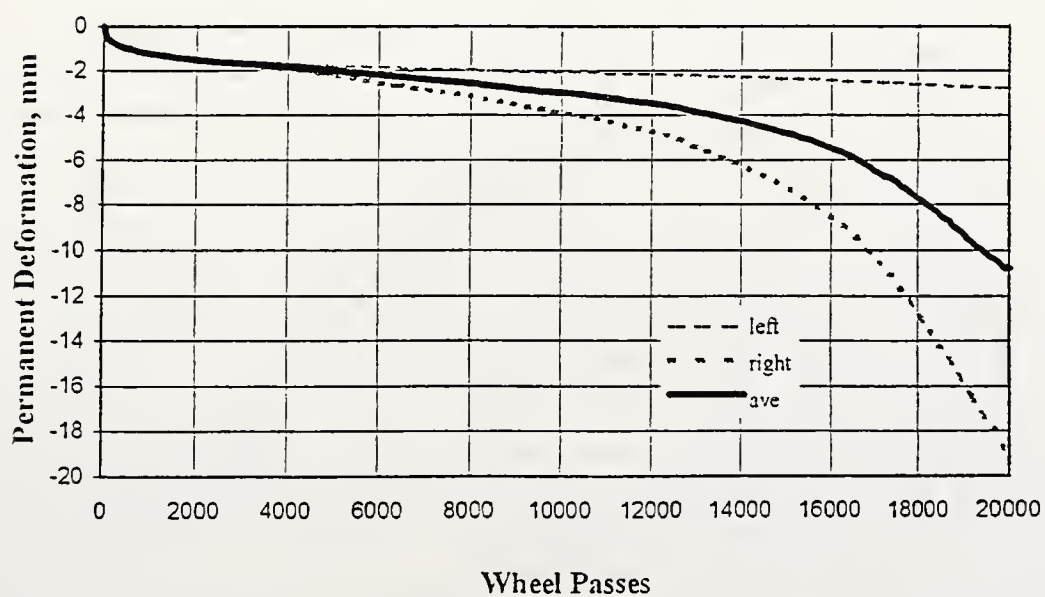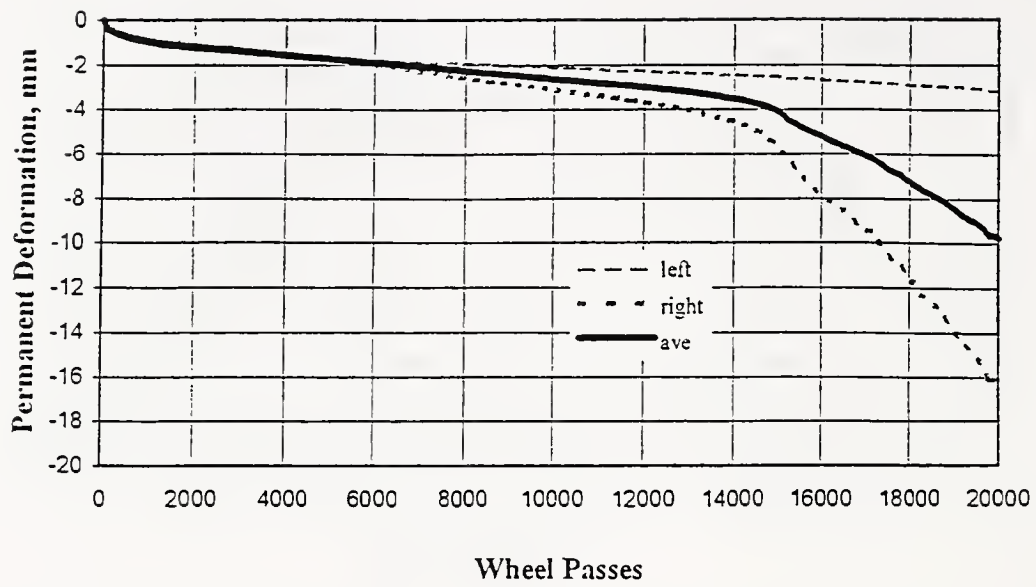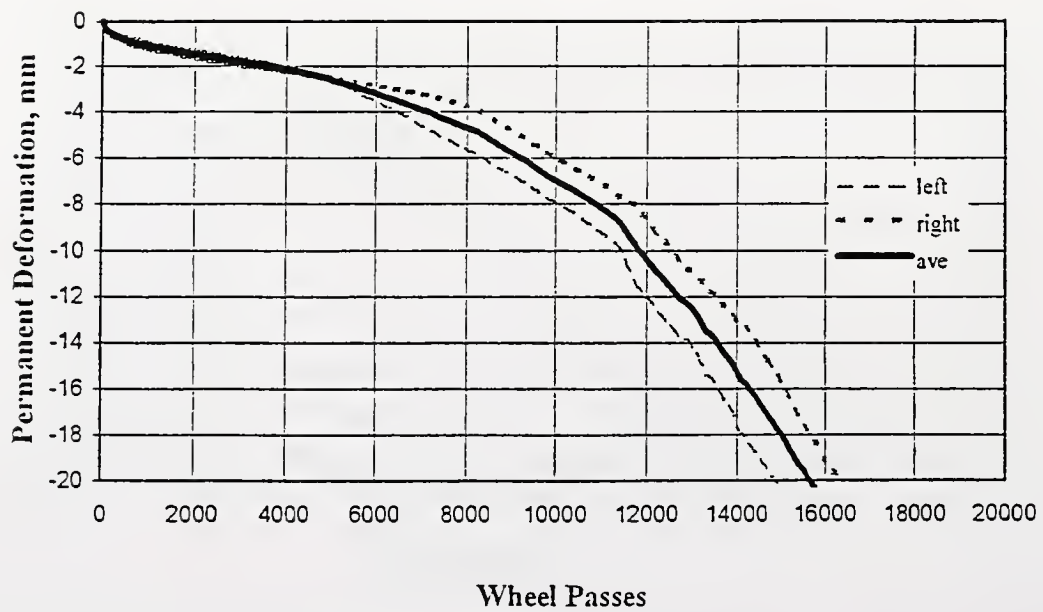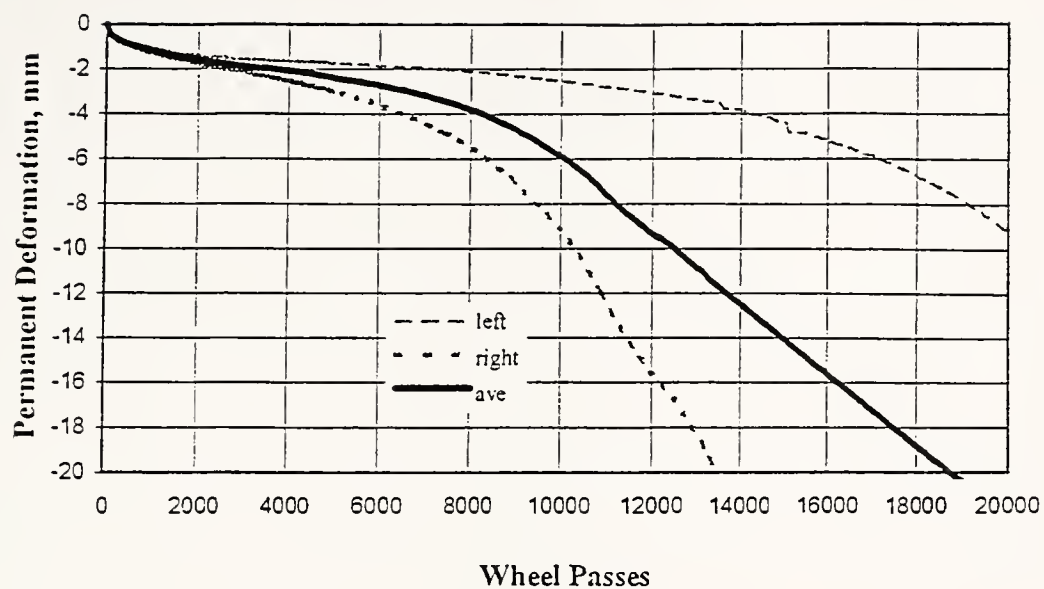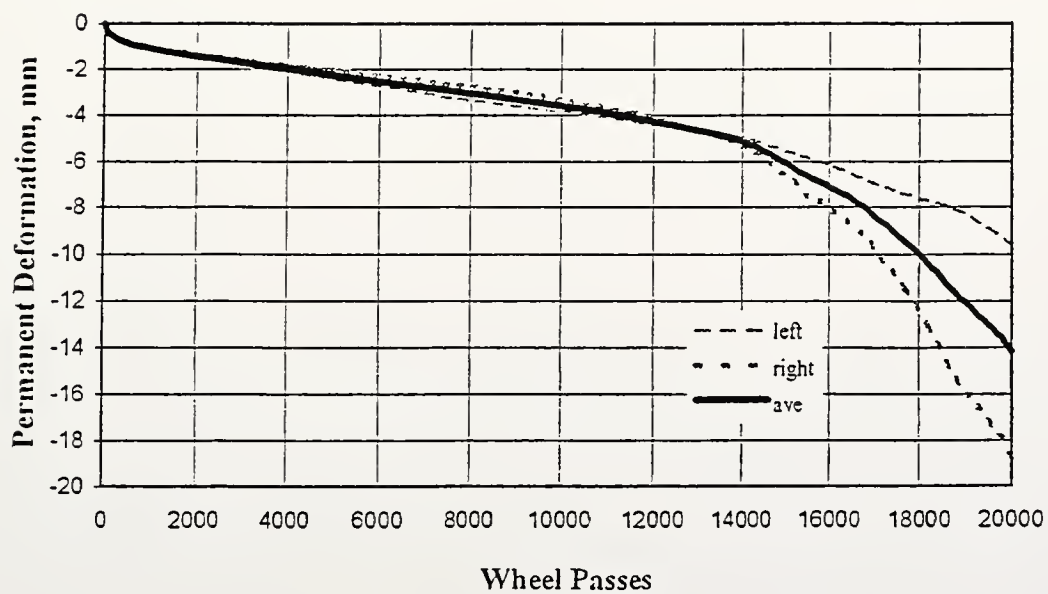Figure D-8 The Results for AC-20 Mixtures with 15% CB

Figure D-9 The Results for AC-20 Mixtures with 10% CB_p

Figure D-10 The Results for AC-20 with 15% CB_p

APPENDIX E.

SYNTHESIS OF CONCLUSIONS AND RECOMMENDATIONS

E-1 Summary

This study, which is based on various laboratory tests and evaluations, investigates the usefulness and potential of using pyrolyzed carbon black (CB_p) from scrap tires as an additive in hot mix asphalt. The fundamental characteristics and performance of asphalt binders and asphalt mixtures modified with pyrolyzed carbon black are determined and compared to asphalt mixtures modified with carbon black (CB) and unmodified asphalt binders and mixtures.

In order to investigate the fundamental properties and characteristics of asphalt binder modified with CB_p and CB, done by Zeng and Lovell (1995), laboratory tests were conducted at INDOT, which is including specific gravity test, kinematic viscosity test, penetration test, softening point test, ductility test and aging test.

Two different types of aggregates, limestone done by Park and Lovell (1995), as well as slag done by Lee, Slagado and Lovell (1996), which have been used in common in Indiana, were employed in mixture design. The optimum binder content and the relationship of density and voids were determined from Marshall mix design. The range of the optimum binder content was 6.3 % to 7.8 % for slag mixtures and 4.2 % to 5.7 % for limestone mixtures, respectively. The Marshall stability as a strength value and flow at 140°F increased within the accepted ranges due to the inclusion of CB_p. The gyratory tests to determine the stress-strain behavior of the mixtures modified with CB_p were conducted by U.S. Army Corps Engineer 8A/6B/4C model. The resilient modulus test and indirect tensile test were conducted to determine the stiffness of the mixtures at low temperatures, which is related to cracking potential of pavement. The inclusion of CB and CB_p produced an increase of M_R and tensile strength. Dynamic confined creep tests were carried out to check the rutting potential of pavement at high temperature, which is one of the important problems with pavements. The mixtures modified by CB_p showed lower creep strain than the unmodified mixtures.

E-2 Conclusions

Within the limited laboratory testing in this study, the following principal conclusions can be drawn:

- The pyrolysis of scrap tires may be one of the most desirable techniques form an economic and environmental standpoint.

- The inclusion of pyrolyzed carbon black will improve the temperature susceptibility of asphalt cements, and hence the service life of hot mix asphalt pavements.

- Penetration of the asphalt cements modified both by carbon black and pyrolyzed carbon black decrease steadily. The higher the test temperature, the larger the penetration value for the same percentage of carbon black added.

- Softening point of the asphalt cements mixed with carbon black or pyrolyzed carbon black increases when the quantity of carbon black added increases. The later one has a higher softening point than the former one.

- Though the results may not indicate much improvement of temperature susceptibility, the addition of pyrolyzed carbon black will not have adverse effect on asphalt properties.

- The performance and characteristics of asphalt binders modified with CB_p are somewhat dependent on the characteristics of the asphalt cement. The use of CB_p in AC-10 mixtures provides more benefits than in AC-20 mixtures for limestone and slag.

- The measured flexural creep stiffness of AC-20 binder from the bending beam rheometer test is higher than that of AC-10 binder at the same testing temperature and loading time, because the viscosity of AC-20 asphalt is much higher than that of AC-10 asphalt.

- The inclusion of CB and CB_p for both asphalts, AC-10 and AC-20, increases flexural creep stiffness at each testing temperature and increases the time to reach a failure (larger bending). This implies that the inclusion of CB and CB_p causes the flexural

creep stiffness to increase, and CB and CB_p can be used as reinforcing additives in asphalt.

- The flexural creep stiffness at lower temperature (less than 0°C) shows a linear relationship as the loading time increases. The change of the flexural creep stiffness becomes smaller as the testing temperature decreases.

- According to the recommendation by King et al. (1993), the asphalt stiffness should be less than 200 MPa at loading of 60 seconds to avoid low temperature cracking. In this study, the temperature to meet King's recommendation is around -13°C for AC-10 binder and -10°C for AC-20 binder.

- As the inclusion of carbon black and pyrolyzed carbon black increases, air-voids of the mixtures tend to increase. The change of air-voids in CB_p mixtures is larger than in CB mixtures, due to the non-uniformity of the particles. The bulk specific gravity of the blended aggregate is not a constant. It depends on the shape and surface texture of the aggregate, and the characteristics of the binder (asphalt+additive).

- The use of iron blast furnace slag as an aggregate for binder courses of pavement produces a high Marshall stability, an average about 20000 N. Also, as the inclusion amounts of CB or CB_p increase, the Marshall stability increases. However, the effect on the Marshall stability for AC-20 mixtures with carbon black (CB) is not as significant as in the other cases.

- The inclusion of CB and CB_p increases flow values, but these remain within the acceptable ranges. The optimum binder content tends to increase as the content of CB and CB_p increases.

- As the GTM revolutions increase, air voids decease. The air voids of AC-10 mixture increased with increasing percent of CB and CB_p, but AC-20 mixtures did not show a similar trend.

- Considering the value of GSI, AC-10 CB_p mixtures represented very stable mixtures. The inclusion of CB_p had the effect of producing a very stable mixture during long loading applications. Only AC-10 mixtures and AC-20 mixtures with 20 percent of CB indicated instability for long loading application due to the flushing of binder.

Compactibility of the CB_p mixtures is independent on the inclusion of CB_p. The inclusion of CB_p in both grades of asphalt mixtures improves the shear resistance of the pavement, and the plastic deformation can be controlled by the appropriate amount of CB_p.

- The flow of AC-10 mixtures with CB and CB_p remained in an acceptable range after long loading application, but that of AC-20 mixtures with CB and CB_p was out of the acceptable range. In all the mixtures, the flow stabilized after long loading applications.

- The M_R at low temperature, 5°C, is around 2 to 3 times larger than at high temperature, 25°C. The rate of change of M_R is larger for Marshall compacted specimens than for gyratory compacted specimens.

- The grade of asphalt cement has a significant effect on the M_R and tensile strength of the mixtures. The higher the asphalt grade, the higher M_R and tensile strength.

- The effect of compaction method for the M_R is relatively significant. The Marshall compaction shows relatively poor reproducibility, however, gyratory compaction does not. The use of M_R for Marshall compacted specimens is overestimated at high temperature and underestimated at low temperature.

- The inclusion of CB and CB_p produces an increase of M_R and tensile strength. In the case of AC-10 mixtures, CB_p can produce a greater difference than CB at low temperature. However, CB is better than CB_p at high temperature.

- In the case of slag mixtures, tensile strength of CB_p mixtures up to 10 %, is better than CB mixtures. However, that of CB mixtures, larger than 10 %, is better than CB_p mixtures. The tensile strength of the mixtures would depend on the effective asphalt film thickness of the mixtures. In the case of the limestone mixtures, the increase of tensile strength due to the inclusion of CB_p is not significant for either grade of asphalt. Thus the tensile strength is independent of the inclusion of CB_p.

- The unmodified mixtures followed a ideal creep behavior of viscoelastic materials, including primary stage, steady state region, and failure stage. However, the modified mixtures followed only the first two stages, primary and steady state. This

means that the inclusion of CB and CB_p can make more stable mixtures which take a longer time to reach failure.

- Although some of mixtures reached the failure mode, the mixtures used showed relatively good quality and performance in accordance with the recommendation of Gabrielson, less than 0.1 mm/mm of permanent strain.

- The viscosity of asphalt should be the major factor at high testing temperature ($50^{\circ}C$) to control the creep strain, creep strain rate, creep modulus, and creep modulus rate.

- The Marshall compacted mixtures represent better creep strain rates (lower values) than the gyratory compacted mixtures, due to the crushing of aggregate and different particle orientations during compaction. The creep strain for Marshall compacted specimens maybe underpredicted at high temperature ($50^{\circ}C$) and overpredicted at low temperature ($25^{\circ}C$), because gyratory compaction simulates the field construction better than Marshall compaction.

- AC-10 mixtures modified with CB produce higher creep slopes than with CB_p, however, the inclusion of CB and CB_p in AC-20 mixtures reduces the creep slope. This means that AC-20 mixtures modified with CB and CB_p are more sensitive to rutting than unmodified AC-20 mixtures.

- The additives, CB and CB_p, for AC-10 mixtures increase the stripping inflection point. However, for AC-20 mixtures a poor effect is illustrated, because AC-20 asphalt has a high viscosity.

- The inclusion of CB_p in AC-10 mixtures and AC-20 mixtures is better than that of CB in retaining the original rutting resistance after the mixtures start stripping.

- The slag mixtures shows better performance than the limestone mixtures, including much higher resistance to stripping.

- A 10 % to 15 % of CB_p by weight of asphalt is recommended for the improvement of the asphalt mixtures.

E-3. Recommendations

- The settlement or separation of carbon black and pyrolyzed carbon black in asphalt is quite common. Sufficient stirring or mixing mist be provided in the laboratory.

- It is difficult to mix (poor workability) either the carbon black or pyrolyzed carbon black percentage beyond 20 % for asphalt binder and asphalt mixtures.

- Even though various types of conventional binder tests, including penetration test, softening point test, ductility test, and aging test, were conducted by Zeng and Lovell (1995), more laboratory tests recommended by SHRP are needed. These include: bending beam rheometer (BBR); direct tension test (DTT); dynamic shear rheometer (DSR); rotational viscometer test; as well as rolling thin film oven (RTFO) test for short-term aging, and pressure vessel test for long-term aging, which should be added in order to characterize the complex rheological properties of binders.

- There are of problems in using the pyrolyzed carbon black. One is a handling problem with a powder forms of pyrolyzed carbon black. A possible alternative is to use palletized type of pyrolyzed carbon black with a proper mixing agent. Another is the settlement or segregation of pyrolyzed carbon black after mixing with asphalt due to its relatively heavy weight. In the field, the time from mixing with asphalt to mixing with aggregate should be minimized.

- Although asphalt mixtures modified by pyrolyzed carbon black have showed relatively good performance, the long-term performance should be monitored. Therefore, test sections should be constructed and monitored for a long time, using the mixtures which have been shown to be most effective in the laboratory.

- Reuse and recycling of pyrolyzed carbon black asphalt concrete should be considered and studied due to its usefulness in hot mix asphalt and the lack of natural construction materials.

- The use of waste material in hot mix asphalt may induce unexpected environmental problems. Although undesirable effects due to the use of pyrolyzed carbon black and iron slag have not been identified, long-term monitoring should be conducted.

APPENDIX F.
COMPARISON OF CONSTRUCTION COST

An evaluation the performance of a wide variety of waste materials for use in all aspects of highway construction should be required. Also, there are increasing regulations madating the use of those materials that show adequate or satisfactory performance. Therefore, information about costs related to the use of waste materials is needed. In this appendix, the construction costs between limestone-asphalt pavement and slag-asphalt pavement, which are modified with commercial carbon black and pyrolyzed carbon black, are presented. The costs of raw-materials are as follows :

- Commercial Carbon Black (CB) : 71 cents/lb ($ 1420 / ton)
- Pyrolyzed Carbon Black (CB_p) : 16 cents/lb ($ 320 / ton)
- Limestone (<3/4" with dust, Vulcan Materials) : $ 8.50 / ton
- Slag (<3/4", Levy Company) : $ 7.75 / ton
- AC-10 and AC-20 Asphalt : $ 126 / ton (varies every week)

For the comparison of construction costs, the length of asphalt pavement with 2 lanes is assumed 5 miles. The width of each lane is 12 feet and the thickness of asphalt pavement is 1.5 inch. The optimum binder content for limestone and slag is 5% and 7%, respectively. From the results of laboratory tests, 10 to 15% of additives by weight of asphalt cement showed the best performance. In this calculation, 10% of additive is used. The detailed calculation of construction cost is shown below :

A. Cost of Aggregate Needed

Type	Limestone	Slag
Bulk Specific Gravity	2.40	2.25
Bulk Density (pcf)	149.76	140.4
Weight of Aggregate (lb)	11,860,992	11,119,680*
Weight of Aggregate (ton)	5380.1	5043.9
Cost of Aggregate	$ 45730	$ 39090

* : 5 miles × 5280 ft/mile × (12 ft × 2 lanes) × 1.5/12 × 140.4 = 11,119,680 lb

B. Cost of Asphalt Concrete

Type	Limestone	Slag
Optimum Binder Content	5.0 %	7.0 %
Asphalt Needed	269 ton	353 ton
Cost	$ 33894	$ 44490*

* : 5043.9 ton $\times$ 0.07 $\times$ \$ 126 /ton = \$ 44,490

C. Total Construction Cost

Type	Limestone			Slag		
Additive	Pure	CB	CB_p	Pure	CB	CB_p
Additive Needed (ton)	-	26.9	26.9	-	35.3	35.3
Cost of Additive ($)	-	38198	8608	-	50126	11299*
Cost of Aggregate ($)	45731	45731	45731	39090	39090	39090
Cost of Asphalt ($)	33894	33894	33894	44491	44491	44491
Total Cost ($)**	79625	117823	88233	83581	133707	94880
Cost Increase (%)	-	48.0	10.8	-	60.0	13.5

* : 0.1 (10% of asphalt) $\times$ 353.1 ton $\times$ \$320 / ton = \$ 11,299

** : the summation of material itself (aggregate + asphalt + additive)

As can be seen in the comparison of construction costs, the raw material cost could be cut down significantly by using CB_p compared to using CB. The inclusion of CB_p in hot mix asphalt increases the construction cost about 10.8% for limestone and 13.5 % for slag, respectively. Even though the use of CB_p increases the construction cost, a consideration of life cycle costs rather than initial costs when selecting the construction materials or rehabilitation strategies should be taken into account. Judging from our laboratory test results, the inclusion of CB_p in hot mix asphalt can compensate for the initial construction cost due to its good performance, such as the increase of strength and ductility at high temperature, the increase of rutting resistance, the decrease of the

potential of low-temperature cracking, and the decrease of water-susceptibility. The service life and performance of materials are the most important factors when looking at life cycles. Therefore, a test section should be constructed and monitored for a long time to check the service life and performance of asphalt pavement modified with pyrolyzed carbon black.